ICLIAD 67 (1), 1-164, 2026

p-ISSN 0535-5133
e-ISSN 2477-9393

Volumen 67
No. 1
Marzo
2026

Investigación Clínica

Universidad del Zulia
Facultad de Medicina
Instituto de Investigaciones Clínicas
"Dr. Américo Negrette"
Maracaibo, Venezuela

Investigación Clínica

https://sites.google.com/site/revistainvestigacionesclinicas

Revista arbitrada dedicada a estudios humanos, animales y de laboratorio relacionados con la investigación clínica y asuntos conexos.

La Revista es de Acceso Abierto, publicada trimestralmente por el Instituto de Investigaciones Clínicas "Dr. Américo Negrette", de la Facultad de Medicina, de la Universidad del Zulia, Maracaibo, Venezuela.

Investigación Clínica está indizada en Science Citation Index Expanded (USA), Excerpta Medica/EMBASE y Scopus (Holanda), Tropical Diseases Bulletin y Global Health (UK), Biblioteca Regional de Medicina/BIREME (Brasil), Ulrich's Periodicals, Journal Citation Reports (USA), Index Copernicus (Polonia), SIIEC Data Bases, Sección Iberoamérica (Argentina) e Infobase Index (India), Redalyc y las bases de datos: SciELO (www.Scielo.org.ve), Revencyt, LILACS, LIVECS, PERIODICA y web de LUZ: http://www.produccioncientificaluz.org/revistas

Para cualquier otra información dirigir su correspondencia a:

Dra. Elena Ryder, Editora
Instituto de Investigaciones Clínicas
"Dr. Américo Negrette"
Facultad de Medicina, Universidad del Zulia
Maracaibo, Venezuela.

Teléfono:
+58-0414-6305451

Correos electrónicos:
elenaryder@gmail.com
riclinicas@gmail.com

Páginas web:
https://sites.google.com/site/revistainvestigacionesclinicas

http://www.produccioncientificaluz.org/revistas

For any information please address correspondence to:

Dr. Elena Ryder, Editor
Instituto de Investigaciones Clínicas
"Dr. Américo Negrette"
Facultad de Medicina, Universidad del Zulia
Maracaibo, Venezuela.

Phone:
+58-0414-6305451

E-mails:
elenaryder@gmail.com
riclinicas@gmail.com

Web pages:
https://sites.google.com/site/revistainvestigacionesclinicas

http://www.produccioncientificaluz.org/revistas

Universidad del Zulia
Publicación auspiciada por el
Vicerrectorado Académico
Serbiluz-CONDES

CODEN: ICLIAD
Versión impresa ISSN: 0535-5133
Depósito legal pp 196002ZU37
Versión electrónica ISSN: 2477-9393
Depósito legal ppi 201502ZU4667

Artes finales:
Lisbeny Valencia
lisbenyvalencia@gmail.com

ASESORES CIENTÍFICOS (2025-2027)

Invest Clin 67(1): 1 - 2, 2026 https://doi.org/10.54817/IC.v67n1a00

EDITORIAL
Reconocimientos y logros alcanzados en nuestro 65° Aniversario.

Investigación Clínica celebró en el 2025 su 65 Aniversario con una intensa actividad editorial. Se recibieron más 150 trabajos; de ellos, 120 fueron analizados por el Comité Editorial en reuniones semanales, durante las cuales se fijaron los árbitros internos o externos y se sometieron también a diversas sub-comisiones para verificar los análisis estadísticos, la gramática en castellano e inglés y las expresiones gráficas de las tablas y figuras. Todo este proceso permite obtener la máxima calidad durante la impresión digital y cuidar, a la vez, la idoneidad de los autores y la veracidad de las referencias bibliográficas emitidas. Por otro lado, el Comité Editorial incorporó dos nuevos investigadores: José Luis Arcaya en el área Neurociencias y Nereida Valero-Cedeño en Virología.

En el 2025 publicamos 39 comunicaciones: 4 editoriales y 35 trabajos (28 trabajos originales, 6 revisiones y 1 reporte de caso); de ellos, 11 provenían de Venezuela y 24 eran foráneos (Brasil, España y China). Para la evaluación de los trabajos recibidos fueron consultados 58 árbitros, 37 en Venezuela y 21 foráneos; sin embargo, hay que hacer notar que la mayoría de los foráneos pertenecen al grupo de graduados en universidades venezolanas y realizan su labor profesional en el exterior. A ellos, les agradecemos profundamente el arraigo a su origen.

Mantenemos nuestra inclusión (Q4) en índices internacionales como Scopus y Web of Science y somos la revista médica venezolana con más números indizados por Scielo-Venezuela. En los análisis bibliométricos del 2024 (últimos análisis publicados) el CitiScore de Scopus subió de 0.2 a 0.3 con el reconocimiento de 70 citaciones y un Índice h de 25, mientras que en el Web of Science el Journal Impact Factor (JIF) permanece en 0.1 al igual que el JCI (Journal Citation Indicator) de 0.02, reconociéndonos 203 citaciones.

La inscripción en CrossRef revela que, durante el 2025, trabajos publicados en Investigación Clínica fueron solicitados mensualmente entre 2000 a 4000 veces, lo que indica que esos trabajos han servido de base a investigadores para la preparación de sus comunicaciones científicas. También mantenemos vigilancia de todas las citaciones a través de Google Académico y nos satisface observar que trabajos publicados hace varios años se mantienen citados. En la misma forma, a través de nuestra página web podemos conocer cuáles son los más leídos.

En este primer número del 2026, hemos hecho algunas modificaciones a las Instrucciones a los Autores para adaptarnos a las continuas exigencias de la comunicación científica y algunas para evitar incidentes ocurridos durante los últimos años. Hemos decidido que las propuestas de trabajos sean responsabilidad exclusiva y directa de los autores, a través del autor de correspondencia. Esto se debe a que algunas propuestas hechas a través de individuos reconocidos como promotores o asistentes de edición han generado serios problemas en la idoneidad y estructura del trabajo presentado comprometiendo su calidad lo que, en alguna ocasión, nos ha llevado a considerar la retractación del manuscrito.

La actividad editorial de Investigación Clínica fue reconocida en este año aniversa-

rio por nuestra Alma Mater, la Universidad del Zulia, a través de la Facultad de Medicina y del Consejo de Desarrollo (CONDES) y por el Colegio de Médicos del Estado Zulia en varios actos académicos. En Acto especial, el día Aniversario, el personal adscrito a la revista recibió botones conmemorativos por parte de la Facultad de Medicina y, a la vez, nosotros reconocimos a un grupo de individuos que se distinguieron por su apoyo en la revisión de trabajos y en la difusión de las publicaciones.

Lamentablemente, el 2026 nos sorprendió con una triste noticia, el fallecimiento de nuestra editora entre los años 1972-1990, la viróloga Dra. Slavia Ryder, quien falleció el día 20 de enero. Incluimos en este número un In Memoriam escrito por uno de sus primeros alumnos, el Dr. José Esparza.

Elena Ryder
ORCID 0000-0003-4613-6424

Recognitions and achievements in our 65th Anniversary

Investigacion Clinica celebrated its 65th anniversary in 2025 with a busy publishing season. We received over 150 submissions; of these, 120 were reviewed by the Editorial Committee, which welcomed two new members: José Luis Arcaya (Neuroscience) and Nereida Valero-Cedeño (Virology). We published four editorials and 35 articles: 28 original articles, 6 reviews, and 1 case report. Thirty-one percent of these originated in Venezuela, while 69% came from other countries, including Brazil, Spain, and China. We had 58 reviewers: 64% were Venezuelan, and 36% were from other countries. Notably, most international reviewers graduated from Venezuelan universities but work abroad. We are deeply grateful to them for maintaining their connection to their homeland. We remain included in international indexes such as Scopus and Web of Science, and we are the Venezuelan medical journal with the most issues indexed by SciELO-Venezuela. CrossRef reported that published works are requested 2,000-4,000 times per month. In this first issue of 2026, we have updated the Instructions for Authors to better meet the ongoing demands of scientific communication and to prevent incidents that have occurred in recent years. Specifically, proposals for articles must be the sole responsibility of the authors, through the corresponding author, because some submissions from promoters or editorial assistants raised serious doubts about the work's suitability, compromising the journal's quality and, on some occasions, prompting us to consider retracting the manuscript. Unfortunately, 2026 brought us the sad news of the passing of our editor from 1972 to 1990, virologist Dr. Slavia Ryder, who died on January 20th. This issue includes an In Memoriam written by one of her first students, Dr. José Esparza.

IN MEMORIAM

Dra. Slavia Cristina Ryder Jaksic
(1938–2026)†

Nacida en Maracaibo el 16 de junio de 1938, Slavia Cristina Ryder Jaksic dedicó su vida a la ciencia, a la Universidad del Zulia y al servicio de la salud pública venezolana. Desde temprana edad manifestó una clara vocación por las ciencias naturales, que la condujo a estudiar Medicina en la Universidad del Zulia, donde se graduó con honores en 1962.

Durante su formación como estudiante fue incorporada, bajo la guía del Dr. Américo Negrette, a la incipiente actividad de investigación científica que daría origen al Instituto de Investigaciones Clínicas de la Facultad de Medicina de LUZ. Se especializó en virología y arbovirosis, con especial énfasis en la Encefalitis Equina Venezolana (EEV), enfermedad a la que dedicó más de tres décadas de trabajo ininterrumpido, combinando investigación de laboratorio, estudios de campo y vigilancia epidemiológica en el estado Zulia.

Realizó estudios de posgrado en el Instituto Venezolano de Investigaciones Científicas (IVIC) con el Dr. Gernot Bergold, así como en el Centro para el Control y la Prevención de Enfermedades (CDC) de Atlanta, y efectuó estancias de investigación en instituciones de referencia internacional como la Universidad de Cornell, el Laboratorio de Arbovirus de Fort Collins y el Dengue Branch en Puerto Rico. Su tesis doctoral, presentada en 1972, constituye un trabajo clásico sobre la epidemiología de la EEV en la Guajira venezolana. Sus investigaciones permitieron comprender la dinámica cíclica de las epidemias, identificar poblaciones en riesgo y alertar oportunamente sobre brotes de gran magnitud, como el ocurrido en 1995.

Su producción científica, su compromiso sostenido con la vigilancia epidemiológica regional y su estrecha colaboración con las autoridades sanitarias contribuyeron de manera decisiva al manejo de las epidemias de encefalitis en el occidente del país. Fue pionera en la creación de la Cátedra de Virología de la Universidad del Zulia, formó a numerosas generaciones de profesionales y tuteló múltiples tesis de grado y posgrado, dejando una huella profunda como docente e investigadora.

Un capítulo fundamental de su legado académico fue su contribución decisiva al desarrollo y a la proyección internacional de la revista *Investigación Clínica,* órgano del Instituto de Investigaciones Clínicas de la Facultad de Medicina de LUZ, fundada en 1960 por el Dr. Américo Negrette. Incorporada como Editora en 1972, la Dra. Slavia Ryder lideró durante casi dos décadas un proceso sostenido de modernización editorial que fortaleció el arbitraje científico, amplió la visibilidad de la revista y elevó sus estándares internacionales. Bajo su supervisión, *Investigación Clínica* fue incluida en el *Science Citation Index* en 1974 y posteriormente en *Index Medicus/Medline* en 1989, así como en otros índices internacionales. En 1987, la revista fue distinguida con el Premio CONICIT como Mejor Revista Científica Venezolana, reconocimiento que reflejó la solidez, continuidad y prestigio alcanzados gracias a su visión editorial.

Todos los que, de una u otra manera, fuimos sus estudiantes y colegas, la recordamos con profundo cariño y admiración.

José Esparza

IN MEMORIAM

Dra. Slavia Cristina Ryder Jaksic
(1938–2026)†

Born in Maracaibo on June 16, 1938, Slavia Cristina Ryder Jaksic dedicated her life to science, the University of Zulia, and serving Venezuelan public health.

From a young age, she showed a strong calling for the natural sciences, which led her to study medicine at the University of Zulia, where she graduated with honors in 1962.

During her studies, under the guidance of Dr. Américo Negrette, she became involved in the emerging scientific research activity that led to the creation of the Instituto de Investigaciones Clínicas at the Facultad de Medicina de LUZ. She specialized in virology and arboviruses, focusing especially on Venezuelan Equine Encephalitis (VEE), a disease she dedicated more than 30 years of continuous work to, combining laboratory research, field studies, and epidemiological surveillance in Zulia state.

She pursued postgraduate studies at the Venezuelan Institute for Scientific Research (IVIC) with Dr. Gernot Bergold, and also at the Centers for Disease Control and Prevention (CDC) in Atlanta. Additionally, she conducted research stays at internationally renowned institutions such as Cornell University, the Arbovirus Laboratory in Fort Collins, and the Dengue Branch in Puerto Rico.

Her doctoral thesis, presented in 1972, is a renowned work on the epidemiology of VEE in the Venezuelan Guajira region. Her research enabled understanding the cyclical patterns of epidemics, identifying at-risk populations, and providing early warnings about large-scale outbreaks, such as the one in 1995.

Her scientific output, her sustained commitment to regional epidemiological surveillance, and her close collaboration with health authorities played a crucial role in managing encephalitis epidemics in western Venezuela. She was a pioneer in establishing the Virology Department at the University of Zulia, trained numerous generations of professionals, and supervised many undergraduate and graduate theses, leaving a lasting impact as a teacher and researcher.

A key part of her academic legacy was her decisive role in developing and internationally promoting the journal Investigación Clínica, the official publication of the Instituto de Investigaciones Clínicas at the Facultad de Medicina de LUZ, founded in 1960 by Dr. Américo Negrette. She joined as Editor in 1972 and led a continuous process of editorial modernization for nearly twenty years, enhancing scientific peer review, boosting the journal's visibility, and increasing its international standards. Under her leadership, Investigación Clínica was included in the Science Citation Index in 1974 and later in Index Medicus/Medline in 1989, as well as in other international indexes.

In 1987, the journal received the CONICIT Prize for Best Venezuelan Scientific Journal, a recognition that highlighted the strength, continuity, and prestige it had gained through its editorial vision.

All of us who, in one way or another, were her students and colleagues, remember her with deep affection and admiration.

Invest Clin 67(1): 5 - 18, 2026 https://doi.org/10.54817/IC.v67n1a01

Effects of Vitamin D deficiency and supplementation on 25(OH)D3 levels and neuropsychobehavioral development in premature infants.

Xiaohui Guo[1], Yanfeng Sun[2], Yanhong Chen[1], Feifei Xu[1] and Yanfei Li[1]

[1]Department of Pediatrics, Binzhou People's Hospital, Binzhou City, Shandong Province, China.
[2]Department of Hematology, Binzhou People's Hospital, Binzhou City, Shandong Province, China.

Keywords: Vitamin D; Neuropsychobehavioral development; Premature infants; Vitamin D; 25(OH)D3; Neurodevelopment; Psychomotor Performance; Infant, Premature.

Abstract. This study systematically examined how vitamin D metabolic imbalance impacts 25(OH)D3 levels and neuropsychological development in premature infants and proposed a personalized supplementation approach. Premature infants were classified as adequate, insufficient, or deficient based on umbilical cord blood 25(OH)D3 levels and then randomly assigned to either a standard-dose group (800 IU/d) or an individualized supplementation group (400-1000 IU/d) with vitamin D. In the vitamin D-deficient group, infants receiving personalized supplementation had significantly higher 25(OH)D3 levels at three and nine months, adjusted for gestational age, than those receiving the fixed dose, indicating that 1000 IU/d is more effective than 800 IU/d for correcting deficiency ($p<0.05$). At nine and 18 months adjusted gestational age, infants in the vitamin D-insufficient and deficient groups scored significantly lower on the Gesell Developmental Scales across categories such as gross motor, fine motor, language, adaptive, and social skills compared to the adequate group ($p<0.05$). Within the deficient group, those receiving personalized supplementation scored higher in all five areas at both nine and 18 months adjusted gestational age compared to those on the fixed dose ($p<0.05$). The study highlights notable differences in umbilical cord blood 25(OH)D3 levels among premature infants, emphasizing that a customized vitamin D supplement protocol is more effective for correcting deficiencies.

Corresponding author: Xiaohui Guo, No. 515, Huanghe Seventh Road, Bincheng District, Binzhou City 256610, Shandong Province, China. Email: guoxiaohui3212919@163.com

Efectos de la deficiencia de vitamina D y la suplementación sobre los niveles de 25(OH)D3 y el desarrollo neuropsicológico-conductual en bebés prematuros.

Invest Clin 2026; 67 (1): 5 – 18

Palabras clave: Vitamina D; 25(OH)D3; Desarrollo Neuropsicológico/Desarrollo Psicomotor; Recién Nacido; Prematuro.

Resumen. Este estudio exploró sistemáticamente el impacto del desequilibrio metabólico de la vitamina D en los niveles de 25(OH)D3 y en el desarrollo neuropsicológico de bebés prematuros, y propuso una estrategia de suplementación individualizada. Los bebés prematuros se categorizaron en grupos adecuados, insuficientes y deficientes según los niveles de 25(OH)D3 en la sangre del cordón umbilical, y luego se asignaron aleatoriamente a un grupo con dosis estándar (800 UI/día) o a otro grupo con suplementación individualizada (400-1000 UI/día) con vitamina D. Entre los bebés prematuros con deficiencia de vitamina D, el grupo de suplementación individualizada presentó niveles significativamente más altos de 25(OH)D3 a los 3 y 9 meses de edad gestacional corregida, en comparación con el grupo de dosis estándar, lo que indica que una dosis de 1000 UI/día fue más efectiva que 800 UI/día para corregir la deficiencia de vitamina D ($p<0,05$). A los 9 y 18 meses de edad gestacional corregida, los bebés prematuros de los grupos con insuficiencia y deficiencia de vitamina D obtuvieron puntuaciones significativamente más bajas en las Escalas de Desarrollo de Gesell para la habilidad motora gruesa, la habilidad motora fina, la competencia lingüística, la capacidad adaptativa y la habilidad personal-social en comparación con el grupo adecuado ($p<0,05$). Dentro del grupo deficiente, el grupo de suplementación individualizada obtuvo puntuaciones más altas en las cinco habilidades a los 9 y 18 meses de edad gestacional corregida en comparación con el grupo de dosis estándar ($p<0,05$). Existen diferencias significativas en los niveles de 25(OH)D3 en la sangre del cordón umbilical entre los bebés prematuros, y un protocolo de suplementación de vitamina D específico para cada individuo es más eficaz para corregir la deficiencia de vitamina D.

Received: 17-07-2025 Accepted: 07-09-2025

INTRODUCTION

Premature infants, defined as those born before 37 weeks of gestation, encounter various health issues after birth because their organ systems are not fully developed[1]. In recent years, with the continued development of perinatal medicine and significant advances in neonatal intensive care and diagnostic techniques, the treatment of premature infants has been greatly enhanced, resulting in a rising survival rate [2]. Subsequent to their survival, long-term issues such as abnormal neurological development in premature infants have also received increasing attention [3]. The normal development of the nervous system is directly related to the future quality of life of premature infants, including cognition, motor skills, language, and other aspects [4]. Therefore, identifying

factors that affect the neuropsychological and behavioral development of premature infants and implementing effective interventions are of great significance for improving their prognosis.

Vitamin D, a crucial fat-soluble nutrient, holds a fundamental position in maintaining human health [5]. In recent years, in-depth research on vitamin D and its roles in bone health, immune function, and neurodevelopment has received increasing attention [6, 7]. Especially among premature infants, pediatric research has increasingly focused on vitamin D status and corresponding supplementation strategies [8]. Premature infants often suffer from vitamin D deficiency [9, 10]. On the one hand, premature infants have inadequate vitamin D stores during pregnancy, especially in the late gestational period, when the amount of vitamin D obtained by the fetus from the mother gradually increases; however, premature birth leads to relatively insufficient vitamin D stores [11]. On the other hand, premature infants have a limited capacity to synthesize vitamin D through their skin after birth, and breast milk, typically their primary source of nutrition, provides insufficient vitamin D to meet their rapid growth and developmental demands [12, 13]. Furthermore, premature infants may not receive adequate sunlight exposure during their hospitalization, thereby hindering vitamin D synthesis[14]. Humans obtain vitamin D primarily from two sources: skin synthesis of 7-dehydrocholesterol under UV-B light to form vitamin D3, and dietary intake of vitamin D2 [15]. Both vitamin D forms undergo hepatic hydroxylation to yield 25(OH)D3, which then undergoes renal metabolism to form its biologically active form, 1,25(OH)2D3 [16]. This metabolic pathway requires the collaboration of various organs, with 25(OH)D3 being the main circulating form and the key indicator for evaluating vitamin D levels [17].

Vitamin D deficiency not only affects the bone development of premature infants but may also have far-reaching impacts on their neuropsychological and behavioral development [18]. Research indicates that insufficient vitamin D levels in premature infants may impair growth and development, including intellectual and motor abilities, at one year of age [19]. Moreover, insufficient vitamin D levels may affect the neurological and behavioral development of preterm infants, particularly if they do not receive adequate supplementation shortly after birth[20]. A study demonstrated a positive association between serum 25(OH)D3 levels in premature infants and neuropsychological developmental quotient scores, which were enhanced by vitamin D supplementation administered both prenatally and postnatally [21]. This suggests that adequate vitamin D supplementation has a positive effect on the neurodevelopment and cognitive function of premature infants. Timely vitamin D supplementation can alleviate vitamin D deficiency and mitigate its adverse effects on neurodevelopment, making it crucial for improving the long-term prognosis of premature infants [22]. Vitamin D influences the morphogenesis and physiological functions of the nervous system through diverse mechanisms, including regulating the expression of neurotrophic factors, influencing neurotransmitter synthesis, and modulating calcium signaling pathways [23]. Vitamin D and its receptor (VDR) are ubiquitously expressed across diverse tissues and cell types in the human body, including neurons and glial cells in the central nervous system, and participate in neuronal proliferation, differentiation, and apoptosis. Vitamin D is essential for neurodevelopment via epigenetic regulation mediated by VDR [24, 25]. 1,25(OH)2D3 upregulates the expression of synaptic proteins such as Synaptophysin and PSD-95, promoting synaptic plasticity. Additionally, vitamin D influences behavioral control and cognitive function by regulating the activity of the dopamine synthesis rate-limiting enzyme (tyrosine hydroxylase) and the glutamate transporter (EAAC-1) [26, 27]. Therefore, examining the impact of vitamin D insufficiency and augmentation on serum 25[OH]D3 concentrations, alongside neuro-

cognitive and behavioral progress in preterm infants, possesses considerable theoretical and practical significance.

At present, there is no universally agreed standard for the dose and schedule of vitamin D supplements for premature babies, with variations in recommendations among countries and organizations [28, 29]. Generally speaking, the range of vitamin D supplementation for premature infants is 400-1000 IU/day, and the specific dosage needs to be adjusted according to factors such as gestational age, birth weight, and feeding mode [30]. Numerous studies have explored the effects of vitamin D supplementation on 25(OH)D3 levels in premature infants, revealing that adequate supplementation can significantly elevate serum 25(OH)D3 levels; nonetheless, it is crucial to recognize that the connection between dosage and 25(OH)D3 levels is non-linear, and excessively high doses may pose a risk of vitamin D excess or toxicity [31, 32]. Secondly, the duration of supplementation also affects the outcome, with studies showing that long-term supplementation maintains stable 25(OH)D3 levels better than short-term supplementation[33]. In addition, factors such as gestational age, birth weight, and liver and kidney function status in premature infants also affect the metabolism and utilization efficiency of vitamin D [34]. One of the research hotspots is the comparison of the effects of different supplementation regimens. Drawing on the aforementioned research background and evidence, this study aims to determine the optimal dose and schedule for administering vitamin D supplements to premature infants, while comprehensively assessing the potential long-term effects of such supplementation on their 25(OH)D3 levels and neuropsychobehavioral development.

Patients and Methods

This is a clinical study conducted in the neonatal unit at our hospital's Children's Medical Center. The designed operational procedure is shown below.

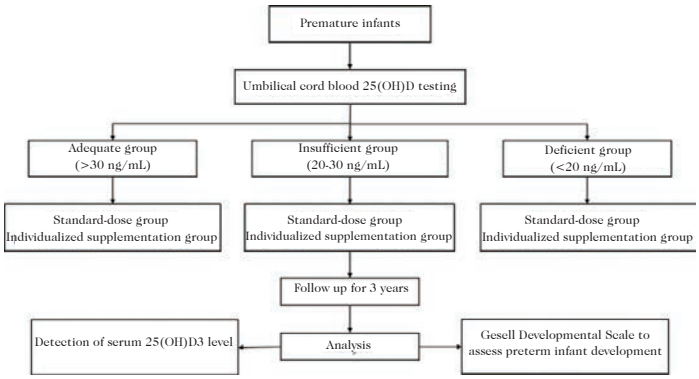

Clinical data

A total of 175 premature infants admitted between January 2020 and December 2021 who underwent umbilical cord blood 25(OH)D3 testing within 24 hours after birth were selected as study subjects. Inclusion criteria included: gestational age less than 37 weeks; no severe complications; stable vital signs; mothers without severe pregnancy-related complications; and participants free from conditions or medications that could affect calcium and vitamin D metabolism. Exclusion criteria included: twin or multiple pregnancies; congenital malformations affecting normal body structure and function; genetic metabolic diseases; brain hypoplasia with obvious neurological abnormalities; and mothers with hypertension, diabetes, metabolic diseases, or other conditions during pregnancy that could negatively impact the fetus.

Grouping and intervention

All premature infants underwent umbilical cord blood 25(OH)D3 testing within 24 hours of birth and were classified into three groups: adequate (>30 ng/mL), insufficient (20-30 ng/mL), and deficient (<20 ng/mL). Each group was further divided into a standard vitamin D dosage group or an individualized supplementation group. All premature infants received vitamin D3 supplementation starting on the first day after birth. The standard-dose group received a routine supplementation of 800 IU/day, while the individualized group received 400, 800, or 1000

IU/day for three months, depending on their 25(OH)D3 levels (adequate, insufficient, or deficient, respectively). After three months, the dose was increased to 400 IU/day for all infants and maintained at this level until age 3 years. Follow-up visits occurred in the outpatient clinic over three years, and cases lost to follow-up were excluded. Ultimately, 175 infants completed the follow-up: 51 in the adequate group (25 in the standard dosage group and 26 in the individualized group), 54 in the insufficient group (26 in the standard dosage group and 28 in the individualized group), and 70 in the deficient group (35 in each group). All premature infants received oral vitamin D3 drops in capsule form [400 IU/capsule, Sinopharm Xingsha Pharmaceutical (Xiamen) Co., Ltd.].

Observation indicators

(1) Serum 25(OH)D3 levels served as a crucial indicator for assessing vitamin D nutritional status. Regular monitoring of serum 25(OH)D3 levels at 24 hours after birth, at 3 months, at 9 months' corrected gestational age (CGA), and at 18 months' CGA can provide insights into the dynamic changes in vitamin D status in premature infants and evaluate the effectiveness of vitamin D supplementation.

(2) The Gesell Developmental Scales were used to evaluate the developmental status of premature infants. This scale covers adaptive ability, gross motor skills, fine motor skills, language ability, and personal-social skills, offering a comprehensive view of the children's intellectual development. Assessments with the Gesell Developmental Scales were performed at 9 months CGA and 18 months CGA. A pediatric nurse trained to administer the scales conducted these assessments at each time point. The scale includes adaptive ability, gross motor skills, fine motor skills, linguistic ability, and personal-social ability, fully reflecting children's intellectual growth. For children aged 0-3, the scale contains 514 items, all completed within 60 minutes. Results are expressed as a Developmental Quotient (DQ). DQ is calculated as Measured Developmental Age divided by Chronological Age, multiplied by 100. A DQ of 130 or higher indicates superior development; 110 to 129, good development; 80 to 109, average development; 70 to 79, borderline low development; and below 70, indicates intellectual developmental delay.

Statistical analysis

Statistical analysis was done with SPSS 25.0. Normally distributed data were reported as mean ± SD and analyzed using a t-test (for two groups) or ANOVA with Bonferroni correction (for multiple groups). Categorical data were presented as the number of individuals and the composition ratio (%), and the chi-square test was employed for analysis. A p-value < 0.05 was considered statistically significant.

RESULTS

Comparison of Baseline characteristics

Baseline demographic features showed no significant differences among the adequate, insufficient, and deficient groups ($p > 0.05$), ensuring comparability of subsequent intervention effects (Table 1).

Comparison of 25(OH)D3 levels among the three groups of infants at 24 hours after birth, 3 months after birth, 9 months CGA, and 18 months CGA

At 24 hours after birth, 3 months after birth, and 9 months CGA, the 25(OH)D3 levels in both the vitamin D insufficient group and the deficient group were lower than those in the adequate group ($p<0.05$). At 18 months CGA, there were no statistically significant differences in 25(OH)D3 levels among the three groups of infants ($p>0.05$ (Table 2).

Table 1. Comparison of baseline characteristics.

Variables	Adequate group (n=51)	Insufficient group (n=54)	Deficient group (n=70)	F/χ^2	p
Gender (n, %)					
male	23 (45.10)	25 (46.30)	33 (47.14)	0.050	0.975
female	28 (54.90)	29 (53.70)	37 (52.86)		
Mode of delivery (n, %)					
spontaneous labor	25 (49.02)	26 (48.15)	31 (44.29)	0.318	0.853
cesarean section	26 (50.98)	28 (51.85)	39 (55.71)		
Gestational age (weeks)	35.33±0.74	35.43±0.63	35.40±0.71	0.248	0.781
Birth weight (g)	2462.82±211.96	2489.46±212.43	2459.87±205.66	0.344	0.709
Mother age (years)	28.96±5.38	28.76±4.59	28.94±5.33	0.026	0.974
1 min Apgar score (scores)	8.33±0.62	8.30±0.71	8.30±0.73	0.046	0.955
5 min Apgar score (scores)	9.04±0.34	9.11±0.32	9.04±0.27	0.971	0.381

Baseline characteristics are presented as mean ± SD or n (%). Between-group differences were assessed using one-way ANOVA for continuous variables and the χ^2 test for categorical variables.

Table 2. Comparison of 25(OH)D3 levels at different time points in the 3 groups.

Groups	n	24 h after birth	3 months after birth	9 months CGA	18 months CGA
Adequate group	51	35.74±4.27	34.95±4.38	35.82±3.88	35.18±4.83
Insufficient group	54	24.15±2.14[a]	29.48±3.44[a]	31.07±4.38[a]	34.53±4.61
Deficient group	70	13.18±2.31[ab]	23.54±4.24[ab]	29.93±5.00[a]	34.65±4.10
F		853.143	118.449	26.8893	0.327
p		0.000	0.000	0.000	0.722

Data are presented as mean ± SD in ng/mL. Between-group comparisons at each time point were performed using one-way ANOVA, followed by Bonferroni post hoc tests. [a]$p<0.05$ vs. Adequate group; [b]$p<0.05$ vs. Insufficient group. CGA: corrected gestational age.

Comparison of 25(OH)D3 levels between the standard dosage group and the individualized supplementation group within the deficient group

Within the deficient group, there were no statistically significant differences in 25(OH)D3 levels between the standard-dose and individualized-supplementation groups at 24 hours after birth ($p>0.05$). However, at 3 months after birth, 9 months CGA, and 18 months CGA, the 25(OH)D3 levels in the individualized supplementation group were significantly higher than those in the standard dose group ($p<0.05$) (Table 3).

Comparison of Gesell Developmental Scales scores among the three groups of infants at 9 months CGA and 18 months CGA

At both the 9- and 18-month CGAs, significant differences were observed in scores across the five abilities among the three infant groups ($p<0.05$). Pairwise comparisons revealed that the scores for the five abilities in both the insufficient and deficient groups were lower than those in the adequate group ($p<0.05$). Nonetheless, the scores of the five abilities did not show significant statistical differences when comparing the insufficient and deficient groups ($p>0.05$) (Tables 4 and 5).

Table 3. Comparison of 25(OH)D3 levels between the standard dosage group and the individualized supplementation group within the deficient group.

Groups	*n*	24 h after birth	3 months after birth	9 months CGA	18 months CGA
Standard dose group	35	13.15±2.46	21.34±3.55	27.29±4.18	32.82±3.81
Individualized supplementation group	35	13.22±2.18	25.74±3.73	32.56±4.37	36.47±3.55
t		0.126	5.049	5.146	4.152
p		0.900	0.000	0.000	0.000

Data are presented as mean ± SD in ng/mL. Between-group differences were evaluated using two-sample t-tests for independent samples. CGA: corrected gestational age.

Table 4. Comparison of Gesell Developmental Scales scores among the three groups of infants at 9 months CGA.

Groups	*n*	gross motor ability	fine motor ability	linguistic competence	adaptive capacity	personal-social ability
Adequate group	51	96.31±8.61	97.45±9.36	96.49±7.79	97.22±10.24	96.22±9.88
Insufficient group	54	88.63±6.22[a]	88.78±8.51[a]	90.46±7.35[a]	91.56±8.21[a]	90.11±10.19[a]
Deficient group	70	87.57±5.65[a]	87.34±9.62[a]	89.70±9.23[a]	90.50±9.57[a]	88.64±9.60[a]
F		16.216	19.494	11.165	8.224	9.258
p		0.000	0.000	0.000	0.000	0.000

Data are presented as mean ± SD. Between-group comparisons at each time point were performed using one-way ANOVA, followed by Bonferroni post hoc tests. [a]$p<0.05$ vs. Adequate group. CGA: corrected gestational age.

Table 5. Comparison of Gesell Developmental Scales scores among the three groups of infants at 18 months of CGA.

Groups	*n*	gross motor ability	fine motor ability	linguistic competence	adaptive capacity	personal-social ability
Adequate group	51	96.45±9.16	97.78±10.22	97.65±7.84	97.98±10.21	97.35±10.21
Insufficient group	54	92.61±7.98[a]	91.35±8.77[a]	92.33±8.64[a]	93.44±8.16[a]	92.65±8.54[a]
Deficient group	70	90.06±7.92[a]	89.67±8.64[a]	90.71±7.97[a]	92.84±7.33[a]	91.90±7.33[a]
F		8.721	12.223	11.164	6.012	6.503
p		0.000	0.000	0.000	0.003	0.002

Data are presented as mean ± SD. Between-group comparisons at each time point were performed using one-way ANOVA, followed by Bonferroni post hoc tests. [a]$p<0.05$ vs. Adequate group. CGA: corrected gestational age.

Comparison of Gesell Developmental Scales scores between the standard dosage group and the individualized supplementation group within the deficient group at 9 months CGA and 18 months CGA

Within the deficient group, at both 9-month and 18-month CGA, infants in the individualized supplementation group scored higher on gross motor ability, fine motor ability, linguistic competence, adaptive capacity, and personal-social ability than those in the standard dosage group ($p<0.05$). See Tables 6 and 7.

Table 6. Comparison of Gesell Developmental Scales scores between the standard dosage group and the individualized supplementation group within the deficient group at 9 months CGA.

Groups	*n*	gross motor ability	fine motor ability	linguistic competence	adaptive capacity	personal-social ability
Standard dosage group	35	85.20±9.57	84.37±9.66	86.97±8.01	87.31±9.77	85.29±9.51
Individualized supplementation group	35	91.29±8.53	90.31±8.74	92.43±9.66	93.69±8.35	92.00±8.57
F		2.809	2.698	2.573	2.933	3.103
p		0.007	0.009	0.012	0.005	0.003

Note: Data are presented as mean ± SD. Between-group differences were evaluated using two-sample t-tests for independent samples. CGA: corrected gestational age.

Table 7. Comparison of Gesell Developmental Scales scores between the standard dosage group and the individualized supplementation group within the deficient group at 18 months CGA.

Groups	*n*	gross motor ability	fine motor ability	linguistic competence	adaptive capacity	personal-social ability
Standard dosage group	35	86.43±7.18	86.49±8.03	86.77±7.53	88.91±6.29	87.57±5.65
Individualized supplementation group	35	93.69±6.98	92.86±8.14	94.66±6.34	96.77±6.15	96.23±6.21
F		4.288	3.297	4.738	5.284	6.100
p		0.000	0.002	0.000	0.000	0.000

Data are presented as mean ± SD. Between-group differences were evaluated using two-sample t-tests for independent samples. CGA: corrected gestational age.

DISCUSSION

Vitamin D plays numerous physiological roles in the human body, including maintaining bone health, modulating the immune system, influencing cell differentiation, and contributing to neurodevelopment, among other functions [35]. Vitamin D can affect the development of the normal fetal brain by regulating the expression of neurotrophic factors, modulating cytokines activity, synthesizing neurotransmitters, modulating intracellular calcium signaling, and controlling the activity of genes and proteins responsible for neuronal differentiation and metabolic processes [36]. During the final stage of pregnancy, the fetus's need for vitamin D increases significantly to support rapid bone growth and calcification [37]. The mother transfers vitamin D to the fetus through the placenta, helping the fetus establish sufficient vitamin D stores to meet early postnatal growth demands [38]. Premature infants, due to their shorter gestational age at birth, have relatively inadequate vitamin D stores, and their rapid growth and development further increase their need for vitamin D [39]. Additionally, premature infants have thinner skin and less subcutaneous fat, which decreases their ability to synthesize vitamin D, making them more vulnerable to deficiency [40]. In our study, we examined 25(OH)D3 levels in the umbilical cord blood of preterm infants, revealing a high rate of vitamin D deficiency in this population.

The results of this research indicate that preterm infants with insufficient vitamin D had significantly lower 25(OH)D3 concentrations at 24 hours, 3 months, and 9 months CGA than those with normal vita-

min D levels. This suggests that variations in umbilical cord blood vitamin D levels at birth significantly influence 25(OH)D3 levels in premature infants during the early postnatal period. Despite postnatal vitamin D3 supplementation, premature infants in the deficient group did not achieve 25(OH) D3 levels comparable to those in the adequate group within a relatively short timeframe. This may relate to the physiological characteristics of premature infants, whose livers and kidneys are not fully developed, limiting their ability to metabolize and convert vitamin D, resulting in a slower increase in 25(OH)D3 levels after supplementation in the deficient group [41]. It may also be affected by the dosage of supplementation and individual differences. Although a standard vitamin D3 supplement was given, absorption and utilization efficiency vary among individuals, making it difficult for premature infants in the deficient group to quickly correct their deficiency [42]. By 18 months CGA, there were no statistically significant differences in 25(OH)D3 levels among the three infant groups. This indicates that, after a period of supplementation, premature infants in the deficient group had sufficient time to increase their levels, gradually closing the gap with the adequate group and eventually reaching comparable levels at 18 months CGA. This improvement may be due to the gradual maturation of liver and kidney function as infants grow, enhancing their ability to metabolize vitamin D, thereby allowing better utilization of supplemental vitamin D3 and a subsequent rise in 25(OH)D3 levels [43]. It may also be related to the cumulative effect of the dose and duration of supplementation. After a longer period, premature infants in the deficient group gradually compensated for their intrauterine vitamin D deficiency, resulting in 25(OH)D3 levels comparable to those in the other groups. At 3, 9, and 18 months of CGA, the group receiving individualized supplementation exhibited significantly higher 25(OH)D3 levels than the standard-dosage group. In the early postnatal period, infants with vitamin D deficiency should undergo closer monitoring of 25(OH)D3 levels and dosage and route of supplementation adjusted to individual circumstances to promote a rapid increase in 25 (OH) D3 levels. By approximately 18 months CGA, monitoring frequency can be adjusted, as vitamin D levels among the groups have converged. Additionally, these findings support the development of more scientifically grounded and rational vitamin D supplementation protocols for premature infants, such as stratifying infants by umbilical cord blood vitamin D levels and applying targeted strategies at different stages to ensure adequate vitamin D for healthy growth.

This study investigates how vitamin D deficiency affects the neuropsychological and behavioral development of preterm infants. At 9 and 18 months CGA, preterm infants with insufficient or deficient vitamin D levels scored significantly lower on the Gesell Developmental Scales in areas such as gross motor, fine motor, language, adaptive behavior, and personal-social skills compared to those with adequate vitamin D levels. These findings indicate that vitamin D deficiency may adversely affect the neuropsychological and behavioral development of preterm infants. Vitamin D plays several roles in the nervous system, including supporting neuronal development and differentiation and regulating the production and release of neurotransmitters [44, 45]. A deficiency of vitamin D may slow nervous system development, impairing cognitive functions, motor coordination, and social skills in premature infants [46, 47]. Moreover, within the deficiency group, at both 9 and 18 months CGA, infants receiving individualized vitamin D supplementation scored higher across all five skill areas than those given a standard dose. This suggests that an individualized vitamin D supplementation approach not only more effectively corrects deficiency but also enhances the neuropsychological and behavioral development of preterm infants. Such tailored supplementa-

tion more effectively addresses the specific needs of premature infants for vitamin D, thereby maintaining healthy serum levels and supporting nervous system development. Adequate vitamin D levels are crucial for the proper development and function of nerve cells, the formation and connectivity of neural synapses, and overall neuropsychological and behavioral health in preemies. Additionally, personalized supplementation may also modulate immune function, lower infection rates, and indirectly support nervous system development [48]. These findings underscore the importance of customized vitamin D supplementation strategies in the care of preterm infants.

The results of this study carry important implications for clinical practice. Firstly, it reminds healthcare professionals to routinely test umbilical cord blood 25(OH)D3 levels in premature infants at birth to promptly identify those with vitamin D deficiency. Secondly, a personalized approach to vitamin D supplementation offers an efficient way to address vitamin D deficiency in premature infants and cater to their unique requirements. In clinical settings, healthcare providers can develop customized vitamin D supplementation plans for premature infants based on individual circumstances to enhance overall health and well-being.

Limitations of the Study

Although this study provides valuable insights, it is important to acknowledge its limitations. First, the relatively small sample size may introduce bias into the results. Second, the observation period of the study is relatively short, extending only to 18 months CGA, and the long-term effects on the neuropsychological and behavioral development of premature infants remain unclear. Future research should increase the sample size and conduct multicenter, large-sample studies to enhance the reliability and generalizability of the findings. Additionally, extending the observation period to follow premature infants into school age or even adulthood would allow for a more comprehensive assessment of the long-term impact of vitamin D deficiency and supplementation on their neuropsychological and behavioral development. Further research could also explore the specific molecular mechanisms by which vitamin D influences neuropsychological and behavioral development in premature infants, providing a theoretical foundation for developing more targeted treatment strategies. Moreover, combining other nutrients and treatment approaches could help evaluate their overall effect on the growth and development of premature babies, offering more comprehensive support for their healthy development.

This study systematically examined how vitamin D metabolic imbalance affects 25(OH)D3 levels and neuropsychological and behavioral development in premature infants, while proposing an individualized supplementation strategy. The results show significant differences in umbilical cord blood 25(OH)D3 levels among premature babies, and that a tailored vitamin D supplement plan is more effective at correcting deficiency. This personalized approach not only resolves vitamin D deficiency in premature infants but also positively influences their neuropsychological and behavioral growth.

Acknowledgment

None.

Funding

Special Fund for Inspection and Testing Science and Technology of China International Scientific Exchange Foundation (Z2021LSD009).

Consent to publish

The manuscript has neither been previously published nor is under consideration by any other journal. The authors have all approved the content of the paper.

Consent to Participate

We obtained a signed informed consent form from each participant's representative.

Ethic Approval

This study was approved by the Ethics Committee of the Binzhou People's Hospital.

Data Availability Statement

The data that support the findings of this study are available from the corresponding author upon reasonable request.

ORCID number of authors

- Xiaohui Guo (XG): 0009-0001-7638-8078
- Yanfeng Sun (YS): 0009-0006-2636-6846
- Yanhong Chen (YC): 0009-0005-0502-5287
- Feifei Xu (FX): 0009-0007-5341-7992
- Yanfei Li (YL): 0009-0001-1945-3347

Author contribution

XG: Edited and refined the manuscript with a focus on critical intellectual contributions. YC, FX, YL: Participated in collecting, assessing, and interpreting the data. Made significant contributions to date interpretation and manuscript preparation. XG, YS: Provided substantial intellectual input during the drafting and revision of the manuscript.

Conflicts of interest

The authors declare that they have no financial conflicts of interest.

REFERENCES

1. **Visscher MO, Carr AN, Narendran V.** Premature infant skin barrier maturation: status at full-term corrected age. J Perinatol. 2021;41(2):232-239. *https://doi.org/10.1038/s41372-020-0704-3.*
2. **Kaempf JW, Gautham K.** Do small baby units improve extremely premature infant outcomes? J Perinatol. 2022;42(2):281-285. *https://doi.org/10.1038/s41372-021-01076-9.*
3. **De Beritto TV, Chu A.** The Evolving Need for Neonatal Care: From the Premature Infant to the Rare Disease. Pediatr Ann. 2023;52(8):e282. https://doi.org/10.3928/19382359-20230613-03.
4. **Flake AW.** A supportive physiologic environment for the extreme premature infant: Improving life outside the womb. J Pediatr Surg. 2022;57(2):167-171. *https://doi.org/10.1016/j.jpedsurg.2021.10.025.*
5. **Mansur JL, Oliveri B, Giacoia E, Fusaro D, Costanzo PR.** Vitamin D: Before, during and after Pregnancy: Effect on Neonates and Children. Nutrients. 2022;14(9):1900. *https://doi.org/10.3390/nu14091900.*
6. **Zhang H, Wang S, Tuo L, Zhai Q, Cui J, Chen D, Xu D.** Relationship between Maternal Vitamin D Levels and Adverse Outcomes. Nutrients. 2022;14(20):4230. https://doi.org/10.3390/nu14204230.
7. **Abrams SA.** Vitamin D and bone minerals in neonates. Early Hum Dev. 2021;162:105461. *https://doi.org/doi: 10.1016/j.earlhumdev.2021.105461.*
8. **Chinnappan A, Sharma A, Agarwal R, Thukral A, Deorari A, Sankar MJ.** Fortification of Breast Milk with Preterm Formula Powder vs Human Milk Fortifier in Preterm Neonates: A Randomized Noninferiority Trial. JAMA Pediatr. 2021;175(8):790-796. *https://doi.org/10.1001/jamapediatrics.2021.0678.*
9. **Chacham S, Pasi R, Chegondi M, Ahmad N, Mohanty SB**. Metabolic Bone Disease in Premature Neonates: An Unmet Challenge. J Clin Res Pediatr Endocrinol. 2020;12(4):332-339. *https://doi.org/10.4274/jcrpe.galenos.2019.2019.0091.*

10. **Stoica AB, Mărginean C.** The Impact of Vitamin D Deficiency on Infants' Health. Nutrients. 2023;15(20):4379. *https://doi.org/10.3390/nu15204379.*
11. **Jafari N, Taslimi Taleghani N, Kazemi SA, Abouoasef S, Motamed N, Jalilvand A.** Association between Vitamin D Insufficiency and Respiratory Problems in Premature Neonates. Arch Iran Med. 2022;25(1):32-36. *https://doi.org/10.34172/aim.2022.06.*
12. **Taiorazova G, Alimbaeva A, Tanatarov S.** The role of vitamin D and trace elements in premature newborns with congenital pneumonia. Bratisl Lek Listy. 2023;124(8):572-577. *https://doi.org/10.4149/BLL_2023_089.*
13. **Vivanti AJ, Monier I, Salakos E, Elie C, Tsatsaris V, Senat MV, et al.** Vitamin D and pregnancy outcomes: Overall results of the FEPED study. J Gynecol Obstet Hum Reprod. 2020;49(8):101883. *https://doi.org/10.1016/j.jogoh.2020.101883.*
14. **Cheng H, Chi P, Zhuang Y, Alifu X, Zhou H, Qiu Y, et al.** Association of 25-Hydroxyvitamin D with Preterm Birth and Premature Rupture of Membranes: A Mendelian Randomization Study. Nutrients. 2023;15(16):3593. *https://doi.org/10.3390/nu15163593.*
15. **Barbosa O, Sim-Sim M, Silvestre MP, Pedro C, Cruz D.** Effects of vitamin D levels during pregnancy on prematurity: a systematic review protocol. BMJ Open. 2024;14(2):e076702. *https://doi.org/10.1136/bmjopen-2023-076702.*
16. **van den Heuvel EG, Lips P, Schoonmade LJ, Lanham-New SA, van Schoor NM.** Comparison of the Effect of Daily Vitamin D2 and Vitamin D3 Supplementation on Serum 25-Hydroxyvitamin D Concentration (Total 25(OH)D, 25(OH)D2, and 25(OH) D3) and Importance of Body Mass Index: A Systematic Review and Meta-Analysis. Adv Nutr. 2024;15(1):100133. *https://doi.org/10.1016/j.advnut.2023.09.016.*
17. **Płudowski P, Kos-Kudła B, Walczak M, Fal A, Zozulińska-Ziółkiewicz D, Sieroszewski P, et al.** Guidelines for Preventing and Treating Vitamin D Deficiency: A 2023 Update in Poland. Nutrients. 2023;15(3):695. *https://doi.org/10.3390/nu15030695.*
18. **Liu CC, Huang JP.** Potential benefits of vitamin D supplementation on pregnancy. J Formos Med Assoc. 2023;122(7):557-563. *https://doi.org/10.1016/j.jfma.2023.02.004.*
19. **Kumar M, Shaikh S, Sinha B, Upadhyay RP, Choudhary TS, Chandola TR, et al.** Enteral Vitamin D Supplementation in Preterm or Low Birth Weight Infants: A Systematic Review and Meta-analysis. Pediatrics. 2022;150(Suppl 1):e2022057092K. *https://doi.org/10.1542/peds.2022-057092K.*
20. **Fisher M, Marro L, Arbuckle TE, Potter BK, Little J, Weiler H, et al.** Association between toxic metals, vitamin D and preterm birth in the Maternal-Infant research on environmental chemicals study. Paediatr Perinat Epidemiol. 2023;37(5):447-457. *https://doi.org/10.1111/ppe.12962.*
21. **Guo H, Xie J, Yu X, Tian Y, Guan M, Wei J.** Effects of vitamin D supplementation on serum 25(OH)D(3) levels and neurobehavioral development in premature infants after birth. Sci Rep. 2024;14(1):23972. *https://doi.org/10.1038/s41598-024-75191-w.*
22. **Chen GD, Pang TT, Li PS, Zhou ZX, Lin DX, Fan DZ, et al.** Early pregnancy vitamin D and the risk of adverse maternal and infant outcomes: a retrospective cohort study. BMC Pregnancy Childbirth. 2020;20(1):465. *https://doi.org/10.1186/s12884-020-03158-6.*
23. **Motlagh AJ, Davoodvandi A, Saeieh SE.** Association between vitamin D level in mother's serum and the level of vitamin D in the serum of pre-term infants. BMC Pediatr. 2023;23(1):97. *https://doi.org/10.1186/s12887-023-03854-0.*
24. **Bollen SE, Bass JJ, Fujita S, Wilkinson D, Hewison M, Atherton PJ.** The Vitamin D/Vitamin D receptor (VDR) axis in muscle atrophy and sarcopenia. Cell Signal. 2022;96:110355. *https://doi.org/10.1016/j.cellsig.2022.110355.*
25. **Aggeletopoulou I, Thomopoulos K, Mouzaki A, Triantos C.** Vitamin D-VDR Novel

Anti-Inflammatory Molecules-New Insights into Their Effects on Liver Diseases. Int J Mol Sci. 2022;23(15):8465. *https://doi.org/10.3390/ijms23158465.*

26. **Voutsadakis IA.** Vitamin D receptor (VDR) and metabolizing enzymes CYP27B1 and CYP24A1 in breast cancer. Mol Biol Rep. 2020;47(12):9821-9830. *https://doi.org/10.1007/s11033-020-05780-1.*
27. **Usategui-Martín R, De Luis-Román DA, Fernández-Gómez JM, Ruiz-Mambrilla M, Pérez-Castrillón JL.** Vitamin D Receptor (VDR) Gene Polymorphisms Modify the Response to Vitamin D Supplementation: A Systematic Review and Meta-Analysis. Nutrients. 2022;14(2):360. *https://doi.org/10.3390/nu14020360.*
28. **Bacchetta J, Edouard T, Laverny G, Bernardor J, Bertholet-Thomas A, Castanet M, et al.** Vitamin D and calcium intakes in general pediatric populations: A French expert consensus paper. Arch Pediatr. 2022;29(4):312-325. *https://doi.org/10.1016/j.arcped.2022.02.008*.
29. **Artman A, Huang A, Bowker R, Cerwinske L, Cooper S, Johnson T, et al.** Evaluation of vitamin D protocol in the neonatal intensive care unit at Rush University Medical Center. JPEN J Parenter Enteral Nutr. 2022;46(3):618-625. *https://doi.org/10.1002/jpen.2138.*
30. **Golan-Tripto I, Bistritzer J, Loewenthal N, Staretz-Chacham O, Dizitzer Y, Goldbart A.** The effect of vitamin D administration on vitamin D status and respiratory morbidity in late premature infants. Pediatr Pulmonol. 2020;55(11):3080-3087. *https://doi.org/10.1002/ppul.25006.*
31. **Irwinda R, Hiksas R, Lokeswara AW, Wibowo N.** Vitamin D supplementation higher than 2000 IU/day compared to lower dose on maternal-fetal outcome: Systematic review and meta-analysis. Womens Health (Lond). 2022;18:17455057221111066. *https://doi.org/10.1177/17455057221111066.*
32. **Rizzoli R.** Vitamin D supplementation: upper limit for safety revisited? Aging Clin Exp Res 2021;33(1):19-24. *https://doi.org/10.1007/s40520-020-01678-x.*
33. **Kołodziejczyk-Nowotarska A, Bokiniec R, Seliga-Siwecka J.** Monitored Supplementation of Vitamin D in Preterm Infants: A Randomized Controlled Trial. Nutrients. 2021;13(10):3442. *https://doi.org/10.3390/nu13103442.*
34. **Matejek T, Zapletalova B, Stepan M, Malakova J, Palicka V.** Dynamics of the vitamin D C3-epimer levels in preterm infants. Clin Chem Lab Med. 2023;61(6):1084-94. *https://doi.org/10.1515/cclm-2022-1128.*
35. **Romero-Lopez M, Tyson JE, Naik M, Pedroza C, Holzapfel LF, Avritscher E, et al.** Randomized controlled trial of enteral vitamin D supplementation (ViDES) in infants <28 weeks gestational age or <1000 g birth weight: study protocol. Trials. 2024;25(1):423. *https://doi.org/10.1186/s13063-024-08274-8.*
36. **Jung JH, Kim EA, Lee SY, Moon JE, Lee EJ, Park SH.** Vitamin D Status and Factors Associated with Vitamin D Deficiency during the First Year of Life in Preterm Infants. Nutrients. 2021;13(6):2019. *https://doi.org/10.3390/nu13062019.*
37. **Aristizabal N, Holder MP, Durham L, Ashraf AP, Taylor S, Salas AA.** Safety and Efficacy of Early Vitamin D Supplementation in Critically Ill Extremely Preterm Infants: An Ancillary Study of a Randomized Trial. J Acad Nutr Diet. 2023;123(1):87-94. *https://doi.org/10.1016/j.jand.2022.06.012.*
38. **Lo ACQ, Lo CCW.** The effect of vitamin D supplementation on glycemic control/glucose metabolism and maternal-neonatal outcomes in women with established gestational diabetes mellitus: An updated meta-analysis. Clin Nutr. 2022;41(10):2420-2423. *https://doi.org/10.1016/j.clnu.2022.08.014.*
39. **Cho MC, Cho IA, Seo HK, Kang MJ, Jo JY, Shin JK, et al.** Serum vitamin D-binding protein (VDBP) concentration and rs7041 genotype may be associated with preterm labor. J Matern Fetal Neonatal Med 2022;35(25):9422-9429. *https://doi.org/10.1080/14767058.2022.2040475.*

40. **Tang WQ, Ma N, Meng LY, Luo YW, Wang YJ, Zhang D.** Vitamin D supplementation improved physical growth and neurologic development of Preterm Infants receiving Nesting Care in the neonatal Intensive Care Unit. BMC Pediatr 2023;23(1):248. *https://doi.org/10.1186/s12887-023-04075-1.*
41. **Jamali Z, Ghorbani F, Shafie'ei M, Tolooefar F, Maleki E.** Risk factors associated with vitamin D deficiency in preterm neonates: a single-center step-wise regression analysis. BMC Pediatr 2023;23(1):324. *https://doi.org/10.1186/s12887-023-04088-w.*
42. **Lian RH, Qi PA, Yuan T, Yan PJ, Qiu WW, Wei Y, et al.** Systematic review and meta-analysis of vitamin D deficiency in different pregnancy on preterm birth: Deficiency in middle pregnancy might be at risk. Medicine (Baltimore). 2021;100(24):e26303. *https://doi.org/10.1097/MD.0000000000026303.*
43. **Sarıdemir H, Surmeli Onay O, Aydemir O, Tekin AN.** Questioning the adequacy of standardized vitamin D supplementation protocol in very low birth weight infants: a prospective cohort study. J Pediatr Endocrinol Metab 2021;34(12):1515-1523. *https://doi.org/10.1515/jpem-2021-0390.*
44. **Treiber M, Mujezinović F, Pečovnik Balon B, Gorenjak M, Maver U, Dovnik A.** Association between umbilical cord vitamin D levels and adverse neonatal outcomes. J Int Med Res 2020;48(10):300060520955001. *https://doi.org/10.1177/0300060520955001.*
45. **Ashrafizadeh M.** Cell Death Mechanisms in Human Cancers: Molecular Pathways, Therapy Resistance and Therapeutic Perspective. J Can Biomol Therap 2024;1(1):17-40. *https://doi.org/10.62382/jcbt.v1i1.13.*
46. **Jiang X, Lu J, Zhang Y, Teng H, Pei J, Zhang C, et al.** Association between maternal vitamin D status with pregnancy outcomes and offspring growth in a population of Wuxi, China. Asia Pac J Clin Nutr 2021;30(3):464-476. *https://doi.org/10.6133/apjcn.202109_30(3).0013.*
47. **Ren J.** Advances in combination therapy for gastric cancer: integrating targeted agents and immunotherapy. Adv Clin Pharmacol Ther 2024;1(1):1-15. *https://doi.org/10.63623/9k14tf70.*
48. **Amiri M, Rostami M, Sheidaei A, Fallahzadeh A, Ramezani Tehrani F.** Mode of delivery and maternal vitamin D deficiency: an optimized intelligent Bayesian network algorithm analysis of a stratified randomized controlled field trial. Sci Rep 2023;13(1):8682. *https://doi.org/10.1038/s41598-023-35838-6.*

Invest Clin 67(1): 19 - 29, 2026 https://doi.org/10.54817/IC.v67n1a02

The impact of complement C1q/tumor necrosis factor-related protein 6-mediated cardiomyocyte pyroptosis on myocardial fibrosis in rats with myocardial infarction.

Qiu Zhang, Xin Chen, Hao Pan and Zengguang Chen

Department of Cardiology, The Second People's Hospital of Changzhou, The Third Affiliated Hospital of Nanjing Medical University, Changzhou, JiangSu, China.

Keywords: Myocardial Infarction; Pyroptosis; Fibrosis; Inflammatory Response.

Abstract. Complement C1q/tumor necrosis factor-related protein 6 (CTRP6) has anti-inflammatory and metabolic regulatory properties, but its role in ameliorating post-myocardial infarction (MI) myocardial fibrosis via pyroptosis inhibition is unclear. This study investigated whether CTRP6 improves post-MI myocardial fibrosis and cardiac dysfunction by suppressing cardiomyocyte pyroptosis through the NLRP3/caspase-1/GSDMD pathway. Thirty Sprague-Dawley rats were randomized to sham-operated (Sham), MI model (MI), or CTRP6-treated (MI+CTRP6) groups. MI was induced by left anterior descending coronary artery ligation; MI+CTRP6 rats received daily subcutaneous recombinant CTRP6 (0.2 mg/kg) from day 3 post-surgery for 28 days. Cardiac function, fibrosis markers, pyroptosis-related proteins, and inflammatory cytokines were assessed via Western blot, Masson staining, and ELISA. CTRP6 expression was lower in MI vs. Sham ($p<0.05$). CTRP6 treatment restored its expression, reduced fibrosis markers and collagen deposition, and improved cardiac function ($p<0.05$). It also downregulated pro-inflammatory cytokines and increased anti-inflammatory cytokines ($p<0.05$). In other words, exogenous CTRP6 ameliorated fibrosis and cardiac function by directly inhibiting the NLRP3/caspase-1/GSDMD pyroptosis pathway.

Corresponding author. Zengguang Chen. Department of Cardiology, The Second People's Hospital of Changzhou, The Third Affiliated Hospital of Nanjing Medical University,No.68, Ge Hu Middle Road, Wujin District, China, Changzhou, Jiangsu, 213000, China. Email:zengguangchen@126.com.

Impacto de la piroptosis de cardiomiocitos mediada por CTRP6 en la fibrosis miocárdica en ratas con infarto de miocardio.

Invest Clin 2026; 67 (1): 19 – 29

Palabras clave: Infarto de Miocardio; Piroptosis; fibrosis; Respuesta Inflamatoria.

Resumen. La proteína 6 relacionada con el factor de necrosis del complemento C1q/tumor (CTRP6) tiene propiedades antiinflamatorias y reguladoras metabólicas, pero su papel en la reducción de la fibrosis del miocardio postinfarto (MI) mediante la inhibición de la piroptosis no está claro. Este estudio investigó si el CTRP6 mejora la fibrosis miocárdica post-MI y la disfunción cardíaca al suprimir la piroptosis de cardiomiocitos mediante la vía NLRP3/caspasa-1/GSDMD. Treinta ratas Sprague-Dawley se asignaron aleatoriamente a grupos operados con simulación (Sham), modelo MI (MI) o tratados con CTRP6 (MI + CTRP6). El MI fue inducido por ligadura de la arteria coronaria descendente anterior izquierda. Las ratas MI+CTRP6 recibieron CTRP6 recombinante por vía subcutánea diaria (0,2 mg/kg) a partir del día 3 tras la cirugía durante 28 días. La función cardíaca (ecocardiografía), los marcadores de fibrosis, las proteínas relacionadas con la piroptosis y las citocinas inflamatorias se evaluaron mediante transferencia Western, tinción de Masson y ELISA. La expresión de CTRP6 fue menor en MI que en Sham ($p<0,05$). El tratamiento con CTRP6 restableció su expresión, redujo los marcadores de fibrosis y de deposición de colágeno, y mejoró la función cardíaca ($p<0,05$). También disminuyó la regulación de las citocinas proinflamatorias y aumentó la regulación antiinflamatoria ($p<0,05$). El CTRP6 protege contra la fibrosis miocárdica post-MI inhibiendo la piroptosis de cardiomiocitos a través de la vía NLRP3/caspasa-1/GSDMD, reduciendo las citocinas proinflamatorias y la activación de fibroblastos.

Received: 12-08-2025 Accepted: 20-10-2025

INTRODUCTION

Myocardial infarction (MI) represents one of the most life-threatening cardiovascular disorders globally, with its pathological hallmark being the ischemic necrosis of cardiomyocytes followed by progressive fibrosis, which ultimately culminates in heart failure and life-threatening arrhythmias [1]. Epidemiological data reveal a striking age-dependent incidence pattern, with MI affecting approximately 3.8% of the population below 60 years compared to 9.5% in individuals over 60 years [2]. While contemporary therapeutic strategies, including revascularization procedures and pharmacological interventions, have markedly enhanced acute-phase survival rates, the inexorable advancement of myocardial fibrosis continues to pose significant challenges to long-term patient outcomes and quality of life [3]. The scientific community has recently focused on elucidating the contributions of programmed cell death pathways to myocardial injury pathophysiology [4]. Among these, pyroptosis—a lytic form of cell death mediated by inflammasome activation—exacerbates local inflammatory responses and drives fibroblast activation

through the release of pro-inflammatory cytokines such as IL-1β and IL-18, potentially serving as a key trigger for myocardial fibrosis [5]. Despite these insights, the regulatory network of pyroptosis in MI and its molecular link with fibrosis remain incompletely elucidated.

Within the complement C1q/tumor necrosis factor-related protein (CTRP) family, CTRP6 has gained prominence as a multifunctional regulator, demonstrating simultaneous involvement in both glucolipid metabolism and inflammatory modulation, thereby positioning it as a molecule of particular interest in metabolic syndrome research [6]. Emerging evidence indicates that CTRP6 exerts protective effects against vascular endothelial inflammation by inhibiting the NF-κB signaling cascade and exhibits anti-fibrotic properties in the context of diabetic cardiomyopathy [7]. Notably, in myocardial ischemia-reperfusion (I/R) injury models, CTRP6 expression levels correlate positively with cardiomyocyte survival rates [8]. However, direct evidence on whether CTRP6 influences myocardial fibrosis by modulating pyroptosis remains lacking. The study by Liang et al.[9] established that serum CTRP6 levels were substantially diminished in I/R-injured rats and inversely associated with both pyroptosis markers (GSDMD-N and caspase-1) and the extent of collagen deposition, suggesting a potential role for CTRP6 in restraining fibrosis via pyroptosis inhibition. Nevertheless, the specific involvement of CTRP6 in MI pathophysiology has not yet been systematically investigated.

In this study, we present a novel conceptual framework that proposes a "CTRP6-pyroptosis-fibrosis" regulatory axis in MI. The primary objective is to delineate the molecular mechanisms by which CTRP6 attenuates cardiomyocyte pyroptosis by modulating the NLRP3/caspase-1/GSDMD signaling pathway, thereby mitigating fibroblast activation and pathological collagen accumulation. The findings are expected to yield two significant contributions: first, the identification of new therapeutic targets for combating post-MI fibrotic complications; and second, the establishment of a robust theoretical platform that supports the translational potential of CTRP6, moving it from its traditional recognition as a metabolic modulator to its emerging role as a cardiovascular protective agent.

MATERIALS AND METHODS

Animal subjects

A total of thirty male Sprague-Dawley (SD) rats, aged 4–6 weeks and weighing 200 ± 20 g, were obtained from Beijing Vitalstar Biotechnology Co., Ltd. (License No.: SCXK2023-0014). The animals were housed under standardized conditions, with free access to water, in a controlled environment (temperature: 20–25°C; relative humidity: 60–70%) under a 12-hour light/dark cycle. Following a one-week acclimatization period, the experiments were conducted in compliance with the 3Rs (Replacement, Reduction, Refinement) principles and were approved by the Institutional Animal Ethics Committee (No. 20210301002).

MI model establishment

The rats were randomly allocated into three groups (n=10 per group). In two of the groups, MI was surgically induced. Briefly, the rats were anesthetized, secured in a supine position, and intubated, after which mechanical ventilation was initiated. After thoracotomy, the heart was gently extruded, and the left anterior descending coronary artery was rapidly ligated approximately 2–3 mm distal to the aortic root, near the junction between the left auricle and the pulmonary artery cone, for MI modeling [10]. The MI model was considered successful if the left ventricular ejection fraction (LVEF) measured by Doppler echocardiography was <50%. The third group underwent an identical surgical procedure without left anterior descending ligation and served as the sham group. Among the two MI groups, one

received daily subcutaneous injections of recombinant human CTRP6 (0.2 mg/kg) starting three days post-MI induction and continuing for 28 consecutive days (CTRP6 group). The other MI group received an equivalent volume of saline and was designated the model group.

Evaluation of cardiac function

Upon completion of the treatment regimen, transthoracic echocardiography was performed on all animals using a high-resolution color Doppler ultrasound system equipped with a 15 MHz linear transducer. Key cardiac functional parameters, including LVEF, left ventricular fractional shortening (LVFS), left ventricular end-diastolic diameter (LVEDD), and left ventricular end-systolic diameter (LVESD), were recorded for comparative analysis.

Western blot analysis of myocardial protein expression

Following euthanasia, myocardial tissue samples were immediately collected, and total protein was extracted by homogenizing the tissues in a RIPA lysis buffer at a 1:5 ratio, followed by incubation at 4°C for 40 minutes. Protein concentrations were measured using the bicinchoninic acid (BCA) protein assay kit. Then, equal amounts of protein (30 μg per sample) were separated with 10% SDS-PAGE and transferred to polyvinylidene difluoride (PVDF) membranes using a wet transfer system. After blocking for two hours at room temperature, the membranes were incubated overnight at 4°C with primary antibodies (all diluted 1:1000 in blocking buffer): anti-CTRP6 (ab300583, Abcam), anti-Collagen III (ab7535, Abcam), anti-α-smooth muscle actin (α-SMA) (ab314895, Abcam), anti-transforming growth factor-β1 (TGF-β1) (ab315254, Abcam), anti-NOD-like receptor family pyrin domain containing 3 (NLRP3) (ab263899, Abcam), anti-cl-Caspase-1 (ab198447, Abcam), anti-gasdermin D (GSDMD) (ab219800, Abcam), anti-N terminal (NT)-GSDMD (ab215203, Abcam), anti-interleukin (IL)-1β (ab315084, Abcam), and GAPDH (ab8245, Abcam). Subsequently, the membranes were incubated with appropriate horseradish peroxidase (HRP)-conjugated secondary antibodies (goat anti-rabbit or goat anti-mouse IgG, 1:5000 dilution, ab308009, Abcam) for two hours at room temperature. Using enhanced chemiluminescence (ECL) detection reagents, protein bands were visualized and photographed. Finally, relative protein expression levels were quantified.

Histopathological examination of myocardial tissues

Cardiac tissues were fixed in 10% paraformaldehyde for 24 hours, then processed through a graded ethanol series for dehydration. After xylene clearing, tissues were embedded in paraffin and sectioned at 3-5 μm thickness. Subsequently, sections were stained with hematoxylin and eosin (H&E) and examined under a light microscope at 200× magnification to evaluate myocardial morphology (focusing on muscle fiber arrangement and ventricular wall thickness). For myocardial fibrosis assessment, tissue fixation and section preparation followed the same procedures as for H&E staining. The sections were then stained using a Masson's trichrome kit according to the manufacturer's instructions. Fibrotic changes in myocardial tissue were evaluated under light microscopy at 200× magnification, with collagen fibers appearing blue in the stained sections.

Measurement of serum inflammatory cytokines

Blood samples (3 mL) were obtained from the abdominal aorta into sterile tubes, and serum was separated by centrifugation. Serum levels of IL-1β (CSB-E08055r-IS), tumor necrosis factor-alpha (TNF-α) (CSB-E11987r), IL-6 (CSB-E04640r), IL-8 (CSB-E07451r), and IL-10 (CSB-E04595r) were measured using commercially available enzyme-linked immunosorbent assay (ELISA)

kits (Wuhan Huamei Biological Engineering Co., LTD.) according to the manufacturer's instructions.

Endpoints

The endpoints of this study included (1) a quantitative assessment of CTRP6 protein expression levels in myocardial tissues after MI, and (2) a comprehensive evaluation of CTRP6's therapeutic effects on myocardial fibrosis, histopathological damage, cardiac function, and pyroptosis.

Statistical analysis

All statistical analyses were performed using SPSS version 25.0 (IBM Corp., USA). Continuous variables with normal distribution were presented as mean ± standard deviation ($\bar{x} \pm sd$). An independent-samples t-test was used to compare the two groups. For multiple-group comparisons, one-way repeated-measures analysis of variance (ANOVA) was employed, followed by Fisher's least significant difference (LSD) post hoc test for pairwise comparisons. A two-tailed p of less than 0.05 was considered statistically significant for all analyses.

RESULTS

MI model establishment and CTRP6 expression

All rats in the sham group survived. In both the CTRP6 and model groups, one rat died in each group, while the surviving rats successfully met the MI model criteria (LVEF <50%). Western blot analysis showed that CTRP6 protein expression in myocardial tissue was significantly lower in the model group than in the sham group ($p<0.001$), indicating downregulation of CTRP6 in MI (Fig. 1).

CTRP6 attenuates myocardial fibrosis and pathological damage in MI rats

Protein expression analysis showed that although CTRP6 levels in the CTRP6 group remained lower than those in the sham controls, they were significantly higher than in the model group ($p<0.001$), confirming successful CTRP6 upregulation through recombinant human CTRP6 administration. Additionally, the model group displayed markedly increased expression of fibrotic markers, including Collagen III, α-SMA, and TGF-β1, compared with the sham group ($p<0.01$). Importantly, CTRP6 treatment significantly reduced the expression of these fibrotic proteins compared with the model group ($p<0.01$), suggesting its potential to mitigate the progression of myocardial fibrosis. Histopathological examination with H&E staining showed well-organized myocardial fibers and intact tissue structure in the sham controls. In contrast, the model group exhibited characteristic pathological changes, such as disorganized myocardial fibers and ventricular wall thinning. CTRP6 treatment markedly alleviated these abnormalities, resulting in increased ventricular wall thickness and more

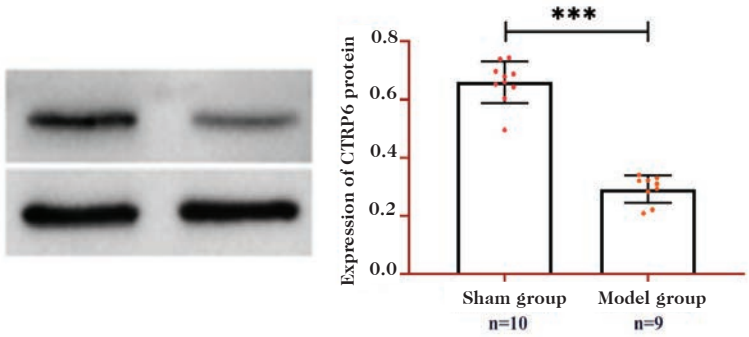

Fig. 1. CTRP6 protein expression in MI. An independent-samples t-test was used to compare groups (***$p<0.001$). CTRP6:complement C1q/tumor necrosis factor-related protein 6. MI: Myocardial infarction.

organized fiber alignment compared with untreated MI rats. Masson's trichrome staining supported these results, with the sham group showing minimal collagen deposition (indicated by blue staining). The model group exhibited extensive myocardial fibrosis, whereas CTRP6-treated animals showed significantly reduced collagen accumulation and better-preserved myocardial structure (Fig. 2).

CTRP6 ameliorates cardiac dysfunction in MI rats

The echocardiographic assessment revealed significant cardiac dysfunction in the MI model group compared to sham-operated controls. Specifically, the model group exhibited markedly reduced LVEF and LVFS, accompanied by increased LVEDD and LVESD ($p<0.05$). Notably, CTRP6 administration effectively attenuated these pathological changes, with treated animals demonstrating significantly improved LVEF and LVFS, along with reduced LVEDD and LVESD, compared with untreated MI rats ($p<0.05$; Fig. 3).

CTRP6 attenuates pyroptotic cell death in infarcted myocardium

Analysis of inflammatory mediators showed a strong pro-inflammatory state in the myocardial tissue of the model group, with significantly increased levels of IL-1β, TNF-α, IL-6,

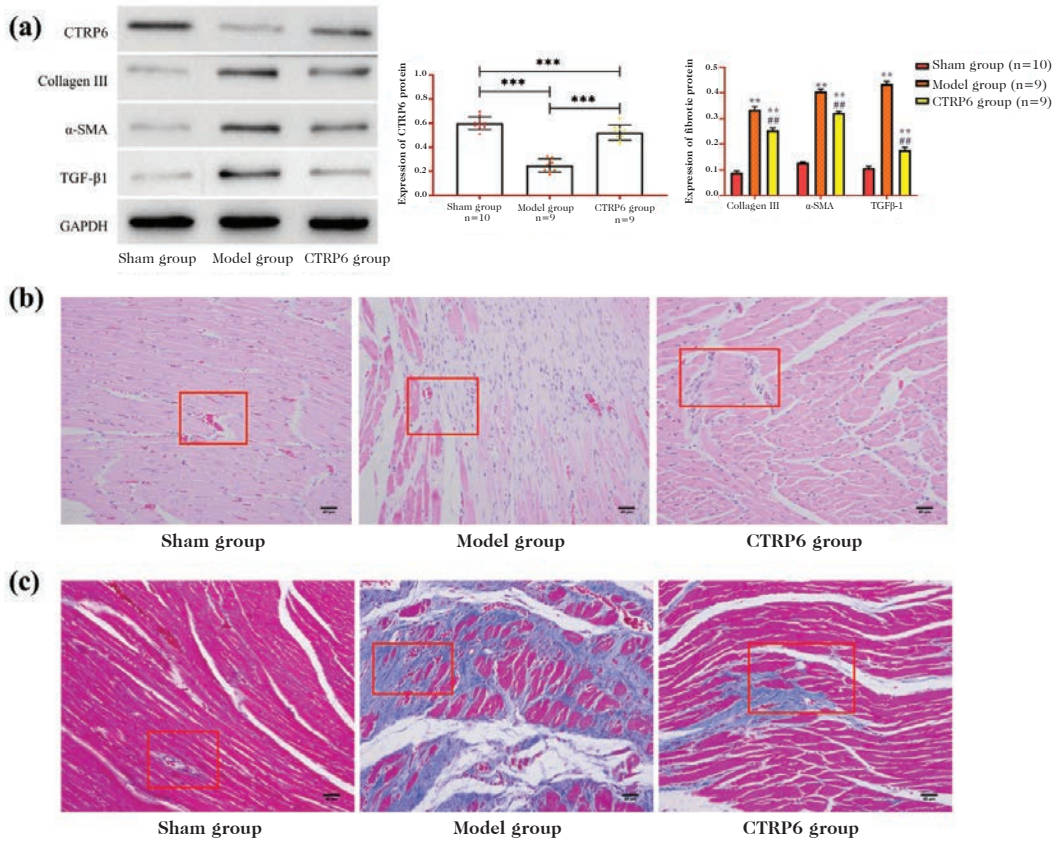

Fig. 2. Effect of CTRP6 on myocardial fibrosis and tissue damage in MI rats. (a) Measurement of myocardial fibrosis-related protein expression in MI rats treated with exogenous CTRP6. (b) Hematoxylin and eosin (H&E) staining of myocardial tissue (200×). (c) Masson staining of myocardial tissue (200×). Repeated-measures analysis of variance and LSD intra-group tests were used to compare multiple groups: ***$p<0.001$ compared with the sham group; **$p<0.01$ compared with the model group; ##$p<0.01$. Complement C1q/tumor necrosis factor-related protein 6 (CTRP6), α-smooth muscle actin (α-SMA), and transforming growth factor-β1 (TGF-β1). The portion of inflammatory cell infiltration is highlighted in the figure. MI: Myocardial infarction.

and IL-8, alongside decreased IL-10, compared to sham controls ($p<0.05$). CTRP6 treatment effectively adjusted this inflammatory imbalance, significantly reducing pro-inflammatory cytokines (IL-1β, TNF-α, IL-6, and IL-8) while boosting anti-inflammatory IL-10 expression ($p<0.05$). Regarding pyroptosis-related proteins, western blot analysis revealed substantial upregulation of NLRP3, cleaved Caspase-1, GSDMD, NT-GSDMD, and IL-1β in both the model and CTRP6 groups compared to the sham group ($p<0.05$); however, their levels were lower in the CTRP6 group than in the control group ($p<0.05$). These findings suggest that CTRP6 suppresses myocardial pyroptosis in MI rats (Fig 4).

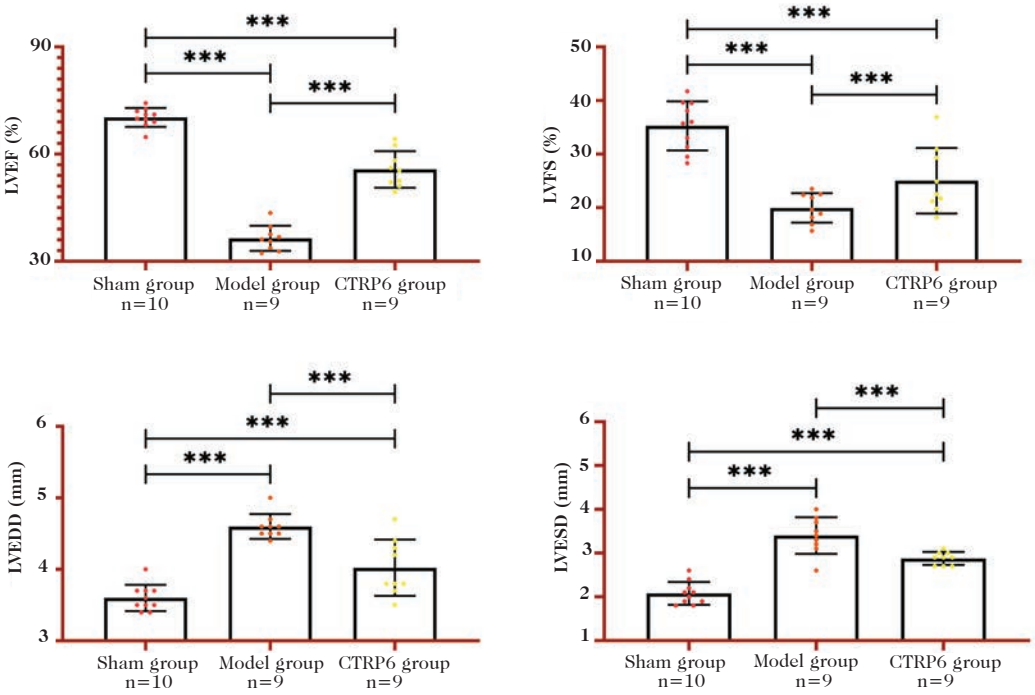

Fig. 3. Effect of CTRP6 on cardiac function (LVEF, LVFS, LVEDD, LVESD) in MI rats. Repeated-measures analysis of variance and LSD intra-group tests were used to compare multiple groups; ****p<0.001*. Left ventricular ejection fraction (LVEF), left ventricular fractional shortening (LVFS), left ventricular end-diastolic diameter (LVEDD), and left ventricular end-systolic diameter (LVESD). MI: Myocardial infarction; CTRP6: Complement C1q/tumor necrosis factor-related protein 6.

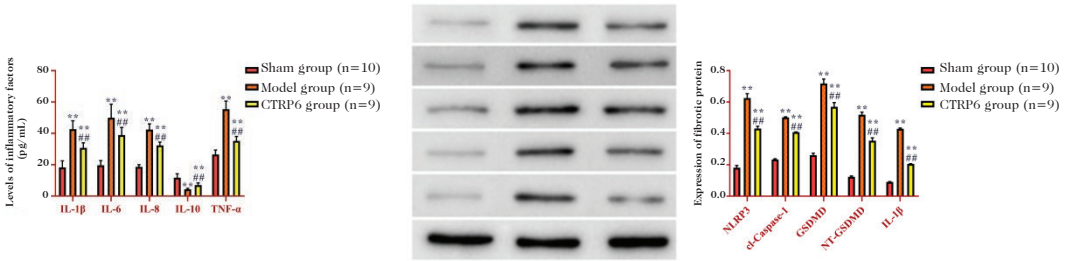

Fig. 4. Effect of CTRP6 on myocardial pyroptosis in MI rats. (a) Effect of CTRP6 on the levels of inflammatory factors (IL-1β, TNF-α, IL-6, IL-8, IL-10) in myocardial tissues of MI rats. (b) Effect of CTRP6 on the expression of focal death proteins (NLRP3, cl-Caspase-1, GSDMD, NT-GSDMD, IL-1β) in myocardial tissues of MI rats. Repeated-measures analysis of variance and LSD intra-group tests were used to compare multiple groups, compared with the sham group **$p<0.01$, and the model group *##p<0.01*. NOD-like receptor family pyrin domain containing 3 (NLRP3), gasdermin D (GSDMD), N-terminal (NT), interleukin (IL), tumor necrosis factor-α (TNF-α). MI: Myocardial infarction; CTRP6: Complement C1q/tumor necrosis factor-related protein 6.

DISCUSSION

Through MI modeling in rats and exogenous CTRP6 intervention experiments, this study demonstrates that CTRP6 exerts cardioprotective effects in MI via a novel mechanism that suppresses cardiomyocyte pyroptosis, thereby ameliorating myocardial fibrosis and restoring cardiac function. These findings not only substantiate the previously hypothesized protective role of CTRP6 in ischemic myocardial injury but also offer novel therapeutic avenues by identifying the pyroptosis-fibrosis axis as a potential target for myocardial repair strategies. Specifically, the therapeutic benefits of CTRP6 were: (1) recovery of cardiac function: LVEF was improved by subcutaneous injection of 0.2 mg/kg/ day (28 days) in MI rats; (2) Anti-fibrosis: reduced collagen deposition and blocked the TGF-β1 pathway.

In the present study, we initially observed significantly decreased CTRP6 protein levels in the myocardial tissue of MI model rats (Fig. 1), suggesting CTRP6's potential role in MI development and progression. This finding supports the findings of Tabatabaei SA et al., who reported a similar reduction in CTRP6 in patients with coronary artery disease [11]. The subsequent administration of exogenous CTRP6 effectively restored CTRP6 levels and yielded two clinically relevant outcomes: a significant reduction in fibrotic markers (Collagen III, α-SMA, and TGF-β1) and improved cardiac function parameters (LVEF and LVFS) (Figs. 2-3). These linked effects provide preliminary evidence for CTRP6's therapeutic potential in the treatment of MI. By analyzing our data systematically and integrating it with existing literature, we identified two complementary mechanisms through which CTRP6 likely exerts its cardioprotective effects: (1) Modulation of inflammation leading to reduced fibrosis: Our results clearly show that CTRP6 treatment causes a significant change in cytokine profiles, characterized by decreased levels of pro-inflammatory mediators (IL-1β, TNF-α, IL-6, and IL-8) and increased levels of the anti-inflammatory cytokine IL-10 (Fig. 4). These findings extend previous research [12] suggesting that CTRP6 may regulate inflammatory responses by inhibiting the NF-κB signaling pathway, ultimately preventing NLRP3 inflammasome activation. This mechanism would decrease pro-inflammatory cytokine release and reduce inflammation in the myocardial environment. (2) Direct inhibition of fibrotic pathways: Our study further confirms the work of Yan et al. [13], showing that CTRP6 suppresses the TGF-β1/Smad3 pathway, preventing the transformation of fibroblasts into myofibroblasts. This is supported by our observed reductions in TGF-β1 and α-SMA protein levels, as well as notably less collagen deposition (particularly Collagen III) in rats treated with CTRP6. Notably, our findings highlight the connection between CTRP6's anti-fibrotic effects and its ability to inhibit pyroptosis [14]. This connection is evident because IL-1β and IL-18, produced during pyroptosis, are potent activators of fibroblasts and promote excessive extracellular matrix (ECM) production [15]. Therefore, we propose that CTRP6 coordinates a multi-faceted anti-fibrotic approach by sequentially blocking "pyroptosis → cytokine release → fibroblast activation". In addition, our study presents the first experimental evidence that CTRP6 suppresses cardiomyocyte pyroptosis by modulating the NLRP3/caspase-1/GSDMD signaling pathway. The underlying mechanisms may involve the following aspects: Upstream regulation: CTRP6 likely initiates its protective effects through activation of the AMPKα pathway, which subsequently attenuates reactive oxygen species (ROS)-mediated NLRP3 inflammasome assembly [16]. Diminished ROS production reduces NLRP3 oligomerization, suppresses caspase-1 self-cleavage (as evidenced by decreased cl-caspase-1 expression), and ultimately prevents GSDMD proteolytic activation (manifested as reduced NT-GSDMD fragments) (Fig. 4). Downstream effects: By inhibiting the pyrop-

tosis executioner protein GSDMD, CTRP6 diminishes plasma membrane pore formation, thereby preventing the release of IL-1β and IL-18 and consequently disrupting the vicious cycle of "pyroptosis-inflammation-fibrosis" (Fig. 4). While the current literature offers limited precedents for CTRP6's role in pyroptosis regulation, our findings align with established clinical evidence that identifies lipid peroxidation and membrane disruption as fundamental prerequisites for pyroptotic cell death [17,18]. Given that CTRP6 functions as a lipid metabolism regulator, it may enhance cellular resistance to pyroptosis by maintaining membrane phospholipid homeostasis, such as by increasing sphingomyelin levels [19]. This intriguing hypothesis warrants further investigation through comprehensive lipidomic profiling in future studies.

Furthermore, this study is the first to establish the "CTRP6-pyroptosis-fibrosis" regulatory axis, elucidating the molecular mechanism by which CTRP6 attenuates post-MI fibrosis via targeting the NLRP3/caspase-1/GSDMD pathway. Using a well-established MI rat model, we demonstrated that intravenous administration of exogenous CTRP6 improves cardiac function. These findings provide crucial experimental evidence supporting the development of CTRP6-based therapeutic approaches, including both gene therapy and protein replacement strategies. Our research suggests several promising clinical applications that warrant further investigation: First, regular monitoring of serum CTRP6 levels could potentially serve as a valuable biomarker for evaluating the risk of fibrosis development in MI patients. Second, combinatorial regimens pairing CTRP6 with established pyroptosis inhibitors (such as MCC950) may produce enhanced anti-fibrotic effects through synergistic mechanisms. Third, the dual protective properties of CTRP6—targeting both metabolic and cardiovascular systems—may be particularly beneficial for the management of diabetic patients with MI, potentially yielding superior therapeutic outcomes in this high-risk population.

While our study provides important insights, several limitations must be considered. First, the precise molecular mechanism remains unclear—we cannot determine whether CTRP6 exerts its anti-pyroptotic effects through direct interaction with NLRP3 or via indirect modulation of upstream regulatory kinases, such as ASK1. Second, our experimental design did not incorporate sex-based analyses, despite existing evidence suggesting estrogen may influence CTRP6 expression patterns [20]. Third, the absence of clinical specimen data prevents validation of the observed relationship between CTRP6 levels and pyroptosis markers.

As a conclusion, CTRP6 ameliorates myocardial fibrosis and enhances cardiac function by inhibiting NLRP3/caspase-1/GSDMD-mediated cardiomyocyte pyroptosis, thereby reducing pro-inflammatory cytokine release and fibroblast activation in an MI animal model. These findings not only expand our understanding of CTRP6's role in cardiovascular diseases but also provide novel strategies for precision medicine in the treatment of MI.

Acknowledgements

Not applicable.

Funding

The authors declare that no funds, grants, or other support were received during the preparation of this manuscript.

Ethical approval

The study protocol was approved by the Ethics Committee of The Second People's Hospital of Changzhou (Approval number:20210301002).

Conflict of interest

The authors had no separate personal, financial, commercial, or academic conflicts of interest.

Availability of data and material

All data generated or analyzed during this study are included in this published article.

ORCID numbers of authors

- Qiu Zhang (QZ): 0009-0002-5874-7484
- Xin Chen (XC): 0009-0005-6572-9323
- Hao Pan (HP): 0009-0005-4335-9325
- Zengguang Chen (ZGC): 0000-0002-0895-3215

Author contributions

Study conception and design: ZGC, QZ; Data collection: XC; Data analysis and interpretation: HP; Drafting of the article: QZ. Critical revision of the article: All authors.

REFERENCES

1. **Frampton J, Ortengren AR, Zeitler EP.** Arrhythmias After Acute Myocardial Infarction. Yale J Biol Med. 2023; 96(1): 83-94. *https://doi.org/10.59249/LSWK8578*
2. **Salari N, Morddarvanjoghi F, Abdolmaleki A, Rasoulpoor S, Khaleghi AA, Hezarkhani LA, et al.** The global prevalence of myocardial infarction: a systematic review and meta-analysis. BMC Cardiovasc Disord. 2023; 23(1): 206. *https://doi.org/10.1186/s12872-023-03231-w*
3. **Kaier TE, Alaour B, Marber M.** Cardiac troponin and defining myocardial infarction. Cardiovasc Res. 2021; 117(10): 2203-2215. *https://doi.org/10.1093/cvr/cvaa331*
4. **Weng L, Ye J, Yang F, Jia S, Leng M, Jia B, et al.** TGF-beta1/SMAD3 Regulates Programmed Cell Death 5 That Suppresses Cardiac Fibrosis Post-Myocardial Infarction by Inhibiting HDAC3. Circ Res. 2023; 133(3): 237-251. *https://doi.org/10.1161/CIRCRESAHA.123.322596*
5. **Chai R, Ye Z, Xue W, Shi S, Wei Y, Hu Y, et al.** Tanshinone IIA inhibits cardiomyocyte pyroptosis through TLR4/NF-kappaB p65 pathway after acute myocardial infarction. Front Cell Dev Biol. 2023; 11: 1252942. *https://doi.org/10.3389/fcell.2023.1252942*
6. **Cai S, Zhang B, Huang C, Deng Y, Wang C, Yang Y, et al.** CTRP6 protects against ferroptosis to drive lung cancer progression and metastasis by destabilizing SOCS2 and augmenting the xCT/GPX4 pathway. Cancer Lett. 2023; 579: 216465. *https://doi.org/10.1016/j.canlet.2023.216465*
7. **Xu E, Yin C, Yi X, Liu Y.** Knockdown of CTRP6 inhibits high glucose-induced oxidative stress, inflammation and extracellular matrix accumulation in mesangial cells through regulating the Akt/NF-kappaB pathway. Clin Exp Pharmacol Physiol. 2020; 47(7): 1203-1211. *https://doi.org/10.1111/1440-1681.13289*
8. **Senthil Kumar J, Mehboob MZ, Lei X.** Exploring CTRP6: a biomarker and therapeutic target in metabolic diseases. Am J Physiol Endocrinol Metab. 2025; 328(2): E139-E147. *https://doi.org/10.1152/ajpendo.00353.2024*
9. **Liang S, Han J, Cheng W, Chen X.** C1q/tumor necrosis factor-related protein-6 exerts protective effects on myocardial ischemia-reperfusion injury through the modulation of the Akt-GSK-3beta-Nrf2 signaling cascade. Int Immunopharmacol. 2023; 115: 109678. *https://doi.org/10.1016/j.intimp.2023.109678*
10. **Konijnenberg LSF, Luiken TTJ, Veltien A, Uthman L, Kuster CTA, Rodwell L, et al.** Imatinib attenuates reperfusion injury in a rat model of acute myocardial infarction. Basic Res Cardiol. 2023; 118(1): 2. *https://doi.org/10.1007/s00395-022-00974-z*
11. **Tabatabaei SA, Fadaei R, Moradi N, Farrokhi V, Vatannejad A, Afrisham R, et al.** Circulating levels of C1q/TNF-alpha-related protein 6 (CTRP6) in coronary artery disease and its correlation with inflammatory markers. J Diabetes Metab Di-

sord. 2024; 23(1): 1233-1241. *https://doi.org/10.1007/s40200-024-01415-5*

12. **Yan S, Ding J, Wang Z, Zhang F, Li J, Zhang Y, et al.** CTRP6 regulates M1 macrophage polarization via the PPAR-gamma/NF-kappaB pathway and reprogramming glycolysis in recurrent spontaneous abortion. Int Immunopharmacol. 2023; 124(Pt A): 110840. *https://doi.org/10.1016/j.intimp.2023.110840*
13. **Yan S, Ding J, Wang Z, Zhang Y, Xu Y, Jia Y, et al.** CTRP6 alleviates endometrial fibrosis by regulating Smad3 pathway in intrauterine adhesion. Biol Reprod. 2024; 111(2): 322-331. *https://doi.org/10.1093/biolre/ioae016*
14. **Fan T, Zhu N, Li M, Wang Z, Lin X.** CTRP6-mediated cardiac protection in heart failure via the AMPK/SIRT1/PGC-1alpha signalling pathway. Exp Physiol. 2024; 109(12): 2031-2045. *https://doi.org/10.1113/EP092036*
15. **Guo Q, Chen X, Chen J, Zheng G, Xie C, Wu H, et al.** STING promotes senescence, apoptosis, and extracellular matrix degradation in osteoarthritis via the NF-kappaB signaling pathway. Cell Death Dis. 2021; 12(1): 13. *https://doi.org/10.1038/s41419-020-03341-9*
16. **Xie YH, Xiao Y, Huang Q, Hu XF, Gong ZC, Du J.** Role of the CTRP6/AMPK pathway in kidney fibrosis through the promotion of fatty acid oxidation. Eur J Pharmacol. 2021; 892: 173755. *https://doi.org/10.1016/j.ejphar.2020.173755*
17. **Hsu CG, Chavez CL, Zhang C, Sowden M, Yan C, Berk BC.** The lipid peroxidation product 4-hydroxynonenal inhibits NLRP3 inflammasome activation and macrophage pyroptosis. Cell Death Differ. 2022; 29(9): 1790-1803. *https://doi.org/10.1038/s41418-022-00966-5*
18. **Liu C, Yao K, Tian Q, Guo Y, Wang G, He P, et al.** CXCR4-BTK axis mediate pyroptosis and lipid peroxidation in early brain injury after subarachnoid hemorrhage via NLRP3 inflammasome and NF-kappaB pathway. Redox Biol. 2023; 68: 102960. *https://doi.org/10.1016/j.redox.2023.102960*
19. **Li M, Zhou S, Feng Z, Zhang C.** Role of C1q/TNF-Related Protein 6 for the Evaluation of Coronary Heart Disease Associated with Type 2 Diabetes. Ther Clin Risk Manag. 2024; 20: 289-296. *https://doi.org/10.2147/TCRM.S464007*
20. **Sadeghi A, Fadaei R, Moradi N, Fouani FZ, Roozbehkia M, Zandieh Z, et al.** Circulating levels of C1q/TNF-alpha-related protein 6 (CTRP6) in polycystic ovary syndrome. IUBMB Life. 2020; 72(7): 1449-1459. *https://doi.org/10.1002/iub.2272*

Invest Clin 67(1): 30 - 44, 2026 https://doi.org/10.54817/IC.v67n1a03

Assessment of the efficacy of tamsulosin and potassium citrate in promoting spontaneous ureteral stone expulsion.

Lihua Liu[1], Kai Zhang[1] and Daichang Li[2]

[1]Huzhou Wuxing District People's Hospital, Huzhou Wuxing District Matemal and Child Health Hospital, Huzhou, Zheijan Province, China.
[2]Department of Urology, Wuyi Branch, Run Run Shaw Hospital, Shuxi Sub-district, Wuyi County, Jinhua Zhejiang Province, China.

Keywords: Tamsulosin; Potassium Citrate; Ureteral Calculi; Lithotripsy; Spontaneous Expulsion.

Abstract. This study aimed to evaluate the effectiveness of tamsulosin combined with potassium citrate in promoting the spontaneous passage of ureteral stones ≤10 mm. A retrospective analysis was performed on 100 patients admitted between January 2020 and December 2023. Patients were divided into four groups: tamsulosin (0.4 mg/day), potassium citrate (3 g/day), combined treatment (tamsulosin + potassium citrate), and a control group (analgesics only + regular water intake). Primary outcomes assessed over four weeks included stone passage rate, passage time, stone location and composition, and safety. Secondary outcomes covered pain control, imaging and laboratory indicators, and quality of life. Baseline characteristics were comparable across groups. The combined treatment group showed the highest stone expulsion rate, which was significantly higher than that of the tamsulosin, potassium citrate, and control groups ($p<0.05$). The median stone expulsion time was also shortest in the combined group ($p<0.05$). Expulsion rates for lower ureteral stones, uric acid stones, and calcium stones were significantly higher in the combined group ($p<0.05$), while the rate for upper stones was not statistically significant ($p>0.05$). No serious adverse events occurred, and safety profiles were similar across all groups. Secondary outcomes, including pain control and quality of life, showed significant improvements in the combined group compared with the other groups ($p<0.05$). The combination of tamsulosin and potassium citrate significantly increases the rate and shortens the time of spontaneous ureteral stone expulsion, with good safety and improved quality of life, supporting its role in medical expulsive therapy.

Corresponding author: Daichang Li. Department of Urology, Wuyi Branch, Run Run Shaw Hospital, Shuxi Sub-district, Wuyi County, Jinhua Zhejiang Province, China. Email: Li1908chang@hotmail.com

Evaluación de la eficacia de tamsulosina y citrato de potasio en la promoción de la expulsión espontánea de cálculos ureterales.

Invest Clin 2026; 67 (1): 30 – 44

Palabras clave: Tamsulosina; Citrato de Potasio; Cálculos Ureterales; Litotricia p; Expulsión Espontánea.

Resumen. Este estudio tuvo como objetivo evaluar la eficacia de la tamsulosina combinada con citrato de potasio para promover la expulsión espontánea de cálculos ureterales de menos de 10 mm. Se realizó un análisis retrospectivo de 100 pacientes ingresados entre enero de 2020 y diciembre de 2023. Los pacientes se dividieron en cuatro grupos: tamsulosina (0,4 mg/día), citrato de potasio (3 g/día), tratamiento combinado (tamsulosina + citrato de potasio) y un grupo de control (solo analgesia + ingesta hídrica regular). Los resultados primarios evaluados durante 4 semanas fueron la tasa y el tiempo de expulsión del cálculo, la ubicación y composición del cálculo, y la seguridad. Los resultados secundarios incluyeron el control del dolor, los indicadores de imagen y de laboratorio y la calidad de vida. Las características basales fueron comparables entre los grupos. El grupo de tratamiento combinado presentó la tasa de expulsión de cálculos más alta, significativamente mayor que la de los grupos de tamsulosina, citrato de potasio y control ($p<0,05$). La mediana del tiempo de expulsión del cálculo también fue la más corta en el grupo combinado ($p<0,05$). Las tasas de expulsión de cálculos en el uréter inferior, de ácido úrico y de calcio fueron significativamente más altas en el grupo combinado ($p<0,05$), mientras que la tasa de expulsión de cálculos superiores no fue estadísticamente significativa ($p>0,05$). No se registraron eventos adversos graves y los perfiles de seguridad fueron similares en todos los grupos. Los resultados secundarios, incluidos el control del dolor y la calidad de vida, mostraron una mejoría significativa en el grupo combinado en comparación con los demás grupos ($p<0,05$). La combinación de tamsulosina y citrato de potasio aumenta significativamente la tasa y acorta el tiempo de la expulsión espontánea de cálculos ureterales, con buena seguridad y mejora de la calidad de vida, lo que respalda su valor en la terapia médica expulsiva.

Received: 18-08-2025 Accepted: 21-12-2025

INTRODUCTION

Ureteral stones are a common condition of the urinary system, and their occurrence is rising worldwide. Approximately 80% of patients with ureteral stones less than 10 mm in diameter can pass them spontaneously with conservative treatment [1], but this process is often accompanied by severe pain and potential complications [2]. Despite recent advances in diagnostic and therapeutic methods, pharmacological excretory therapy (MET) is increasingly recognized as an important non-surgical treatment option [3, 4].

Tamsulosin, a highly selective α1A/D adrenergic receptor blocker, has been shown

in several studies to reduce intraureteral pressure by relaxing the smooth muscle of the lower ureter, thereby promoting stone expulsion [5]. Its mechanism of action mainly includes [6, 7]: (1) selectively blocking the α1D receptor on ureteral smooth muscle, reducing the frequency and amplitude of ureteral peristalsis; (2) reducing the edema of the ureteral wall; and (3) improving the urinary drainage proximal to the stone. Clinical studies have shown that tamsulosin significantly increases the rate and shortens the duration of stone expulsion from the distal ureter and reduces episodes of renal colic [8]. Potassium citrate, as an alkaline drug, has multiple roles in the treatment of urinary stones [9-11]: (1) increase the solubility of uric acid and cystine stones by alkalinizing the urine; (2) inhibit the formation of calcium salt crystals; and (3) replenish citrate to correct hypo-citraturia. In recent years, potassium citrate has been found to promote stone expulsion by altering stone surface charge and reducing their adhesion to the urinary tract epithelium. Some studies have shown that combination therapy is superior to monotherapy, and the rationale for combination therapy is that the two drugs may synergize to promote stone clearance through different mechanisms: tamsulosin acts primarily on ureteral dynamics, and potassium citrate may alter the physicochemical properties of the stone [12].

In clinical practice, the choice of treatment for ureteral stones requires consideration of several factors, including stone size, location, composition, symptom severity, and individual patient characteristics. In general, stones <5 mm in diameter have a high rate of spontaneous expulsion, whereas those 5-10 mm in diameter have a significantly lower rate of spontaneous expulsion[13]. Stone location is also an important factor influencing stone expulsion, with distal ureteral stones typically having a higher expulsion rate than proximal stones [14]. In addition, stone composition, ureteral anatomical variations, and previous history of stone evacuation can affect treatment outcomes. Therefore, the search for a more effective pharmacological lithotripsy regimen is of great clinical importance. The aim of this study was to systematically evaluate the promotion effect of tamsulosin and potassium citrate alone and in combination on the spontaneous expulsion of ureteral stones, to compare the differences in stone expulsion rate, time to expulsion, and degree of pain relief, and to explore the effect of stone composition on drug efficacy, with a view to providing an evidence-based basis for the clinical development of an individualized treatment regimen. The results of the study will help optimize the conservative treatment strategy for ureteral stones, reduce patient pain, and medical costs.

MATERIALS AND METHODS

Study design and participants

This is a clinical retrospective study aimed at evaluating the clinical effectiveness of tamsulosin therapy and potassium citrate in promoting the spontaneous passage of ureteral stones. The clinical data of patients with ureteral stones admitted to our hospital from January 2020 to December 2023 were collected, and 100 patients were ultimately included. These patients were divided into four groups based on their treatment protocols: tamsulosin group (0.4 mg/d), potassium citrate group (3 g/d), combined treatment group (tamsulosin + potassium citrate), and a control group (symptomatic treatment only). The flow chart of this study is shown in Fig. 1.

Inclusion, exclusion, and withdrawal criteria

Inclusion criteria: age 18-70 years; unilateral primary ureteral stone diagnosed by abdominal Computed Tomography (CT) scanning [15]; maximum stone diameter 5-10 mm (longest diameter measured by CT) [16]; receiving at least 2 weeks of standardized medication; having complete 4-week follow-

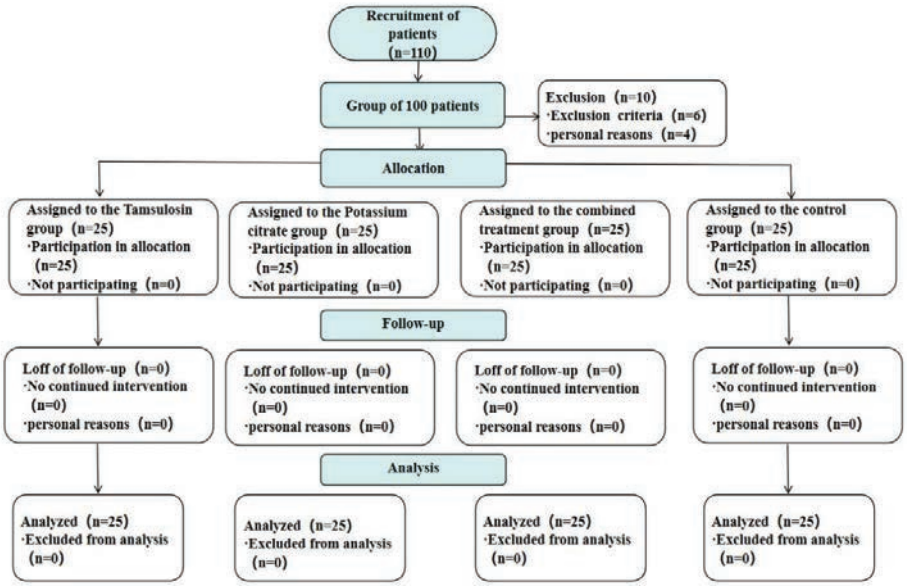

Fig. 1. Flow diagram of patients included in the analysis.

up data; and a normal contralateral urinary tract.

Exclusion criteria: renal insufficiency; history of previous ureteral surgery on the affected side; pregnant women; recurrent renal colic during the follow-up period, ineffective conservative treatment, requiring surgical treatment; comorbidity with severe urinary tract infections requiring surgical treatment; and recent use of oral calcium channel blockers or alpha-1 receptor blockers.

Withdrawal criteria: exacerbation of the condition during follow-up (worsening of infection or recurrent renal colic); due to non-collection of stones (e.g., complete dissolution of stones or stone exclusion not detected); and stone composition analysis (using chemical analysis) in all patients, if the composition of the stones is non-uric acid stones.

Ethics statement

The study strictly followed the requirements of the Declaration of Helsinki and the ethical guidelines of the Wuxing District People's Hospital of Huzhou City and was approved by this Hospital's Ethics Committee.

Research methodology

Patients' baseline data (age, gender, stone characteristics, etc.) were collected, and the calculus clearance achieved by 4-week follow-up was recorded. The primary observation index was the rate of stone expulsion (confirmed by ultrasound or CT), and the secondary indexes included the time of expulsion, the number of pain episodes and the adverse drug reactions. Blinded, unifactorial and multifactorial logistic regression were used to analyze the relevant factors affecting stone expulsion.

How the medication was administered: 2 packets of potassium citrate three times a day, dissolved in warm boiled water. Tamsulosin 0.2 mg/d, 1 time/d, taken orally after meals. During follow-up, each group had episodes of renal colic and was given diclofenac for pain relief. The placebo group was given diclofenac only at the onset of renal colic and no other medication. Patients in each group were asked to drink >2 L of water per day [17]. The follow-up period was four weeks and was terminated if the stone was expelled within that period. Surgery was recommended for those who had not expelled the stone within four weeks.

Observation indicators

General information

Age, BMI (Body Mass Index), stone size, stone location, CT value [Hounsfield Unit (HU)], blood creatinine, uric acid, urine hydrogen ion concentration (pH), hypertension, diabetes mellitus, and the presence of hyperuricemia were recorded for the patients. A total of 110 patients met the inclusion and exclusion criteria for this trial, but 10 were excluded. The remaining 100 patients were divided into four groups based on the intervention method: 25 patients in the tamsulosin group, 25 in the potassium citrate group, 25 in the combined treatment group (tamsulosin + potassium citrate), and 25 in the control group (symptomatic treatment only).

Observation indicators

1. Recorded imaging assessment (4-week rate of complete stone expulsion)

All patients underwent low-dose unenhanced CT scans before (baseline) and after 4 weeks (±3 days) of treatment to independently assess the rate of complete stone expulsion using a blinded method.

2. Median time to stone expulsion

Confirmation of median stone expulsion time by imaging.

3. Stone location and composition

The location and composition of stones were examined using imaging and infrared spectroscopy, respectively, in each patient group.

4. Adverse reactions

Hypotension, nausea, vomiting, abdominal pain, diarrhea, and allergic reactions were recorded in each group.

5. Pain control effects

The visual analogue scale (VAS) was used to assess pain, with 0 indicating no pain and 10 representing the worst pain imaginable; higher scores indicate greater pain. The maximum reduction in VAS score was identified by noting the time when the patient first reported a significant decrease in pain and counting the number of pain episodes recorded daily, starting from the time of drug administration.

6. Imaging and laboratory indicators

The location of the stone was determined by CT before treatment, and CT was reviewed after treatment to measure the new position of the stone, calculate the three-dimensional spatial travel distance using the software Mimics Imaging, compare the average speed of stone movement (mm/day) among different treatment groups, and record the separate distances of stone movement. Multislice spiral CT scanning was used to calculate changes in fluid volume with the software Mimics. The 24-hour urinary citrate level was recorded through sample collection.

7. Quality of life indicators

The patients were evaluated using the EuroQol 5-Dimensions 5-Levels (EQ-5D-5L) scale, which assesses mobility, self-care, daily activities, pain or discomfort, and anxiety or depression. Higher scores indicated poorer health status. The time taken to return to daily activities was also recorded, with shorter times reflecting higher patient satisfaction.

Statistical analyses

Per protocol, statistical analysis was conducted using SPSS 26.0. Efficacy endpoints (measured as mean ± SD) were analyzed with ANCOVA, adjusting for baseline values. Safety data (categorical) were compared using χ^2 tests with Yates' correction. The significance level was kept at 0.05 without applying multiplicity adjustment for this exploratory analysis.

RESULTS

Comparison of general information

A total of 110 patients met the inclusion and exclusion criteria for this trial; 10 declined to participate and were excluded. The remaining 100 patients were allocated

25 per group to the tamsulosin, potassium citrate, combined treatment, and control groups, according to the intervention modality. The demographic characteristics and baseline data of the subjects in the four groups were analyzed and were not statistically significant ($p>0.05$), indicating that the four groups were comparable at the pretreatment level. As shown in Table 1.

Comparison of the efficacy of tamsulosin, potassium citrate and combination therapy in promoting spontaneous ureteral stone expulsion

The analysis of the effectiveness of the index in promoting spontaneous ureteral stone discharge is shown in Table 2. The stone discharge rate in the combined treatment group was optimal, with an 84.6% rate at 84.6 weeks, which was significantly higher than the rates in the single-drug groups (68.2% in the tamsulosin group and 62.1% in the potassium citrate group) and the control group (46.3%). This difference was statistically significant ($p<0.001$). This suggests that the combined treatment may significantly improve stone discharge efficiency through a synergistic effect (tamsulosin relaxes the ureter + potassium citrate dissolves uric acid stones). The median time to stone expulsion was shortest in the combination therapy group (6.5 days), shorter than in the monotherapy groups (9.3 days in the tamsulosin group and 11.7 days in the potassium citrate group), and significantly shorter than in the control group (14.0 days; $p<0.0001$). These findings indicate that the combined therapy not only enhances the expulsion rate but also accelerates the stone passage process and may reduce patients' pain duration.

Table 1. Comparison of patients' general information.

Variables	Tamsulosin group (n=25)	Potassium citrate group (n=25)	Combined treatment group (n=25)	Control group (n=25)	$-/\chi^2/F$	p
Age (years, mean ± SD)	43.2±11.8	41.7±12.5	42.8±12.1	42.1±12.7	0.25	0.87
Males (%)	68.0	64.0	68.0	64.0	0.18	0.98
BMI (kg/m^2, mean ± SD)	24.1±3.0	24.5±3.3	24.0±2.9	24.6±3.2	0.41	0.76
Stone size (mm, mean ± SD)	7.1±1.4	7.3±1.6	7.0±1.3	7.4±1.7	0.59	0.65
Upper segment (%)	28.0	24.0	28.0	24.0	0.21	0.98
Mid-range (%)	36.0	36.0	36.0	36.0	0.00	1.00
Lower segment (%)	36.0	40.0	36.0	40.0	0.17	0.98
CT values (HU, mean ± SD)	670±205	690±215	665±200	695±220	0.45	0.72
Blood creatinine (μmol/L)	77.8±17.5	79.2±18.8	78.0±17.9	79.1±19.0	0.16	0.91
Uric acid (μmol/L)	348±82	362±90	350±84	360±88	0.48	0.69
Urine pH (mean ± SD)	5.7±0.6	5.9±0.8	5.8±0.7	5.8±0.7	0.31	0.83
Hypertensive	16.0	12.0	16.0	16.0	-	1.00
Diabetes	8.0	12.0	12.0	12.0	-	1.00
Hyperuricemia	20.0	24.0	20.0	24.0	0.23	0.97

BMI: Body Mass Index, CT: Computed Tomography, HU: Hounsfield Unit, Combined treatment group: tamsulosin + potassium citrate. χ^2: Chi-square Test, F: ANCOVA, -: Fisher exact. The p represents the overall difference across the four groups (Tamsulosin, Potassium citrate, Combined treatment, and Control).

Table 2. Comparison of outcomes of patients with spontaneous ureteral stone expulsion.

Variables	Tamsulosin group (n=25)	Potassium citrate group (n=25)	Combined treatment group (n=25)	Control group (n=25)	χ^2/H	*p*
4-week stone expulsion rate (%)	68.2	62.1	84.6	46.3	15.72	<0.001
Median discharge interval (days, 95% CI)	9.3 (8.1-10.5)	11.7 (10.2-13.2)	6.5 (5.8-7.2)	14.0 (12.5-15.5)	28.45	<0.0001

Combined treatment group: tamsulosin + potassium citrate. χ^2: Chi-square Test, *H*: Kruskal-Wallis H. The *p* represents the overall difference across the four groups (Tamsulosin, Potassium citrate, Combined treatment, and Control).

Comparison of efficacy by stone location and composition

A comparison of efficacy based on stone location and composition is shown in Table 3. The lower segment stone treatment group achieved the best results, with an expulsion rate of 91.2%, which was significantly higher than the tamsulosin group (79.5%), the potassium citrate group (73.2%), and the control group (58.6%). This difference was statistically significant ($p<0.001$), indicating that the smooth muscle of the lower ureter is more responsive to α-blockers like tamsulosin, and that combining potassium citrate may further aid stone movement and dissolution. Upper segment stones had lower expulsion rates across all groups, with no significant difference between them ($p=0.12$). This suggests that upper stones are harder to expel naturally due to their anatomical position and gravity, and that medication alone has limited effectiveness. More aggressive treatments, such as extracorporeal lithotripsy, might be necessary. The expulsion rate for uric acid stones was notably higher in the potassium citrate group (78.9%) compared to the tamsulosin group (61.2%, $p=0.03$), and increased further to 85.4% in the combination group. This indicates that urine alkalinization with potassium citrate dissolves uric acid stones, while tamsulosin has a weaker mechanical effect on them. The clearance rate of calcium stones was higher in the tamsulosin group (70.5%) than in the potassium citrate group (55.8%), and reached 83.1% in the combined group ($p<0.01$). This suggests that calcium stones are resistant to dissolution and that tamsulosin helps promote their passage by relaxing the ureter, whereas potassium citrate has limited impact on them.

Analysis of safety results

The safety results are shown in Table 4, and there was no statistically significant difference in adverse reactions ($p>0.05$). No serious adverse reactions occurred. The combination therapy group experienced a higher rate of gastrointestinal adverse reactions, such as nausea (24%), vomiting (16%), and abdominal pain (12%), compared to other groups, indicating that the drug combination may irritate the gastrointestinal tract. The occurrence of diarrhea was significantly higher in the potassium citrate group (16%) than in the other groups (0-8%), with the p-value reaching statistical significance ($p=0.05$), suggesting that potassium citrate may increase the risk of diarrhea. The incidence of hypotension was relatively higher in the tamsulosin group (12%), but there was no significant difference compared to the other groups. The rate of allergic reactions was low across all groups, indicating a favorable safety profile.

Assessment of pain control effectiveness

As shown in Table 5, the first pain relief time was shortest in the combination group,

Table 3. Comparison of the efficacy of patients in terms of stone location and composition.

Variables	Tamsulosin group (n=25)	Potassium citrate group (n=25)	Combined treatment group (n=25)	Control group (n=25)	χ^2	*p*
Lower segment stones (%)	79.5	73.2	91.2	58.6	18.34	<0.001
Upper segment stones (%)	42.1	38.5	47.8	28.3	5.67	0.12
Uric acid stones (CT<500HU) (%)	61.2	78.9	85.4	42.9	9.12	0.03
Calcium stones (%)	70.5	55.8	83.1	47.2	13.45	<0.01

Combined treatment group: tamsulosin + potassium citrate. χ^2: Chi-square Test. The p represents the overall difference across the four groups (Tamsulosin, Potassium citrate, Combined treatment, and Control).

Table 4. Analysis of patient safety outcomes.

Variables	Tamsulosin group (n=25)	Potassium citrate group (n=25)	Combined treatment group (n=25	Control group (n=25)	χ^2	*p*
low blood pressure	3 (12%)	1 (4%)	2 (8%)	0 (0%)	3.21	0.36
nausea	4 (16%)	5 (20%)	6 (24%)	1 (4%)	5.78	0.12
vomiting	2 (8%)	3 (12%)	4 (16%)	1 (4%)	2.94	0.40
stomach pain	1 (4%)	2 (8%)	3 (12%)	0 (0%)	4.15	0.25
constipation	0 (0%)	4 (16%)	2 (8%)	0 (0%)	7.62	0.05
allergic reaction	1 (4%)	0 (0%)	1 (4%)	0 (0%)	2.04	0.56

Combined treatment group: tamsulosin + potassium citrate. χ^2: Chi-square Test. The *p*-represents the overall difference across the four groups (Tamsulosin, Potassium citrate, Combined treatment, and Control).

Table 5. Comparison of patients' pain control outcome assessment.

Variables	Tamsulosin group (n=25)	Potassium citrate group (n=25)	Combined treatment group (n=25)	Control group (n=25)	*F*	*p*
Time to first pain relief (hours)	6.2±2.1	7.5±2.8	4.8±1.7	9.3±3.4	12.36	<0.01
Number of pain episodes (times/week)	1.8±0.9	2.1±1.2	1.2±0.6	2.7±1.5	9.54	<0.05
Maximum VAS score reduction (Δ)	-3.5±1.2	-2.9±1.0	-4.2±1.4	-2.1±0.8	18.72	<0.001

VAS: Visual Analogue Scale. Combined treatment group: tamsulosin + potassium citrate. *F*: ANCOVA. The *p* represents the overall difference across the four groups (Tamsulosin, Potassium citrate, Combined treatment, and Control).

taking only 4.8 hours, which was significantly faster than the single-drug group (6.2 hours for tamsulosin and 7.5 hours for potassium citrate) and the control group (9.3 hours). This difference was statistically significant (p<0.01), indicating that the two-drug combination had a synergistic analgesic effect. The frequency of pain episodes was only 1.2 times per week in the combination therapy group, significantly lower than the single-drug group (1.8 times for tamsulosin and 2.1 times for potassium citrate)

and the control group (2.7 times) ($p<0.05$). This suggests that the combination therapy can reduce the need for analgesic medication, improve patients' quality of life, and decrease emergency room visits. The improvement in pain intensity, measured by the VAS score, was greatest in the combination therapy group (-4.2 points), which was significantly better than the monotherapy groups (tamsulosin -3.5 points, potassium citrate -2.9 points) and the control group (-2.1 points) ($p<0.001$). This indicates that the combination therapy effectively reduces pain intensity.

Comparison of imaging and laboratory index assessment

A comparison of imaging and laboratory index assessments is shown in Table 6. The stone movement distance was greatest in the combined treatment group (12.3±4.1 mm), which was significantly better than that in the single-drug group (8.7±3.2 mm for tamsulosin and 6.5±2.8 mm for potassium citrate) and the control group (4.2±2.1 mm) ($p<0.001$). This suggests that tamsulosin can relax the smooth muscle to widen the ureter lumen, while potassium citrate reduces crystalline deposits on the stone surface; the combined treatment produces a synergistic pro-excretory effect. The improvement rate of hydronephrosis in the combined treatment group reached 78.2%, significantly higher than in the single-drug group (65.3% for tamsulosin and 58.7% for potassium citrate) and the control group (42.6%) ($p<0.01$). This reflects the relief of ureteral obstruction, which can prevent renal damage caused by long-term hydronephrosis. Urinary citrate excretion increased most notably in the potassium citrate and combined groups (+142±38 mg/24h and +158±42 mg/24h), significantly differing from the control group (+8±5 mg/24h) ($p<0.001$). Potassium citrate significantly elevated urinary citrate levels. Renal function, assessed by creatinine, improved most in the combined treatment group, with a decrease of -18.6±7.2 μmol/L, which was significantly better than the single-drug and control groups ($p<0.05$). This indicates the recovery of renal function after relief of obstruction, with the combination treatment providing the most comprehensive protection for renal health.

Assessment of quality of life indicators

Quality of life indicators were evaluated as shown in Table 7, and the most notable enhancement was seen in the combined

Table 6. Comparison of patients' imaging and laboratory index assessment.

Variables	Tamsulosin group (n=25)	Potassium citrate group (n=25)	Combined treatment group (n=25)	Control group (n=25)	χ^2/F	p
Stone travelling distance (mm, CT)	8.7±3.2	6.5±2.8	12.3±4.1	4.2±2.1	24.73	<0.001
Improvement rate of hydronephrosis (%)	65.3	58.7	78.2	42.6	14.28	<0.01
24-hour urinary citrate (mg/24h, Δ)	25±12	142±38	158±42	8±5	32.15	<0.001
Decrease in serum creatinine (μmol/L)	-15.2±6.8	-12.7±5.9	-18.6±7.2	-8.3±4.1	12.34	<0.05

CT: Computed Tomography. Combined treatment group: tamsulosin + potassium citrate. χ^2: Chi-square Test, F: ANCOVA. The p represents the overall difference across the four groups (Tamsulosin, Potassium citrate, Combined treatment, and Control).

Table 7. Patients Comparison of quality of life indicators assessed.

Variables	Tamsulosin group (n=25)	Potassium citrate group (n=25)	Combined treatment group (n=25)	Control group (n=25)	*p*
EQ-5D-5L Scoring Improvement (Δ)	0.21±0.08	0.18±0.07	0.28±0.09	0.12±0.05	<0.01
Resumption of daily activities (days)	5.1±1.8	6.3±2.1	3.7±1.2	7.5±2.6	<0.001

EQ-5D-5L: Euro Qol 5-Dimensions 5-Levels, Combined treatment group: tamsulosin + potassium citrate. *F*: ANCOVA. The p represents the overall difference across the four groups (Tamsulosin, Potassium citrate, Combined treatment, and Control).

treatment group (+0.28±0.09 points), surpassing the single-drug groups (tamsulosin +0.21, potassium citrate +0.18) and the control group (+0.12) ($p<0.01$). This reflects overall improvement in pain management and activity levels. The quickest recovery of daily activities occurred in the combination therapy group (3.7±1.2 days), which was 30-40% shorter than the single-drug group (5.1 days for tamsulosin and 6.3 days for potassium citrate), and significantly faster than the control group (7.5 days) ($p<0.001$), indicating that the combination therapy increases patient satisfaction with treatment.

DISCUSSION

Ureteral stones are a common disease of the urinary system, often leading to renal colic, urinary tract obstruction, and infection, seriously affecting the quality of life of patients [18]. For stones with a small diameter (usually<10 mm), conservative treatment to promote their spontaneous expulsion is the preferred clinical strategy, but the rate of spontaneous stone expulsion is affected by factors such as stone size, location, and local inflammatory reaction in the ureter [19, 20]. Potassium citrate may further synergize with tamsulosin in stone expulsion rates. Therefore, the aim of this study was to systematically evaluate the efficacy and safety of tamsulosin and potassium citrate, alone or in combination, on the spontaneous excretion of ureteral stones, and to provide an evidence-based basis for optimal clinical decision-making.

Ureteral stone is a common emergency in the urinary system, this trial investigated the differences in efficacy, action characteristics and effects on different types of stones between tamsulosin and potassium citrate used alone and in combination, and systematically evaluated the differences in efficacy between these two drugs in terms of stone expulsion rate, time of expulsion, and pain control through a controlled trial. The study showed that the combination demonstrated superior efficacy compared to both monotherapy and control groups in terms of the main efficacy indicators ($p<0.01$). It was further found that the combined treatment was particularly effective in lower segment stone discharge rate and uric acid stones. In terms of safety, although the rate of adverse reactions was slightly higher in the combination therapy group, it was dominated by mild dizziness and gastrointestinal reactions, and there was no significant increase in serious adverse events. The results showed that the combination of tamsulosin and potassium citrate had a synergistic effect in promoting stone expulsion, shortening the expulsion time and relieving pain, and the efficacy was significantly better than that of single-drug treatment or natural stone expulsion.

The choice of therapeutic strategy for ureteral stones requires a comprehensive consideration of stone location and compositional characteristics [21]. The efficacy of pharmacological lithotripsy as an important

means of non-surgical treatment varies significantly in patients with different anatomical locations and stone compositions [22]. In this study, we investigated differences in the efficacy of these two drugs across patients with varying stone characteristics. The results showed that stone location and composition significantly influenced the drugs' effectiveness: in patients with lower-segment stones, the combination therapy group had a significantly higher expulsion rate than the monotherapy and control groups ($p<0.001$), confirming the specific effect of tamsulosin on the lower ureteral segments; whereas, in patients with upper-segment stones, the efficacy in all groups was limited (combination group vs. control group, $p=0.12$), and upper-segment stones may require surgical intervention more often. Analysis of stone composition revealed that potassium citrate was significantly more effective in uric acid stones ($p=0.03$), while tamsulosin was more effective in calcium stones. Notably, the combination treatments consistently maintained their superiority, indicating broad-spectrum efficacy. These findings highlight the importance of personalized treatment, and clinical drug selection should consider stone location and composition.

Drug safety assessment is a crucial aspect when choosing a treatment plan [23]. In pharmacological management of ureteral stones, the safety profiles of tamsulosin and potassium citrate, commonly used medications, need to be carefully evaluated [24]. Tamsulosin can cause side effects such as postural hypotension and dizziness, while potassium citrate, as an alkaline agent, may lead to gastrointestinal discomfort and electrolyte imbalances [25]. The present study thoroughly examined the safety profiles of these two drugs individually and in combination. Results showed that gastrointestinal side effects like nausea, vomiting, and abdominal pain were more common across all groups, likely due to the side effects of both drugs. Importantly, no serious adverse reactions were observed, suggesting a favorable safety profile for the combination therapy. These findings indicate that although the combination may increase the frequency of minor adverse reactions, it does not pose a risk of serious adverse events.

Renal colic caused by urinary stones is a common urological emergency, and rapid pain relief along with a reduction in episode frequency are essential goals of clinical treatment [26, 27]. In this study, the analgesic effects of different treatment options were systematically assessed by measuring the time to initial pain relief, the frequency of pain episodes, and the reduction in VAS scores. The time to first pain relief was significantly shorter in the combination group compared to the monotherapy and control groups, indicating a synergistic analgesic effect of the two drugs. The frequency of pain episodes was significantly lower in the combination treatment group than in the other groups ($p<0.05$), suggesting that the combination regimen not only provides quick pain relief but also effectively prevents recurrent episodes. The combination group exhibited the greatest improvement in pain levels, which was significantly higher than that of monotherapy ($p<0.001$), further confirming the analgesic benefit of combination therapy. The combination of tamsulosin and potassium citrate offers notable advantages in managing pain associated with urinary tract stones, providing faster relief and more sustained reduction in both the frequency and severity of pain episodes [28].

The assessment of treatment efficacy of urinary tract stones needs to consider not only the stone expulsion rate, but also focus on comprehensive factors such as stone mobility, improvement of renal function and changes in urinary biochemical indexes [29, 30]. In the present investigation, we comprehensively evaluated the effects of different treatment regimens on stone kinetics and renal function using objective indicators, including stone mobility distance measured by CT, improvement in hydronephrosis, changes in 24-hour urinary

citrate, and decreases in serum creatinine. Stone movement distance: the combined treatment group showed the greatest stone movement, which was significantly greater than the single-drug group ($p<0.001$), confirming that the combination of the two drugs synergistically enhanced stone mobility. Improvement of hydronephrosis: the highest improvement rate was observed in the combination group ($p<0.01$), suggesting that the combination therapy could more effectively relieve urinary tract obstruction. Change in urinary citrate: urinary citrate increased significantly in the potassium citrate and combination groups, reflecting the pharmacodynamic effect of potassium citrate. Renal function improvement: Serum creatinine decreased most significantly in the combination group, showing its advantage in protecting renal function. The study confirms that the combined treatment of tamsulosin and potassium citrate has a synergistic effect in promoting stone movement, improving hydronephrosis, and protecting renal function [31], which provides an objective basis for the clinical combined drug regimen. In particular, the combination group was significantly better than monotherapy across all indicators, suggesting that combination therapy may be a better choice for patients who require stone expulsion while improving the urinary environment and renal function.

The outcome of treatment for urinary stones requires not only objective clinical indicators, but also patient-reported outcomes (PROs) and quality of life improvement [32, 33]. The EQ-5D-5L, an internationally recognized quality-of-life assessment tool, provides a comprehensive picture of the patient's health status across five dimensions: mobility, self-care, activities of daily living, pain and discomfort, and anxiety and depression [34]. Meanwhile, the time to resume daily activities is an important indicator for assessing the impact of treatment on patients' social functioning [35]. This study assessed the impact of different treatment regimens on patients' overall recovery through these two patient-centered outcome indicators. Improvement in EQ-5D-5L scores: the combination therapy group showed the greatest improvement in quality of life and demonstrated superior efficacy compared with both monotherapy and control groups ($p<0.01$), suggesting that combination therapy has a synergistic advantage in improving patients' overall health status. The study results confirmed that combination therapy with tamsulosin and potassium citrate significantly improved patients' quality of life and accelerated functional recovery. This advantage may stem from the fact that tamsulosin relieves pain symptoms faster, potassium citrate improves the urinary environment to reduce discomfort, and the synergistic effect of the two drugs shortens the overall recovery process.

In conclusion, for ureteral wall stones measuring ≤10 mm, the combination treatment was more effective than tamsulosin alone, without a significant increase in adverse drug reactions. The combination of tamsulosin and potassium citrate notably improved the stone expulsion rate for these stones and therefore warrants further clinical observation and research. Although current evidence supports the effectiveness of tamsulosin and potassium citrate in promoting spontaneous ureteral stone expulsion, this study has several limitations a lack of validation through large-scale, multicenter randomized controlled trials (RCTs), affecting the reliability of the findings. Moving forward, larger, more rigorous studies are needed, along with standardized efficacy criteria and extended follow-up periods to better establish its clinical value.

Acknowledgment

None.

Funding

None.

Consent to publish

The manuscript has neither been previously published nor is under consideration by any other journal. The authors have all approved the content of the paper.

Consent to participate

We secured a signed informed consent form from every participant.

Ethic approval

The study strictly followed the requirements of the Declaration of Helsinki and the ethical guidelines of Wuxing District People's Hospital of Huzhou City and was approved by this Hospital's Ethics Committee # 2025LW003).

Data availability statement

The data supporting the findings of this study are available from the corresponding author upon request.

ORCID numbers of authors

- Lihua Liu (LL): 0009-0006-9873-2323
- Kai Zhang (KZ): 0009-0002-7817-1048
- Daichang Li (DL): 0009-0006-4532-0931

Author contribution

LL: Conceived and designed the research, and analyzed data. Drafted and revised the manuscript critically for important intellectual content. KZ: Contributed to the acquisition, analysis, and interpretation of data. Provided substantial intellectual input during the drafting and revision of the manuscript. DL: Participated in the conception and design of the study. Played a key role in data interpretation and manuscript preparation. All authors have read and approved the final version of the manuscript.

Conflicts of interest

The authors affirm that they have no financial conflicts of interest.

REFERENCES

1. **Razi A, Ghiaei A, Dolatabadi FK, Haghighi R.** Unraveling the association of bacteria and urinary stones in patients with urolithiasis: an update review article. Front Med. 2024;11:1401808. *https://doi.org/10.3389/fmed.2024.1401808.*
2. **Hassan MA**. Presentation and management outcome of symptomatic epididymal cysts in children: A case series. Int J Surg Open. 2023;55:100626. *https://doi.org/10.1016/j.ijso.2023.100626*
3. **Hasan A, Kumar V, Kant Kumar S, M M**. Radiological and Hematological Parameters Predicting Success of Medical Expulsive Therapy in Patients with Ureteral Calculus. Cureus. 2024;16(8):e67356. *https://doi.org/10.7759/cureus.67356.*
4. **Ren J.** Advances in combination therapy for gastric cancer: integrating targeted agents and immunotherapy. Adv Clin Pharmacol Ther. 2024;1(1):1-15. *https://doi.org/10.63623/9k14tf70*
5. **Jung HD, Cho KS, Jun DY, Jeong JY, Moon YJ, Chung DY, et al**. Silodosin versus Tamsulosin for Medical Expulsive Therapy of Ureteral Stones: An Updated Systematic Review and Meta-Analysis of Randomized Controlled Trials. Medicina (Kaunas). 2022;58(12):1794. *https://doi.org/10.3390/medicina58121794.*
6. **Hong SH, Jang EB, Hwang HJ, Park SY, Moon HS, Yoon YE.** Effect of α1D-adrenoceptor blocker for the reduction of ureteral contractions. Investig Clin Urol. 2023;64(1):82-90. *https://doi.org/10.4111/icu.20220254.*
7. **Jalali S, Borumandnia N, Basiri A, Nagiee M, Amiri FB, Tavasoli S, et al.** A Comparison of Boron Supplement and Tamsulosin as Medical Expulsive Therapy for Urinary Stones After Extracorporeal Shock Wave Lithotripsy: a Randomized Controlled Clinical Trial. Biol Trace Elem

Res. 2023;201(11):5126-5133. *https://doi.org/10.1007/s12011-023-03597-0.*

8. **Ye Z, Zeng G, Yang H, Tang K, Zhang X, Li H, et al.** Efficacy and Safety of Tamsulosin in Medical Expulsive Therapy for Distal Ureteral Stones with Renal Colic: A Multicenter, Randomized, Double-blind, Placebo-controlled Trial. Eur Urol. 2018;73(3):385-391. *https://doi.org/10.1016/j.eururo.2017.10.033.*
9. **Rodriguez-Hesles CA, Alkhatatbeh H, Alonso Bartolomé MB, Valladares Ferreiro CA, Ayllón Blanco HR, Calzas Montalvo C, et al.** Urine alkalinization for dissolution of uric acid stones and treatment of other urological diseases with a treatment combining potassium magnesium citrate and theobromine. Arch Ital Urol Androl. 2025;97(1):13824. *https://doi.org/10.4081/aiua.2025.13824.*
10. **Sun P, Yue J, Lu C, Ji K, Yang R, Lu J, et al.** Targeting urinary calcium oxalate crystallization with inulin-type AOFOS from Aspidopterys obcordata Hemsl. for the management of rat urolithiasis. J. Ethnopharmacol.. 2024;329:118149. *https://doi.org/10.1016/j.jep.2024.118149.*
11. **Maisto M, Schiano E, Luccheo G, Luccheo L, Alfieri E, Piccolo V, et al.** Efficacy of a Multicomponent Nutraceutical Formulation for the Prevention and Treatment of Urinary Tract Stones. Int J Mol Sci. 2023;24(9):8316. *https://doi.org/10.3390/ijms24098316.*
12. **Dogha MM, Sherif IGA, Madney YM, Harb HS, Rabea H.** Comparative study between silodosin, tamsulosin, silodosin plus tadalafil, and tamsulosin plus tadalafil as a medical expulsive therapy for lower ureteral stones: a prospective randomized trial. Int Urol Nephrol. 2025;57(6):1827-1833. *https://doi.org/10.1007/s11255-024-04356-3.*
13. **Belkovsky M, Zogaib GV, Passerotti CC, Artifon ELA, Otoch JP, da Cruz JAS.** Tamsulosin vs. Tadalafil as medical expulsive therapy for distal ureteral stones: a systematic review and meta-analysis. Int Braz J Urol. 2023;49(6):668-676. *https://doi.org/10.1590/S1677-5538.IBJU.2023.0345.*
14. **Ramadhani MZ, Kloping YP, Rahman IA, Yogiswara N, Soebadi MA, Renaldo J.** Silodosin as a medical expulsive therapy for distal ureteral stones: A systematic review and meta-analysis. Indian J Urol. 2023;39(1):21-26. *https://doi.org/10.4103/iju.iju_115_22.*
15. **Selvi I, Baydilli N, Tokmak TT, Akinsal EC, Basar H.** CT-related parameters and Framingham score as predictors of spontaneous passage of ureteral stones ≤ 10 mm: results from a prospective, observational, multicenter study. Urolithiasis. 2021;49(3):227-237. *https://doi.org/10.1007/s00240-020-01214-6.*
16. **Abdel-Basir Sayed M, Moeen AM, Saada H, Nassir A, Tayib A, Gadelkareem RA.** Mirabegron as a Medical Expulsive Therapy for 5-10 mm Distal Ureteral Stones: A Prospective, Randomized, Comparative Study. Turk J Urol. 2022;48(3):209-214. *https://doi.org/10.5152/tud.2022.22014.*
17. **Welty J, Geurin MD.** Is potassium citrate effective for preventing kidney stone recurrence in patients with calcium-containing stones? Evid Based Pract. 2018;21(1):E11. *https://doi.org/10.1097/01.EBP.0000541948.12657.ee*
18. **Sinanoglu O, Yildirim S, Suceken FY, Bicaklioglu F, Aydin ME, Uslu M, et al.** Bilateral ureteral stones; factors affecting treatment decision. Urolithiasis. 2024;52(1):76. *https://doi.org/10.1007/s00240-024-01573-4.*
19. **Abdel-Kader MS, Sayed AM, Sayed SM, AbdelRazek M.** Evaluation of the efficacy and safety of either or both mirabegron and silodosin, as a medical expulsive therapy for distal ureteric stones. Int. Urol. Nephrol. 2024;56(5):1605-1610. *https://doi.org/10.1007/s11255-023-03880-y.*
20. **Aghaways I, Bapir R, Siwaily NS, Abdalqadir AM, Said SH, Mustafa AM, et al.** Role of inflammatory markers in predicting spontaneous passage of ureteral stones less than 10 mm. Arch Ital Urol Androl. 2024;96(4):12997. *https://doi.org/10.4081/aiua.2024.12997.*
21. **Papatsoris A, Alba AB, Galán Llopis JA, Musafer MA, Alameedee M, Ather H, et**

al. Management of urinary stones: state of the art and future perspectives by experts in stone disease. Arch Ital Urol Androl. 2024;96(2):12703. *https://doi.org/10.4081/aiua.2024.12703.*

22. **Falahatkar S, Akhavan A, Esmaeili S, Amin A, Kazemnezhad E, Jafari A.** Efficacy of tamsulosin versus tadalafil as medical expulsive therapy on stone expulsion in patients with distal ureteral stones: A randomized double-blind clinical trial. Int Braz J Urol. 2021;47(5):982-988. *https://doi.org/10.1590/S1677-5538.IBJU.2020.1007.*
23. **Beilmann M, Adkins K, Boonen HCM, Hewitt P, Hu W, Mader R, et al.** Application of new approach methodologies for nonclinical safety assessment of drug candidates. Nat Rev Drug Discov. 2025;24(9):705-725. *https://doi.org/10.1038/s41573-025-01182-9.*
24. **Alenezi NA, Zanaty F, Hodhod A, El-Gharabawy M, El-Sherif E, Badawy A, et al.** The safety of ureteral stenting with the use of potassium citrate for management of renal uric acid stones. Urol Ann. 2020;12(1):37-41. *https://doi.org/10.4103/UA.UA_60_19.*
25. **Ch'ng LS, Toh CC, Sathiyananthan JR, Malek R.** Does alkalinised urine reduce the rate of encrustation in patients with ureteric stents? A randomised controlled study. Int Urol Nephrol. 2022;54(3):509-515. *https://doi.org/10.1007/s11255-022-03105-8.*
26. **Kachkoul R, Touimi GB, El Mouhri G, El Habbani R, Mohim M, Lahrichi A**. Urolithiasis: History, epidemiology, aetiologic factors and management. Malays J Pathol. 2023;45(3):333-352. PMID: 38155376.
27. **Qu LG, Chan G, Gani J.** Clinician training level impacts prescribing practices for the conservative management of acute renal colic: a contemporary update. Int Urol Nephrol. 2021;53(4):661-667. *https://doi.org/10.1007/s11255-020-02686-6.*
28. **El-Gamal O, El-Bendary M, Ragab M, Rasheed M.** Role of combined use of potassium citrate and tamsulosin in the management of uric acid distal ureteral calculi. Urol Res. 2012;40(3):219-224. *https://doi.org/10.1007/s00240-011-0406-6.*
29. **Simmons KE, Nair HR, Phadke M, Motamedinia P, Singh D, Montgomery TA, et al.** Risk factors for common kidney stones are correlated with kidney function independent of stone composition. Am J Nephrol. 2023;54(7-8):329-336. *https://doi.org/10.1159/000531046.*
30. **Moretto S, Saita A, Scoffone CM, Talso M, Somani BK, Traxer O, et al.** Ureteral stricture rate after endoscopic treatments for urolithiasis and related risk factors: systematic review and meta-analysis. World J Urol. 2024;42(1):234. *https://doi.org/10.1007/s00345-024-04933-2.*
31. **Mohammadi A, Rakebi MM, Gholamnezhad M, Ahmadi Pishkuhi M, Aghamir SMK.** Does potassium citrate administration change the type and composition of encrusted material on Double-J stent compared to primary stone? Int Urol Nephrol. 2021;53(9):1797-1803. *https://doi.org/10.1007/s11255-021-02891-x.*
32. **Joshi HB, Johnson H, Pietropaolo A, Raja A, Joyce AD, Somani B, et al.** Urinary Stones and Intervention Quality of Life (USIQoL): Development and Validation of a New Core Universal Patient-reported Outcome Measure for Urinary Calculi. Eur Urol Focus. 2022;8(1):283-290. *https://doi.org/10.1016/j.euf.2020.12.011.*
33. **Okada T, Hamamoto S, Taguchi K, Okada S, Inoue T, Ando R, et al.** Quality of life after urinary stone surgery based on Japanese Wisconsin Stone Quality of Life questionnaire: multicenter analysis from SMART study group. Urolithiasis. 2023;51(1):113. *https://doi.org/10.1007/s00240-023-01486-8.*
34. **Feng YS, Kohlmann T, Janssen MF, Buchholz I.** Psychometric properties of the EQ-5D-5L: a systematic review of the literature. Qual Life Res. 2021;30(3):647-73. *https://doi.org/10.1007/s11136-020-02688-y.*
35. **Sawant R, Paret K, Petrillo J, Koenig A, Wolowacz S, Ronquest N, et al.** Health state utility estimates for value assessments of novel treatments in Huntington's disease: a systematic literature review. Health Qual Life Outcomes. 2024;22(1):33. *https://doi.org/10.1186/s12955-024-02242-1.*

Invest Clin 67(1): 45 - 56, 2026 https://doi.org/10.54817/IC.v67n1a04

Factores de virulencia y su efecto sobre la sensibilidad a los fármacos antifúngicos de *Candida albicans* causante de vulvovaginitis candidiásica recurrente.

Xiomara Moreno-Calderón[1,2], Angie Cantero-Alvarado[3], María G. Vivas-Parababire[4], María M. Panizo-Domínguez[5]

[1]Departamento de Microbiología. Instituto Médico La Floresta, Caracas-Venezuela.
[2]Departamento de Microbiología. Cátedra de Bacteriología. Facultad de Medicina, Escuela de Bioanálisis. Universidad Central de Venezuela, Caracas-Venezuela.
[3]Veneurgencias CA, Laboratorio. Caracas-Venezuela.
[4]Departamento de Virología. Laboratorio de Pruebas Especiales Hepatitis y SIDA. Instituto Nacional de Higiene "Rafael Rangel",Caracas, Venezuela
[5]Cátedra de Salud Pública, Escuela de Bioanálisis. Facultad de Medicina, Universidad Central de Venezuela, Caracas-Venezuela.

Palabras clave: *Candida albicans*; Vulvovaginitis; Virulencia; Susceptibilidad; Fluconazol; Voriconazol; Anfotericina B.

Resumen. La vulvovaginitis candidiásica (VVC) recurrente es causada principalmente por *Candida albicans*. Se valoró la actividad de fosfolipasas, proteasas, hemolisinas y biopelículas como factores de virulencia en *C. albicans* causante de VVC recurrente y sus efectos en la sensibilidad a los antifúngicos a fin de aportar en el conocimiento de los factores de virulencia y su influencia sobre la sensibilidad a los antifúngicos. Se analizaron 22 cepas de *C. albicans* aisladas de pacientes con VVC recurrente que acudieron al Departamento de Microbiología del Instituto Médico La Floresta, Caracas–Venezuela, desde julio 2023 hasta junio de 2024. Se determinó la actividad de fosfolipasas, proteasas, hemolisinas y la formación de biopelículas, así como el perfil de sensibilidad por concentración mínima inhibitoria para fluconazol, voriconazol y anfotericina B por Vitek 2 Compact® mediante la tarjeta AST-YSO1®. El 100% de las cepas produjeron hemolisinas, 77% presentó actividad fosfolipasa y el 27,3% expresó proteasas. El 82% de las cepas tuvo capacidad de formar biopelículas. El 82% de las cepas fueron resistentes a fluconazol, 73% presentó resistencia a voriconazol y el 100% fue sensible a anfotericina B. No hubo relación estadísticamente significativa entre los tres fármacos ensayados con los factores de virulencia estudiados. Los factores de virulencia participan en las diferentes etapas de la infección y se asocian al cuadro clínico de la VVC recurrente, pero son variables independientes al perfil de sensibilidad antifúngica.

Autor de correspondencia: Xiomara Moreno-Calderón. Cátedra de Bacteriología, Escuela de Bioanálisis. Facultad de Medicina, Universidad Central de Venezuela, Caracas-Venezuela. Departamento de Microbiología, Instituto Médico la Floresta, Caracas-Venezuela. Teléfonos: +58-0212-2846897; +58-0414-3722227.
E-mail: xmorenoc1356@gmail.com

Virulence factors and their effect on antifungal sensitivity of *Candida albicans* causing recurrent vulvovaginal candidiasis.

Invest Clin 2026; 67 (1): 45 – 56

Keywords: *Candida albicans*; Vulvovaginitis; Virulence; Susceptibility; Fluconazole; Voriconazole; Amphotericin B.

Abstract. Candidal vulvovaginitis (CVV) is mainly caused by Candida albicans. The activities of phospholipases, proteases, hemolysins, and biofilms were evaluated as virulence factors in *C. albicans* causing recurrent CVV, and their effects on antifungal susceptibility were assessed to understand their influence on antifungal sensitivity. A total of 22 *C. albicans* strains isolated from patients with recurrent CVV who attended the Microbiology Department of the La Floresta Medical Institute, Caracas–Venezuela, from July 2023 to June 2024 were analyzed. Phospholipase, protease, and hemolysin activity, along with biofilm formation and the minimum inhibitory concentration (MIC) susceptibility profiles for fluconazole, voriconazole, and amphotericin B, were determined using the Vitek 2 Compact® assay with the AST-YSO1® card. All strains produced hemolysins; 77% exhibited phospholipase activity, and 27.3% expressed proteases. 82% were capable of forming biofilms. Resistance rates were 82% for fluconazole and 73% for voriconazole; all strains were susceptible to amphotericin B. There was no statistically significant relationship between the three drugs tested and the virulence factors studied. Virulence factors are independent variables in the antifungal susceptibility profile but participate in different stages of infection and are associated with the clinical presentation of CVV.

Recibido: 18-08-2025 Aceptado: 29-01-2026

INTRODUCCIÓN

Entre las causas más comunes de asistencia a la consulta ginecológica se encuentra la vulvovaginitis, observándose actualmente una elevada incidencia de esta infección causadas por levaduras del género *Candida* [1].

La vulvovaginitis candidiásica (VVC) es una infección común del aparato reproductor femenino, causada principalmente por el hongo polimórfico complejo *Candida. albicans,* que forma parte de la microbiota humana habitual, por lo que suele colonizar el canal vaginal sin producir síntomas. Sin embargo, puede actuar como patógeno oportunista bajo ciertas condiciones al alterarse el ambiente vaginal, favoreciendo el crecimiento excesivo del hongo [2,3], entre otras causas se describen los cambios de pH, alteración en el metabolismo de carbohidratos, tratamiento con antimicrobianos y/o corticosteroides, embarazo e inmunodeficiencias [4,5].

La VVC es la infección por *Candida* spp. con mayor prevalencia y se estima que afecta aproximadamente al 75% de la población femenina por lo menos una vez en su vida [2]. Los principales síntomas incluyen ardor, dolor, prurito, enrojecimiento de la vulva y presencia de flujo vaginal grumoso; éstos suelen intensificarse durante la etapa premenstrual, cuando se incrementa la acidez en la vagina [2,3,6].

La virulencia de *Candida albicans*, específicamente la capacidad de formar micelio verdadero, producir enzimas hidrolíticas y biopelículas, contribuyen a la adherencia y posterior invasión y persistencia en el epitelio vaginal [1,7], lo que incide negativamente en el bienestar de las mujeres con VVC [6,8,9]. Por lo tanto, con la finalidad de disminuir el malestar ocasionado por los síntomas de la infección, lo más común es que se suministre tratamiento de forma empírica, sin realizar el estudio microbiológico que incluya toma de la muestra, cultivo y pruebas de sensibilidad a los antifúngicos. El fluconazol se utiliza usualmente como primera opción de tratamiento, no obstante, la exposición prolongada a este antifúngico ha sido un factor desencadenante para el desarrollo de la resistencia, lo cual se traduce en falla terapéutica y episodios recurrentes de la infección observados en la actualidad [10-12].

Con lo anteriormente descrito, nos preguntamos si existe relación entre la expresión de factores de virulencia en cepas de *C. albicans* y la alteración del perfil de sensibilidad a los principales antifúngicos utilizados para tratar la vulvovaginitis candidiásica recurrente. En Venezuela se han realizado investigaciones sobre la expresión de los factores de virulencia de *C. albicans*, en especial de las enzimas proteolíticas, lipasas y la capacidad de formar biopelículas [1,13]. Sin embargo, son escasos los estudios que se han centrado en investigar la posible influencia de estos factores en la expresión de la sensibilidad o resistencia a los antifúngicos. El propósito de este trabajo fue valorar la actividad de fosfolipasas, proteasas, hemolisinas y biopelículas como factores de virulencia y sus efectos en la sensibilidad a los antifúngicos en *C. albicans* causante de vulvovaginitis candidiásica recurrente.

MATERIALES Y MÉTODOS

Estudio descriptivo, prospectivo y transversal con una muestra finita, intencional y no probabilística, conformada por 22 cepas de *C. albicans* aisladas de pacientes con VVC recurrente que acudieron al Departamento de Microbiología del Instituto Médico La Floresta Caracas-Venezuela, solicitando cultivo de secreción vaginal y cepas provenientes de Clínica El Ávila, Clínica Santa Sofía y Centro Médico Docente La Trinidad, aisladas de pacientes con VVC recurrente que fueron derivadas para verificación de su identificación taxonómica y pruebas de sensibilidad a los antifúngicos, durante julio 2023 hasta junio 2024.

La investigación cumple con los principios bioéticos establecidos en la Declaración de Helsinki y en las Directrices Internacionales para la Investigación Médica de la Organización Mundial de la Salud. Se obtuvo el consentimiento informado de los participantes y se mantuvo la confidencialidad de los datos. La investigación fue aprobada por el Comité de Bioética de la Escuela de Bioanálisis de la Universidad Central de Venezuela.

Identificación de las cepas

Los aislados identificados como complejo *Candida albicans* fueron preservados en agua destilada por Método de Castellani [14] y guardados a temperatura ambiente hasta el momento de realizar el estudio experimental. Posteriormente estos aislados se inocularon en agar Sabouraud dextrosa (ASD, Oxoid®-USA) y se incubaron durante 24-48 h a 35 °C, para constatar su viabilidad y pureza. La identificación taxonómica se realizó mediante pruebas fenotípicas como resistencia a la cicloheximida (agar Mycosel, Oxoid®), producción de pigmento en agar cromógeno (CHROMagar, Oxoid®), visualización de la morfología microscópica en agar harina de maíz e identificación automatizada mediante el equipo Vitek 2 Compact® (bioMérieux, Marcy-l'Étoile, Francia).

Determinación de la actividad de la fosfolipasa

La actividad de la fosfolipasa se determinó por el método semicuantitativo en placa de ASD suplementado con yema de huevo (AS-

DYH) descrito por Echeverría *et al.* [15]. Cada cepa de *C. albicans* fue inoculada en lugares distantes del medio por triplicado e incubada a 35 °C ± 2. Posterior a su crecimiento, se midió con una regla la zona densa y blanca de la hidrólisis bien definida, generada por la actividad enzimática de la levadura a las 24, 48 y 72 h. Se calculó el índice de actividad enzimática (Pz) dividiendo el diámetro de crecimiento de la colonia entre el diámetro de la zona de hidrólisis enzimática [16]. El índice Pz puede tomar valores que van de cero a uno, correspondiendo aquellos más próximos a cero a niveles máximos de actividad enzimática, mientras que los índices con valores próximos o iguales a uno son indicativos de un bajo nivel o ausencia de actividad, respectivamente, de la siguiente forma: 1 (Sin actividad enzimática); 0,90-0,99 (+); 0,80-0,89 (++); 0,70-0,79 (+++); ≤ 0,69 (++++) [16].

Determinación de la actividad de proteasa

La actividad de proteasa se determinó mediante el ensayo de Aoki *et al.* [17], inoculando cada una de las cepas en lugares diferentes en un medio agar base de carbono para levaduras (1,17%) suplementado con 0,2% de albúmina de suero bovino (YCB-BSA), por triplicado, y se incubaron a 35 °C ± 2. Los diámetros de las colonias y de las zonas de precipitación generadas por la actividad enzimática se midieron a las 24, 48, 72 h, hasta los 7 d. Las mediciones, los cálculos de la actividad proteolítica y la interpretación se realizaron de acuerdo con el método de Price *et al.* [16], descrito anteriormente.

Para valorar la actividad de las fosfolipasas y proteasas se utilizaron como control de referencia las cepas *Pichia kudriaavzevii* (*Candida krusei*) ATCC® 6258[18], *Candida parapsilosis* ATCC® 22019, *Candida albicans* ATCC® 28367, *Candida albicans* 36801 y *Candida parapsilosis* ATCC® 22019.

Determinación de la actividad de la hemolisina

La actividad hemolítica se evaluó con modificaciones de las técnicas descritas por De Melo *et al.* [19] y Ortolan *et al.* [20] en cuanto a la procedencia de la sangre y porcentaje de glucosa, en ASD más sangre humana fresca al 5%. Los ensayos se realizaron por triplicado y se incubaron a 35°C ± 2. La lectura fue realizada a las 24 y 48 h. La presencia de hemólisis beta (total) o alfa (parcial) fue considerada como un resultado positivo. La actividad hemolítica (Índice hemolítico, IH) se midió dividiendo el diámetro de la colonia entre la zona de hemólisis más el diámetro de la colonia, siguiendo la metodología descrita por de Paula Menezes *et al.* [21]. La interpretación del IH fue la siguiente: negativo (IH=1); moderado (IH= < 1-0,63); alto (IH= ≤0,63).

El control de calidad para la presencia de actividad hemolítica se utilizó la cepa ATCC®: *Staphylococcus aureus* y para la confirmación del complejo género/especie de *C. albicans* se utilizó la cepa *Candida albicans* ATCC® 10231.

Determinación de la formación de biopelículas

- *Preparación del inóculo para el análisis de biopelículas*. De los aislados obtenidos, previa verificación de viabilidad y pureza, se preparó una suspensión en solución salina estéril al 0,85%, con una turbidez de 0,5 en la escala McFarland (1-5 x10^6 UFC/mL). 200 μL de la suspensión se colocaron en 19,8 mL de caldo infusión cerebro corazón (BHI, Oxoid®), obteniendo así una dilución 1:100 [22].

- *Método en microplacas de poliestireno*. Se utilizaron microplacas de titulación de poliestireno (MPS) de fondo plano, en cuyos pocillos se añadieron 200 μL de la dilución en caldo BHI 1:100, siguiendo la metodología adaptada para *Candida* spp. por Moreno *et al.* [22]. Cada aislado se estudió por triplicado. Para la interpretación de los resultados, se utilizó la metodología estadística establecida por Stepanovic

et al. [23], para la cuantificación de biopelículas en *Staphylococcus* adaptada a microorganismos fúngicos; las mismas fueron clasificadas, realizando las lecturas por densidad óptica (DO) a 490 nm, como: no formadoras (DO < DOc), poco formadoras (DOc < DO < 2DOc), moderadamente formadoras (2DOc < DO < 4DOc) y fuertemente formadoras (4DOc < DO). DOc (punto de corte o cut-off). Se utilizaron como controles positivos para la formación de biopelículas las cepas *C. albicans* ATCC® 28367, *C. albicans* 36801.

Perfil de sensibilidad a los antifúngicos por Vitek 2 Compact®

Las tarjetas AST YSO1® del sistema Vitek 2 Compact® contienen una serie de diluciones seriadas para anfotericina B (0,25 a 16 μg/mL), voriconazol (0,125 a 8 μg/mL) y fluconazol (1 a 64 μg/mL) y se siguieron las recomendaciones del fabricante para la ejecución de las pruebas de sensibilidad [24]. La interpretación de la concentración mínima inhibitoria (CMI) de fluconazol y voriconazol se realizó tomando en cuenta los puntos de corte clínico del documento CLSI [25], mientras que para la interpretación de la CMI de anfotericina B se tomaron en consideración los puntos de corte sugeridos por Pfaller *et al.* [26]. Para el control de calidad en la identificación del complejo *C. albicans* (género y especie) se utilizó la cepa *C. albicans* ATCC® 10231.

Métodos estadísticos

Las variables se describieron utilizando estadística descriptiva y medidas de tendencia central. Se utilizó la prueba de Kolmogorov-Smirnov para verificar la normalidad de los datos cuantitativos. Se utilizaron pruebas estadísticas no paramétricas. Para determinar la correlación entre las variables sensibilidad a los antifúngicos y los factores de virulencia se utilizó la prueba exacta de Fisher y la prueba de correlación de rangos de Spearman. La fuerza de la correlación de los datos pareados se interpretó con el coeficiente de correlación de Spearman (r_s). Se consideró un valor de $p \leq 0,05$ como significancia estadística. El análisis estadístico se realizó utilizando el programa Statgraphics 19® Centurion.

Una limitante del estudio es la cantidad de cepas evaluadas (n=22).

RESULTADOS

Las pacientes con vulvovaginitis candidiásica (VVC) recurrente estaban en edad reproductiva, con edades comprendidas entre 24 y 45 años y una media de 31,5 años. De las 22 cepas analizadas, 17 cepas (77%) expresaron actividad de fosfolipasas como se muestra en la Fig. 1 A y 1 B, seis cepas (27,3%) fueron capaces de producir proteasas (Fig. 1 C y D) y todas las cepas de *C. albicans* evaluadas produjeron hemolisinas (Fig. 1 E y F). A nivel general, evaluando la actividad de estas tres enzimas en los aislados estudiados, 17 (77%) expresaron dos de las enzimas analizadas al mismo tiempo (fosfolipasas y hemolisinas), tres aislados (13,6%) presentaron las tres enzimas de manera simultánea y solo un aislado (4,5%) expresó actividad hemolítica alta; los demás presentaron actividad hemolítica moderada.

La mayoría de las cepas (82%) estudiadas formaron biopelículas, siendo clasificadas como formadoras débiles, cuya DO estuvieron dentro del rango entre 0,1013-0,2024, clasificadas de acuerdo con el valor de la media de las tres lecturas, mientras que el 18% (cuatro cepas) no formó biopelículas conforme a los rangos de DO obtenidos.

De los 22 aislados analizados, 18 cepas fueron resistentes a fluconazol, mientras que cuatro presentaron sensibilidad dependiente de la dosis. En cuanto a la sensibilidad a voriconazol, sólo uno de los aislados fue sensible, cinco aislados presentaron un rango intermedio, mientras que 16 fueron resistentes. No obstante, todos los aislados fueron sensibles a anfotericina B como antifúngico de amplio espectro, como se observa en la Tabla 1.

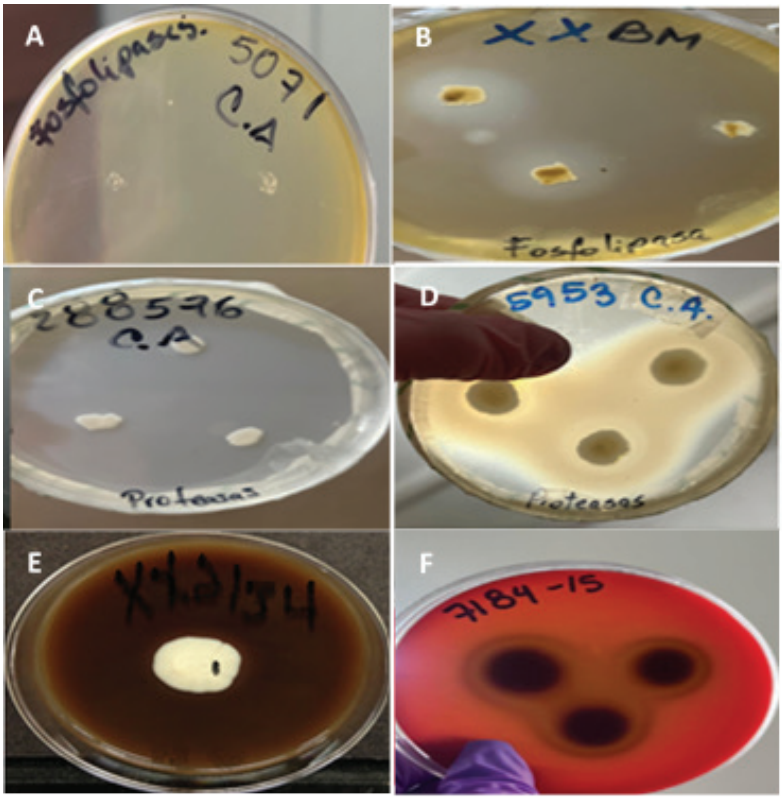

Fig. 1. Actividad de los factores de virulencia de *C. albicans* aisladas de secreciones vaginales de pacientes con VVC recurrente. A: actividad fosfolipasa negativa en ASDYH. B: actividad fosfolipasa positiva en ASDYH. C: actividad proteasa negativa en YCB-BS. D: actividad proteasa positiva en YCB-BSA. E: actividad hemolítica negativa en ASD más sangre humana fresca al 5%. F: actividad hemolítica positiva en ASD más sangre humana fresca al 5%. VVC: vulvovaginitis candidiásica; ASD: agar Sabouraud dextrosa; ASDYH: ASD suplementado con yema de huevo; YCB-BS: agar base de carbono para levaduras suplementado con albúmina de suero bovino.

Tabla 1. Rangos y parámetros estadísticos de sensibilidad de *Candida albicans* a tres antifúngicos por el sistema Vitek 2 Compact®.

Antifúngico	Rangos (μg/mL)	MG	M	DE	Porcentaje (%)			
					S	SDD	I	R
FZ	4 - 64	17,91	64,00	23,77	-	18	-	82
VO	0,12 - 16	2,15	1,00	3,45	4	-	23	73
AB	0,12 - 1	0,40	0,50	0,22	100	-	-	-

FZ: fluconazol. VO: voriconazol. AB: anfotericina B. MG: media geométrica. M: moda. DE: desviación estándar. S: sensibilidad. SDD: sensibilidad dependiente de la dosis. I: intermedio. R: resistente.

La prueba de correlación de rangos de Spearman no pudo ser aplicada para correlacionar los factores de virulencia y los resultados obtenidos con la anfotericina B, debido a que todas las cepas de *C. albicans* ensayadas fueron sensibles a este antifúngico. Sin embargo, se pudo aplicar la prueba exacta de Fisher, mostrando que la asociación entre las variables no fue significativa.

DISCUSIÓN

Candida albicans es el principal agente causal de VVC, enfermedad muy frecuente que afecta aproximadamente al 75% de las mujeres en edad fértil al menos una vez en su vida [2]. El desarrollo de la candidiasis se asocia con una inmunosupresión del huésped, así como con los cambios transcripcionales del hongo en respuesta a un entorno

cambiante del huésped que están prácticamente ausentes durante la colonización, favoreciendo la transición de comensal a patógeno [27], incrementándose la carga fúngica y la alteración de la microbiota vaginal (disminución de *Lactobacillus* spp. o alteración en la distribución de las especies). Esto a su vez promueve la formación de hifas que pueden penetrar directamente las células epiteliales de la mucosa vaginal o desarrollarse entre las uniones intercelulares, lo cual genera daño y produce consecuentemente una respuesta inflamatoria que se asocia a la aparición de las manifestaciones clínicas de la infección [28].

Las enzimas hidrolíticas que degradan los fosfolípidos presentes en la membrana de la célula fúngica. Las fosfolipasas, permiten la invasión de la célula al tejido del huésped, causando un importante daño tisular [11]. En este estudio, las cepas con actividad fosfolipasa fueron similares a las obtenidas por Samaranayake *et al.* [29], donde el 79% de las cepas de *C. albicans* analizadas presentaron actividad fosfolipasa; y discordantes con los obtenidos por Panizo *et al*. [14], donde el 100% de las cepas de *C. albicans* mostraron actividad fosfolipasa.

Por otra parte, enzimas como las proteasas favorecen la colonización, invasión de tejidos y evasión del sistema inmunológico al degradar proteínas de defensa [11]. Estudios como los de Pandey *et al*. [30], hallaron que *C. albicans* mostró fuerte actividad de la proteasa en un 93,75% [30]; igualmente Sriphannam *et al.* [11], y Panizo *et al*.[13], reportaron que el 100% de las cepas de *C. albicans* analizadas presentaron actividad de la proteasa, estos resultados fueron diametralmente opuestos a los obtenidos en el presente estudio, donde sólo el 27,3% de los aislados analizados presentó actividad proteasa. Las diferencias observadas con respecto a la actividad fosfolipasa y proteasa pudieran estar relacionadas con varios factores tales como: variaciones en el tiempo de la incubación, la fórmula de preparación del medio de cultivo y/o el lugar de procedencia de las muestras biológicas utilizadas para el aislamiento de *C. albicans* en cada estudio. De igual forma, es importante destacar que la patogenia de *C. albicans* también está asociada a factores dependientes del huésped y no se relaciona con un único factor de virulencia, sino con el conjunto de éstos [31].

Otro mecanismo de virulencia de *C. albicans* es la producción de enzimas hemolíticas capaces de lisar glóbulos rojos, descomponer la hemoglobina y liberar el hierro, promoviendo así la supervivencia a largo plazo de *Candida* y la invasión por parte de las hifas a los tejidos del hospedador [21,32]. El 100 % de las cepas estudiadas fueron capaces de producir hemolisinas, lo cual se relaciona con la investigación realizada por de Paula *et al.* [33] quienes observaron que la mayoría de las cepas de *C. albicans* (71,4%) expresaron alta actividad hemolítica y, además, reflejaron mayor capacidad para producir hemolisinas con respecto a otras especies de *Candida* estudiadas. Sin embargo, en la presente investigación la mayoría de las cepas (95%) presentó un índice hemolítico moderado y sólo una cepa (4,5%) presentó una actividad hemolítica alta. En otro estudio, realizado por Pakshir *et al*. [34], también se observó actividad hemolítica en todos los aislados de *C. albicans* analizados.

La formación de biopelículas como mecanismo de virulencia en *C. albicans permite* la unión compacta a superficies vivas o inertes, colonización de tejidos, incremento de la patogenicidad, cooperación metabólica, captura de nutrientes y comunicación célula a célula, aumentando de esta forma su tolerancia a ambientes hostiles y al tratamiento antifúngico [35]. Moreno *et al*. [22], estudiaron la capacidad de formación de biopelículas en 19 aislados provenientes de secreciones vaginales, informando que todos fueron capaces de formar biopelículas, donde 14 (73,7%) fueron formadoras débiles, dos (10,5%) formadoras moderadas y tres (15,8%) formadoras fuertes [1].

El presente estudio el 82% de las cepas estudiadas formaron biopelículas y todas fueron clasificadas como formadoras débiles. De forma similar, de Paula *et al*. [33], registraron que el 86,5% de las cepas de *C. albicans* estudiadas fueron capaces de producir biopelículas, cuya clasificación fue: 42,8% como formadoras débiles y 42,8% como formadoras moderadas. Así mismo, Morales-López *et al*. [36], informaron que de 300 aislamientos de *C. albicans,* 246 resultaron positivos a la formación de biopelículas: 85 aislados (28%) se clasificaron como fuertemente formadores; 86 (29%) como formadores moderados y 74 (25%) como formadores débiles. *C. albicans* tiene un amplio potencial para formar biopelículas, propiciando la invasión y diseminación de la infección, ya que confiere protección a las levaduras dentro de las capas más internas de las mucosas, impidiendo la penetración de los antifúngicos y su efecto farmacológico, favoreciendo la supervivencia del hongo y la aparición de episodios recurrentes de la infección [35,37].

La resistencia a los antifúngicos es un tema de gran preocupación, en especial la resistencia a los azoles como el fluconazol, que es el más utilizado para el tratamiento de la candidiasis. La resistencia a los antifúngicos ocurre con frecuencia en entornos clínicos y puede estar relacionado a factores como la exposición prolongada a estos fármacos [7,37]. Además, se ha demostrado que la resistencia a los azoles trae como resultado una estimulación de los factores de virulencia dependiendo de la especie [38]. Los resultados obtenidos de las pruebas de sensibilidad a los antifúngicos son similares a un estudio realizado por Moreno *et al*. [1], donde encontraron que de los 19 aislados de *C. albicans* provenientes de secreciones vaginales, todos fueron sensibles a anfotericina B, mientras que el 89,5% presentaron elevada resistencia a los azoles evaluados (voriconazol, itraconazol y fluconazol), enfatizando que el fluconazol exhibió el mayor porcentaje de cepas resistentes.

La elevada resistencia a los azoles se puede asociar a una exposición prolongada de *C. albicans* a fluconazol. Por otra parte, la anfotericina B podría ser una alternativa terapéutica para tratar la VVC, sin embargo, este antifúngico no posee presentación oral [1]. La nistatina, que también es un polieno, tiene presentación tópica, por lo cual pudiera ser utilizada como segunda opción de tratamiento en pacientes con VVC recurrente [1,6].

Las cepas de *C. albicans* ensayadas frente a fluconazol resultaron sensibles dependientes de la dosis (SDD) y resistentes (R), mientras que frente a voriconazol fueron intermedias (I) y R; ninguna mostró sensibilidad a los antifúngicos, por lo tanto, los resultados de la CMI no poseen una distribución normal en términos estadísticos, al igual que la anfotericina B, ya que todas las cepas ensayadas fueron sensibles al antifúngico y, al no obtener cepas resistentes, la distribución de las CMI tampoco es normal. Probablemente por esta razón, no se observaron los resultados reportados en la literatura donde los factores de virulencia están relacionados a la resistencia antifúngica [7,38]. Además la muestra fue muy pequeña, intencional y no probabilística de pacientes con VVC recurrente, en estas pacientes, *C. albicans* suele expresar resistencia secundaria a fluconazol, debido a que es el tratamiento de primera elección indicado con frecuencia para la afección de VVC [10,39]. El uso reiterado de fluconazol genera presión selectiva en la microbiota vaginal, seleccionando resistencia secundaria, y dicha presión selectiva también genera la presencia de otras especies de *Candida* causantes de VVC [40,41].

La resistencia a fluconazol puede inducir resistencia cruzada a otros azoles que se utilizan como opciones de tratamiento alternativo en la VVC, como voriconazol e itraconazol [42]. Esto se pudo observar en los resultados obtenidos al ensayar las cepas de *C. albicans* a fluconazol y voriconazol, similares a los encontrados por Moreno *et al*. [1], quienes demostraron estadísticamente la presen-

cia de reacción cruzada en cepas de *C. albicans* aisladas de secreciones vaginales.

Finalmente, los resultados obtenidos evidenciaron que los factores de virulencia como las fosfolipasas, hemolisinas, formación de biopelículas y en menor grado la presencia de proteasas, son factores de virulencia que están presentes en las cepas *C. albicans* evaluadas. Aunque no se encontró una relación directa de estos factores con la resistencia al fármaco de primera línea, el fluconazol, ni tampoco con voriconazol, estos hallazgos podrían haber estado influenciados por el tamaño de la muestra, por lo tanto, es necesario aumentar el número de esta e incluir cepas de *C. albicans* sensibles a los antifúngicos azólicos. La expresión de los factores de virulencia de *C. albicans* estudiados se considera independiente a la sensibilidad antifúngica; su papel es generar un efecto estimulante que permite con mayor facilidad la invasión, multiplicación y daño a los tejidos del hospedador por parte del hongo, produciendo el cuadro clínico de VVC recurrente, sin estar asociado con la presencia de resistencia a los fármacos azólicos. Se sugiere continuar con esta investigación valorando un mayor número de aislados que incluyan cepas con sensibilidad y resistencia a los azoles para definir si los factores de virulencia analizados están relacionados con la resistencia a los antífúngicos como lo han descrito otros autores.

Financiamiento

Este estudio ha sido financiado por el Departamento de Microbiología del Instituto Médico La Floresta y con fondos internos de la Cátedra de Bacteriología de la Escuela de Bioanálisis de la Universidad Central de Venezuela.

Conflicto de intereses

Los autores declaran no tener conflictos de intereses.

Número ORCID de los autores

- Xiomara Moreno Calderón (XMC): 0000-0002-5924-6158
- Angie Cantero Alvarado (ACA): 0009-0006-8845-6759
- María G. Vivas Parababire (MGVP): 0009-0002-0204-4763
- María M. Panizo Domínguez (MMPD): 0000-0001-8438-4993

Contribución de los autores

XMC Conceptualización y diseño del estudio, investigación; análisis e interpretación de resultados, preparación, redacción, revisión y edición del manuscrito final. ACA y MGVP Investigación, análisis, interpretación de resultados y edición del manuscrito final. MMPD estadístico y análisis, revisión y edición del manuscrito final.

REFERENCIAS

1. **Moreno X, Núñez G, Rosales O, Ferrara G, Panizo MM.** Evaluación de factores de virulencia y perfil de susceptibilidad en *Candida albicans* provenientes de secreciones vaginales. Acta Cient Soc Venez Bioanal Esp. 2021; 24(2):70-78. Disponible en: http://saber.ucv.ve/ojs/index.php/rev_ACSVBE/article/view/26181/144814492171
2. **Leite-Jr DP, Vivi-Oliveira VK, Maia MLS, Macioni MB, Oliboni GM, de Oliveira, et al.** The *Candida* Genus complex: biology, evolution, pathogenicity and virulence, beyond the *Candida albicans* paradigm. A comprehensive review. Virol Immunol J. 2023; 7(2):000331. *https://doi.org/10.23880/vij-16000331.*
3. **Willems HME, Ahmed SS, Liu J, Xu Z, Peters BM**. Vulvovaginal candidiasis: A current understanding and burning questions. J Fungi (Basel). 2020; 6(1):27. *https://doi.org/10.3390/jof6010027.*
4. **Arenas Guzmán R.** Candidosis (Candidiasis). En: Arenas Guzmán R, editor. Mi-

cología Médica Ilustrada. 5ª ed. México: McGraw-Hill; 2014. p. 242-248. Disponible en: https://biblioteca-digital-cefamus.webnode.mx/micologia-medica2/

5. **Life Worldwide.** Mucosal *Candida*. Fungal Education. 2019 [citado el 28 de diciembre de 2024]. Disponible en: https://en.fungaleducation.org/mucosal-candida/.
6. **Miró MS, Rodríguez E, Vigezzi C, Icely PA, Gonzaga de Freitas Araújo M, Riera FO, et al.** Candidiasis vulvovaginal: una antigua enfermedad con nuevos desafíos. Rev Iberoam Micol. 2017; 34(2):65-71. *https://doi.org/10.1016/j.riam.2016.11.006.*
7. **Mohammadi F, Ghasemi Z, Familsatarian B, Salehi E, Sharifynia S, Barikani A, et al.** Relationship between antifungal susceptibility profile and virulence factors in *Candida albicans* isolated from nail specimens. Rev Soc Bras Med Trop. 2020; 53: e20190214. *https://doi.org/10.1590/0037-8682-0214-2019.*
8. **Achkar JM, Fries BC.** *Candida* infections of the genitourinary tract. Clin Microbiol Rev. 2010; 23(2):253-273. *https://doi.org/10.1128/cmr.00076-09.*
9. **Cassone A.** Vulvovaginal *Candida albicans* infections: pathogenesis, immunity and vaccine prospects. BJOG. 2015; 122(6):785-794. *https://doi.org/10.1111/1471-0528.12994.*
10. **Sobel JD, Sobel R.** Current treatment options for vulvovaginal candidiasis caused by azole-resistant *Candida* species. Expert Opin Pharmacother. 2018; 19(9):971-977. *https://doi.org/10.1080/14656566.2018.1476490.*
11. **Sriphannam C, Nuanmuang N, Saengsawang K, Amornthipayawong D, Kummasook A.** Anti-fungal susceptibility and virulence factors of *Candida* spp. isolated from blood cultures. J Mycol Med. 2019; 29(4):325-330. *https://doi.org/10.1016/j.mycmed.2019.08.001.*
12. **Lamoth F, Lockhart SR, Berkow EL, Calandra T.** Changes in the epidemiological landscape of invasive candidiasis. J Antimicrob Chemother. 2018; 73(1):i4-i13. *https://doi.org/10.1093/jac/dkx444.*
13. **Panizo MM, Reviákina V, Flores Y, Montes W, González G.** Actividad de fosfolipasas y proteasas en aislados clínicos de *Candida* spp. Rev Soc Ven Microbiol. 2005; 25(2):64-71. Disponible en: https://ve.scielo.org/scielo.php?pid=S1315-25562005000200006&script=sci_arttext.
14. **Castellani A.** Further researches on the long viability and growth of many pathogenic fungi and some bacteria in sterile distilled water. Mycopathol Mycol Appl. 1963; 20:1-6. *https://doi.org/10.1007/bf02054872.*
15. **Echeverría A, Durante AG, Arechavala A, Negroni R.** Estudio comparativo de dos medios de cultivo para la detección de la actividad de fosfolipasa en cepas de *Candida albicans* y *Cryptococcus neoformans*. Rev Iberoam Micol. 2002; 19:95-98. Disponible en: https://reviberoammicol.com/2002-19/095098.pdf.
16. **Price MF, Wilkinson ID, Gentry LO.** Plate method for detection of phospholipase activity in *Candida albicans*. Sabouraudia. 1982; 20(1):7-14. *https://doi.org/10.1080/00362178285380031.*
17. **Aoki S, Ito-Kuwa S, Nakamura Y, Masuhara T.** Comparative pathogenicity of wild-type strains and respiratory mutants of *Candida albicans* in mice. Zentralbl Bakteriol. 1990; 273:332-343. *https://doi.org/10.1016/S0934-8840(11)80437-8.*
18. **Cruz Choappa R, Vieille Oyarzo P.** Nuevos nombres para antiguas especies fúngicas de importancia médica. Rev Chil Infectol. 2023; 40(5): 461-464. *http://doi.org/10.4067/s0716-10182023000500461.*
19. **De Melo Riceto ÉB, de Paula Menezes R, Penatti MPA, dos Santos Pedroso R.** Enzymatic and hemolytic activity in different *Candida* species. Rev Iberoam Micol. 2015; 32(2):79-82. *https://doi.org/10.1016/j.riam.2013.11.003.:79-82.*
20. **Ortolan Rörig KC, Colacite J, Abegg MA.** Produção de fatores de virulência *in vitro* por espécies patogênicas do gênero *Candida*. Rev Soc Bras Med Trop. 2009; 42(2):225-227. *https://doi.org/10.1590/S0037-86822009000200029.*

21. **de Paula Menezes R, de Melo Riceto ÉB, Borges AS, de Brito Roder DV, dos Santos Pedroso R.** Evaluation of virulence factors of *Candida albicans* isolated from HIV-positive individuals using HAART. Arch Oral Biol. 2016; 66:61-65. *https://doi.org/10.1016/j.archoralbio.2016.02.004.*
22. **Moreno X, Ventura M, Panizo MM, Garcés MF.** Evaluación de la formación de biopelículas en aislamientos bacterianos y fúngicos por el método semicuantitativo de microtitulación con cristal violeta y el cualitativo de agar con rojo Congo. Biomédica. 2023; 43(Suppl 1):77-88. *https://doi.org/10.7705/biomedica.6732.*
23. **Stepanovic S, Vukovic D, Dakic I, Savic B, Svabic-Vlahovic M.** A modified microtiter-plate test for quantification of staphylococcal biofilm formation. J Microbiol Methods. 2000; 40(2):175-179. *https://doi.org/10.1016/s0167-7012(00)00122-6.*
24. **Ochiuzzi ME, Arechavala A, Guelfand L, Maldonado I, Soloaga R, Red de Micología CABA, Argentina.** Evaluación de las tarjetas AST-YSO1 del sistema Vitek 2 para determinar la sensibilidad a antifúngicos de levaduras del género *Candida*. Rev Argent Microbiol. 2014; 46(2):111-118. *https://doi.org/10.1016/S0325-7541(14)70058-6.*
25. **Clinical and Laboratory Standards Institute (CLSI).** Performance Standards for Antifungal Susceptibility Testing of Yeasts. 2nd ed. CLSI Supplement M60- Ed 2. Wayne, PA: Clinical and Laboratory Standards Institute; 2020. Disponible en: wwiw.clsi.org.
26. **Pfaller MA, Espinel-Ingroff A, Canton E, Castanheira M, Cuenca-Estrella M, Diekema DJ, et al.** Wild-type MIC distributions and epidemiological cutoff values for amphotericin B, flucytosine, and itraconazole and *Candida* spp. as determined by CLSI broth microdilution. J Clin Microbiol. 2012; 50(6):2040-2046. *https://doi.org/10.1128/JCM.00248-12.*
27. **Hube B.** From commensal to pathogen: stage- and tissue-specific gene expression of *Candida albicans*. Curr Opin Microbiol. 2004;7(4):336–341. *https://doi.org/10.1016/j.mib.2004.06.003.*
28. **Jacobsen ID.** The role of host and fungal factors in the commensal-to-pathogen transition of *Candida albicans*. Curr Clin Microbiol Rep. 2023; 10(2):55-65. *https://doi.org/10.1007/s40588-023-00190-w.*
29. **Samaranayake LP, Raeside JM, Macfarlane TW.** Factors affecting the phospholipase activity of *Candida* species *in vitro*. Sabouraudia. 1984; 22(3):201-207. *https://doi.org/10.1080/00362178485380331.*
30. **Pandey N, Gupta MK, Tilak R.** Extracellular hydrolytic enzyme activities of the different *Candida* spp. isolated from the blood of the intensive care unit-admitted patients. J Lab Physicians. 2018; 10(4):392-396. *https://doi.org/10.4103/JLP.JLP_81_18.*
31. **Hernández-Solís SE, Rueda-Gordillo F, Rojas-Herrera RA.** Actividad de la proteinasa en cepas de *Candida albicans* aisladas de la cavidad oral de pacientes inmunodeprimidos, con candidiasis oral y sujetos sanos. Rev Iberoam Micol. 2014; 31(2):137-140. *https://doi.org/10.1016/j.riam.2013.09.003.*
32. **Tiwari P, Aishwarya N, Tiwari K, Tanushree P, Munesh Kumar G, Tilak R.** *In vitro* determination of antifungal susceptibility and virulence factors in *Candida* species causing candidemia in North India region. Discov Public Health. 2024: 21:50. *https://doi.org/10.1186/s12982-024-00175-0.*
33. **de Paula Menezes R, Silva FF, Melo SGO, Alves PGV, Brito MO, de Souza Bessa MA, et al.** Characterization of *Candida* species isolated from the hands of the healthcare workers in the neonatal intensive care unit. Med Mycol. 2019; 57(5):588-594. *https://doi.org/10.1093/mmy/myy101.*
34. **Pakshir K, Bordbar M, Zomorodian K, Nouraei H, Khodadadi H.** Evaluation of CAMP-like effect, biofilm formation, and discrimination of *Candida africana* from vaginal *Candida albicans* species. J Pathog. 2017; 2017:7126258. *https://doi.org/10.1155/2017/7126258.*
35. **Castrillón LE, Palma A, Padilla MC.** Biopelículas fúngicas. Dermatol Rev Mex. 2013; 57 (5):350-361. Disponible en: https://www.esi.academy/wp-content/uploads/Biopeliculas_fungicas.pdf

36. **Morales-López S, Ustate K, Pedrozo Z, Torres Y.** Tipificación bioquímica y evaluación de la patogenicidad de aislamientos vulvovaginales del complejo *Candida albicans*. Biomed. 2023; 43(1):194-205. *https://doi.org/10.7705/biomedica.6861.*
37. **López-**Ávila K, Dzul-Rosado KR, Lugo-Caballero C, Arias-León JJ, Zavala-Castro JE. Mecanismos de resistencia antifúngica de los azoles en *Candida albicans*. Una revisión. Rev Biomédica. 2016; 27(3):127-136. *https://doi.org/10.32776/revbiomed.v27i3.541.*
38. **Siddiqui R, Mendiratta D, Siddiqui A, Rukadikar A.** A study of the association between virulence factors and antifungal susceptibility profile of *Candida* species recovered from cases of vulvovaginal candidiasis. J Family Med Prim Care. 2023; 12(1):152-159. *https://doi.org/10.4103/jfmpc.jfmpc_1479_22.*
39. **Berkow E, Lockhart S.** Fluconazole resistance in *Candida* species: a current perspective. Infect Drug Resist. 2017; 10:237-245. *https://doi.org/10.2147/idr.s118892.*
40. **Tapia C.** Candidiasis vulvovaginal. Rev Chil Infectol. 2008; 25(4):312. *https://doi.org/10.4067/S0716-10182008000400016.*
41. **Makanjuola O, Bongomin F, Fayemiwo SA.** An update on the roles of non-*albicans Candida* species in vulvovaginitis. J Fungi (Basel). 2018; 4(4):121. *https://doi.org/10.3390/jof4040121*
42. **Quindós G, Cantón E, Espinel A, López J, Pemán F, Mazuelos E, et al.** Resistencia a los fármacos antifúngicos. En: Quindós G. Micología Clínica. 1era ed. Elsevier; Barcelona, España: 2015. p 265-278. Disponible en: https://books.google.co.ve/books?id=MuJiCAAAQBAJ&printsec=frontcover&hl=es#v=onepage&q&f=false

Invest Clin 67(1): 57 - 72, 2026 https://doi.org/10.54817/IC.v67n1a05

Study on the predictive model of response of patients with inflammatory bowel disease to infliximab treatment.

Ru Ding[1], Mengdi Fan[2], Juanjuan Gu[1] and Zhangning Zhou[1]

[1]Department of Gastroenterology, Shulan (Hangzhou) Hospital, Shulan International Medical College, Zhejiang Shuren University, Hangzhou, P.R. China.
[2]Department of General Practice, Shulan (Hangzhou) Hospital, Shulan International Medical College, Zhejiang Shuren University, Hangzhou, P.R, China.

Keywords: Inflammatory Bowel Diseases; Infliximab; Drug Therapy; Response; Disease forecasting models.

Abstract. This study aimed to develop a predictive model for how patients with inflammatory bowel disease (IBD) respond to infliximab (IFX) treatment. One hundred adult IBD patients admitted to Shulan (Hangzhou) Hospital from August 2023 to November 2024 were included and divided into response and non-response groups based on their reaction to IFX. The response group consisted of 57 patients (57.0%), while the non-response group had 43 patients (43.0%). Clinical data, including gender, age, BMI, disease type (Crohn's disease/ulcerative colitis), disease activity indices (CDAI/UCAI), history of IFX treatment, and infusion reactions, were collected and compared between the two groups. Additionally, biomarker levels, such as TNF-α, CRP, calprotectin, anti-infliximab antibody (ATI), IL-6, and IL-8, were measured during the midcourse of IFX treatment. Single-factor analysis identified variables that differed, and logistic regression showed that calprotectin level (OR=1.099, 95%CI=1.039-1.163), ATI (OR=3.756, 95%CI=1.222-11.546), IL-6 (OR=1.261, 95%CI=1.069-1.488), and IL-8 (OR=1.014, 95%CI=1.004-1.024) were key factors influencing treatment response ($p < 0.05$). A nomogram was created using these factors to predict treatment response in IBD patients. ROC analysis showed AUC values of 0.809, 0.762, 0.850, and 0.775 for calprotectin, ATI, IL-6, and IL-8, respectively, with corresponding 95% confidence intervals. The calibration curve indicated good model fit. These findings underscore the important roles of these cytokines in IBD pathogenesis and the action of IFX, as well as the high predictive power of the nomogram model.

Corresponding author: Zhangning Zhou. Department of Gastroenterology, Shulan (Hangzhou) Hospital, Shulan International Medical College, Zhejiang Shuren University, Hangzhou 310022, P.R. China.
Email: zjsrxy2024@hotmail.com

Estudio sobre el modelo predictivo de la respuesta de los pacientes con enfermedad inflamatoria intestinal al tratamiento con infliximab.

Invest Clin 2026; 67 (1): 57 – 72

Palabras clave: Enfermedades Inflamatorias del Intestino; Infliximab; Tratamiento Farmacológico; Respuesta; Modelos de predicción de enfermedades.

Resumen. Este estudio tuvo como objetivo desarrollar un modelo predictivo de la respuesta de los pacientes con enfermedad inflamatoria intestinal (EII) al tratamiento con infliximab (IFX). Se incluyeron un total de 100 pacientes adultos con EII ingresados en el Hospital Shulan (Hangzhou) desde agosto de 2023 hasta noviembre de 2024, y se dividieron en grupos de respuesta y no respuesta según su reacción al IFX. El grupo de respuesta tenía 57 pacientes (57,0%), mientras que el de no respuesta, 43 (43,0%). Se recolectaron y compararon datos clínicos, como género, edad, IMC, tipo de enfermedad (Crohn/colitis ulcerosa), índices de actividad de la enfermedad (CDAI/UCAI), historial de tratamiento con IFX y reacciones a la infusión, entre ambos grupos. Además, se midieron los niveles de biomarcadores, incluidos TNF-α, PCR, calprotectina, ATI, IL-6 e IL-8, durante el período intermedio del tratamiento con IFX. El análisis de variables individuales identificó diferencias significativas, y el análisis de regresión logística reveló que los niveles de calprotectina (OR=1,099, IC95%=1,039-1,163), ATI (OR=3,756, IC95%=1,222-11,546), IL-6 (OR=1,261, IC95%=1,069-1,488) e IL-8 (OR=1,014, IC95%=1,004-1,024) eran factores clave que influyen en la respuesta al tratamiento ($p<0,05$). Se construyó un nomograma basado en estos factores para predecir la respuesta al tratamiento en pacientes con EII. El análisis de la curva ROC mostró valores de AUC de 0,809, 0,762, 0,850 y 0,775 para calprotectina, ATI, IL-6 e IL-8, respectivamente, con los rangos del IC del 95% correspondientes. La curva de calibración indicó un buen ajuste del modelo. Estos hallazgos destacan el papel importante de estas citocinas en la patogénesis de la EII y en el mecanismo terapéutico del IFX, así como el alto valor predictivo del nomograma.

Received: 29-06-2025 *Accepted: 23-11-2025*

INTRODUCTION

Inflammatory Bowel Disease (IBD) is a complex, chronic gastrointestinal inflammatory condition that mainly includes Crohn's disease and ulcerative colitis. Its pathogenesis has not been fully understood yet [1]. Globally, the incidence and prevalence of IBD are continuously rising, especially in Western developed countries. However, in recent years, its incidence has also sharply increased in newly industrialized regions like Asia [2]. IBD causes long-term pain and suffering for patients, seriously affecting their quality of life, and also places a significant economic burden on the healthcare system [3].

The approach to treating IBD has shifted greatly from traditional medications to biological therapies. During the era of conventional treatments, 5-aminosalicylic acid drugs, corticosteroids, and immunosuppressants were the primary options for managing IBD. However, these medications often faced challenges such as limited effectiveness and notable side effects, making it difficult to fully meet clinical needs [4, 5]. With a deeper understanding of IBD's causes, especially the development of targeted therapies aimed at inflammatory mediators like tumor necrosis factor (TNF), there has been groundbreaking progress in IBD treatment. Infliximab (IFX), the first TNF-α inhibitor approved for treating IBD, effectively reduces intestinal inflammation and significantly improves patients' symptoms and quality of life by specifically binding to and neutralizing TNF-α [6, 7]. The successful use of infliximab not only offers new treatment options for IBD patients but also encourages widespread use and ongoing research of biological agents in managing IBD.

Although IFX has shown a remarkable curative effect in the treatment of IBD, there are significant individual differences in patients' treatment response. Some patients responded well to IFX, achieving rapid symptom relief and a significant reduction in disease activity. However, some patients exhibit poor responses and even primary or secondary treatment failure. The heterogeneity of this therapeutic response is a key problem that urgently requires resolution in the treatment of IBD [8].

Heterogeneity in treatment response not only affects patients' clinical prognosis but also increases medical costs and psychological burden. For patients with poor response, it may be necessary to try other biological agents or immunosuppressants, which not only increase treatment costs but may also bring additional drug-related side effects and risks [9,10]. In addition, heterogeneity in treatment response poses challenges for physicians in developing treatment plans. Doctors need to provide patients with personalized treatment programs, given limited medical resources, to achieve optimal treatment outcomes.

To optimize treatment strategies for IBD patients and improve IFX efficacy, researchers have begun exploring factors that affect treatment response. These factors include, but are not limited to, the patient's age, sex, disease type, disease activity, previous treatment history, complications, serological marker levels, and genetic background[11,12]. However, given the complexity of IBD pathogenesis and interpatient variability, it is often difficult for a single factor to fully account for the heterogeneity of treatment responses. Therefore, it has become a challenging and forward-looking research direction to develop a predictive model that comprehensively considers multiple factors and individually predicts the treatment response of IBD patients to IFX [13,14].

A prediction model is a mathematical system based on large datasets that generates predictions for specific events or outcomes by analyzing and processing input data. In medicine, predictive models are widely used in areas including disease diagnosis, prognosis assessment, treatment strategy selection, and others [15,16]. In the treatment of IBD, the potential of prediction models also remains broad [17, 18].

First, the prediction model can help physicians more accurately evaluate IBD patients' responses to infliximab, enabling more personalized treatment plans. Using the model, doctors can identify patients unlikely to respond to infliximab in advance and adjust treatment strategies accordingly to avoid unnecessary drug use and waste of medical resources [19]. Additionally, the model can suggest other potentially effective treatments or strategies tailored to individual patient conditions, thereby improving overall treatment outcomes. Second, the prediction model can also offer more comprehensive health management services for patients with IBD. By regularly monitoring relevant

indicators and dynamically evaluating them with the model, healthcare providers can detect changes in patients' conditions promptly and implement appropriate interventions, effectively preventing disease recurrence and complications. This approach not only enhances patients' quality of life but also helps reduce medical costs and social burdens [20, 21]. Finally, research on the prediction model can also advance understanding of IBD's pathogenesis and treatment strategies. By analyzing the key factors identified by the model, researchers can further uncover the molecular mechanisms and immune regulatory networks involved in IBD, providing a theoretical basis and experimental evidence for the development of new drugs and therapies [22]. This will promote continuous innovation and progress in IBD treatment.

Given the variability in IBD patients' responses to infliximab and the wide-ranging applications and challenges of predictive models in IBD treatment, this study aims to develop a predictive model for infliximab response in IBD patients through retrospective analysis. It will utilize existing medical resources, gather comprehensive patient data, and apply scientific methods to clean and standardize the data, build an accurate and reliable prediction model, and rigorously validate and evaluate it. The importance of this study lies in: providing more personalized treatment plans for IBD patients, enhancing treatment efficiency and success rates, reducing medical costs and patient burden, and equipping doctors with more precise tools for disease management and prediction. This enables timely detection of changes in patients' conditions and the implementation of appropriate interventions to improve overall treatment outcomes and quality of life. Additionally, it promotes an in-depth understanding of IBD pathogenesis and treatment strategies, offers a theoretical basis and experimental evidence for developing new therapies, and supports continuous innovation and advancement in IBD treatment.

PATIENTS AND METHODS

One hundred adult patients with IBD admitted to Shulan (Hangzhou) Hospital, Shulan International Medical College, Zhejiang Shuren University, from August 2023 to November 2024 were included.

Inclusion criteria

- Inflammatory bowel disease (IBD) was diagnosed by professional doctors through endoscopy and imaging findings.
- No recent (within six months) treatment with other biological agents or immunosuppressants.
- 20~65 years old.
- Patients treated with infliximab for a certain period (more than 14 weeks).
- The patient and his family agreed and signed the informed consent form.

Exclusion criteria

- Clinical data were incomplete.
- Have a clear history of infection in the respiratory system or urinary system recently.
- Taking aspirin and other anticoagulants recently.
- Complicated with serious diseases such as heart, liver, kidney, biliary system, and hematopoietic system.
- Combined with autoimmune diseases.
- Have a history of trauma and operation during pregnancy and within three months.
- Previous history of biological treatment.

METHOD

Baseline data collection

Baseline data of all IBD patients were collected before the initiation of infliximab

(IFX) treatment, including gender, age, BMI index, disease type [Crohn's disease (CD) or ulcerative colitis (UC)], baseline disease activity [Crohn's disease activity index (CDAI) [23] and ulcerative colitis activity index (UCAI) [24]], prior IFX treatment history, and the occurrence of infusion-related reactions (e.g., chest tightness or chest pain) during previous treatments. In addition, baseline biomarkers—such as serum levels of tumor necrosis factor-α (TNF-α), C-reactive protein (CRP), anti-Infliximab antibody (ATI), interleukin-6 (IL-6), interleukin-8 (IL-8), and fecal calprotectin—were measured prior to treatment initiation to assess their predictive value for treatment response.

Assessment instrument

The CDAI score consists of many factors, including symptoms (such as abdominal pain, diarrhea, weight loss, etc.), signs (such as abdominal mass, perforation, intestinal obstruction, etc.), laboratory indicators (such as hemoglobin level and white blood cell count) and complications (such as peripheral arthritis, skin lesions, etc.). The score ranges from 0 to 600, and higher scores indicate more severe disease. Specific scoring criteria: remission period: < 150 points; mild activity period: 150~220 points; moderate activity period: 221~450 points; severe activity period: > 450 points.

The UCAI score is primarily based on patients' clinical manifestations, including defecation frequency, presence of blood in stool, endoscopic findings, and physicians' overall assessment. For example, the improved Mayo scoring system is a common form of UCAI, and its scoring comprises four components: daily defecation frequency, presence of blood in stool, degree of mucosal injury under endoscopic examination, and overall physician assessment. The scoring range is usually 0~12 points. Specific grading: remission period: UCAI score < 2; mild activity period: 2~3 points; moderate activity period: 4~6 points; severe activity period: > 6 points.

Biochemical index detection method

Four mL of fasting venous blood was routinely collected and placed in a disposable vacuum blood collection tube without anticoagulant for later use. The ELISA method (the kits were purchased from Beijing Baiao Innovation Technology Co., Ltd., Beijing Suolaibao Technology Co., Ltd., Aimeijie Technology Co., Ltd., Jianglai Biology and Wuhan Feien Biotechnology Co., Ltd. in turn; the serial numbers/goods numbers are (E-EL-H0109c, SEKH-0138, KA4933, JL14113, QT-EH0205) was used to detect serum tumor necrosis factor -α (TNF-α), C-reactive protein (CRP), anti-infliximab antibody (ATI), and interleukins (IL).

An ELISA kit (article number HR0593; purchased from Suzhou Herui Pharmaceutical Technology Co., Ltd.) was used to measure calprotectin levels in the supernatant of routinely collected fecal samples from patients.

The above indicators are included in the baseline data.

Response vs. Non-response evaluation standard

Based on post-IFX treatment responses, patients were classified into a response group and a non-response group.

Response group: After treatment, clinical symptoms such as diarrhea, abdominal pain, bloody stool, and intestinal absorption disorder resolved or improved significantly, and no new complications, including oral ulcer, gallstone, arthritis, and gastrointestinal bleeding, occurred. Colonoscopy showed that intestinal mucosal inflammation, including congestion, edema, erosion, and ulceration, was significantly reduced or absent. Intestinal mucosal healing is good, as evidenced by reduced ulcer size, increased mucosal smoothness, and reduced submucosal edema. The intestinal stenosis or dilatation has improved, and intestinal patency has increased.

Unresponsive group: there was no significant change or aggravation of clinical symptoms after treatment; symptoms such

as diarrhea, abdominal pain, and others persisted or worsened. New complications may have occurred, or the original complications may have been aggravated. Colonoscopy showed that there was no significant change or aggravation of intestinal mucosal inflammation, such as the expansion of the lesion scope and the increase in ulcer depth. Intestinal stenosis or dilatation has not been improved or aggravated.

Ethical considerations

This study strictly adheres to the principles of the Declaration of Helsinki, and all research procedures comply with international ethical standards. Strictly adheres to ethical principles to ensure the rationality of the research design, the compliance with data use, and the full protection of participants' privacy. The research should aim to improve treatment effectiveness, respect the rights and interests of all participants, avoid bias, and ensure the fairness and transparency of the research results.

Statistical methods

SPSS 22.0 was used for statistical analysis. Measurement data that conformed to the normal distribution were presented as (S), t-test; count data were presented as n (%), χ^2-test; and Logistic regression was used for correlation factor analysis. The nomogram model was constructed in R, and the Bootstrap method was used for internal validation. A calibration curve and receiver operating characteristic (ROC) curve were drawn to evaluate the nomogram model. Inspection standard $\alpha=0.05$.

RESULTS

Immune response

A total of 57 cases, accounting for 57.0% of all IBD patients, were included in the response group. The remaining 43 patients were unresponsive (43.0%) and were included in the non-response group.

Baseline data analysis

In the baseline data of the two groups, the levels of TNF-α, CRP, calprotectin, ATI, IL-6, IL-8, and other cytokines were lower than those of the non-response group. There was no significant difference in other data (Table 1).

Logistic regression analysis

The treatment response of patients with IBD was used as the dependent variable (response = 0, non-response = 1). The data with a statistically significant difference in Table 1 were included in the independent variable, and Logistic regression analysis was conducted. The results showed that the levels of calprotectin (*OR*=1.099, 95%*CI*=1.039~1.163), ATI (*OR*=3.756, 95%*CI*=1.222~11.546), IL-6 (OR=1.261, 95%CI=1.069~1.488), and IL-8 (OR=1.014, 95%CI=1.004~1.024) are the key factors affecting the response of patients with IBD after treatment ($p<0.05$) (Table 2).

Construction and verification of the nomogram model

Based on the results of the logistic regression analysis, a nomogram was developed to predict treatment response in IBD patients (Fig. 1). ROC curve analysis showed that the AUC values for calprotectin level, ATI level, IL-6 level, and IL-8 level in this model were 0.809, 0.762, 0.850, and 0.775, with 95% confidence intervals of 0.719–0.881, 0.666–0.841, 0.765–0.913, and 0.681–0.853 (Fig. 2). The calibration curve indicates a good fit for the nomogram model (Fig. 3).

DISCUSSION

Analysis of baseline data difference between response and non-response groups

In this retrospective study, we examined how patients with inflammatory bowel disease (IBD) responded to infliximab (IFX) and developed a predictive model.

Table 1. Comparison of two groups of baseline data.

Index		Group		χ^2/t	p
		Response group (n=57)	Non-response group (n=43)		
Gender [n (%)]	Male	33 (57.89)	28 (65.12)	0.537	0.464
	Female	24 (42.11)	15 (34.88)		
BMI (kg/m^2)		22.07±0.90	21.86±0.63	1.275	0.205
Type of disease [n (%)]	CD	20 (35.09)	17 (39.53)	0.208	0.648
	UC	37 (64.91)	26 (60.47)		
Age (years)	CD	33.24±3.09	34.34±4.86	0.834	0.410
	UC	37.52±5.48	38.48±4.32	0.743	0.460
Disease activity (points)	CDAI	219.25±16.83	222.37±21.65	0.492	0.626
	UCAI	4.89±0.53	5.04±0.66	1.020	0.312
History of IFX treatment [n (%)]	Existent	3 (5.26)	7 (16.28)	3.305	0.069
	Non-existent	54 (94.74)	36 (83.72)		
Infusion reaction [n (%)]	Chest Tightness/ Chest pain	1 (1.75)	1 (2.33)	1.283	0.733
	Dyspnea	0	1 (2.33)		
	Flushing/Urticaria	0	1 (2.33)		
	Generate heat	1 (1.75)	2 (4.65)		
Gastrointestinal reaction [n (%)]	Nausea/Vomiting	3 (5.26)	4 (9.30)		
	Abdominalgia	0	1 (2.33)	0.774	0.679
	Diarrhea/ Constipation	1 (1.75)	1 (2.33)		
TNF-α level (ng/L)		24.65±3.26	26.57±3.81	2.700	0.008
CRP level (mg/L)		7.58±1.21	9.23±1.87	5.329	<0.001
Calprotectin level (μg/g)		105.09±14.68	123.34±14.74	6.146	<0.001
ATI level (ng/mL)		3.17±0.64	3.82±0.74	4.665	<0.001
IL-6 level (pg/mL)		30.04±5.66	37.70±5.32	6.879	<0.001
IL-8 level (pg/mL)		567.48±78.63	662.70±89.59	5.646	<0.001

BMI: Body Mass Index; CD: Crohn's Disease; UC: Ulcerative Colitis; CDAI: Crohn's Disease Activity Index; UCAI: Ulcerative Colitis Activity Index; TNF-α: Tumor Necrosis Factor-α; CRP: C-reactive Protein; ATI: Anti-Infliximab Antibody; IL-6: Interleukin-6; IL-8: Interleukin-8.

Data is expressed as n (%) or mean +- standard deviation. t: independent-samples t-test, χ^2: Chi-square test.

The results showed that 57 patients (57.0%) responded in this study, and these patients were included in the response group. The remaining 43 patients were non-responders (43.0%) and were included in the non-response group. This proportion distribution suggests that although IFX therapy has a certain effect on IBD patients, there are still many patients who can't get the ideal therapeutic effect.

Table 2. Logistic regression analysis of related influencing factors

Correlative factor	β	SE	Wald χ^2	*p*-value	OR	95%*CI*
TNF-α level	0.068	0.107	0.400	0.530	1.070	0.867~1.319
CRP level	0.323	0.272	1.408	0.235	1.381	0.810~2.354
Calprotectin level	0.094	0.029	10.596	0.001	1.099	1.039~1.163
ATI level	1.323	0.573	5.334	0.021	3.756	1.222~11.546
IL-6 level	0.232	0.084	7.622	0.006	1.261	1.069~1.488
IL-8 level	0.014	0.005	7.732	0.008	1.014	1.004~1.024

Note: TNF-α: Tumor Necrosis Factor-α; CRP: C-reactive Protein; ATI: Anti-Infliximab Antibody; IL-6: Interleukin-6; IL-8: Interleukin-8.

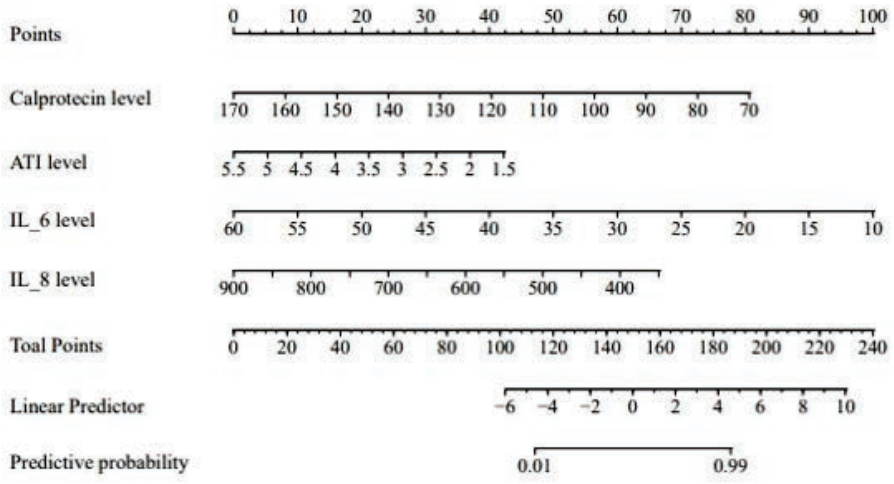

Fig 1. Risk prediction nomogram model.

ATI: Anti-Infliximab Antibody; IL-6: Interleukin-6; IL-8: Interleukin-8.

Risk prediction nomogram model is a visual, point-based tool that translates the final logistic-regression model into a clinician-friendly graphic. It is built on the four independent predictors that remained significant after multivariable adjustment: Calprotectin level, ATI level, IL-6 level, IL-8 level. Locate each biomarker value on its axis, sum the corresponding points, drop the total to the probability scale to read the predicted chance of non-response to infliximab.

Upon further comparison of baseline characteristics between responders and non-responders, this study revealed significant variations in TNF-α, CRP, calprotectin, ATI, IL-6, and IL-8 levels. Specifically, the levels of these cytokines in the response group were lower than those in the non-response group. This discovery provides an important clue and a basis for developing a predictive model in the future.

As IFX's direct target, TNF-α is crucial in IBD development [25]. This study found that, although TNF-α concentrations in both the response and non-response groups exceeded normal levels, they were notably lower in the response group than in the non-response group. This result suggests that TNF-α levels may reflect the intensity of intestinal inflammation and, in turn, influence the therapeutic outcome of IFX. In patients receiving effective IFX treatment, the decrease in TNF-α levels may indicate that IFX neutralizes TNF-α more effectively, thereby reducing intestinal inflammation [26].

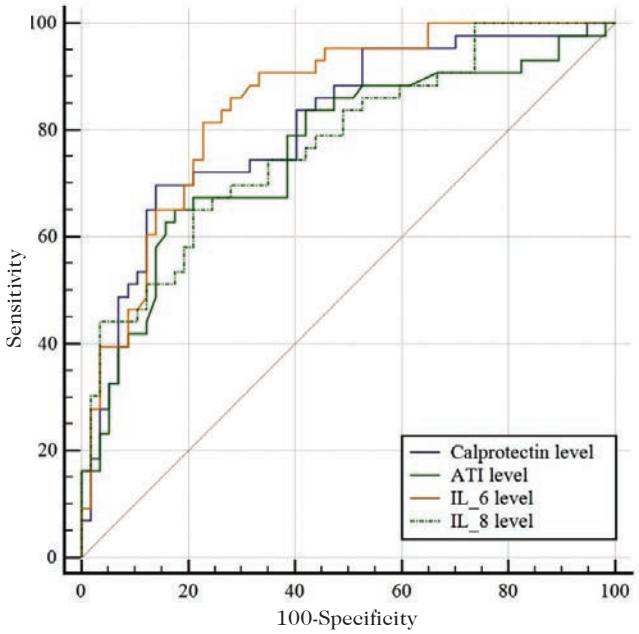

Fig. 2. ROC curve.
ATI: Anti-Infliximab Antibody; IL-6: Interleukin-6; IL-8: Interleukin-8.

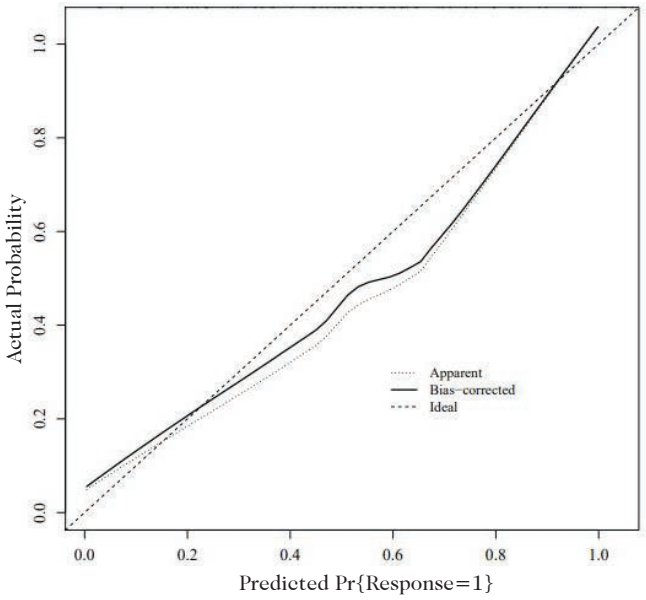

Fig 3. Calibration curve.

CRP serves as a marker of acute inflammation, indicating the body's inflammatory activity level [27]. This study revealed lower CRP levels among responders than among non-responders, consistent with trends in TNF-α levels. A decrease in CRP levels may indicate relief of intestinal inflammation and thus serve as an auxiliary index for predicting the IFX response. However, it is worth noting that CRP levels may be influenced by multiple factors, such as infection and trauma, and therefore should be considered comprehensively in clinical practice.

In addition to the above cytokines, we compared differences in age, sex, disease type, and history between the response and non-response groups. However, this study found no significant difference between the two groups in the baseline data. This result suggests that the treatment response to IFX may be more influenced by the intestinal local inflammatory environment.

Correlation analysis between key cytokines and IFX treatment response

Calprotectin: a sensitive marker of intestinal inflammation and a potential predictor of IFX response.

This study found a notable disparity between response and non-response groups, with Logistic regression analysis confirming calprotectin level as a crucial predictor of IBD patients' response to IFX treatment (OR=1.099, 95%CI=1.039~1.163). This discovery implies that calprotectin is crucial for monitoring IBD inflammation and may serve as a predictive indicator of IFX treatment response.

Calprotectin is a calcium-binding protein primarily secreted by neutrophils, and its elevated expression in the intestine is often closely linked to the severity of the intestinal inflammation [28]. In patients with IBD, an increase in calprotectin levels usually indicates active intestinal inflammation. However, the research revealed that, although calprotectin levels in responders were above normal, they were markedly lower than those of non-responders, potentially because IFX treatment alleviated intestinal inflammation. As an anti-TNF-α monoclonal antibody, IFX can reduce intestinal inflammation by specifically neutralizing TNF-α. Therefore, we speculate that the decrease in calpro-

tectin levels in patients receiving effective IFX may reflect the alleviation of intestinal inflammation and could serve as a sensitive index for predicting the IFX response.

Deeper insights into calprotectin's role in the IFX response suggest its potential involvement in modulating the NF-κB pathway. NF-κB serves as a crucial regulatory protein essential for inflammatory responses. When the intestine is injured or infected, NF-κB is activated, inducing the expression of a series of inflammatory cytokines, including TNF-α, IL-6, and IL-8. The release of calprotectin may affect NF-κB activity through an unknown mechanism, thereby indirectly influencing the expression levels of inflammatory factors [29,30]. In patients receiving effective IFX treatment, a decrease in calprotectin levels may indicate inhibition of the NF-κB signaling pathway, thereby reducing the production of inflammatory mediators and promoting the regression of intestinal inflammation.

ATI: Correlation between Drug Antibody Reaction and Response State of IFX

In this study, the ATI (anti-IFX antibody) level has also been established as a crucial predictor of IBD patients' response to IFX treatment (*OR*=3.756, 95%*CI*=1.222~11.546). This discovery underscores the importance of ATI in the treatment response to IFX and suggests that ATI levels may be a key factor influencing the efficacy of IFX.

In patients, the therapeutic effect of IFX may be influenced by the immune system. When IFX is administered, some patients may develop antibodies (ATI) against IFX, which may bind to IFX, thereby reducing its biological activity and further affecting its therapeutic effect [31]. Therefore, the increase in ATI level often indicates a decrease in the IFX treatment response.

Further analysis of the molecular mechanism of ATI in the IFX response indicates that ATI may influence the pharmacokinetics and pharmacodynamics of IFX. On the one hand, the combination of ATI and IFX may accelerate the clearance of IFX, thereby reducing its concentration in the body and potentially affecting its therapeutic effect. On the other hand, the combination of ATI and IFX may also affect the binding of IFX to TNF-α, thereby reducing the neutralizing activity of IFX [32, 33]. Therefore, in patients receiving effective IFX treatment, a decrease in ATI levels may indicate that IFX maintains high biological activity in vivo, thereby neutralizing TNF-α more effectively and reducing intestinal inflammation.

IL-6 and IL-8: Dual Roles of Inflammatory Factors and Predictive Value of IFX Response

Research revealed IL-6 and IL-8 concentrations as crucial indicators of IBD patients' response to IFX treatment (IL-6: *OR*=1.261, 95%*CI*=1.0691.488; IL-8: *OR*=1.014, 95%*CI*=1.0041.024). This discovery reveals the important roles of IL-6 and IL-8 in the pathogenesis of IBD and in the therapeutic response to IFX.

IL-6 and IL-8 are two key inflammatory cytokines that play a central role in the pathogenesis of IBD. On the one hand, IL-6 and IL-8 can induce inflammatory responses in intestinal mucosal cells and promote the progression of intestinal inflammation. On the other hand, they can also affect the function of the intestinal immune system and further exacerbate the progression of intestinal inflammation [34, 35]. Therefore, the increase of IL-6 and IL-8 levels often indicates the aggravation of IBD patients.

However, this study found that although IL-6 and IL-8 levels in the response group were higher than normal, they were markedly lower than in the non-response group. This result suggests that the decrease in IL-6 and IL-8 levels may reflect the relief of intestinal inflammation in patients with effective IFX treatment. Further analysis of the molecular mechanisms of IL-6 and IL-8 in the IFX response indicates that they may regulate multiple signaling pathways, including the JAK-STAT, NF-κB, and MAPK pathways [36,37]. Abnormal activation of these

signaling pathways is often closely linked to the pathogenesis of IBD. IFX therapy may inhibit the activity of these signaling pathways by neutralizing TNF-α, thereby reducing IL-6 and IL-8 expression and promoting the regression of intestinal inflammation [38, 39].

Construction and verification of the nomogram model

Using logistic regression results, this study developed a predictive model to forecast IBD patients' responses to IFX treatment. The model contains the key influencing factors such as calprotectin level, ATI level, IL-6 level, and IL-8 level, and can accurately predict the response of IBD patients to IFX treatment.

To evaluate the model's predictive performance, we use ROC and calibration curves. The ROC curve analysis results show that the AUC values for calprotectin, ATI, IL-6, and IL-8 levels in this model for predicting the response of IBD patients after treatment are 0.809, 0.762, 0.850, and 0.775, respectively, indicating high predictive accuracy. The results of calibration curve analysis also indicate that the nomogram model has a good fit and can accurately predict the response of IBD patients to IFX treatment.

Discussion on the mechanism of response and loss of response: signal pathway and molecular network

Neutralization of TNF-α Signal Pathway and IFX

As an important inflammatory factor, TNF-α plays a key role in the pathogenesis of IBD. TNF-α activates downstream signaling pathways, such as the NF-κB and MAPK pathways, by binding to its cell-surface receptor, thereby inducing a series of inflammatory responses [40]. As an anti-TNF-α monoclonal antibody, IFX can specifically neutralize TNF-α, thereby blocking activation of its downstream signaling pathways. In patients receiving effective IFX treatment, inhibition of the TNF-α signaling pathway may alleviate intestinal inflammation and promote mucosal healing [41].

Interaction between calprotectin and the NF-κB signaling pathway

As mentioned above, calprotectin may be involved in the regulation of the NF-κB signaling pathway. In patients with IBD, calprotectin release may modulate NF-κB activity via unknown mechanisms, thereby indirectly influencing the expression levels of inflammatory factors. In patients with effective IFX treatment, the decrease of calprotectin level may mean the inhibition of NF-κB signaling pathway, thus reducing the production of inflammatory factors [42, 43]. This interaction may constitute an important molecular mechanism of IFX therapeutic response.

Interaction between ATI and IFX pharmacokinetics

The production of ATI can affect the pharmacokinetics of IFX in vivo. On one side, combining ATI with IFX might speed up the clearance of IFX, lowering its concentration and half-life in the body. On the other side, ATI production can also impair IFX's ability to bind to TNF-α, thereby reducing its capacity to neutralize TNF-α [44, 45]. Therefore, in patients effectively treated with IFX, decreasing ATI levels could allow IFX to sustain high biological activity and concentration in vivo, resulting in more effective neutralization of TNF-α and relief from intestinal inflammation.

Limitations and future prospects of research

Despite certain advancements, the study harbors limitations. Notably, being retrospective, it may be subject to issues such as selection and information biases. Compared with prospective cohort studies, this study is retrospective and inherently has a higher risk of selection bias and information bias. The reliance on 100 patients from a single center (Shulan Hospital) severely limited the universality of the nomogram. To overcome these limitations, we need to further increase the sample size and conduct multicenter prospective research to validate

the study's conclusions. Furthermore, the model relies solely on internal validation (Bootstrap). A robust predictive model must be validated using an independent cohort of patients (external validation) to confirm its clinical utility in different settings.

Secondly, the study examined only the effects of cytokines such as calprotectin, ATI, IL-6, and IL-8 on IFX outcomes in IBD patients, without considering other potential biomarkers or genetic factors. To fully understand the pathogenesis of IBD and the therapeutic mechanism of IFX, we need to conduct further exploration. For example, we can use gene chips, protein genomics, and other technologies to screen for additional biomarkers and apply machine learning algorithms to build multivariate predictive models [46, 47]. The application of these new technologies and methods will help us understand the pathogenesis of IBD and the therapeutic mechanism of IFX, and provide stronger support for individualized treatment.

In addition, we need to consider the long-term effects and safety of IFX in the treatment of IBD. Although IFX can significantly improve the clinical symptoms of patients in the short term, long-term use may increase the risk of infection and malignant tumors [48]. Therefore, we need to conduct long-term follow-up of patients to identify and address potential adverse reactions in a timely manner. At the same time, we need to explore additional effective treatment modalities and strategies to further improve treatment outcomes and quality of life in patients with IBD.

In sum, this study developed a predictive tool for IBD patients' IFX outcomes based on a retrospective analysis and validated its predictive performance. The results indicated that calprotectin, ATI, IL-6, and IL-8 concentrations were pivotal in determining the IFX treatment response in IBD patients. These cytokines play important roles in the pathogenesis of IBD and in the therapeutic mechanism of IFX. In the future, we need to further expand the sample size, more deeply explore the pathogenesis of IBD and the treatment mechanism of IFX, and leverage new technologies and methods to develop a more precise and stable predictive model, thereby providing a more comprehensive foundation for personalized treatment. Meanwhile, attention should be given to the long-term efficacy and safety of IFX in IBD treatment to ensure optimal patient outcomes.

Through this study, we not only identified the key determinants of IBD patients' responses to IFX treatment but also developed a predictive model with clinical applicability. This achievement provides strong support for individualized treatment of IBD and also provides an important reference for follow-up research. We believe that in the near future, as our comprehension of IBD's disease processes and IFX's therapeutic mechanisms deepens, as well as the continuous emergence of new technologies and methods, we can provide more accurate and effective treatment strategies for patients with IBD and help them get rid of the disease and regain their health and happiness.

Acknowledgment

None.

Funding

None.

Consent to publish

The manuscript has neither been previously published nor is under consideration by any other journal. The authors have all approved the content of the paper.

Consent to participate

We secured a signed informed consent form from every participant.

Ethic approval

This study was approved by the Ethics Committee of the Shulan (Hangzhou) Hospital, Shulan International Medical College, Zhejiang Shuren University (KY2025018)

Data availability statement

The data that support the findings of this study are available from the corresponding author upon reasonable request.

ORCID numbers of authors

- Ru Ding (RD): 0009-0009-9395-5853
- Mengdi Fan (MF): 0009-0000-2327-2146
- Juanjuan Gu (JG): 0009-0000-9408-912X
- Zhangning Zhou (ZZ): 0009-0002-3277-4142

Participation of each author

RD: Edited and refined the manuscript with a focus on critical intellectual contributions. MF, JG: Participated in collecting, assessing, and interpreting the data. Made significant contributions to date interpretation and manuscript preparation. ZZ: Provided substantial intellectual input during the drafting and revision of the manuscript.

Conflicts of interest

The authors declare that they have no financial conflicts of interest.

REFERENCES

1. **Bruner LP, White AM, Proksell S**. Inflammatory Bowel Disease. Prim Care. 2023;50(3):411-427. *https://doi.org/10.1016/j.pop.2023.03.009*
2. **Singh N, Bernstein CN**. Environmental risk factors for inflammatory bowel disease. United European Gastroenterol J. 2022;10(10):1047-1053. *https://doi.org/10.1002/ueg2.12319.*
3. **Bisgaard TH, Allin KH, Keefer L, Ananthakrishnan AN, Jess T**. Depression and anxiety in inflammatory bowel disease: epidemiology, mechanisms and treatment. Nat Rev Gastroenterol Hepatol. 2022;19(11):717-726. *https://doi.org/10.1038/s41575-022-00634-6.*
4. **Liu D, Saikam V, Skrada KA, Merlin D, Iyer SS**. Inflammatory bowel disease biomarkers. Med Res Rev. 2022;42(5):1856-1887. *https://doi.org/10.1002/med.21893.*
5. **Wang CR, Tsai HW**. Seronegative spondyloarthropathy-associated inflammatory bowel disease. World J Gastroenterol. 2023;29(3):450-468. *https://doi.org/10.3748/wjg.v29.i3.450.*
6. **Ashton JJ, Beattie RM**. Inflammatory bowel disease: recent developments. Arch Dis Child. 2024;109(5):370-376. *https://doi.org/10.1136/archdischild-2023-325668.*
7. **Kumar M, Murugesan S, Ibrahim N, Elawad M, Al Khodor S**. Predictive biomarkers for anti-TNF alpha therapy in IBD patients. J Transl Med. 2024;22(1):284. *https://doi.org/10.1186/s12967-024-05058-1*
8. **Buisson A, Nachury M, Reymond M, Yzet C, Wils P, Payen L, et al.** Effectiveness of Switching From Intravenous to Subcutaneous Infliximab in Patients With Inflammatory Bowel Diseases: the REMSWITCH Study. Clin Gastroenterol Hepatol. 2023;21(9):2338-2346.e3. *https://doi.org/10.1016/j.cgh.2022.08.011*
9. **Peyrin-Biroulet L, Arkkila P, Armuzzi A, Danese S, Guardiola J, Jahnsen J, et al.** Comparative efficacy and safety of infliximab and vedolizumab therapy in patients with inflammatory bowel disease: a systematic review and meta-analysis. BMC Gastroenterol. 2022;22(1):291. https://doi.org/10.1186/s12876-022-02347-1
10. **Herrlinger KR, Stange EF**. Prioritization in inflammatory bowel disease therapy. Expert Rev Gastroenterol Hepatol. 2023;17(8):753-767. *https://doi.org/10.1080/17474124.2023.2240699*
11. **Kapizioni C, Desoki R, Lam D, Balendran K, Al-Sulais E, Subramanian S, et al.** Biologic Therapy for Inflammatory Bowel Disease: Real-World Comparative Effectiveness and Impact of Drug Sequencing in 13 222 Patients within the UK IBD BioResou-

rce. J Crohns Colitis. 2024;18(6):790-800. *https://doi.org/10.1093/ecco-jcc/jjad203*

12. **Sharma KK, Gupta S, Bisen PS**. Enhancing Gastrointestinal (GI) Cancer Therapies with Ganoderma Lucidum: A Review of Mechanisms and Efficacy. J Can Biomol Therap 2025;2(1):15-44. *https://doi.org/10.62382/jcbt.v2i1.28*
13. **Qiu Y, Hu S, Chao K, Huang L, Huang Z, Mao R, et al.** Developing a Machine-Learning Prediction Model for Infliximab Response in Crohn's Disease: Integrating Clinical Characteristics and Longitudinal Laboratory Trends. Inflamm Bowel Dis. 2025;31(5):1334-1343. *https://doi.org/10.1093/ibd/izae176*
14. **Meng X**. Therapeutic Efficacy of Platinum Based Medicines Combined with Various Nanoparticles in the Treatment of Colorectal Cancer: A Comprehensive Review. J Can Biomol Therap 2025;2(1):57-72. *https://doi.org/10.62382/jcbt.v2i1.32*
15. **Lee C, Jo B, Woo H, Im Y, Park RW, Park C**. Chronic Disease Prediction Using the Common Data Model: Development Study. JMIR AI. 2022;1(1):e41030. *https://doi.org/10.2196/41030*
16. **Rahman MS, Islam KR, Prithula J, Kumar J, Mahmud M, Alam MF, et al.** Machine learning-based prognostic model for 30-day mortality prediction in Sepsis-3. BMC Med Inform Decis Mak. 2024;24(1):249. *https://doi.org/10.1186/s12911-024-02655-4*
17. **Huang L, Li H, Wang S, Ren Y**. Prediction of early mucosal healing of Crohn's disease after treatment with biologics- a novel nomogram based on radiomics and clinical risk factors. Front Pharmacol. 2025;16:1586300. *https://doi.org/10.3389/fphar.2025.1586300*
18. **Wang Y, Song J, Zheng Z, Peng X, Li X, Wu W**. Development and Validation of a Machine Learning Model to Predict Anti-Drug Antibody Formation During Infliximab Induction in Crohn's Disease. Biomedicines. 2025;13(10):2464. *https://doi.org/10.3390/biomedicines13102464.*
19. **Caenepeel C, Falony G, Machiels K, Verstockt B, Goncalves PJ, Ferrante M, et al.** Dysbiosis and Associated Stool Features Improve Prediction of Response to Biological Therapy in Inflammatory Bowel Disease. Gastroenterology. 2024;166(3):483-495. *https://doi.org/10.1053/j.gastro.2023.11.304*
20. **Pinton P**. Impact of artificial intelligence on prognosis, shared decision-making, and precision medicine for patients with inflammatory bowel disease: a perspective and expert opinion. Ann Med. 2023;55(2):2300670. *https://doi.org/10.1080/07853890.2023.2300670*
21. **Li M, Tao Y, Sun Y, Wu J, Zhang F, Wen Y, et al.** Constructing a prediction model of inflammatory bowel disease recurrence based on factors affecting the quality of life. Front Med (Lausanne). 2023;10:1041505. *https://doi.org/10.3389/fmed.2023.1041505*
22. **Xiong Z, Fang Y, Lu S, Sun Q, Huang J**. Identification and Validation of Signature Genes and Potential Therapy Targets of Inflammatory Bowel Disease and Periodontitis. J Inflamm Res. 2023; 16:4317-4330. *https://doi.org/10.2147/jir.S426004*
23. **Lahiff C, Safaie P, Awais A, Akbari M, Gashin L, Sheth S, et al.** The Crohn's disease activity index (CDAI) is similarly elevated in patients with Crohn's disease and in patients with irritable bowel syndrome. Aliment Pharmacol Ther. 2013;37(8):786-794. *https://doi.org/10.1111/apt.12262*
24. **Gürel S, Kiyici M**. Ulcerative colitis activity index: a useful prognostic factor for predicting ulcerative colitis outcome. J Int Med Res. 2005;33(1):103-110. *https://doi.org/10.1177/147323000503300111*
25. **Little RD, McKenzie J, Srinivasan A, Hilley P, Gilmore RB, Chee D, et al.** Switching from Dose-Intensified intravenous to SubCutaneoUS infliximab in Inflammatory Bowel Disease (DISCUS-IBD): protocol for a multicentre randomised controlled trial. BMJ Open. 2024;14(7):e081787. *https://doi.org/10.1136/bmjopen-2023-081787*
26. **Zheng M, Zhai Y, Yu Y, Shen J, Chu S, Focaccia E, et al.** TNF compromises intestinal bile-acid tolerance dictating colitis progression and limited infliximab respon-

se. Cell Metab. 2024;36(9):2086-2103. e9. *https://doi.org/10.1016/j.cmet.2024.06.008*

27. **Levinson T, Wasserman A**. C-Reactive Protein Velocity (CRPv) as a New Biomarker for the Early Detection of Acute Infection/Inflammation. Int J Mol Sci. 2022;23(15):8100. *https://doi.org/10.3390/ijms23158100*
28. **Tung KK, Chen ST, Lee CH, Tung CF, Wei JC**. Calprotectin in spondyloarthritis and gut inflammation, is it clinically meaningful? Int J Rheum Dis. 2023;26(4):609-612. *https://doi.org/10.1111/1756-185x. 14619*
29. **Kostrzewska P, Całkosiński A, Majewski M, Malinowski K**. [Fecal calprotectin as a diagnostic marker of inflammatory bowel disease]. Pol Merkur Lekarski. 2022;50(295):58-61. PMID: 35278302.
30. **Costa MHM, Sassaki LY, Chebli JMF**. Fecal calprotectin and endoscopic scores: The cornerstones in clinical practice for evaluating mucosal healing in inflammatory bowel disease. World J Gastroenterol. 2024;30(24):3022-3035. *https://doi.org/10.3748/wjg.v30.i24.3022*
31. **Levitte S**. Point-of-Care Assays for Infliximab Therapeutic Drug Monitoring in Patients with IBD: Is Quicker Better? Dig Dis Sci. 2024;69(1):5-6. *https://doi.org/10.1007/s10620-023-08140-8*
32. **Smith PJ, Critchley L, Storey D, Gregg B, Stenson J, Kneebone A, et al.** Efficacy and Safety of Elective Switching from Intravenous to Subcutaneous Infliximab [CT-P13]: A Multicentre Cohort Study. J Crohns Colitis. 2022;16(9):1436-1446. *https://doi.org/10.1093/ecco-jcc/jjac053*
33. **Zhu K, Ding X, Chen Z, Xi Q, Pang X, Chen W, et al.** Association between genetic variants and development of antibodies to infliximab: A cross-sectional study in Chinese patients with Crohn's disease. Front Pharmacol. 2023;14:1096816. *https://doi.org/10.3389/fphar.2023.1096816*
34. **Tataru C, Livni M, Marean-Reardon C, Franco MC, David M**. Cytokine induced inflammatory bowel disease model using organ-on-a-chip technology. PLoS One. 2023;18(12):e0289314. *https://doi.org/10.1371/journal.pone.0289314*
35. **Kuenstner JT, Xu Q, Bull TJ, Foddai ACG, Grant IR, Naser SA, et al.** Cytokine expression in subjects with Mycobacterium avium ssp. paratuberculosis positive blood cultures and a meta-analysis of cytokine expression in Crohn's disease. Front Cell Infect Microbiol. 2024;14:1327969. *https://doi.org/10.3389/fcimb.2024.1327969*
36. **Mukherjee T, Kumar N, Chawla M, Philpott DJ, Basak S**. The NF-κB signaling system in the immunopathogenesis of inflammatory bowel disease. Sci Signal. 2024;17(818):eadh1641. *https://doi.org/10.1126/scisignal.adh1641*
37. **Ren J.** Advances in Combination Therapy for Gastric Cancer: Integrating Targeted Agents and Immunotherapy. Adv Clin Pharmacol Ther. 2024;1(1):1-15. *https://doi.org/10.63623/9k14tf70*
38. **Salah N, Dubuquoy L, Carpentier R, Betbeder D**. Starch nanoparticles improve curcumin-induced production of anti-inflammatory cytokines in intestinal epithelial cells. Int J Pharm X. 2022;4:100114. *https://doi.org/10.1016/j.ijpx.2022.100114*
39. **Podolski M, Požgaj L, Faraho I, Petrinić Grba A, Belamarić D, Paravić Radičević A, et al.** Correlation of ex vivo cytokine secretion profiles with scoring indices in ulcerative colitis. Eur J Clin Invest. 2023;53(12):e14070. *https://doi.org/10.1111/eci.14070*
40. **Gros B, Kaplan GG**. Ulcerative Colitis in Adults: A Review. JAMA. 2023;330(10):951-965. *https://doi.org/10.1001/jama.2023.15389*
41. **Griffin H, Ceron-Gutierrez L, Gharahdaghi N, Ebrahimi S, Davies S, Loo PS, et al.** Neutralizing Autoantibodies against Interleukin-10 in Inflammatory Bowel Disease. N Engl J Med. 2024;391(5):434-441. *https://doi.org/10.1056/NEJMoa2312302*
42. **Hu T, Zhang Z, Song F, Zhang W, Yang J**. Evaluation of Mucosal Healing in Ulcerative Colitis by Fecal Calprotectin vs. Fecal Immunochemical Test: A Systematic Review and Meta-analysis. Turk J Gastroen-

terol. 2023;34(9):892-901. *https://doi.org/10.5152/tjg.2023.22812*

43. **Newman KL, Higgins PDR**. Fecal calprotectin level is nonlinearly associated with GI pathogen detection in patients with and without inflammatory bowel disease. J Clin Microbiol. 2023;61(12):e0094623. *https://doi.org/10.1128/jcm.00946-23*
44. **Zhu K, Ding X, Xue L, Liu L, Wang Y, Li Y, et al.** Optimising infliximab induction dosing to achieve clinical remission in Chinese patients with Crohn's disease. Front Pharmacol. 2024;15:1430120. *https://doi.org/10.3389/fphar.2024.1430120*.
45. **Kampa KC, Loures MR, Ivantes CAP, Petterle RR, Pedroso MLA**. The evaluation of infliximab trough level favors maintenance therapy of patients with inflammatory bowel disease. Arq Gastroenterol. 2023;60(1):48-56. *https://doi.org/10.1590/s0004-2803.202301000-07*.
46. **Pandey H, Jain D, Tang DWT, Wong SH, Lal D**. Gut microbiota in pathophysiology, diagnosis, and therapeutics of inflammatory bowel disease. Intest Res. 2024;22(1):15-43. *https://doi.org/10.5217/ir.2023.00080*.
47. **Liu X, Reigle J, Prasath VBS, Dhaliwal J**. Artificial intelligence image-based prediction models in IBD exhibit high risk of bias: A systematic review. Comput Biol Med. 2024;171:108093. *https://doi.org/10.1016/j.compbiomed.2024.108093*.
48. **Wijnands AM, Penning de Vries BBL, Lutgens M, Bakhshi Z, Al Bakir I, Beaugerie L, et al.** Dynamic Prediction of Advanced Colorectal Neoplasia in Inflammatory Bowel Disease. Clin Gastroenterol Hepatol. 2024;22(8):1697-1708. *https://doi.org/10.1016/j.cgh.2024.02.014*.

Invest Clin 67(1): 73 - 91, 2026 https://doi.org/10.54817/IC.v67n1a06

Withaferin-A induces apoptosis and autophagy in colorectal cancer cell lines via down-regulated expression of histone deacetylase 1.

Qiong Wang[1,2] and Caixia Li[3]

[1]Qilu Hospital of Shandong University, Jinan, Shandong, China.
[2]Endoscopy Center, Weifang NO.2 People's Hospital, Weifang, Shandong, China.
[3]Department of Stomatology, Shandong Provincial People's Hospital, Jinan, Shandong, China.

Keywords: Apoptosis; Autophagy; Histone Deacetylase 1; Aberrant Crypt Foci; Chemoprevention.

Abstract. Colorectal cancer (CRC) remains the third most common malignancy worldwide, and there is an urgent need for low-toxicity, mechanism-based preventives or adjuvants. Withaferin-A (WA), a plant-derived steroidal lactone, exhibits broad antitumor activity; however, its role in CRC and its interactions with epigenetic regulators, such as histone deacetylase 1 (HDAC1), remain unclear. Therefore, we investigated whether WA suppresses CRC growth by down-regulating HDAC1 while inducing apoptosis and autophagy. Caco2 and HT-29 cells were treated with 0–5 μM WA; viability, colony formation, and migration decreased significantly (IC_{50} 0.70–1.52 μM). Techniques such as Annexin-V/7-AAD flow cytometry, MDC staining, TEM, and LC3B immunofluorescence showed that 1 μM WA notably increased apoptosis and autophagic flux, along with reduced HDAC1 and p62 levels, higher LC3B-II/I ratios, and an increased Bax/Bcl-2 ratio. Overexpression of HDAC1 via a lentiviral vector reversed these effects, confirming dependence on HDAC1. For translational relevance, eight-week-old C57BL/6J mice were first exposed to the food-borne carcinogen IQ (2-amino-3-methyl-3H-imidazo[4,5-f]quinoline, 100 mg/kg) every other day for three weeks to induce aberrant crypt foci (ACF). Starting the day after the first IQ dose, animals received WA (2 mg/kg) or vehicle (corn oil) by gavage every other day for the same period. WA reduced the number of macroscopic ACF by more than 60%, restored HDAC1-related LC3B and p62 expression to normal levels, and showed no toxicity based on body weight or general health assessments. These findings suggest that WA provides potent, low-toxicity chemopreventive effects against CRC lesion formation through HDAC1-dependent induction of apoptosis and autophagy, supporting its further consideration as a preventive or adjuvant agent.

Corresponding author: Qiong Wang. Endoscopy Center. Qilu Hospital of Shandong University. 107 Wenhuaxi Road, Jinan, Shandong 250012, China. Tel: +86 13563606469. Email: Wangqiong7979@163.com

La withaferina-A induce la apoptosis y la autofagia en líneas celulares de cáncer colorrectal mediante la regulación negativa de la expresión de la histona deacetilasa 1.

Invest Clin 2026; 67 (1): 73 – 91

Palabras clave: Apoptosis; Autofagia; Histona Desacetilasa 1; Focos de Criptas Aberrantes; Quimioprevención.

Resumen. El cáncer colorrectal (CCR) sigue siendo la tercera malignidad más común en todo el mundo, y existe una necesidad urgente de preventivos o adyuvantes de baja toxicidad basados en mecanismos. Withaferin-A (WA), una lactona esteroide derivada de plantas, ha mostrado una amplia actividad antitumoral, pero su papel en el CRC y su interacción con reguladores epigenéticos, como la histona deacetilasa 1 (HDAC1), no están claros. Por lo tanto, se evaluó si WA suprime el crecimiento de CRC al regular la actividad de HDAC1 hacia abajo e inducir concomitantemente apoptosis y autofagia. Las células Caco2 y HT-29 se expusieron a WA 0–5 μM; la viabilidad, la formación de colonias y la migración se inhibieron marcadamente (IC_{50} 0.70–1.52 μM). La citometría de flujo con Annexin-V/7-AAD, la tinción con MDC, la inmunofluorescencia de TEM y de LC3B mostraron que WA a 1 μM aumentó significativamente la apoptosis y el flujo autofágico, acompañados de la regulación descendente de HDAC1 y p62, la regulación ascendente de LC3B-II/I y un aumento en la relación Bax/Bcl-2. La sobreexpresión de HDAC1 mediada por lentivirus revertió todos estos efectos, lo que confirma la dependencia de HDAC1. Para evaluar la relevancia traslacional, a ratones C57BL/6J de ocho semanas de edad se les administró primero el carcinógeno el carcinógeno de origen alimentario, 2-amino, 2-amino-3-metil-3H-imidazo[4,5-f]quinoline (100 mg/kg), cada dos días durante 3 semanas, para inducir focos de cripta aberrantes (ACF). A partir del día siguiente a la primera dosis de carcinógeno, los animales recibieron, adicionalmente, WA (2 mg/kg) o vehículo (aceite de maíz) por gavage cada dos días durante el mismo período. WA redujo el número macroscópico de ACF en más del 60%, restableció la expresión de LC3B y p62 asociada a HDAC1 a niveles normales y no mostró toxicidad ni en el peso corporal ni en el monitoreo general de la salud. Estos datos indican que WA ejerce una quimioprevención potente y de baja toxicidad contra la formación de lesiones de CRC mediante la inducción de apoptosis y autofagia dependientes de HDAC1, lo que respalda su desarrollo adicional como agente preventivo o adyuvante.

Received: 15-10-2025 Accepted: 21-12-2025

INTRODUCTION

Colorectal cancer (CRC) is the third most diagnosed malignancy and the second leading cause of cancer-related death worldwide [1]. Despite advances in surgery, radiotherapy, and targeted agents, the 5-year survival rate of patients with advanced CRC remains below 20%, largely because of chemo-resistance and dose-limiting toxicities [2]. Therefore, the development of low-toxicity, mechanism-based preventive or adjuvant therapies is urgently needed.

Plant-derived small molecules have gained prominence due to their widespread antitumor effects and favorable safety profiles [3]. Withaferin-A (WA), a steroidal lactone derived from *Withania somnifera*, has demonstrated potent antiproliferative, proapoptotic, and antimetastatic effects across various solid tumors [4-6]. These effects are linked to proteasome inhibition, reactive oxygen species production, and modulation of key cancer-related signaling pathways, including STAT3 and NF-κB [7–9]. However, the role of WA in CRC and the exact molecular mechanisms underlying its activity remain incompletely understood.

An increasing body of evidence suggests that epigenetic dysregulation—especially abnormal histone acetylation—plays a key role in CRC initiation and progression[10,11]. Histone deacetylases (HDACs) remove acetyl groups, thereby repressing tumor-suppressor genes, and HDAC1 is often overexpressed in CRC tissues [12,13]. Small-molecule HDAC inhibitors (e.g., Trichostatin A) can restore acetylation balance and induce growth arrest or apoptosis, but their clinical use is limited by systemic toxicity [14]. Whether WA affects HDAC activity in CRC remains unexplored.

The present study, therefore, aimed to evaluate the anti-proliferative, pro-apoptotic, and anti-migratory effects of WA in human CRC cell lines and to determine whether these effects are mediated by downregulation of HDAC1-dependent epigenetic mechanisms. To assess translational relevance, we also examined WA activity in a murine model of colitis-associated CRC.

MATERIALS AND METHODS

Cell lines and culture conditions

Caco2 and HT-29 human CRC cells were obtained from Shanghai ZhongQiao Xin Zhou Biotechnology Co., Ltd. They were grown as monolayers in Dulbecco's Modified Eagle Medium (DMEM) (Gibco; Thermo Fisher Scientific, Inc.). The human CRC cell lines were supplemented with 10% fetal bovine serum (FBS, Biological Industries, Israel) and 1% penicillin/streptomycin (PEN/STREP 100×, MILLIPORE, USA). Cells were cultured in a humidified incubator at 37°C in 5% CO_2. The culture medium, including any treatments, was replaced every 48 hours. All treatments and controls contained a final dimethyl sulfoxide (DMSO, D2650, Sigma-Aldrich, USA) concentration of less than 0.1%.

Cell Counting Kit-8 (CCK8) assay

We used the CCK8 kit (K1018-5; APExBIO, USA) to detect cell viability. A total of 5×10^3 cells in 100 μL per well were cultured in five replicate wells of a 96-well plate in medium containing 10% FBS and allowed to adhere overnight. Then, the cells were treated with various concentrations of WA (W4394-5mg, Sigma-Aldrich, Saint Louis, MO, USA) (0, 0.5, 1, 2, 3, 4, 5 μM) for 24 and 48 hours. WA was diluted in 0.1% DMSO. Control cells were treated with 0.1% DMSO in culture medium. Following the manufacturer's instructions, 10 μL of CCK8 reagent was added to 90 μL of DMEM to prepare a working solution, which was then incubated for 30 minutes at 37°C. 100 μL of the working solution was added to each well. The absorbance (OD) was measured at 450 nm using a microplate spectrophotometer (Varioskan Flash 4.0, Thermo Fisher Scientific, Waltham, MA, USA). All experiments were performed in quintuplicate, with five wells per replicate. The viability rate was calculated as: (OD test – OD blank) / (OD control – OD blank) × 100%. The OD blank consisted of wells with 0.1% DMSO in culture medium. The half-maximal inhibitory concentration (IC_{50}) values were determined using GraphPad 8.0. Subsequently, cells were treated in complete medium with or without 1 μM WA for future experiments.

Colony formation assay

CRC cells were seeded into 6-well plates at a density of 1000 cells per well and cultured with 0 or 1 μM WA. They were incubated at 37°C for 14 days to allow colony for-

mation. Finally, the cells were washed with phosphate-buffered saline (PBS), fixed in methanol at room temperature for 30 minutes, washed again with PBS, and stained with 0.1% crystal violet at room temperature for 30 minutes. After washing with PBS, the wells were photographed with a smartphone camera (VIVO X6 PLUS, China), and colonies with at least 50 cells were visually counted and quantified.

Wound healing assay

Wound-healing assays were performed to evaluate CRC cell motility. CRC cells were seeded in 6–well plates at a density of 1×10^6 cells per well. After 24 h, the cell monolayer was scratched with a 10μL pipette tip. The wound-healing assay was performed in monolayer culture, after which the cells were cultured in serum–free medium. Wounds were washed with PBS and incubated in serum-free medium in the presence of 0 or 1 μM WA. Images were captured at different timepoints (0, 24 and 48 h). The wound-healing area was calculated using ImageJ software (version 1.8.0.112; National Institutes of Health).

Transwell (Migration) assay

Migration ability was evaluated using 24-well Transwell chambers (8.0 μm pore size; 3422, Corning Costar, USA). After 48 hours of treatment with the respective agents, CRC cells were digested and suspended in FBS-free medium. Subsequently, 1×10^5 cells were allowed to migrate from the upper chamber, which contained 200 μL of medium without FBS, to the lower chamber, which contained 700 μL of medium with 30% FBS. After incubating the Transwells for 24 hours, non-invading cells in the upper chamber were removed with a cotton swab, and cells that had invaded the membrane were fixed in methanol for 5 minutes and stained with crystal violet for 30 minutes. The cells that migrated through the polycarbonate membrane were counted under a Nikon Ti-E inverted microscope (5 random fields per well, magnification ×100).

Analysis of apoptosis by Flow Cytometry (FCM)

CRC cells were cultured in 60 mm dishes at a density of 1×10^6 cells per well and treated with drugs for 24 hours as previously described. An Annexin V-APC/7-AAD apoptosis detection kit was used to assess cell morphology and apoptosis. Following the manufacturer's instructions, cells were washed twice with cold PBS, then collected and resuspended in 1× Annexin V Binding Buffer. Next, 5 μL of Annexin V-APC conjugate and 5 μL of 7-AAD solution were added to the cell suspension, which was incubated for 15 minutes at 2-8°C in the dark. Afterward, 400 μL of 1× Annexin V Binding Buffer was added to each tube. The samples were analyzed by flow cytometry using a CytoFLEX Flow Cytometer (Beckman Coulter, Inc., USA) within 1 hour of staining. Data were analyzed with CytExpert software.

Monodansylcadaverine (MDC) staining

MDC, an electrophoretic marker of autophagosome formation, was used to quantify autophagy induction. The autofluorescent drug MDC is a selective marker for acidic vesicular organelles (AVOs), such as autophagic vacuoles and autolysosomes. The effects of WA and the control group on autophagy levels in CRC cells were assessed using the MDC method. Normal cells displayed a uniform yellow-green stain, while autophagosomes appeared as densely packed green granules of varying sizes, producing punctate green fluorescence. In brief, after the specified treatment conditions, cells were seeded into a 6-well plate (3×10^6 cells/well) and cultured overnight until reaching 50–60% confluence. As described above, they were divided into two groups for different interventions. At the designated time points, the original medium was removed, cells were washed with 1× wash buffer (diluted in deionized water), incubated with the prepared MDC staining solution at room temperature for 45 minutes in the dark, and then washed three times with 1× wash buffer. Fluores-

cent images were captured using an inverted fluorescence microscope (magnification ×200) (Nikon Microscope, Tokyo, Japan) at an excitation wavelength of 355 nm and an emission filter of 512 nm (Leica, Wetzlar, Germany).

Ultra-structures observed by transmission electron microscopy

To evaluate the effect of WA on cell autophagy in CRC cells, cells were treated with or without WA (1 μM) for 48 hours. The cells were then washed with PBS, collected by centrifugation at 1,000 × g (Eppendorf, Hamburg, Germany), and fixed in cold (4°C) 2.5% glutaraldehyde solution (Servicebio Technology Co., Ltd., Wuhan) for 1 hour. The specimens were subsequently rinsed with 0.1 mL PBS, embedded in agarose for pre-embedding, postfixed in 1% osmium tetroxide (Ted Pella Inc., California, USA) in the dark for 2 hours at room temperature, dehydrated through a graded series of ethanol solutions (30-100%) and two changes of acetone (Sinaopharm Group Chemical Reagent Co., Ltd.), and then infiltrated with EMBed 812 (SPI, USA) for resin penetration and embedding. After polymerization, the resin blocks were sectioned at 60–80 nm on a Leica UC7 ultramicrotome (Leica, Wetzlar, Germany), and the tissues were transferred onto 150-mesh copper grids coated with Formvar film. Copper grids were stained with 2% uranyl acetate in saturated alcohol for 8 minutes, then with 2.6% lead citrate for 8 minutes, with light exposure avoided during staining. The grids were placed on the grid board and dried overnight at room temperature. Representative areas were examined with an HT7800 transmission electron microscope (Hitachi Ltd., Tokyo, Japan).

Immunofluorescence Assay

To further confirm that autophagy was induced by WA, CRC cells were seeded into 24-well cell culture plates at a density of 1.5×10^5 cells per well. The cells were divided into two groups as previously described. After fixing with 4% paraformaldehyde, the cells were permeabilized with 0.3% Triton X-100 for 5 minutes and blocked with 5% normal goat serum for 1 hour. The cells were then incubated with rabbit anti-LC3A/B primary antibody (1:200) overnight at 4°C. After washing with PBS, the cells were immunostained with FITC-conjugated goat anti-rabbit secondary antibody (1:100) for 1 hour at room temperature in the dark. Next, the cell nuclei were stained with 4',6-diamidino-2-phenylindole (DAPI) for 3 minutes. Finally, immunofluorescence images were captured and observed using a fluorescence microscope (magnification, ×400). The Dylight 488, Goat Anti-Rabbit IgG (cat. no. A23220; 1:500) was obtained from Abbkine Scientific Co., Ltd., Wuhan, China.

RNA extraction, Reverse Transcription, and RT-qPCR

CRC cells were treated with 1 μM WA for the indicated duration (48 hours) and harvested using TRIzol reagent (Invitrogen, Thermo Fisher Scientific, Inc.). After adding 1/5 volume of chloroform (Invitrogen, Thermo Fisher Scientific, Inc.), the mixture was centrifuged at 12000g for 15 minutes at 4°C, and the supernatants were transferred to new, clear centrifuge tubes. An equal volume of isopropanol was added to each supernatant and gently mixed. After incubation at room temperature for 30 minutes, the mixture was centrifuged at 12000g for 15 minutes. The pellets were washed once with 75% ethanol and dissolved in RNase-free water at an appropriate volume. Following RNA quantification, reverse transcription (RT) reactions were performed to convert total RNA into cDNA using the SureScript™ First-Strand cDNA Synthesis Kit (cat. no. QP056, GeneCopoeia, Inc., Guangzhou, China) and reverse transcriptase (Takara, Tokyo, Japan) according to the manufacturer's protocol. Cycling parameters were set at 95°C for 30 seconds (denaturation), 95°C for 5 seconds (annealing), and 60°C for 34 seconds (extension), with 40 cycles performed.

The gene-specific primer sequences, synthesized by Generay Biotech Co., Ltd. (Shanghai, China) and derived from PrimerBank, are summarized in Supplemental Table 1. GAPDH was used as an internal control to normalize RNA quantity and quality across samples. The presence of HDAC1, Bax, Bcl-2, p62, and LC3B transcripts was analyzed by Quantitative RT-qPCR (10-μL reaction volume) using the BlazeTaq™ SYBR® Green qPCR Mix 2.0 Kit (cat. no. QP031, GeneCopoeia, Inc., Guangzhou, China). Real-time reverse transcription quantitative PCR (RT-qPCR) was performed on an Applied Biosystems 7500 system according to the manufacturer's instructions. Data were analyzed using the $2^{-\Delta\Delta Cq}$ method, with relative quantification calculated by the formula $2^{-\Delta\Delta Ct}$, where $\Delta Ct = Ct$ of target gene $- Ct$ of GAPDH, and $\Delta\Delta Ct = \Delta Ct$ of treatment $- \Delta Ct$ of control.

Supplemental Table 1. Primers for RT-qPCR.

Gene		Primer sequence, 5'3'
GAPDH	F	GGACCTGACCTGCCGTCTAG
	R	GTAGCCCAGGATGCCCTTGA
Bax	F	CCCGAGAGGTCTTTTTCCGAG
	R	CCAGCCCATGATGGTTCTGAT
Bcl-2	F	GGTGGGGTCATGTGTGTGG
	R	CGGTTCAGGTACTCAGTCATCC
LC3B	F	AAGGCGCTTACAGCTCAATG
	R	CTGGGAGGCATAGACCATGT
HDAC1	F	CGCCCTCACAAAGCCAATG
	R	CTGCTTGCTGTACTCCGACA
p62	F	GACTACGACTTGTGTAGCGTC
	R	AGTGTCCGTGTTTCACCTTCC

F, forward; R, reverse.

Western blotting

Western blotting was performed to assess protein expression levels of the anti-apoptotic Bcl-2 and the pro-apoptotic Bax; the autophagic markers LC3 II/I and p62; and HDAC1. After the specified drug treatments, total protein was extracted from CRC cells at 48 hours. The cells were washed twice with ice-cold PBS and lysed in complete cell lysis buffer (50 mM Tris- HCl, pH 7. 4, 7.4,150 mM NaCl, 1% Triton X- 100, 0. 25% Na-Deoxycholate,1 mM EDTA, 1 mM NaF, 1 mM dithiothreitol, 1 mM PMSF,1 mM activated Na 3 VO 4, 0.02 μM aprotinin, 0. 16 μM leupeptin, and 0.22 μM pepstatin). Protein extracts were heated at 99°C for 5 minutes and then cooled on ice. Protein concentrations were measured using a BCA protein assay kit (Tiangen Biotech Co., Ltd.). Equal amounts (30 μg) of protein from each sample were loaded and separated on a 10% SDS-PAGE gel through 6–12% gels, then transferred onto PVDF membranes (Millipore, USA). The membranes were blocked in rapid sealing fluid for 30 minutes, then incubated overnight at 4°C with primary antibodies. The blots were washed three times for 5 minutes with TBST, then incubated with specific secondary antibodies at room temperature for 1 hour. After washing three additional times for 5 minutes in TBST, the bands were visualized with an ECL detection reagent, quantified using ImageJ, and normalized to GAPDH as the endogenous control. The antibody information is as follows: GAPDH (product no. 5174; 1: 1000 dilution), LC 3 A/B (product no. 12741; 1: 1000 dilution), and HDAC 1 (product no. 34589; 1: 1000 dilution) from Cell Signaling Technology; p 62 (cat. no. ab 109012; 1: 2000 dilution) and Bax (cat. no. ab 182733; 1: 2000 dilution) from Abcam; Bcl- 2 (cat. no. SC 271268; 1: 200 dilution) from Santa Cruz Biotechnology. Goat anti- Rabbit IgG-HRP (cat. no. HA 1001; 1: 10, 000 dilution) and Goat anti- Mouse IgG- HRP (cat. no. HA 1006; 1: 5000 dilution) from Huaan Biotechnology, Co., Ltd. (Hangzhou, China). The secondary antibody diluent buffer (P 0023 D- 100 mL) was obtained from Beyotime Biotechnology (Shanghai, China).

Separation of the nucleus from the cytoplasm

A nucleoprotein extraction kit was used to separate the nucleus from the cytoplasm

according to the manufacturer's protocol. The CRC cells were washed three times with cold PBS and collected into 1.5 mL Eppendorf tubes using a cell scraper. Cells were centrifuged at 500 × g for 3 minutes at 4°C, and the supernatants were discarded. Cell lysates were added to the precipitates. The Eppendorf tubes were then vortexed for 15 seconds at 5-minute intervals, for a total of 3 cycles. Next, the suspensions were centrifuged for 5 minutes at 12,000 × g, and the supernatants were collected as the cytoplasmic fraction. The nuclear lysates were added to the precipitates. After vortexing for 15 seconds every 10 minutes for a total of 4 times, the suspensions were centrifuged for 10 minutes at 12,000 x g, and the supernatants contained the cytoplasmic proteins. Finally, the samples were packaged and stored at -80°C for future use.

Histone acetyltransferase activity/ inhibition assay

Trichostatin A (TSA) is a specific inhibitor of HDACs, and its inhibitory ability has been validated in many experiments. Cells were divided into three groups: control, WA, and TSA. The control and WA groups were treated with medium containing or lacking WA, respectively. The TSA group cells were pretreated with the inhibitor TSA. Nuclear extracts were prepared as described above, and the EpiQuik™ HDAC Activity/Inhibition Kit (Colorimetric) (P-4002) (Epigentek Group Inc.) was used to determine whether WA can inhibit HDACs in CRC cells similarly to TSA. The assay was carried out according to the provided protocol. Activity was expressed as relative OD values per mg protein (OD/mg), based on triplicate measurements (n=4). HDAC activity/inhibition assays were performed either with or without HDAC inhibitors (HDACi). The inhibitory rate (%) was calculated as: {1 - [OD (control – blank) – OD (inhibitor sample – blank)] / [OD (control – blank) – OD (no inhibitor sample – blank)]} × 100%.

Lentivirus-mediated RNA interference

Lentiviral particles and Polybrene were purchased from Shanghai Genechem Co., Ltd. The overexpressed gene was named LV-HDAC1 (14721-1), and the negative control (NC) was labeled as CON238. The procedure was as follows: CRC cells were seeded in 6-well plates at a density of 1×10^5 cells per well. Lentiviral particles with a multiplicity of infection of 10 for HT-29 and 18 for Caco2 were added to the cells. GFP-expressing cells were observed using fluorescence microscopy, and stable transfected cells were selected with puromycin (8 μg/mL). After RNA and protein were collected, and the interference efficiency was calculated, the cells were used for subsequent experiments. Levels of HDAC1 mRNA and protein expression were measured by RT-qPCR and Western blotting. Previous research has shown that HDAC1 expression decreases upon WA treatment. It was hypothesized that WA-induced apoptosis and autophagy in CRC cells were mediated by HDAC1 downregulation. CRC cells transfected with PCMV-HDAC1 or PCMV-NC were treated with 1 μM WA for subsequent experiments, including colony formation, scratch healing, Transwell migration, flow cytometry, Western blotting, and RT-qPCR assays, to verify that WA-induced apoptosis and autophagy were mediated by HDAC1 downregulation.

Studies *in vivo*

Eight-week-old C57BL/6J mice were purchased from SiPeiFu Biotechnology Co., Ltd., Beijing. They were housed under standard laboratory conditions. The animals were kept 3–5 per individually ventilated cage (IVC) under specific-pathogen-free (SPF) conditions at 22 ± 2°C, 40–60% relative humidity, and a 12- hour light/12- hour dark cycle (lights on from 07: 00 to 19: 00). Sterilized squirrel cages, feed (high- fat diet), bedding, and drinking water were regularly replaced. WA (cat. no. T 5687- 250 mg), used in mice, was obtained from Targetmol

Chemicals Inc. (Boston, USA). 2- amino- 3- methyl- 3 H- imidazo [4, 5- f] quinoline IQ was supplied by Toronto Research Chemicals Inc. (Canada). Corn oil was purchased from Jinlongyu, China. Mice were weighed, and their initial body weights were recorded before placement in the cage. Body weights were measured again after 3 weeks on a high- fat diet and prior to each oral (gavage) drug/oil administration. The oil group received 0.2 mL of oil; the IQ group received 100 mg/kg body weight; and the WA group received 2 mg/kg body weight, with both IQ and WA dissolved in corn oil, administered once every two days. Mice were euthanized by cervical dislocation. IQ, a potent heterocyclic aromatic amine (HAA) formed during high-temperature cooking of protein-rich foods, is classified by the International Agency for Research on Cancer as a Group 2A carcinogen. In rodents, oral gavage doses of IQ can rapidly induce DNA adduct formation, chronic inflammation, and result in aberrant crypt foci (ACF) within 3–4 weeks. Eight-week-old C57BL/6J mice (n = 5 per group) were acclimated for 1 week and then maintained on a high-fat diet (Research Diets D12492, 60% kcal from fat) to promote tumor development. Colitis-associated ACF was induced via gavage of IQ dissolved in corn oil at 100 mg/kg body weight (0. 0,1 mL/10 g). Successful induction was defined as having≥20 macroscopically visible ACF per colon, along with histologically confirmed dysplasia at necropsy in the IQ-alone group. Body weight: mice were weighed before being placed in the cage, and initial weights were recorded; body weights were also measured and recorded before each intragastric gavage. General health status, including activity, stool consistency, and rectal bleeding, was assessed daily. This project was approved by the Laboratory Animal Ethics and Welfare Committee of Shandong University Qilu College of Medicine (Approval number: 21099).

Bodies against HDAC1 (cat. no. 10197-1-AP, 1:500) and LC3B (cat. no. 14600-1-AP, 1:1000) used in IHC were obtained from Proteintech Biotechnology, Inc. (Wuhan, China). Colorectal tissues were fixed in 4% paraformaldehyde for 24 hours, dehydrated through graded ethanol, cleared in xylene, and embedded in paraffin. Sections 4 μm thick were cut on a rotary microtome, deparaffinized, rehydrated, and stained with hematoxylin for 5 minutes, followed by eosin for 2 minutes. After dehydration and mounting, whole-slide digital images were captured at 200× magnification. Aberrant crypt foci (ACF) were identified by two independent investigators blinded to treatment groups according to established morphological criteria. The percentage of ACF per colon was calculated. Antigen retrieval was performed by heating sections in 10 mM citrate buffer (pH 6.0) at 95°C for 20 minutes. Endogenous peroxidase activity was blocked with 3% H_2O_2 in methanol for 15 minutes, followed by 5% normal goat serum for 30 minutes. Sections were incubated overnight at 4°C with primary antibodies: rabbit anti-HDAC1 (Proteintech, 10197-1-AP, 1:500) and rabbit anti-LC3B (Proteintech, 14600-1-AP, 1:1000). After PBS washes, horseradish-peroxidase-conjugated goat anti-rabbit IgG (Huaan, HA1001, 1:200) was applied for 1 hour at room temperature. DAB was used as the chromogen; sections were counterstained with hematoxylin, dehydrated, and mounted. Five non-overlapping high-power fields (HPF, 400×) per section were photographed. Integrated optical density (IOD) of positive staining was measured using Image-Pro Plus 6.0 (Media Cybernetics). Data were normalized to the total tissue area in each field and expressed as IOD/μm^2. Mean values from five mice per group were used for statistical analysis.

Statistical analysis

GraphPad Prism 8.0.1 software was used for statistical analysis. The results are presented as mean ± SD (n≥3). Single-point data (e.g., IC_{50} values, apoptotic index, protein densitometry) were first tested for normality (Shapiro–Wilk test) and homoge-

neity of variances (Levene's test). Normally distributed data were compared between two groups using an unpaired Student's t-test or among three or more groups with one-way ANOVA followed by Tukey's post-hoc test. Repeated measurements (such as CCK-8 viability assays and body-weight curves) were analyzed with two-way repeated-measures ANOVA (factors: treatment and time), followed by Bonferroni's post-hoc test when an interaction was detected. The statistical significance of differences between groups ($p<0.05$) was assessed by one-way ANOVA.

RESULTS

Withaferin-A inhibits the proliferation and motility/migration of CRC cells

To evaluate the anticancer effect of WA on CRC cell lines, cells were treated with various concentrations of WA. The CCK8 assay revealed that WA significantly reduced cell viability in a dose- and time-dependent manner compared to the control group (Fig. 1A-C). The half maximal inhibitory concentration (IC_{50}) values are shown in Table 1. Next, the role of WA in colony formation was assessed. Compared to the control group, the number of colonies in the WA group was significantly decreased (Fig. 1D and E). Changes in the motility and migration capacity of CRC cells were examined using wound healing and Transwell (migration) assays. Decreased cell motility was observed in CRC cells treated with WA. The 48-hour wound-healing rate in the WA group differed significantly from that in the control group (Fig. 1F and G). Cell migration capacity was also reduced in the WA-treated group compared with the control. Additionally, the number of CRC cells migrating into the lower chamber differed significantly (Fig. 1H and I). These assay results indicate that cell proliferation, migration, and overall activity were significantly reduced in the WA group compared with the control group.

Withaferin-A induces the apoptosis of CRC cells

To confirm the effect of WA on cell apoptosis in CRC cells, cells treated with 0 and 1 μM of WA for 24 hours were analyzed by flow cytometry. The data showed significant differences in apoptosis rates among the CRC cells; all results are presented in (Fig. 1J and K). WA treatment increased apoptosis in CRC cells, which inhibits their growth.

Withaferin-A induces the autophagy of CRC cells

The results of MDC staining and TEM assays are shown in (Fig. 2A–D). The data indicate a significant difference in the number of autophagosomes between the two groups. As shown in the histogram, fluorescence intensity analysis revealed that autophagic vesicles in the WA group were significantly higher than in the control group. Additionally, LC3B fluorescence intensity indicated a significant difference in autophagy levels between the two groups (Fig. 2E and F).

Effect of Withaferin-A on HDAC1/LC3B / p62/Bax and Bcl-2 expression in CRC cells

RT-qPCR was used to measure the mRNA levels of LC3B, p62, Bax, and Bcl-2 in response to WA. As shown in (Fig. 3A - B), treatment with WA increased LC3B and Bax mRNA levels and decreased p62 and Bcl-2 mRNA levels. Western blotting was performed to detect the protein levels of these molecules, with or without 1 μM WA. The protein expression of HDAC1, p62, Bax, Bcl-2, and the LC3B II/I ratio, as previously described, is shown in (Fig. 3C and D). In summary, there were significant increases in LC3B II/I and the Bax to Bcl-2 ratio in the WA treatment group, alongside a reduction in p62 levels in total protein, as demonstrated in (Fig. 3E and F). The mRNA and total protein expression of HDAC1 were similarly decreased in the WA-treated group (Fig. 3G-I).

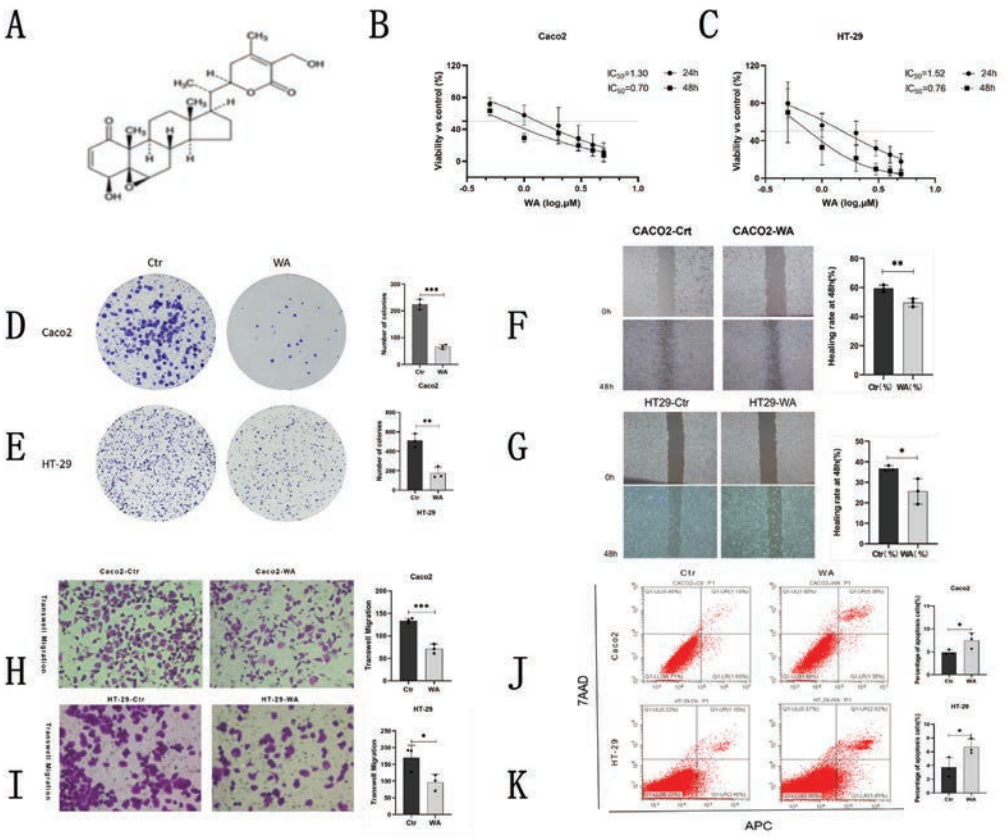

Fig. 1. The molecular structure of WA (A) and the CCK8 assay demonstrated that WA significantly decreased cell viability compared to the control group in a dose- and time-dependent manner. (B and C) IC_{50} values are provided in Table 1. The number of colonies in both groups was quantified, as shown in the graphs, and the corresponding histograms are included (D and E). Wound healing assay results and statistical graphs are shown in (F and G). The number of cells migrating into the lower chamber (H and I) was significantly different. Apoptosis rates in the two groups also showed significant differences (J and K). An unpaired Student's t-test was used, with n=3 replicates, * $p<0.05$, ** $p<0.01$, *** $p<0.001$. WA: Withaferin-A.

Table 1. IC_{50} of Withaferin-A in CRC Cells.

CRC Cells	IC_{50} of WA (μM)	
	24h	48h
CACO2	1.30	0.70
HT-29	1.52	0.76

CRC: colorectal cancer; WA: Withaferin-A. IC_{50}: half-maximal inhibitory concentration; CACO2: human colon adenocarcinoma-derived cell line; HT-29 human colorectal adenocarcinoma epithelial cell line.

Histone Acetyltransferase Activity/ Inhibition Assay

The HDAC Activity/Inhibition Assay demonstrated that WA can inhibit HDACs, similar to Trichostatin A (TSA), a specific HDAC inhibitor. The difference was statistically significant (Fig.4A). HDAC1 expression was notably increased after transfection with a lentiviral vector and purine screening. HDAC1 mRNA and protein levels were measured by RT-qPCR and Western blotting. The upregulation ratio also showed a significant difference (Fig.4B-D). Cell proliferation activity in the PCMV-HDAC1 group (HDAC1 overexpression) was significantly higher compared to the NC group (Fig.4E-H). The CCK8 assay determined the IC_{50} (Table 2) and revealed cell viability at various doses and time points relative to the control group. Additionally, cell motility and migration capacity increased in the PCMV-HDAC1 group (Fig.4I-L).

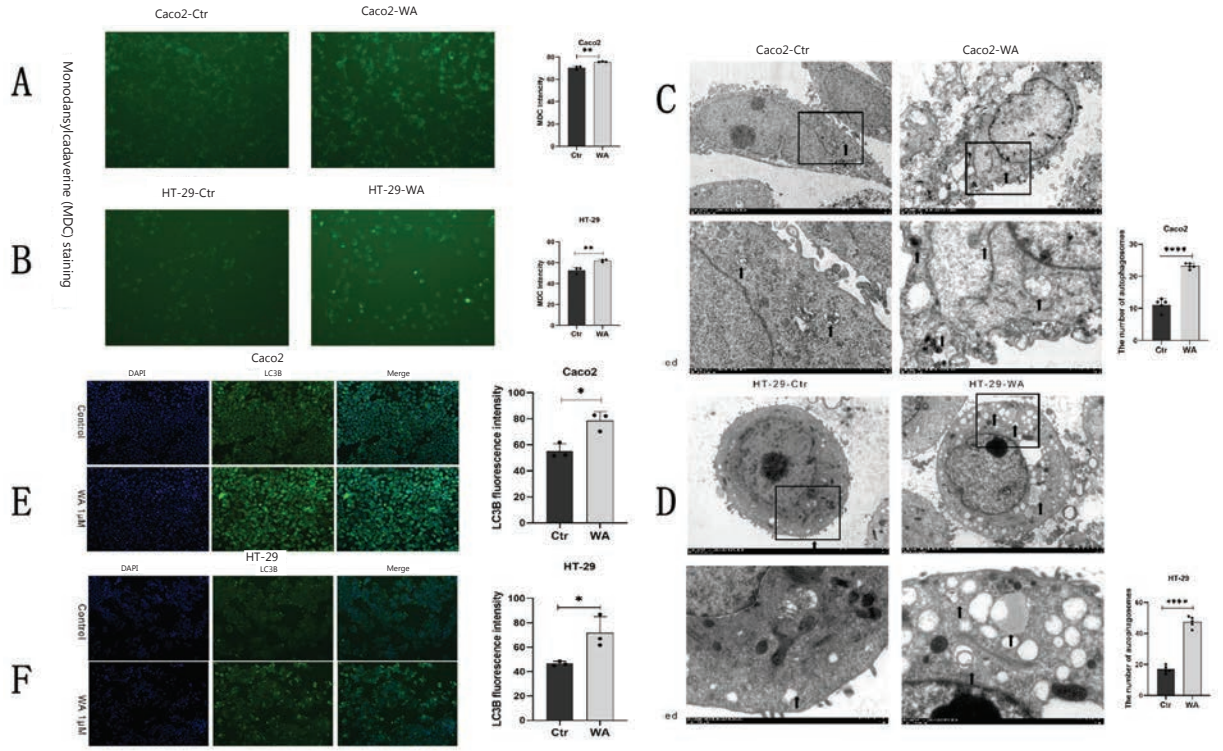

Fig. 2. Experiments using MDC staining were conducted to measure autophagosomes in two groups. Histograms indicated that autophagic vesicles in the WA group were significantly higher compared to the control group. (A-B) TEM analysis is displayed in (C). An enlarged section of the spectrogram (black box) is shown below (D). Autophagosome-like structures are marked with black arrows. Immunofluorescence analysis revealed that LC3B fluorescence intensity, an autophagy marker, varied significantly between the two groups (E and F). An unpaired Student's t-test was used, with n=3 replicates, * $p<0.05$, ** $p<0.01$, **** $p<0.0001$. WA: Withaferin-A; MDC: Monodansylcadaverine; TEM: Transmission Electron Microscope.

The apoptosis rates in the two groups

Flow cytometry analysis of apoptosis was also significantly reduced in the PCMV-HDAC1 group (Fig. 5A and B). Additionally, mRNA expression levels of molecules involved in apoptosis and autophagy were affected. Bax and LC3B expressions were notably decreased, while p62 and Bcl-2 were markedly increased in the PCMV-HDAC1 group (Fig. 5C and D). Protein expression levels of Bax/Bcl-2 and LC3B-II/I were significantly lower, whereas p62 levels were notably higher in the PCMV-HDAC1 group (Fig. 5E-H).

The study *in vivo*

Eight-week-old C57BL/6J mice were fed a high-fat diet for three weeks, then given the colonic carcinogen IQ (100 mg/kg) by gavage once every two days. Starting the day after, animals were gavaged every two days with either vehicle (corn oil) or Withaferin-A (WA, 2 mg/kg) dissolved in corn oil (Fig. 6A, B). Mice were weighed before being placed in the cage, and initial weights were recorded; body weight was also measured before each intragastric gavage. No significant differences were observed among groups at any time point, indicating that WA was well tolerated (Fig. 6C). After sacrifice, colons were excised longitudinally and examined. WA-treated mice showed a significant reduction in the number and size of macroscopically visible aberrant crypt foci (ACF) compared to the IQ-only group (Fig. 6D). HE staining

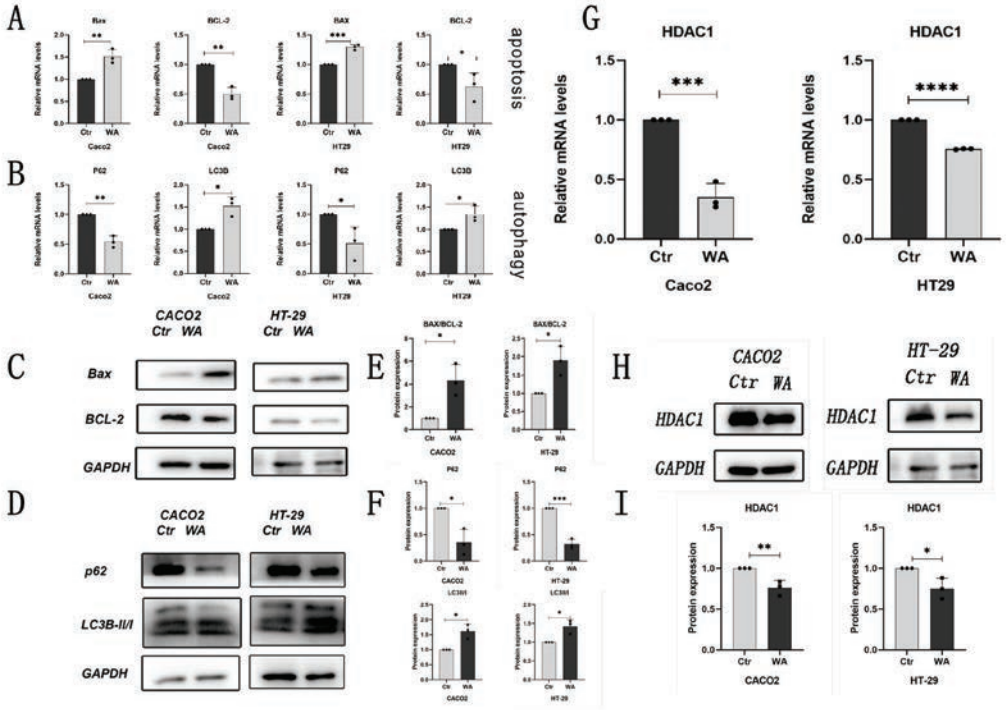

Fig. 3. Significant increases in LC3B/Bax and decreases in Bcl-2/p62 mRNA levels were observed, along with notable changes in protein expression of p62/Bax/Bcl-2 and the LC3B-II/I ratio, all of which were statistically significant. (C-F) RT-qPCR and Western blotting confirmed that HDAC1 mRNA and total protein levels were also significantly reduced in the W-treated group (G-I). An unpaired Student's t-test was used, with n=3 replicates, and significance levels indicated as * $p<0.05$, ** $p<0.01$, *** $p<0.001$, **** $p<0.0001$. WA: Withaferin-A; HDAC1: histone deacetylase 1.

Table 2. IC_{50} of **Withaferin-A** in CRC Cells.

CRC Cells	IC_{50} (WA=1uM)	
CACO2	PCMV-HDAC1	2.341
48h	PCMV-NC	1.738
HT-29	PCMV-HDAC1	3.239
48h	PCMV-NC	2.507

CRC: colorectal cancer; WA: Withaferin-A. IC_{50}: half-maximal inhibitory concentration; CACO2: human colon adenocarcinoma-derived cell line; HT-29 human colorectal adenocarcinoma epithelial cell line; HDAC1: Histone Deacetylase 1 enzyme; PCMV-HDAC1: CRC cells transfected with HDAC1; PCMV-NC: CRC cells not transfected with HDAC1.

was used to analyze the percentage of ACF. Colorectal tissue slices from all three groups were stained, revealing that ACF contained crypt branching, distortion, atrophy, surface irregularity, mucin depletion, Paneth cell metaplasia, cryptitis, crypt abscesses, basal plasmacytosis, or lymphoid aggregates, with statistical significance (Fig. 6E). Representative immunohistochemical images and quantitative analyses of LC3B and p62 expression from different groups are shown in (Fig. 6F). Compared to the IQ group, the WA group showed reduced LC3B and p62 positivity, indicating that WA can reduce the IQ-induced increase in LC3B and p62 expression (Fig. 6F).

DISCUSSION

Over the last few decades, the use of plant-derived edibles and the consumption of highly active, naturally occurring or synthetic, highly specific drugs have increased[15-18]. Plant-derived natural molecules have fewer side effects and are readily available. They have been used in the treatment of various

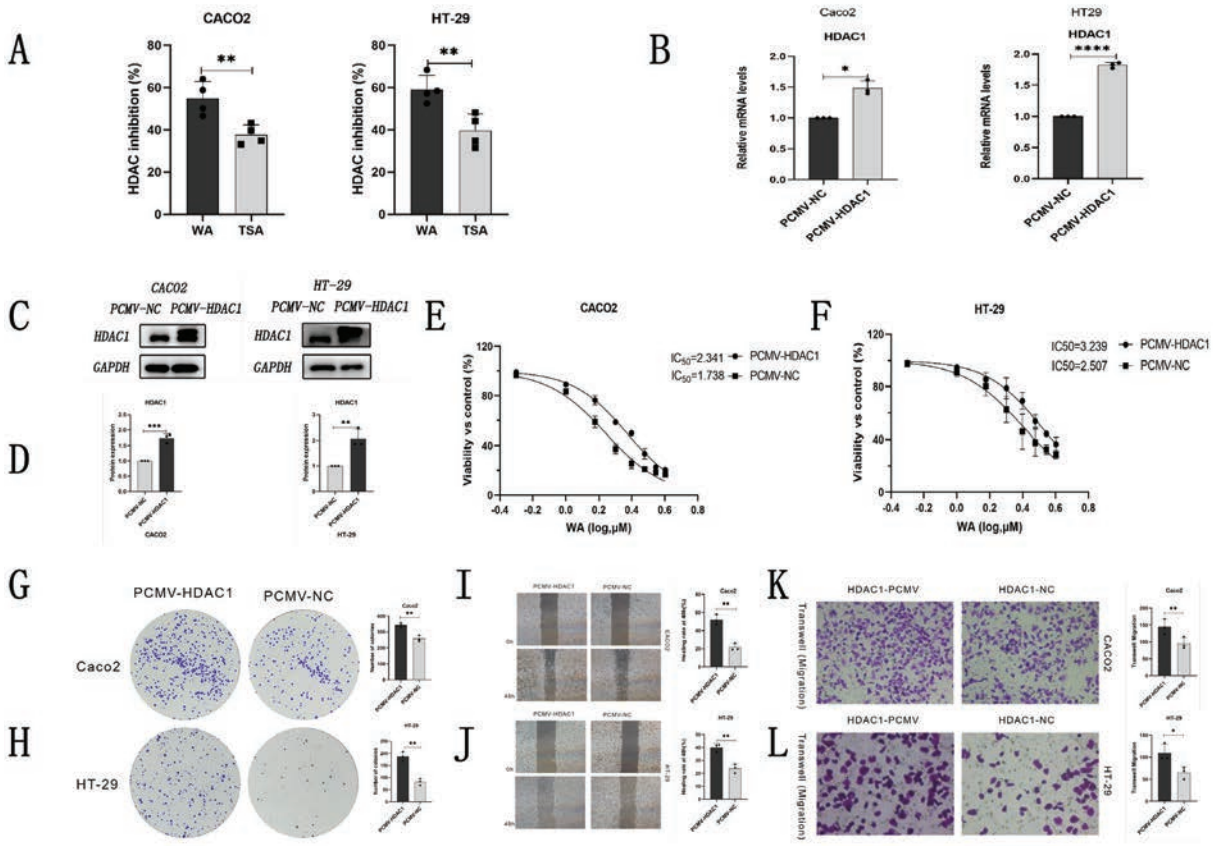

Fig. 4. The HDAC activity/Inhibition Assay showed that both WA and TSA decreased total HDAC mRNA levels, with the difference being statistically significant (A). HDAC1 mRNA and protein levels were measured by RT-qPCR and Western blotting, respectively, and the upregulation ratios indicated a statistically significant difference (B-D). The results of the CCK8 assay are presented in (E and F). The number of colonies for both groups, as shown in the graphs, was quantified and displayed in histograms (G and H). The wound-healing assay and its statistical analysis are shown in (I and J). The number of cells migrating into the lower chamber (K and L) differed significantly. An unpaired Student's t-test was used, with n≥3 replicates. Significance levels are indicated as * $p<0.05$, ** $p<0.01$, **** $p<0.0001$. WA: Withaferin-A; HDAC1: histone deacetylase 1; TSA: Trichostatin A.

diseases [19-21]. WA, a steroidal lactone, is a promising anticancer phytochemical that is abundantly isolated from Withania somnifera (a medicinal plant native to Asia) and exhibits anti-inflammatory, immunomodulatory, and anti-angiogenic properties[22, 23]. The potency of natural drugs or potential toxicity can often be addressed through semi-synthetic approaches. WA exerts its anti-tumorigenic effects in different types of cancer, especially in breast cancer [24].

Anticancer effect of WA contains its effects on cancer-relevant cellular processes (e.g., growth arrest, apoptosis induction, autophagy, metabolic adaptation, immune function, etc.) and molecular targets (e.g., suppression of oncogenes such as estrogen receptor-α, signal transducer and activator of transcription 3, etc.) [25, 26]. WA has promising roles in cancer prevention and therapy. It can reduce cellular proliferation and viability in certain cancer cell lines, modulate inflammatory pathways, and induce apoptosis, all of which have piqued interest in its use as a potential chemotherapeutic agent [27].

Some reported its ability to regulate epigenetic processes. However, acetylation has been studied infrequently, particularly

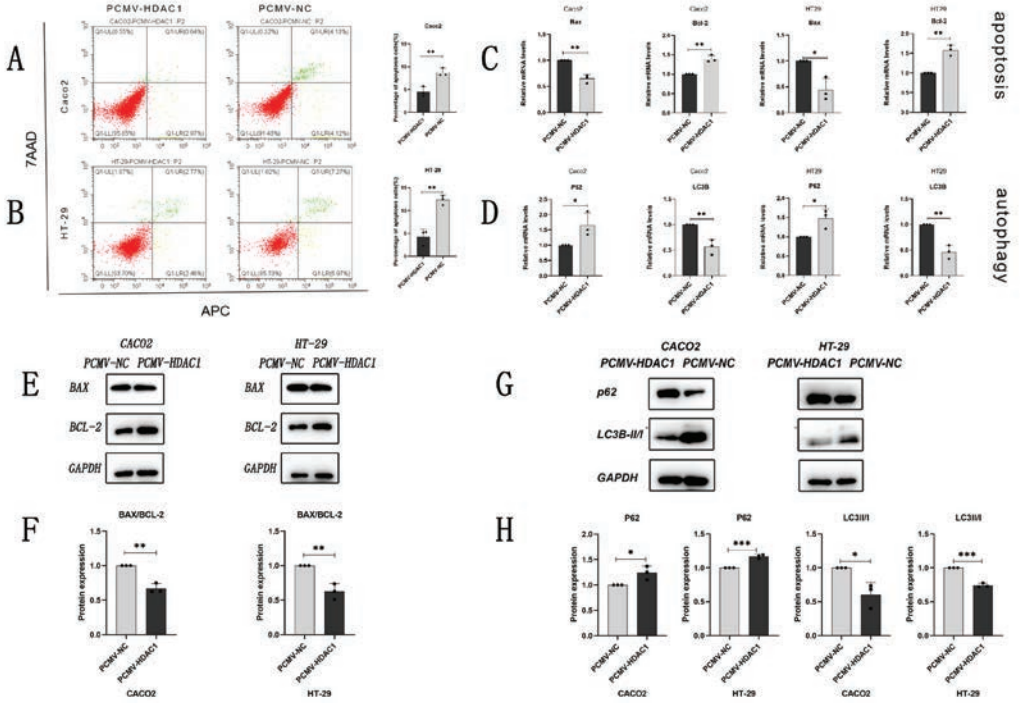

Fig. 5. The apoptosis rates between the two groups also differed significantly (A and B). RT-qPCR assay verified that the mRNA levels (C and D) of LC3B, Bax, Bcl-2, and p62 (E and F) are statistically significant. Western blotting confirmed the total protein expression of p62, LC3B-II/I, and Bax/Bcl-2 (G and H), with statistical significance (G and H). An unpaired Student's t-test was used, with n=3 replicates. * $p<0.05$, ** $p<0.01$, *** $p<0.001$.

in CRC cells. Histone acetylation is catalyzed by histone acetyltransferase (HAT) and HDACs. The goal of this study was to examine the anticancer effects of WA in CRC cells and to elucidate the mechanisms underlying its regulation of acetylation.

Firstly, cell proliferation and motility/migration in the WA group were significantly reduced compared to the control group. Secondly, WA induces apoptosis in CRC cells, with a significant increase in the Bax/Bcl-2 ratio at both the protein and mRNA levels. Thirdly, WA induces autophagy in CRC cells; p62 protein and mRNA expression were significantly decreased, while LC3B-II/I levels were significantly increased. Moreover, MDC staining and the TEC assay confirmed autophagy induction. Fourthly, the HDAC Activity Assay revealed that WA can inhibit HDAC activity, similar to Trichostatin A (TSA), a specific HDAC inhibitor. The differences were statistically significant. In this study, WA also increased the LC3B-II/I ratio and decreased p62 protein and mRNA levels. The increase in LC3B-II could be due to increased autophagosome formation or impaired degradation, whereas p62, an autophagic substrate, shows a continuous decrease, suggesting enhanced rather than blocked autophagic flux. Activation of autophagic flux was further confirmed by TEM observation of numerous autophagosomes, punctate MDC accumulation, and LC3B immunofluorescence. Because p62 also has signal-transduction functions, its degradation can weaken pro-survival pathways, thereby increasing WA cytotoxicity. Notably, HDAC1 overexpression reversed the decrease in p62, suggesting that HDAC1 may "clamp" autophagic flux by transcriptionally repressing certain core autophagy genes or upregulating mTORC1 signaling; after WA relieves this

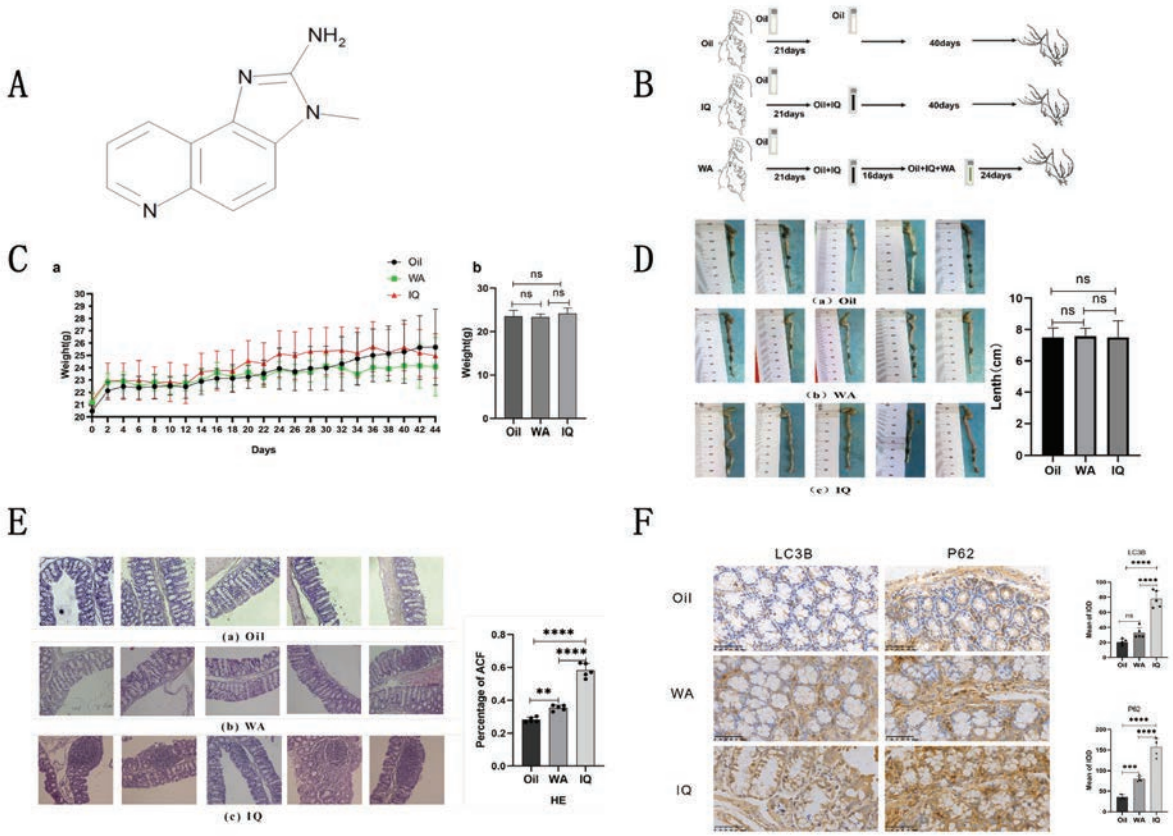

Fig. 6. Structure of IQ (A). Dose and timing of Oil/WA and IQ in different groups (B). Images of mice's dynamic weight (C) and colorectal tissues (D). HE staining showed that the percentage of ACF varied significantly across groups (E). Representative immunohistochemical images and quantitative analyses of LC3B and p62 expression across groups (×200) were also statistically significant (F-test). n=5 mice per group; two-way repeated-measures ANOVA was used for (C), and one-way ANOVA followed by Tukey's post hoc test for (E) and (F). ** $p<0.01$, *** $p<0.001$, **** $p<0.0001$. IQ: 2-amino-3-methyl-3H-imidazo[4,5-f]quinoline; WA: Withaferin-A.

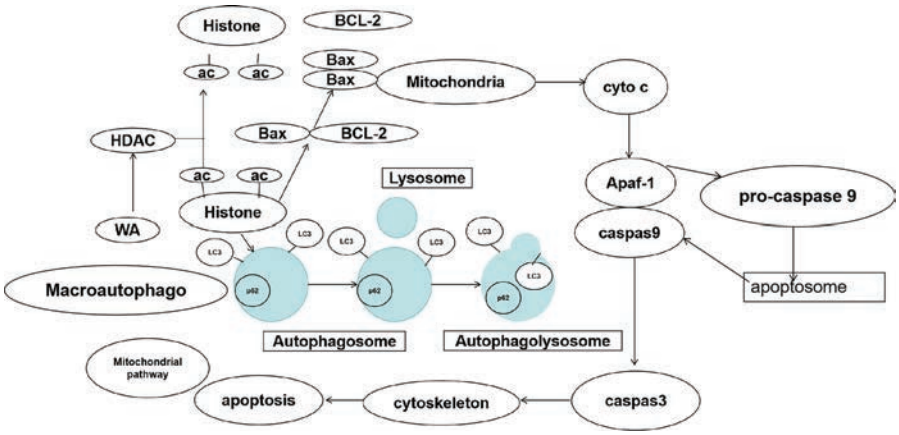

Fig. 7. Mechanism diagram

WA: Withaferin-A, HDAC: Histone deacetylase, Ac: Acetylation, LC3: microtubule-associated protein 1 light chain 3, BCL-2: B cell lymphoma/leukemia-2 protein, Bax: Bcl-2-associated X protein, p62: ubiquitin-binding protein p62.

"clamp," autophagosome formation accelerates along with degradation, leading to p62 consumption. An increased Bax/Bcl-2 ratio is a classic mitochondrial apoptosis switch. HDAC1 binds to the transcriptional repression complex Sin3A/CoREST to deacetylate histone H3K9 at the Bax gene promoter and inhibit transcription; simultaneously, HDAC1 can deacetylate non-histone proteins, thereby weakening their pro-apoptotic functions [14]. Following HDAC1 inhibition by WA, acetylation levels at the Bax promoter region are restored, and transcription is enhanced. Bcl-2 is then downregulated due to the loss of HDAC1-mediated sustained STAT3 activation, leading to an increased Bax/Bcl-2 ratio, greater mitochondrial outer membrane permeability, cytochrome c release, and activation of the caspase-9/3 cascade [22]. Overexpression of HDAC1 again increased histone deacetylation levels and reversed these effects, supporting the HDAC1-acetyl-Bax/Bcl-2-mitochondrial apoptosis axis as a key mechanism of WA.

As previously described, WA may function like a histone deacetylase inhibitor in CRC cells. Therefore, we hypothesized that WA promotes cancer cell death by inhibiting the epigenetic effects of HDACs [15]. Among these, HDAC1 plays an important role. Subsequent experiments confirmed this: HDAC1 expression was significantly upregulated after transfection with a lentiviral vector and purine screening. HDAC1 mRNA and protein levels were measured by RT-qPCR and Western blotting, and the upregulation ratio differed significantly. The CCK8 assay revealed that the IC_{50} values of the two groups also differed significantly. Cell proliferation and motility/migration in the PCMV-HDAC1 group were significantly higher than in the NC group. The rates of apoptosis and autophagy also differed significantly between the two groups. RT-qPCR and Western blotting verified that the mRNA and total protein expression levels of p62/LC3II/I and Bax/Bcl-2 were statistically significant. Based on these results, we found that the anti-cancer effect of WA against the PCMV-HDAC1 group was significantly lower than against the PCMV-NC group.

Finally, to validate our *in vitro* results, we also examined the effects of WA in C57BL/6J mice. The IQ-induced inflammatory CRC model was characterized by a spike in ACF numbers, increased LC3B speckles, and cytoplasmic accumulation of p62 as the main pathological features. After WA treatment, the number of ACFs decreased by more than 60%, and p62/LC3B levels in intestinal tissue decreased significantly. It is important to note that the body weight curve of WA-treated mice was similar to that of the control group, indicating that WA is safe at effective doses and provides a solid basis for its potential future use as an HDAC1-targeted CRC chemopreventive or adjuvant therapy.

This novel treatment may offer a strategy for CRC treatment. In addition to the previously mentioned detection of HDAC1 expression, WA could also inhibit other HDACs in CRC cells. Acetylation of histones can serve as specific anchors for recruiting transcription factors. Finding downstream transcription factors may further elucidate the anti-cancer mechanism of WA. A mechanism diagram is shown in Fig. 7.

These results demonstrate that WA can inhibit CRC cell proliferation and migration. The treatments also decreased Bcl-2 expression and increased Bax expression, thereby elevating the Bax/Bcl-2 ratio. Undeniably, WA enhanced apoptosis in CRC cells. WA also promotes autophagy in CRC cells. Furthermore, we examined the molecular mechanisms underlying WA-induced apoptosis and autophagy in CRC cells. When HDAC1 was overexpressed using a lentiviral vector, all prior effects were abolished. We confirm that these effects are mediated by HDAC1 downregulation. Finally, we tested whether WA had similar effects in CRC cells in vitro. It significantly affected p62 and LC3B levels compared to the oil and IQ groups. The animal model yielded similar results.

Although this study offers initial evidence for the anticancer effects of WA in colorectal cancer and indicates that these effects may be mediated through HDAC1-dependent regulation of apoptosis and autophagy, further research using more diverse experimental models, detailed mechanistic studies, and thorough safety assessments is essential to advance its clinical application. Only Caco-2 and HT-29 cell lines were used in vitro, and their molecular characteristics and drug responses may differ from those of primary tumor cells or patient-derived organoids (PDOs). Additionally, the mouse ACF model only represents the early stage of carcinogenesis, and the effectiveness of WA on established tumors has not been evaluated. Therefore, it is crucial to further verify the safety window, optimal dose, and pharmacokinetic properties of WA using primary cultures, PDO/PDX models, and larger-animal studies, providing a foundation for early clinical trials. Future research should identify the specific molecular targets of WA, explore combination therapies, and perform preclinical pharmacokinetic evaluations to determine the feasibility of WA as a candidate for colorectal cancer prevention and treatment.

This study demonstrated, in both in vitro and in vivo models, that WA decreases HDAC1 expression while promoting apoptosis and autophagy in human colorectal cancer cells. This process inhibits cell proliferation, migration, and colony formation, and significantly reduces IQ-induced ACF in mice. These findings support further development of WA as a chemopreventive or adjunct therapy for colorectal cancer. Since WA did not cause weight loss or overt toxicity in mice at effective doses, and its molecular target, HDAC1, is often overexpressed in patients with colorectal cancer, WA seems to be a promising, low-toxicity, epigenetically targeted oral drug candidate.

Funding

This work received no funding support.

Ethical approval

This study was conducted following the principles of the Declaration of Helsinki. Approval was received from the Laboratory Animal Ethical and Welfare Committee of Shandong University Qilu College of Medicine (Approval number: 21099).

Consent to participate

Informed consent was secured from all participants involved in the study.

Competing interests

The authors have no relevant financial or non-financial interests to disclose.

ORCID numbers of authors

- Qiong Wang (QW): 0000-0003-1561-7559
- Caixia Li (CL): 0009-0003-4741-0429

Author contributions

Both authors contributed to the study's conception and design, participated in data collection, and reviewed and edited the manuscript. Both authors read and approved the final version.

REFERENCES

1. **Puspitaningtyas H, Wiranata JA, Wiratama BS, Fachiroh J, Hutajulu SH.** Association of Low Educational Attainment and Higher Colorectal Cancer Risk: Mediatory Effect of Lifestyle-Associated Factors Within Local Context. World J Oncol. 2025; 16(4):388-396. *https://doi.org/10.14740/wjon2599.*
2. **Huang P, Guo K, Tu J, Fang J, Zhou L, Luo X, et al.** Single-Cell RNA Sequencing Reveals LEF1 as a Prognostic Biomarker for Poor Outcomes in Oxaliplatin-Resistant Colorectal Cancer. Hum Mutat. 2025; 2025:6705599. https://doi.org/*10.1155/humu/6705599.*

3. **Shen R, Cheng F, Guo R, Wang W, Yang X, Chen Y, et al.** Dehydroleucodine exerts an antiproliferative effect on human Burkitt's lymphoma Daudi cells via SLC7A11-mediated ferroptosis. Front Pharmacol. 2025; 16:1572364. https://doi.org/*10.3389/fphar.2025.1572364*.
4. **Wu HC, Tsai CC, Hsu PC, Kuo CY.** Herbal Medicine in Breast Cancer Therapy: Mechanisms, Evidence, and Future Perspectives. Curr Issues Mol Biol. 2025; 47(5):362. https://doi.org/*10.3390/cimb47050362*.
5. **Lee J, Seo Y, Roh JL.** Emerging Therapeutic Strategies Targeting GPX4-Mediated Ferroptosis in Head and Neck Cancer. Int J Mol Sci. 2025; 26(13):6452. https://doi.org/*10.3390/ijms26136452*.
6. **Chen X, Ma X, Hu X, Wang C, Zhang X, Yan C.** Mechanisms and potential therapeutic strategies of withaferin A in breast cancer. Pharmacol Rep. 2025; 77: 1163-1176. https://doi.org/*10.1007/s43440-025-00736-3*.
7. **Heyninck K, Lahtela-Kakkonen M, Van der Veken P, Haegeman G, Vanden Berghe W.** Withaferin A inhibits NF-kappaB activation by targeting cysteine 179 in IKKβ. Biochem Pharmacol. 2014; 91(4):501-509. https://doi.org/*10.1016/j.bcp.2014.08.004*.
8. **Choi BY, Kim BW.** Withaferin-A Inhibits Colon Cancer Cell Growth by Blocking STAT3 Transcriptional Activity. J Cancer Prev. 2015; 20(3):185-192. https://doi.org/*10.15430/JCP.2015.20.3.185*.
9. **Yan Z, Guo R, Gan L, Lau WB, Cao X, Zhao J, et al.** Withaferin A inhibits apoptosis via activated Akt-mediated inhibition of oxidative stress. Life Sci. 2018; 211:91-101. https://doi.org/*10.1016/j.lfs.2018.09.020*.
10. **Mirza S, Sharma G, Parshad R, Gupta SD, Pandya P, Ralhan R.** Expression of DNA methyltransferases in breast cancer patients and to analyze the effect of natural compounds on DNA methyltransferases and associated proteins. J Breast Cancer. 2013;16(1):23-31. https://doi.org/*10.4048/jbc.2013.16.1.23*.
11. **Duan N, Hu X, Qiu H, Zhou R, Li Y, Lu W, et al.** Targeting the E2F1/Rb/HDAC1 axis with the small molecule HR488B effectively inhibits colorectal cancer growth. Cell Death Dis. 2023; 14(12):801. https://doi.org/*10.1038/s41419-023-06205-0*.
12. **Yang Z, Su W, Zhang Q, Niu L, Feng B, Zhang Y, et al.** Lactylation of HDAC1 Confers Resistance to Ferroptosis in Colorectal Cancer. Adv Sci (Weinh). 2025; 12(12):e2408845. https://doi.org/*10.1002/advs.202408845*.
13. **Likasitwatanakul P, Li Z, Doan P, Spisak S, Raghawan AK, Liu Q, et al.** Chemical Perturbations Impacting Histone Acetylation Govern Colorectal Cancer Differentiation. Gastroenterology. 2026; 170(1):70-88. S0016-5085(25)05732-4. https://doi.org/*10.1053/j.gastro.2025.07.003*.
14. **Dhingra N, Gupta V, Tyagi A, Agrawala PK, Gupta V.** Trichostatin A ameliorated combined radiation and skin wound injury-induced mortality and hematopoietic suppression in a rat model. Int J Radiat Biol. 2025; 101(9):952-972. https://doi.org/*10.1080/09553002.2025.2537211*.
15. **Al-Rimawi F, Rishmawi S, Ariqat SH, Khalid MF, Warad I, Salah Z.** Anticancer Activity, Antioxidant Activity, and Phenolic and Flavonoids Content of Wild Tragopogon porrifolius Plant Extracts. Evid Based Complement Alternat Med. 2016; 2016:9612490. https://doi.org/*10.1155/2016/9612490*.
16. **Yang R, Sun S, Zhang Q, Liu H, Wang L, Meng Y, et al.** Pharmacological Inhibition of TXNRD1 by a Small Molecule Flavonoid Butein Overcomes Cisplatin Resistance in Lung Cancer Cells. Biol Trace Elem Res. 2025; 203(4):1949-1960. https://doi.org/*10.1007/s12011-024-04331-0*.
17. **Liu P, Zhang B, Li Y, Yuan Q.** Potential mechanisms of cancer prevention and treatment by sulforaphane, a natural small molecule compound of plant-derived. Mol Med. 2024; 30(1):94. https://doi.org/*10.1186/s10020-024-00842-7*.
18. **An T, Yin H, Lu Y, Liu F.** The Emerging Potential of Parthenolide Nanoformulations in Tumor Therapy. Drug Des Devel

Ther. 2022; 16:1255-1272. https://doi.org/*10.2147/DDDT.S355059.*

19. **Vidjeyamannane C, Joy A, Prakash K, Saravanakumar R.** A comprehensive review on the role of plant-derived bioactive metabolites driving ROS-mediated apoptosis in cancer. Med Oncol. 2025; 42(9):420. https://doi.org/*10.1007/s12032-025-02985-x.*
20. **Wang H, Gu B, Wang Z, Zhang X, Shan L, Liu L, et al.** Emodin enhances host antiviral immunity against Micropterus salmoides rhabdovirus by activating RLR signaling in largemouth bass. Fish Shellfish Immunol. 2025; 166:110633. https://doi.org/*10.1016/j.fsi.2025.110633.*
21. **Dzięgielewska M, Tomczyk M, Wiater A, Woytoń A, Junka A.** Targeting Ocular Biofilms with Plant-Derived Antimicrobials in the Era of Antibiotic Resistance. Molecules. 2025; 30(13):2863. https://doi.org/*10.3390/molecules30132863.*
22. **Lee K, Lee D, Kim JY, Shim JJ, Bae JW, Lee JH.** Attenuation Effect of Withania somnifera Extract on Restraint Stress-Induced Anxiety-like Behavior and Hippocampal Alterations in Mice. Int J Mol Sci. 2025; 26(15):7317. https://doi.org/*10.3390/ijms26157317.*
23. **Albalawi AA.** Dual impact of Ashwagandha: Significant cortisol reduction but no effects on perceived stress - A systematic review and meta-analysis. Nutr Health. 2025; *31(4):1395-1408.* https://doi.org/*10.1 177/02601060251363647.*
24. **Elzayat EM, Elsamahy GE, Mansour GH, El-Sherif AA, Hassan N.** The Synergistic and Anticancer Potential of Withania Somnifera (Ashwagandha) Ethanol Extract as an Adjuvant with Doxorubicin in MCF7 Breast Cancer Cell Line. Asian Pac J Cancer Prev. 2025; 26(3):757-766. https://doi.org/*10.31557/APJCP.2025.26.3.757.*
25. **Baghel K, Azam Z, Srivastava R.** Dietary restriction-induced alterations on estrogen receptor alpha expression in regulating fertility in male Coturnix coturnix japonica: Relevance of Withania somnifera in modulation of inflammation and oxidative stress in testis. Am J Reprod Immunol. 2024; 91(2): e13816. https://doi.org/*10.1111/aji.13816.*
26. **White PT, Subramanian C, Motiwala HF, Cohen MS.** Natural Withanolides in the Treatment of Chronic Diseases. Adv Exp Med Biol. 2016; 928:329-373. https://doi.org/*10.1007/978-3-319-41334-1_14.*
27. **Hameed H, Afzal M, Khan MA, Javaid L, Shahzad M, Abrar K.** Unraveling the role of withanolides as key modulators in breast cancer mitigation. Mol Biol Rep. 2025; 52(1):331. https://doi.org/*10.1007/s11033-025-10442-1.*

Invest Clin 67(1): 92 - 107, 2026 https://doi.org/10.54817/IC.v67n1a07

Phyllanthin identified from *Phyllanthus amarus* attenuates arsenite-induced liver and kidney damage: Role of NF-kB pathway inhibition.

Jiarui Xu[1], Smeeta Sadar[2], Hemant Kamble[3] and Yingtao Zhang[4]

[1]Department of Poisoning and Occupational Diseases, Emergency Center, Shandong Provincial Hospital Affiliated to Shandong First Medical University, Jinan, China.
[2]Dr. D. Y. Patil College of Pharmacy, Akurdi, Pune, Maharashtra.
[3]Shri Wagheshwar Gramvikas Pratishthan's Pharate Patil College of Pharmacy, Mandavgan Pharata, Maharashtra, India.
[4]Department of Nephrology, Yan'an People's Hospital, Yan'an, China.

Keywords: Antioxidant; Hepatotoxicity; Nephrotoxicity; NF-κb; Oxidative stress; *Phyllanthus amarus;* Sodium arsenite.

Abstract. Sodium arsenite is a common and highly toxic inorganic arsenic compound that causes liver and kidney damage. *Phyllanthus amarus* is well known for its protective effects on these organs. This study aimed to identify the active phytoconstituents of the methanolic extract of *P. amarus* (PAME) and to explore their effects on arsenite-induced liver and kidney toxicity in experimental rats. The standardization of *P. amarus* extract was performed using high-performance liquid chromatography (HPLC). Male Wistar rats developed liver and kidney toxicity after daily oral administration of sodium arsenite (5 mg/kg) for 4 weeks. The rats were simultaneously given coenzyme Q10 (CoQ10; 10 mg/kg) or PAME (50, 100, and 200 mg/kg). Results showed that HPLC analysis detected phyllanthin at a retention time of 25.41 minutes with an area of 71.84%. Arsenite treatment caused a significant ($p<0.001$) increase in hepatic enzymes (ALT, AST, and ALP), renal markers (BUN, uric acid, and creatinine), and direct and total bilirubin in the serum. It also significantly increased hepatic and renal levels of malondialdehyde, nitric oxide, NF-κB p65, interleukins (ILs), and TNF-α ($p<0.001$), while decreasing hepatic antioxidant enzymes (GSH and SOD) and overall hepatic antioxidant capacity. Notably, P. amarus extract (200 mg/kg) markedly ($p<0.001$) mitigated arsenite-induced changes in these serum markers, oxidative stress indicators, NF-kB p65, and inflammatory cytokines. It also improved the structure of liver and kidney tissues, maintained cellular architecture, and reduced necrosis and inflammation. In conclusion, these results suggest that phyllanthin from *P. amarus* protects against arsenite-induced liver and kidney damage by inhibiting NF-κB activation, reducing inflammatory cytokine release, and decreasing oxidative and nitrosative stress, thereby enhancing overall antioxidant capacity. Therefore, *P. amarus* extract may be a promising treatment for pesticide-related liver and kidney injuries in rats.

Corresponding author: Yingtao Zhang. Department of Nephrology, Yan'an People's Hospital, Yan'an, 716000, China. E-mail: snkzyt@sina.com

La filantina identificada en *Phyllanthus amarus* atenúa el daño hepático y renal inducido por arsenito: papel de la inhibición de la vía NF-Kb.

Invest Clin 2026; 67 (1): 92 – 107

Palabras clave: Antioxidante; Hepatotoxicidad; Nefrotoxicidad; NF-κb; Estrés oxidativo; *Phyllanthus amarus*; Arsenito de sodio.

Resumen. El arsenito de sodio es un compuesto inorgánico de arsénico, de prevalencia elevada y altamente tóxico, que causa toxicidad hepática y renal. *Phyllanthus amarus* está bien documentado por sus efectos hepatoprotectores y nefroprotectores. Este estudio tuvo como objetivo examinar los fitoconstituyentes activos del extracto metanólico de *P. amarus* (PAME) y sus mecanismos de acción sugeridos contra la toxicidad hepática y renal inducida por el arsenito en ratas experimentales. La estandarización del extracto de P. amarus se realizó mediante cromatografía líquida de alta resolución (HPLC). Ratas Wistar machos desarrollaron toxicidad hepática y renal tras la administración oral continua de arsenito de sodio (5 mg/kg) durante 4 semanas. A las ratas se les administró por vía oral coenzima Q10 (CoQ10; 10 mg/kg) o PAME (50, 100 y 200 mg/kg) de forma concomitante. En los resultados, el análisis de HPLC mostró la presencia de filantina con un tiempo de retención de 25,41 min y un área de 71,84%. La administración de arsenito dio lugar a un aumento significativo ($p<0,001$) de las enzimas hepáticas (ALT-alanina aminotransferasa), AST (aspartato aminotransferasa) y ALP (fosfatasa alcalina), de las enzimas renales (BUN (nitrógeno ureico en sangre), ácido úrico y creatinina) y de la bilirrubina directa y total en el suero. También elevó efectivamente ($p<0,001$) los niveles hepáticos y renales de malondialdehído, óxido nítrico, NF-κB (factor nuclear kappa de la cadena ligera de las células B activadas) p65, IL (interleucinas) y TNF-α (factor de necrosis tumoral alfa), y disminuyó las enzimas antioxidantes GSH (glutatión) y SOD (superóxido dismutasa), así como la capacidad antioxidante total hepática. Sin embargo, el extracto de *P. amarus* (200 mg/kg) atenuó notablemente ($p<0,001$) las alteraciones inducidas por el arsenito en estos marcadores séricos, los parámetros de estrés oxidativo, NF-κB p65 y los niveles de citoquinas inflamatorias. También mejoró la histología hepática y renal, preservó la arquitectura celular y redujo la necrosis e inflamación. En conclusión, estos hallazgos sugieren que la filantina de *P. amarus* ejerce efectos protectores contra la hepatotoxicidad y la nefrotoxicidad inducidas por el arsenito al inhibir la activación de NF-κB y disminuir la liberación de citoquinas inflamatorias y el estrés oxidativo-nitrosativo, mejorando así la capacidad antioxidante general. Por lo tanto, el extracto de *P. amarus* podría constituir un tratamiento eficaz para el daño hepático y renal inducido por pesticidas en ratas.

Received: 20-10-2025 Accepted: 12-11-2025

INTRODUCTION

Sodium arsenite is a common, highly toxic inorganic arsenic compound. Environmental exposure to arsenic through drinking arsenic-contaminated groundwater can cause several health hazards, particularly affecting the liver and kidneys [1]. In more than 70 countries, approximately 140 million people drink water with arsenic concentrations exceeding the WHO provisional limit of 10 μg/L [2]. According to models, approximately 94–220 million people are at risk of exposure to high arsenic levels in groundwater[3]. When exposed, sodium arsenite induces inflammation and oxidative stress, primarily in the kidneys and liver, thereby disrupting homeostasis.

Disruption of this balance, along with the reactive nitrogen species (RNS) and reactive oxygen species (ROS)-mediated induction of oxidative stress, triggers hepatocellular injury [4]. Additionally, arsenite-induced hepatotoxicity and nephrotoxicity are characterized by mitochondrial damage and ATP depletion, which in turn lead to oxidative stress. This is evidenced by increased oxidative markers, such as lipid peroxidation (malondialdehyde, MDA) and nitrite/nitrate levels, as well as decreased antioxidant defenses, including glutathione (GSH), catalase, and superoxide dismutase (SOD) [5]. Sodium arsenite enhances pro-inflammatory signaling pathways and induces apoptosis in renal and hepatic tissues by upregulating proteins such as caspase-3 and tumor necrosis factor-alpha (TNF-α) [5,6]. Consequently, researchers aim to strengthen the antioxidant defense system to reduce the production of free radicals induced by arsenite toxicity.

Current therapeutic strategies for arsenite-induced toxicity involve chelation therapy and antioxidant treatment. Chelation therapy is a standard method, with 2,3-dimercaptosuccinic acid (DMSA) being the most commonly used chelating agent, which helps bind and remove arsenic from the bloodstream. However, DMSA alone is not enough to eliminate arsenic from intracellular compartments, leading to toxicity and cell damage. As a result, combined therapies are being investigated to improve their effectiveness [7]. A new approach is to add antioxidants alongside chelators. Coenzyme Q10 (CoQ10), which has antioxidant properties, protects against arsenic-induced intracellular damage and, when used with DMSA, offers enhanced protection against arsenite toxicity [7]. Dual therapy not only promotes the removal of arsenic from the extracellular space but also protects against intracellular arsenic toxicity, demonstrating broader pharmacological benefits in arsenic poisoning. However, these treatments are very costly, necessitating affordable alternatives. Plant-derived medicinal compounds present a promising, low-cost option for addressing arsenite-induced toxicity.

To counteract sodium arsenite toxicity, many studies have examined the protective effects of both natural and synthetic molecules. For example, naringin, hesperidin, and lipoic acid have been shown to reduce arsenic toxicity by restoring biochemical parameters, decreasing oxidative stress, and inhibiting inflammatory and apoptotic cascades[8,9]. These findings support the potential of such molecules to lessen sodium arsenite-induced hepatic and renal damage through their antioxidant and anti-inflammatory properties. *Phyllanthus amarus* Schum. and Thonn., also known as Bhuia amla, is a medicinal herb of great importance in the scientific field of Ayurvedic medicine [10]. It has been traditionally used for over 2000 years to treat secondary hepatitis and various liver injuries [10]. It has numerous traditional uses and is commonly employed to treat conditions such as jaundice, gonorrhea, heavy menstruation, and diabetes [11]. Qualitative analyses of the phytochemical composition of *P. amarus* have identified a wide range of compounds, including lignans (phyllanthin and hypophyllanthin), alkaloids, and bioflavonoids (e.g., quercetin). While it remains to be confirmed which of these possesses anti-

oxidant properties, scientific reports indicate that the herb exerts maximal effects on the liver and kidneys [10,12-14]. Such liver specificity is rooted in its traditional use for jaundice, as evidenced by the report by Santos et al. [15]. Studies have demonstrated the antioxidant effect of the ethanolic extract of *P. amarus*, indicating its protective role in experimental models of kidney and liver damage [11-14]. However, the exact mechanisms underlying the hepatoprotective and nephroprotective effects of these compounds against arsenite-mediated hepatic and renal toxicities still remain unknown. Therefore, this study aimed to investigate the biochemical mechanisms and phytoconstituents responsible for the hepatoprotective effects of *P. amarus* in an experimental model of arsenite-induced liver and kidney damage.

MATERIALS AND METHODS

P. amarus methanolic extract - preparation and identification

Air-dried powder from *P. amarus* aerial parts underwent maceration at ambient temperature using methanol (distilled). This process involved soaking and occasional agitation for 7 days, followed by filtration. The filtrate was dried in a tray dryer at 40°C, yielding a semi-solid *P. amarus* methanolic extract (PAME). Subsequently, colloidal silicon dioxide was incorporated, and the mixture was dried in a vacuum tube. Phytochemical analysis of PAME was conducted using high-performance liquid chromatography (HPLC) to quantify phyllanthin content. Analyses were conducted using an HPLC system (reverse-phase C_{18} column, 250 × 4.6 mm, flow rate 1.5 mL/min). For isolation and detection, a mobile phase comprising acetonitrile and buffer in a 40:60 volume ratio was employed. The buffer was prepared by dissolving potassium hydrogen phosphate (0.136 g) in o-phosphoric acid (0.5 mL). The optimal injection volume was 20 μL, and the detector wavelength was set to 230 nm. The autosampler temperature was maintained at 10°C, and the system operated at 1000 psi [16].

Animals

White male Wistar rats aged 8–10 weeks were obtained from the animal facility at Shandong First Medical University. The rats were kept in an environment with controlled temperature (24 ± 1°C), humidity (45-55%), and a normal light-dark cycle. During the study, the rats had free access to standard pellet feed and water. The Zhinanzhen Biology Ethics Committee approved the research protocol (approval number: A2024000414).

Experimental design

The rats were divided into six groups of 15 animals each and received the following treatments: Group 1: gum acacia (1% suspension, 10 mg/kg; Normal group), Group 2: gum acacia (1% suspension, 10 mg/kg) + Sodium arsenite (5 mg/kg) (vehicle control group), Group 3: Coenzyme Q10 (10 mg/kg, 1% suspension in gum acacia) + sodium arsenite (5 mg/kg) (CoQ10-treated group), and Groups 4 to 6: standardized extract of P. amarus (50 mg/kg, 100 mg/kg, or 200 mg/kg, 1% suspension in gum acacia) + sodium arsenite (5 mg/kg) (PA-treated groups), all administered orally for 28 days.

On the final day of the experiment (day 28), blood samples were collected from anesthetized rats via retro-orbital puncture, stored in glass tubes, and centrifuged for 10 minutes at 2,000 × g at 4°C. Serum levels of albumin, ALT (alanine transaminase), AST (aspartate transaminase), ALP (alkaline phosphatase), bilirubin (direct and total), BUN (Blood Urea Nitrogen), cholesterol, creatinine, LDL (Low-Density Lipoprotein), HDL (High-Density Lipoprotein), LDH (Lactate Dehydrogenase), triglycerides, and uric acid were measured using reagent kits according to the provided procedure (Accurex Biomedical Pvt. Ltd., Mumbai, India). The animals were then euthanized, and the

liver and kidneys were quickly removed and weighed with a balance at temperatures below 4°C. The tissues were divided into three sections and stored at -80°C. One section was used to assess oxidative and nitrosative stress markers (MDA (malondialdehyde), GSH (reduced glutathione), NO (nitric oxide), SOD (superoxide dismutase) activity) and total antioxidant capacity (TAC) following previously reported methods [16-22]. Another portion was analyzed to determine the concentrations of pro-inflammatory cytokines (IL-6, IL-1β, and TNF-α) and NF-κB p65 using a commercially available ELISA kit (Thermo Fisher Scientific, USA). The remaining tissue was examined histologically using hematoxylin and eosin (H&E) staining. Changes observed in the histological characteristics were classified according to a previously established grading system [23].

Statistical analysis

GraphPad Prism software (version 5.0; GraphPad, San Diego, USA) was used for statistical analysis. One-way analysis of variance (ANOVA) followed by Dunnett's post hoc test was performed. A two-sided Fisher's exact test was used to calculate the correlation coefficients. The results are presented as mean ± SEM, with statistical significance set at $p<0.05$.

RESULTS

Phyllanthin - Isolation and identification

PAME had a 59.12% w/w yield and contained glycosides, lignans, steroids, tannins, and phenols. HPLC column analysis lasted 40 minutes, during which phyllanthin was detected at 25.41 minutes, with a peak area of 71.84% (Fig. 1).

Body, liver, kidney, and spleen weights

Body weight was effectively decreased ($p<0.001$), while a significant ($p<0.001$) increase in spleen, kidney, and liver weights (both absolute and relative) was observed in vehicle control rats compared to normal rats. Rats treated with PA (200 mg/kg) showed a significant ($p<0.001$) reduction in the elevated weights of the spleen, kidney, and liver, along with a marked ($p<0.001$) increase in body weight compared to vehicle control rats. However, PA treatment at doses of 50 and 100 mg/kg did not produce any notable changes in the absolute or relative weights of the liver, spleen, and kidneys, nor in body weight, compared to the vehicle control group. CoQ (10 mg/kg) treatment effectively decreased spleen, kidney, and liver weights ($p<0.001$) and increased body weight ($p<0.001$) compared to the vehicle control group (Table 1).

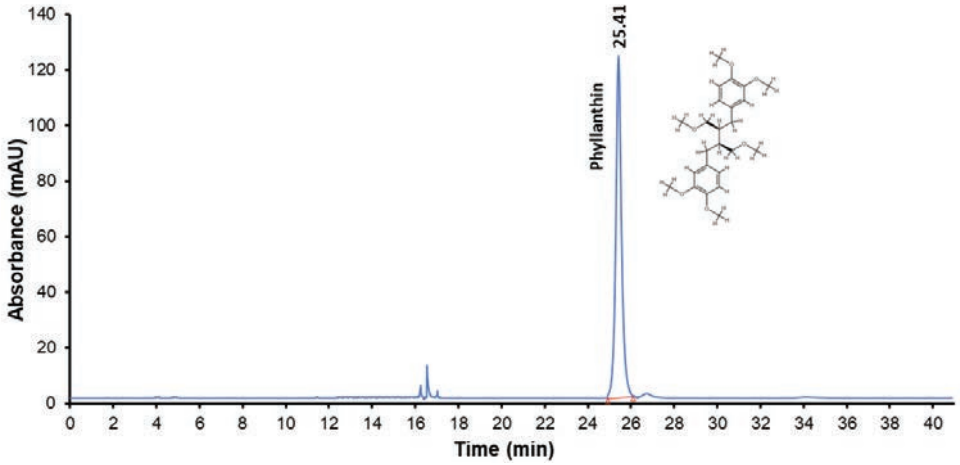

Fig. 1. HPLC chromatogram of the standardized *P. amarus* extract showing a phyllanthin peak at RT = 25.41 min. mAU, milli-absorbance units.

Table 1. Effect of *P. amarus* on body weight and organ weights.

Treatment	Normal	Vehicle control	CoQ (10)	PA (50)	PA (100)	PA (200)
Body weight (g)	239.70 ± 3.81	213.20 ± 3.47$^{###}$	234.70 ± 4.17***	211.70 ± 2.94	218.00 ± 1.39	223.50 ± 2.35***
Liver weight (g)	5.48 ± 0.22	7.34 ± 0.29$^{###}$	5.52 ± 0.33***	7.23 ± 0.30	7.31 ± 0.15	5.73 ± 0.29***
Liver weight / Body weight	22.90 ± 1.11	34.47 ± 1.54$^{###}$	23.65 ± 1.79***	34.20 ± 1.57	33.51 ± 0.60	25.69 ± 1.43***
Kidney weight (g)	1.20 ± 0.01	1.81 ± 0.01$^{###}$	1.29 ± 0.01***	1.77 ± 0.01	1.79 ± 0.01	1.30 ± 0.01***
Kidney weight / Body weight	5.01 ± 0.08	8.49 ± 0.16$^{###}$	5.50 ± 0.14***	8.39 ± 0.13	8.21 ± 0.06	5.81 ± 0.09***
Spleen weight (g)	0.19 ± 0.02	0.75 ± 0.02$^{###}$	0.36 ± 0.02***	0.74 ± 0.03	0.73 ± 0.02	0.52 ± 0.03**
Spleen weight / Body weight ($x10^{-3}$)	0.79 ± 0.08	3.53 ± 0.12$^{###}$	1.54 ± 0.11***	3.52 ± 0.19	3.33 ± 0.07	2.31 ± 0.15**

The results are presented as mean ± SEM, based on a sample size of 6. A one-way analysis of variance (ANOVA) was used for statistical analysis, and Dunnett's test was applied to each parameter individually. **p<0.01, ***p<0.001: vehicle control group, and $^{###}$p<0.001: normal group. CoQ (10), Coenzyme Q (10 mg/kg); PA, *Phyllanthus amarus*.

Serum parameters

Compared to the normal group, serum levels of BUN, uric acid, creatinine, direct and total bilirubin, LDH, ALP, AST, and ALT were significantly (p<0.001) elevated, while albumin levels were notably (p<0.001) decreased in the vehicle control group. These changes suggest substantial hepatic and renal injury caused by sodium arsenite, as these parameters are closely linked to liver and kidney functions. Treatment with PA (200 mg/kg) led to significant improvements, evidenced by a marked (p<0.001) reduction in serum BUN, ALT, AST, creatinine, uric acid, direct bilirubin, total bilirubin, LDH, and ALP levels, along with a significant (p<0.001) increase in albumin compared to the vehicle control group. Additionally, CoQ (10 mg/kg) significantly (p<0.001) inhibited arsenite-induced changes in serum creatinine, BUN, uric acid, albumin, bilirubin (direct and total), LDH, AST, ALT, and ALP levels compared to the control (Tabla 2).

Lipid profile

Following chronic sodium arsenite administration, a significant reduction (p<0.001) in serum HDL and a notable (p<0.001) increase in serum cholesterol, LDL, and triglyceride levels were observed in vehicle control rats compared to normal rats. These decreases in serum HDL and the elevations in cholesterol, LDL, and triglyceride levels were clearly (p<0.001) reduced with PA (200 mg/kg) treatment. Similarly, CoQ (10 mg/kg) administration resulted in significant improvements, increasing (p<0.001) HDL levels and decreasing (p<0.001) LDL, cholesterol, and triglyceride levels in the serum compared to vehicle control rats. However, no significant changes in serum cholesterol, HDL, LDL, or triglyceride levels were seen following PA (50 and 100 mg/kg) treatments (Table 3).

Hepatic and renal antioxidant parameters

Compared with normal rats, sodium arsenite administration significantly reduced hepatic total antioxidant capacity (TAC) in the vehicle control group. However, PA (200 mg/kg) effectively increased hepatic TAC (p<0.001) compared to the vehicle control group. Notably, CoQ (10 mg/kg) also significantly increased hepatic TAC (p<0.01) relative to the vehicle control group (Fig. 2A). Compared to the normal group, sodium arsenite markedly affected hepatic and renal antioxidant levels, as indicated by a significant (p<0.001) decrease in hepatic and renal GSH and SOD levels, followed by

a substantial ($p<0.001$) increase in nitric oxide and MDA levels in the hepatic and renal tissues of the vehicle control group. PA (200 mg/kg) effectively ($p<0.001$) restored GSH and SOD levels and significantly lowered MDA ($p<0.001$) and nitric oxide levels in hepatic and renal tissues compared to the vehicle control group. CoQ (10 mg/kg) administration also demonstrated strong hepatoprotective and nephroprotective effects by effectively increasing ($p<0.001$) hepatic and renal GSH and SOD levels and markedly reducing ($p<0.001$) hepatic and renal nitric oxide and MDA levels relative to the vehicle control group (Fig. 2B-2E).

Table 2. Effect of *P. amarus* on serum hepatic and renal biomarker levels.

Treatment	Normal	Vehicle control	CoQ (10)	PA (50)	PA (100)	PA (200)
BUN (mg/dL)	25.85 ± 1.47	50.72 ± 1.29$^{###}$	31.48 ± 1.26***	47.85 ± 0.89	46.91 ± 1.38	34.38 ± 1.26***
Creatinine (mg/dL)	0.63 ± 0.06	2.07 ± 0.11$^{###}$	0.92 ± 0.07***	2.12 ± 0.13	2.08 ± 0.12	1.57 ± 0.09***
Uric acid (mg/dL)	1.90 ± 0.12	4.41 ± 0.12$^{###}$	2.50 ± 0.06***	4.36 ± 0.11	4.40 ± 0.14	3.26 ± 0.13***
Albumin (mg %)	6.75 ± 0.56	2.39 ± 0.51$^{###}$	6.04 ± 0.41***	2.43 ± 0.50	2.61 ± 0.43	4.46 ± 0.40***
Direct bilirubin (mg %)	0.20 ± 0.01	0.67 ± 0.01$^{###}$	0.29 ± 0.02***	0.66 ± 0.02	0.62 ± 0.01	0.42 ± 0.01***
Total bilirubin (mg %)	0.12 ± 0.01	0.31 ± 0.02$^{###}$	0.16 ± 0.01***	0.31 ± 0.02	0.31 ± 0.01	0.23 ± 0.01***
ALP (IU/L)	50.47 ± 3.77	392.80 ± 3.81$^{###}$	94.35 ± 3.69***	383.80 ± 6.32	367.80 ± 6.12	257.90 ± 3.71***
AST (IU/L)	63.92 ± 13.33	284.30 ± 14.17$^{###}$	102.00 ± 11.65***	289.50 ± 12.34	264.50 ± 10.44	144.00 ± 11.42***
ALT (IU/L)	28.32 ± 7.65	146.50 ± 6.27$^{###}$	42.75 ± 10.28***	145.00 ± 9.97	140.00 ± 6.73	63.36 ± 8.47***
LDH (mg %)	482.00 ± 119.90	3418.00 ± 212.80$^{###}$	682.30 ± 152.20***	3399.00 ± 405.50	3239.00 ± 406.40	1456.00 ± 131.40***

The results are presented as mean ± SEM, based on a sample size of 6. A one-way analysis of variance (ANOVA) was performed for statistical analysis, followed by Dunnett's test applied individually to each parameter. ***$p<0.001$: vehicle control group and $^{###}p<0.001$: normal group. AST, Aspartate transaminase; ALP, Alkaline phosphatase; ALT, alanine transaminase; BUN, Blood Urea Nitrogen; CoQ (10), Coenzyme Q (10 mg/kg); LDH, Lactate Dehydrogenase; PA, *Phyllanthus amarus*.

Table 3. Effect of *P. amarus* on serum lipid profile.

Treatment	Normal	Vehicle control	CoQ (10)	PA (50)	PA (100)	PA (200)
Cholesterol (mg %)	18.71 ± 3.14	65.06 ± 8.72$^{###}$	35.70 ± 2.42***	61.54 ± 4.62	60.73 ± 5.07	29.74 ± 4.02***
HDL (mg %)	60.85 ± 1.09	22.26 ± 3.42$^{###}$	56.31 ± 3.68***	23.99 ± 2.07	21.94 ± 4.74	56.53 ± 3.15***
LDL (mg %)	2.10 ± 0.35	5.02 ± 0.51$^{###}$	2.12 ± 0.45***	5.14 ± 0.47	5.07 ± 0.47	2.34 ± 0.35***
Triglyceride (mg %)	60.33 ± 14.89	185.30 ± 19.41$^{###}$	72.25 ± 9.03***	167.30 ± 17.33	156.90 ± 13.88	122.4 ± 10.23***

The results are presented as mean ± SEM, based on a sample size of 6. A one-way analysis of variance (ANOVA) was conducted for statistical analysis, and Dunnett's test was subsequently applied to each parameter individually. ***$p<0.001$: vehicle control group and $^{###}p<0.001$: normal group. CoQ (10), Coenzyme Q (10 mg/kg); HDL, high-density lipoprotein; LDL, low-density lipoprotein; PA, *Phyllanthus amarus*.

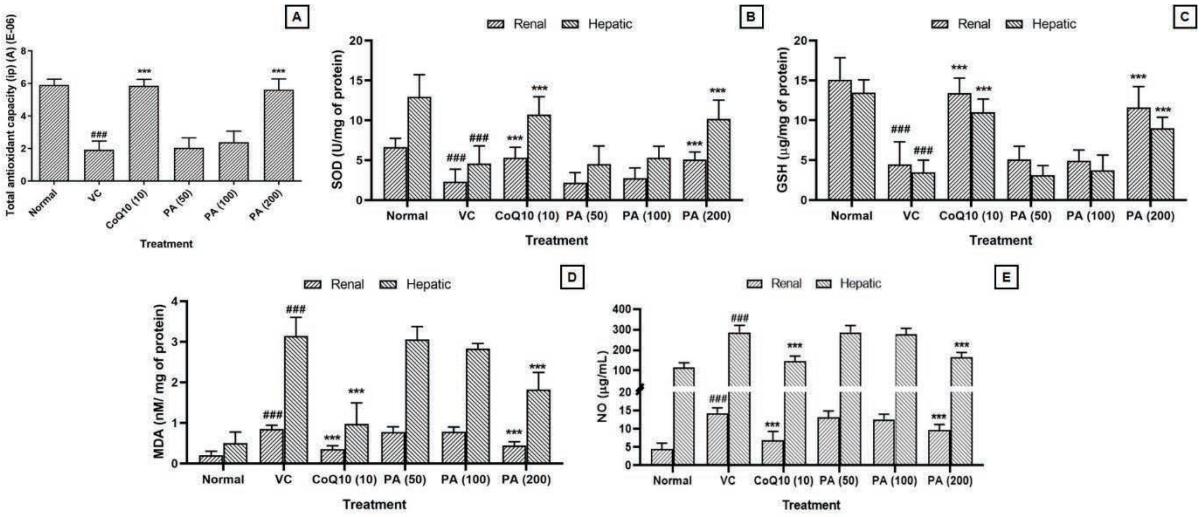

Fig. 2. *P. amarus* effects on hepatic and renal oxidative stress. A quantitative chart of the total antioxidant capacity of the liver (A). Quantitative measurements of SOD (B), GSH (C), MDA (D), and nitric oxide (E) levels in hepatic and renal tissues. Results are presented as mean values with SEM, based on a sample size of 6. One-way ANOVA was used for statistical analysis, with Dunnett's test applied to each parameter separately. ***p<0.001: vehicle control group and ###p<0.001: normal group. CoQ (10), Coenzyme Q (10 mg/kg); GSH, glutathione peroxidase; NO, nitric oxide; MDA, malondialdehyde; PA, Phyllanthus amarus; SOD, superoxide dismutase.

Protein expressions of hepatic and renal ILs, TNF-α, and NF-kB p65

Compared to the normal group, hepatic and renal ILs (IL-6 and IL-1β), TNF-α, and NF-kB p65 protein expression were significantly increased ($p<0.001$) in the vehicle control group. Administration of PA (200 mg/kg) effectively reduced hepatic and renal ILs, TNF-α, and NF-kB p65 protein levels ($p<0.001$) compared with the vehicle control group. Treatment with CoQ (10 mg/kg) demonstrated a substantial ($p<0.001$) protective effect against arsenite-induced liver and kidney damage, as shown by decreased hepatic and renal ILs, TNF-α, and NF-kB p65 protein expression compared to the vehicle control group (Table 4).

There was a strong, positive, and statistically significant correlation between serum ALT levels and hepatic TNF-α ($R2=0.737$ and $p<0.05$), IL-1β ($R2=0.8578$ and $p<0.01$), IL-6 ($R2=0.7493$ and $p<0.05$), and NF-κB p65 ($R2=0.8692$ and $p<0.01$) (Fig. 3A-3D). Serum levels of BUN were positively and significantly correlated with renal TNF-α ($R2=0.7693$ and $p<0.05$), IL-1β ($R2=0.7315$ and $p<0.05$), IL-6 ($R2=0.8323$ and $p<0.01$), and NF-κB p65 ($R2=0.8927$ and $p<0.01$) (Fig. 3E-3H).

Hepatic histopathology

The liver sections from the normal group showed well-preserved architectural features, including hepatocytes arranged in orderly cords radiating from the central vein, with uniform cellular dimensions and transparent cytoplasm. The nuclei were centrally positioned and exhibited normal morphology. No necrosis was observed; however, mild inflammation was noted (Fig. 4A). The histology of hepatic tissue from the vehicle control group showed histopathological changes, including significant ($p<0.001$) necrosis, distorted hepatocyte arrangement, and infiltration of inflammatory cells (Fig. 4B). Histological examination of liver sections from rats treated with CoQ (10 mg/kg) revealed a notable ($p<0.001$) improvement in morphology compared to the vehicle control group. Hepatocytes mostly maintained their normal structure, with mild necrosis

Table 4. Effect of *P. amarus* treatment in hepatic and renal Interleukins and NFkB-P65 levels.

Treatment	Normal	Vehicle control	CoQ (10)	PA (50)	PA (100)	PA (200)
Hepatic TNF-α (pg/mg)	11.23 ± 1.57	56.96 ± 2.54###	22.17 ± 3.18***	52.83 ± 4.32	51.09 ± 4.76	26.16 ± 4.50***
Hepatic IL-1β (pg/mg)	8.61 ± 0.88	111.50 ± 2.67###	24.17 ± 2.71***	109.00 ± 2.80	98.19 ± 5.61	55.69 ± 4.80***
Hepatic IL-6 (pg/mg)	29.19 ± 5.06	169.30 ± 8.19###	81.67 ± 7.37***	152.20 ± 6.82	152.20 ± 10.47	100.60 ± 9.31***
Hepatic NF-kB p65 (pg/mg)	141.50 ± 14.43	653.30 ± 7.00###	168.10 ± 8.93***	646.20 ± 13.25	559.30 ± 20.79	274.60 ± 16.08***
Renal TNF-α (pg/mg)	3.12 ± 0.67	14.13 ± 1.23###	4.42 ± 0.54***	12.46 ± 0.76	11.88 ± 1.00	5.58 ± 0.85***
Renal IL-1β (pg/mg)	11.39 ± 2.17	79.58 ± 5.70###	37.92 ± 4.17***	74.58 ± 4.82	71.94 ± 5.08	48.33 ± 3.71***
Renal IL-6 (pg/mg)	9.09 ± 1.56	97.02 ± 6.43###	22.78 ± 3.20***	94.39 ± 5.91	94.90 ± 1.97	24.70 ± 6.04***
Renal NF-kB p65 (pg/mg)	78.84 ± 1.69	214.70 ± 2.14###	98.41 ± 2.86***	213.10 ± 2.79	203.10 ± 2.48	119.90 ± 2.29***

The results are expressed as mean ± SEM, based on a sample size of 6. A one-way analysis of variance (ANOVA) was used for statistical analysis, and Dunnett's test was subsequently applied to each parameter individually. ***$p<0.001$: vehicle control group and ###$p<0.001$: normal group. CoQ (10), Coenzyme Q (10 mg/kg); ILs, Interleukins; NF-κB, nuclear factor kappa B; PA, *Phyllanthus amarus;* TNF-α, tumor necrosis factor-alpha.

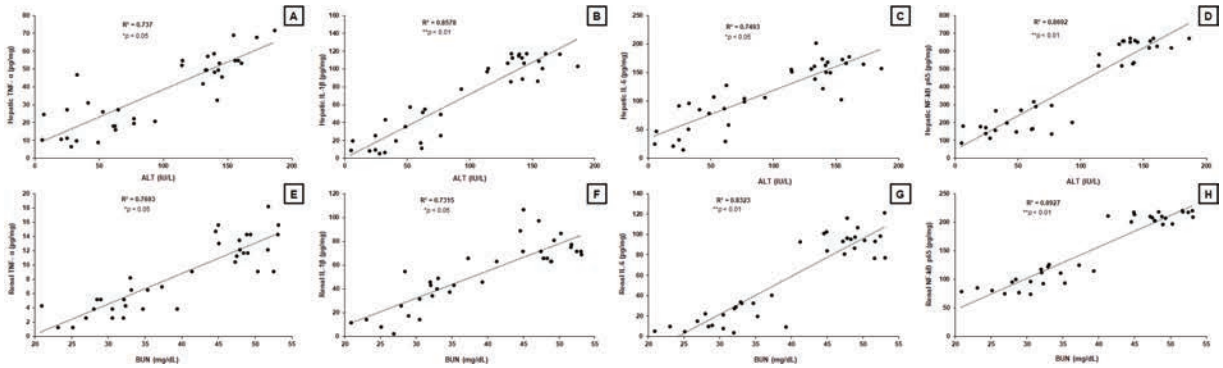

Fig. 3. Simple regression analysis of hepatic TNF-α (A), IL-1β (B), IL-6 (C), and NF-kB p65 (D) with ALT levels, and renal TNF-α (E), IL-1β (F), IL-6 (G), and NF-kB p65 (H) with BUN levels. A two-sided Fisher's test was used to calculate the correlation coefficients. ALT, alanine transaminase; BUN, blood urea nitrogen; ILs, interleukins; NF-κB, nuclear factor kappa B; TNF-α, tumor necrosis factor-alpha.

and inflammation, and their cytoplasm was less eosinophilic than in the vehicle control group (Fig. 4C). Histological analysis of liver tissue from the PA (50 and 100 mg/kg)-treated groups showed infiltration of inflammatory cells, vacuolation, and interstitial edema (Fig. 4D and 4E). Liver sections from the PA (200 mg/kg)-treated group showed mainly preserved hepatocytes, as evidenced by well-maintained cellular architecture and minimal necrotic changes. The cytoplasm showed reduced vacuolation, and inflammatory cell infiltration was significantly decreased ($p<0.001$) compared to the vehicle control group (Fig. 4F, Fig. 4M).

Renal histopathology

The renal sections of the normal group showed well-preserved kidney architecture. The glomeruli and renal tubules were clearly

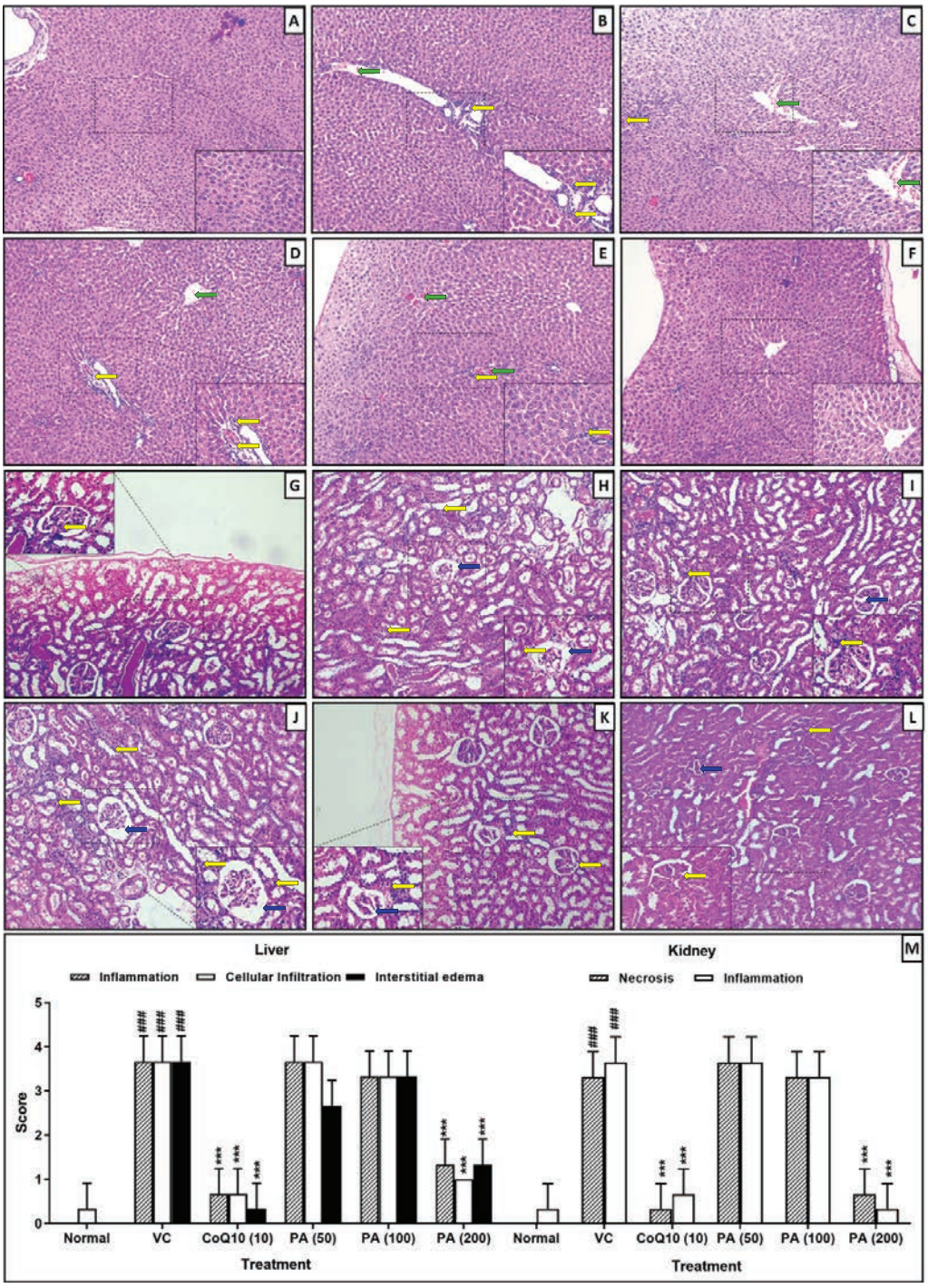

Fig. 4. *P. amarus* on rat hepatic and renal pathology.

Microscopic images of liver (A-F) and kidney (G-L) cross-sections from various rat groups, including normal (A and G), vehicle control (B and H), CoQ (10) treatment (C and I), PA treatment (50 mg/kg) (D and J), PA treatment (100 mg/kg) (E and K), and PA treatment (200 mg/kg) (F and L). H&E staining at 40X and 100X (inset). Quantitative data showing the effect of *P. amarus* treatment on rat hepatic and renal pathologies (M). The results are expressed as mean ± SEM, based on a sample size of 6. One-way ANOVA was used for statistical analysis, followed by Dunnett's test for each parameter. ***p<0.001: vehicle control group; ###p<0.001: normal group. CoQ (10), Coenzyme Q (10 mg/kg); PA, *Phyllanthus amarus*. Inflammatory infiltration (yellow arrow), cellular infiltration (green arrow), and necrosis (blue arrow) are indicated.

defined. No signs of inflammation, necrosis, or other cellular damage were observed (Fig. 4G). In contrast, renal tissue from the vehicle control group exhibited severe kidney damage, with prominent ($p<0.001$) tubular necrosis and infiltration of inflammatory cells (Fig. 4H). Kidney tissue from the CoQ10 (10) treated group demonstrated a significantly preserved renal architecture compared to the vehicle control group ($p<0.001$). Although mild inflammation was present, there was a notable reduction in tubular necrosis and overall structural damage (Fig. 4I). Groups treated with PA (50 and 100 mg/kg) showed extensive renal tissue damage similar to that in the vehicle control group, with clear evidence of inflammation and tubular necrosis (Fig. 4J and 4K). Treatment with PA (200 mg/kg) showed a marked ($p<0.001$) protective effect, comparable to the vehicle control, with kidney architecture largely preserved and only minimal signs of inflammation and reduced tubular damage (Fig. 4L and 4M).

DISCUSSION

Sodium arsenite causes significant toxicity in various biological systems, with effects ranging from genetic damage to organ harm. Studies have shown that the liver and kidneys are especially susceptible to arsenic-related toxicity because of their roles in detoxification and excretion [24,25]. Sodium arsenite triggers notable oxidative stress in both liver and kidney tissues, leading to apoptosis and inflammatory responses that impair their functions. As research advances, the use of antioxidants and other protective agents, such as hesperidin, lycopene, and bosentan, has demonstrated potential in reducing these toxic effects by lowering oxidative stress and inflammation and boosting cellular antioxidant defenses [9,26]. The current study examined the possible mechanisms by which *P. amarus* methanolic extract may protect against arsenite-induced liver and kidney damage in rats.

Chronic administration of sodium arsenite causes acute liver failure and hepatotoxicity, leading to fatal outcomes [25]. Researchers have noted that significant increases in AST, ALT, and ALP levels during arsenite- induced hepatotoxicity serve as indicators of liver function, along with histological changes [25]. Sodium arsenite is absorbed from the gut and detoxified through oxidative methylation in the liver. This process, driven by hepatic enzymes, converts inorganic arsenic into organic forms like monomethylarsonic acid and dimethylarsinic acid [27]. Paradoxically, this detoxification pathway depletes S- Adenosyl methionine and produces trivalent methylated metabolites that are more toxic than the original compound, sodium arsenite, causing hepatocellular damage[25]. Elevated ALT levels are key indicators of the severity of hepatocellular damage. Similar to ALT, AST also increases markedly in arsenite-induced liver injury; however, AST is less specific to the liver. In severe cases, AST levels can match or surpass ALT levels, especially in the later stages of liver necrosis. Therefore, increased ALT and AST levels, along with histological abnormalities during chronic sodium arsenite exposure, confirm its hepatotoxic effects [25]. Additionally, long-term exposure to sodium arsenite results in significant changes in serum biomarkers, such as BUN, uric acid, and creatinine, indicating renal dysfunction [28]. In this study, elevated levels of ALT, AST, ALP, uric acid, BUN, and creatinine were observed following arsenite administration. These increases in serum markers correlate with histological damage in the liver and kidneys, reflecting the hepatotoxic and nephrotoxic effects of sodium arsenite. Further histological analysis supported the protective potential of arsenite against arsenite-induced structural damage in hepatocytes, including irregular and indistinct central veins, cellular damage, tubular necrosis, and increased inflammatory cells, which were alleviated after treatment with *P. amarus*. Previous studies have also documented the hepatoprotective

and nephroprotective effects of *P. amarus* through the inhibition of carbon tetrachloride-induced elevation of hepatic biomarkers and high-salt diet-induced increases in kidney function markers [13,29]. The findings of this study reinforce those from earlier research [13, 29].

Reactive oxygen species (ROS), cytokines, chemokines, and hepatic macrophages are key contributors to liver and kidney damage [30]. The family of transcription factors called nuclear factor-κB (NF-κB) is evolutionarily conserved and remains inactive in the cytoplasm of various cell types. When activated, NF-κB translocates to the nucleus, where it plays a critical role in inflammatory processes, immune responses, and programmed cell death. ROS- induced inflammation is crucial for arsenite- related liver and kidney injury. Excessive production of free radicals triggers NF-κB activation at the inflammation site, leading to the expression of pro-inflammatory genes, including TNF-α and interleukins, ultimately raising cytokine levels. During the acute-phase response, pro-inflammatory cytokines are vital[31,32]. Elevated levels of TNF-α and IL-1β in the liver and kidneys serve as important indicators of hepatic and renal damage in rats [33]. Therefore, the transcriptional regulation of certain inducible inflammatory mediators is significantly affected by NF- κB [34]. Afolabi et al. reported that intestinal ischemia-reperfusion injury caused a significant increase in intestinal and hepatic IL-1β and TNF-α levels compared to the sham group [31]. However, administering the methanolic extract of *P. amarus* to rats with ischemia-reperfusion injury significantly inhibited hepatic IL-1β and TNF-α levels [31]. Furthermore, previous research demonstrated that *P. amarus* ethanolic extract suppresses NF-κB, a major regulator of inflammation, in RAW 264.7 cells [35]. Additionally, Phyllanthin from *P. amarus* has been shown to reduce elevated pro- inflammatory cytokine levels by inhibiting NF- κB activation in high- fat diet- induced fatty liver[36]. In this study, Phyllanthin from *P. amarus* also reduced arsenite-induced increases in pro-inflammatory cytokine production by inhibiting NF-κB. Therefore, the protective effects of phyllanthin from *P. amarus*, through its anti-inflammatory properties, align with earlier research [31]. Moreover, this investigation consistently showed that the extent of organ damage, as measured by serum markers ALT for the liver and BUN for the kidney, was strongly and significantly correlated with the local inflammatory response in these organs. Higher levels of organ injury were associated with increased tissue concentrations of proinflammatory cytokines and transcription factors. The high correlation coefficients ($R2 > 0.7$ for all plots) and statistical significance ($p<0.05$) across all analyses provide strong evidence supporting this relationship.

P. amarus has been extensively studied for treating chronic Hepatitis B infection. A randomized trial involving chronic Hepatitis B patients (n=60) who received *P. amarus* extract for 12 weeks showed a significant reduction in Hepatitis B virus (HBV) DNA levels [37,38]. Its antiviral effectiveness inhibits viral replication and raises liver enzymes (ALT and AST) [37,38]. Patients with chronic Hepatitis B (n=123) treated with *P. amarus* for 6 months experienced decreased HBV surface antigen (HBsAg) levels, supporting its antiviral and liver-protective properties[39]. Additionally, patients with type 2 diabetes treated with P. amarus for 10 weeks had significant reductions in fasting blood glucose and glycosylated hemoglobin levels [40]. Moreover, in individuals with non-alcoholic fatty liver disease, *P. niruri* supplementation lowered elevated oxidative stress markers such as malondialdehyde (MDA), resulting in an increased overall antioxidant capacity[41]. Safety assessments have also shown that *P. amarus* is well tolerated. Therefore, *P. amarus* appears to be a promising herbal treatment for pesticide-induced liver and kidney damage. However, further research is needed to determine its clinical effectiveness in these conditions.

CONCLUSION

The results of this study showed that *P. amarus* methanolic extract effectively protects against sodium arsenite-induced liver and kidney damage in rats. The protective effect of *P. amarus* is likely due to the presence of phyllanthin, which reduces NF-κB activation, thereby decreasing inflammation and oxidative-nitrosative stress, and boosting overall antioxidant capacity. Clinically, *P. amarus* standardized capsules or liquid extracts can be taken orally, with dosing carefully controlled based on safety and effectiveness data from preclinical studies. The dose should consider factors such as the severity of arsenic poisoning, the patient's body weight, and how long the exposure lasts, with treatment lasting long enough for detoxification and tissue healing. Using *P. amarus* extract as an additional therapy alongside traditional chelation could improve patient outcomes by lowering arsenic levels and reducing biochemical problems caused by arsenic toxicity.

Acknowledgments

Medical writing support for this manuscript, under the authors' guidance, was provided by Yonnova Scientific Consultancy Pvt. Ltd. in accordance with Good Publication Practice Guidelines.

Funding

This study did not receive any funding.

Conflict of interest

No conflict of interest.

Data availability

The raw data supporting this article will be provided to the corresponding author upon reasonable request.

Ethical statements

The research protocol was approved by the Institutional Animal Ethics Committee (IAEC) of the Zhinanzhen Biology Ethics Committee (approval number: A2024000414). This study was conducted following the National Institutes of Health Guide for the Care and Use of Laboratory Animals.

ORCID numbers auhors

- Jiarui Xu (JK): 0000-0003-4925-2770
- Smeeta Sadar (SS): 0000-0001-8682-303X
- Hemant Kamble (HK): 0009-0003-2865-5172
- Yingtao Zhang (YZ): 0009-0003-9376-7381

Authors contribution

Each author has contributed significantly to the development of this manuscript. JX and HK: conceived and designed the evaluation, performed parts of the statistical analysis, and drafted the manuscript; SS and YZ: conducted data collection and drafted the manuscript. All authors have read and approved the final version of the manuscript.

REFERENCES

1. **Fatoki JO, Badmus JA**. Arsenic as an environmental and human health antagonist: A review of its toxicity and disease initiation. Journal of Hazardous Materials Advances 2022;5:100052. *https://doi.org/10.1016/j.hazadv.2022.100052*
2. **World Health Organization.** Arsenic. World Health Organization; 2012.
3. **Podgorski J, Berg M**. Global threat of arsenic in groundwater. Science 2020;368:845-

850. *https://doi.org/10.1126/science.aba1510*

4. **Alkully T, El-Refaei MF, Abdallah EAA**. Protective Effects of Ellagic Acid Against Arsenic-Induced Hepatotoxicity in Male Wistar Rats: Impact of Heme Oxygenase-1 Upregulation. Food Sci Nutr 2025;13:e70344. *https://doi.org/10.1002/fsn3.70344*
5. **Opeyemi Olaoluwa L, Joseph- Peace A, Okikijesu O, Emeka Gabriel E, Precious O, Tella A** *et al.* Protective effects of Butylated Hydroxytoluene (BHT) against sodium Arsenite (NaAsO2) - Induced hepatotoxicity in Wistar Rats. International Journal of Science and Research Archive 2024;12:067-102. *https://doi.org/10.30574/ijsra.2024.12.2.1130*
6. **Gong X, Ivanov VN, Davidson MM, Hei TK**. Tetramethylpyrazine (TMP) protects against sodium arsenite-induced nephrotoxicity by suppressing ROS production, mitochondrial dysfunction, pro-inflammatory signaling pathways and programed cell death. Arch Toxicol 2015;89:1057-1070. *https://doi.org/10.1007/s00204-014-1302-y*
7. **Mwaeni VK, Nyariki JN, Jillani N, Omwenga G, Ngugi M, Isaac AO**. Coenzyme Q(10) protected against arsenite and enhanced the capacity of 2,3-dimercaptosuccinic acid to ameliorate arsenite-induced toxicity in mice. BMC Pharmacol Toxicol 2021;22:19. *https://doi.org/10.1186/s40360-021-00484-z*
8. **Ma G, Yan X, Wang C, Ran X, Liang Z, Chen X** *et al.* Mechanism of arsenic-induced liver injury in rats revealed by metabolomics and ionomics based approach. Ecotoxicol Environ Saf 2025;293:118038. *https://doi.org/10.1016/j.ecoenv.2025.118038*
9. **Turk E, Kandemir FM, Yildirim S, Caglayan C, Kucukler S, Kuzu M**. Protective Effect of Hesperidin on Sodium Arsenite-Induced Nephrotoxicity and Hepatotoxicity in Rats. Biol Trace Elem Res 2019;189:95-108. *https://doi.org/10.1007/s12011-018-1443-6*
10. **Bose Mazumdar Ghosh A, Banerjee A, Chattopadhyay S**. An insight into the potent medicinal plant Phyllanthus amarus Schum. and Thonn. Nucleus (Calcutta) 2022;65:437-472. *https://doi.org/10.1007/s13237-022-00409-z*
11. **Krithika R, Verma RJ, Shrivastav PS, Suguna L**. Phyllanthin of Standardized Phyllanthus amarus Extract Attenuates Liver Oxidative Stress in Mice and Exerts Cytoprotective Activity on Human Hepatoma Cell Line. J Clin Exp Hepatol 2011;1:57-67. *https://doi.org/10.1016/S0973-6883(11)60123-0*
12. **Faremi TY, Suru SM, Fafunso MA, Obioha UE**. Hepatoprotective potentials of Phyllanthusamarus against ethanol-induced oxidative stress in rats. Food Chem Toxicol 2008;46:2658-2664. *https://doi.org/10.1016/j.fct.2008.04.022*
13. **Olorunnisola OS, Fadahunsi OS, Adegbola PI, Ajilore BS, Ajayi FA, Olaniyan LWB**. Phyllanthus amarus attenuated derangement in renal-cardiac function, redox status, lipid profile and reduced TNF-alpha, interleukins-2, 6 and 8 in high salt diet fed rats. Heliyon 2021;7:e08106. *https://doi.org/10.1016/j.heliyon.2021.e08106*
14. **Karuna R, Bharathi VG, Reddy SS, Ramesh B, Saralakumari D**. Protective effects of Phyllanthus amarus aqueous extract against renal oxidative stress in Streptozotocin -induced diabetic rats. Indian J Pharmacol 2011;43:414-418. *https://doi.org/10.4103/0253-7613.83112*
15. **Santos AR, Filho VC, Yunes RA, Calixto JB**. Analysis of the mechanisms underlying the antinociceptive effect of the extracts of plants from the genus Phyllanthus. Gen Pharmacol 1995;26:1499-1506. *https://doi.org/10.1016/0306-3623(95)00030-5*
16. **Kandhare AD, Ghosh P, Ghule AE, Zambare GN, Bodhankar SL**. Protective effect of *Phyllanthus amarus* by modulation of endogenous biomarkers and DNA damage in acetic acid induced ulcerative colitis: Role of phyllanthin and hypophyllanthin. Apollo Med 2013;10:87-97.
17. **Kandhare AD, Kumar VS, Adil M, Rajmane AR, Ghosh P, Bodhankar SL**. Investigation of gastro protective activity of *Xanthium strumarium* L. by modulation of cellular and biochemical marker. Orient Pharm Exper Med 2012;12:287-299.

18. **Kandhare AD, Raygude KS, Ghosh P, Ghule AE, Bodhankar SL**. Neuroprotective effect of naringin by modulation of endogenous biomarkers in streptozotocin induced painful diabetic neuropathy. Fitoterapia 2012;83:650-659. *https://doi.org/10.1016/j.fitote.2012.01.010*
19. **Gosavi TP, Ghosh P, Kandhare AD, Kumar VS, Adil M, Rajmane AR** *et al.* Therapeutic effect of *H. pylori* nosode, a homeopathic preparation in healing of chronic *H. pylori* infected ulcers in laboratory animals. Asian Pac J Trop Dis 2012;2:S603-S611.
20. **Gosavi TP, Kandhare AD, Ghosh P, Bodhankar SL**. Anticonvulsant activity of Argentum metallicum, a homeopathic preparation. Der Pharmacia Lettre 2012; 4:626-637.
21. **Momen-Beitollahi J, Mansourian A, Momen-Heravi F, Amanlou M, Obradov S, Sahebjamee M**. Assessment of salivary and serum antioxidant status in patients with recurrent aphthous stomatitis. Med Oral Patol Oral Cir Bucal 2010;15:e557-561. *https://doi.org/10.4317/medoral.15.e557*
22. **Kandhare AD, Bodhankar SL, Mohan V, Thakurdesai PA**. Effect of glycosides based standardized fenugreek seed extract in bleomycin-induced pulmonary fibrosis in rats: Decisive role of Bax, Nrf2, NF-kappaB, Muc5ac, TNF-alpha and IL-1beta. Chem Biol Interact 2015;237:151-165. *https://doi.org/10.1016/j.cbi.2015.06.019*
23. **Honmore V, Kandhare A, Zanwar AA, Rojatkar S, Bodhankar S, Natu A**. Artemisia pallens alleviates acetaminophen induced toxicity via modulation of endogenous biomarkers. Pharm Biol 2015;53:571-581. *https://doi.org/10.3109/13880209.2014.934382*
24. **Concessao PL, Prakash J**. Arsenic-induced nephrotoxicity: Mechanisms, biomarkers, and preventive strategies for global health. Kidney 2025;13:15.
25. **Wen J, Li A, Wang Z, Guo X, Zhang G, Litzow MR** *et al.* Hepatotoxicity induced by arsenic trioxide: clinical features, mechanisms, preventive and potential therapeutic strategies. Front Pharmacol 2025;16:1536388. *https://doi.org/10.3389/fphar.2025.1536388*
26. **Sharma AK, Kaur J, Kaur T, Singh B, Yadav HN, Pathak D** *et al.* Ameliorative role of bosentan, an endothelin receptor antagonist, against sodium arsenite-induced renal dysfunction in rats. Environ Sci Pollut Res Int 2021;28:7180-7190. *https://doi.org/10.1007/s11356-020-11035-0*
27. **Zhang W, Miao AJ, Wang NX, Li C, Sha J, Jia J** *et al.* Arsenic bioaccumulation and biotransformation in aquatic organisms. Environ Int 2022;163:107221. *https://doi.org/10.1016/j.envint.2022.107221*
28. **Khodayar MJ, Shirani M, Shariati S, Khorsandi L, Mohtadi S**. Antioxidant and anti-inflammatory potential of vanillic acid improves nephrotoxicity induced by sodium arsenite in mice. Int J Environ Health Res 2024;ahead-of-print:1-11. *https://doi.org/10.1080/09603123.2024.2439452*
29. **Ogunmoyole T, Awodooju M, Idowu S, Daramola O**. Phyllanthus amarus extract restored deranged biochemical parameters in rat model of hepatotoxicity and nephrotoxicity. Heliyon 2020;6:e05670. *https://doi.org/10.1016/j.heliyon.2020.e05670*
30. **Adil M, Kandhare AD, Visnagri A, Bodhankar SL**. Naringin ameliorates sodium arsenite-induced renal and hepatic toxicity in rats: decisive role of KIM-1, Caspase-3, TGF-beta, and TNF-alpha. Ren Fail 2015;37:1396-1407. *https://doi.org/10.3109/0886022X.2015.1074462*
31. **Afolabi AO, Akhigbe TM, Odetayo AF, Anyogu DC, Hamed MA, Akhigbe RE**. Restoration of Hepatic and Intestinal Integrity by Phyllanthus amarus Is Dependent on Bax/Caspase 3 Modulation in Intestinal Ischemia-/Reperfusion-Induced Injury. Molecules 2022;27:5073. *https://doi.org/10.3390/molecules27165073*
32. **Kandhare AD, Liu Z, Mukherjee AA, Bodhankar SL**. Therapeutic Potential of Morin in Ovalbumin-induced Allergic Asthma Via Modulation of SUMF2/IL-13 and BLT2/NF-kB Signaling Pathway. Curr Mol Pharmacol 2019;12:122-138. *https://doi.org/10.2174/1874467212666190102105052*
33. **Sarkate AP, Murumkar PR, Lokwani DK, Kandhare AD, Bodhankar SL, Shinde DB** *et al.* Design of selective TACE inhibitors

using molecular docking studies: Synthesis and preliminary evaluation of anti-inflammatory and TACE inhibitory activity. SAR QSAR Environ Res 2015;26:905-923. *https://doi.org/10.1080/1062936X.2015.1095240*

34. **Zhou Z, Kandhare AD, Kandhare AA, Bodhankar SL**. Hesperidin ameliorates bleomycin-induced experimental pulmonary fibrosis via inhibition of TGF-β1/Smad3/AMPK and IκBα/NF-κB pathways. EXCLI Journal 2019;18:723-745.
35. **Kiemer AK, Hartung T, Huber C, Vollmar AM**. Phyllanthus amarus has anti-inflammatory potential by inhibition of iNOS, COX-2, and cytokines via the NF-kappaB pathway. J Hepatol 2003;38:289-297. *https://doi.org/10.1016/s0168-8278(02)00417-8*
36. **Jagtap S, Khare P, Mangal P, Kondepudi KK, Bishnoi M, Bhutani KK**. Protective effects of phyllanthin, a lignan from Phyllanthus amarus, against progression of high fat diet induced metabolic disturbances in mice. RSC Advances 2016;6:58343-58353. *https://doi.org/10.1039/c6ra10774e*
37. **Thyagarajan SP, Subramanian S, Thirunalasundari T, Venkateswaran PS, Blumberg BS**. Effect of Phyllanthus amarus on chronic carriers of hepatitis B virus. Lancet 1988;2:764-766. *https://doi.org/10.1016/s0140-6736(88)92416-6*
38. **Xin-Hua W, Chang-Qing L, Xing-Bo G, Lin-Chun F**. A comparative study of Phyllanthus amarus compound and interferon in the treatment of chronic viral hepatitis B. Southeast Asian J Trop Med Public Health 2001;32:140-142.
39. **Wang M, Cheng H, Li Y, Meng L, Zhao G, Mai K**. Herbs of the genus Phyllanthus in the treatment of chronic hepatitis B: observations with three preparations from different geographic sites. J Lab Clin Med 1995;126:350-352.
40. **Moshi MJ, Lutale JJ, Rimoy GH, Abbas ZG, Josiah RM, Swai AB**. The effect of Phyllanthus amarus aqueous extract on blood glucose in non-insulin dependent diabetic patients. Phytother Res 2001;15:577-580. *https://doi.org/10.1002/ptr.780*
41. **Abu Hassan MR, Hj Md Said R, Zainuddin Z, Omar H, Md Ali SM, Aris SA** *et al.* Effects of one-year supplementation with Phyllanthus niruri on fibrosis score and metabolic markers in patients with non-alcoholic fatty liver disease: A randomized, double-blind, placebo-controlled trial. Heliyon 2023;9:e16652. *https://doi.org/10.1016/j.heliyon.2023.e16652.*

Invest Clin 67(1): 108 - 124, 2026 https://doi.org/10.54817/IC.v67n1a08

Treatment strategies and mortality risk factors in patients with multidrug-resistant *Acinetobacter baumannii* pneumonia: A retrospective analysis.

Lili Liu[#,1], Wen Lu[#,2], Gege Fang[3] and Wei Zhang[2]

[1]Infection Control Department, The Third People's Hospital of Yichang City, No. 23, Gangyao Road, Xiling District, Yichang City, Hubei Province, China.
[2]Department of Critical Care Medicine, The Third People's Hospital of Yichang City, No. 23, Gangyao Road, Xiling District, Yichang City, Hubei Province, China.
[3]Department of Pulmonary Medicine III, The Third People's Hospital of Yichang City, No. 23, Gangyao Road, Xiling District, Yichang City, Hubei Province, China.
[#]These authors contributed equally to this work as co-first authors.

Keywords: *Acinetobacter baumannii*; Pneumonia; Drug Resistance; Multiple; Risk Factors; Tigecycline.

Abstract. This study aimed to investigate the determinants of drug resistance risk factors, 30-day all-cause mortality risk factors, and related clinical treatment strategies in patients with multidrug-resistant *Acinetobacter baumannii* (MDRAB) pneumonia. This retrospective study analyzed data from 168 patients with MDRAB pneumonia and 141 patients with non-MDRAB pneumonia between February 2022 and February 2025. On the second day of admission, the severity of illness and use of carbapenems, tigecycline, etc., were higher in MDRAB pneumonia patients than in non-MDRAB pneumonia patients ($p<0.05$). The risk factors significantly associated with MDRAB pneumonia included ICU stay prior to AB infection ($p<0.001$), APACHE II score ≥ 18 ($p=0.002$), invasive procedures ($p<0.001$), septic shock ($p=0.002$), and drug abuse ($p<0.001$). Length of ICU stay before culture, recent surgery, APACHE II score ≥18, tigecycline-containing treatment, and the use of two or more antibiotic types (all $p<0.05$) were significantly linked to 30-day mortality. In a cohort of 168 MDRAB patients, the non-tigecycline treatment group (n=85) showed a significantly lower 30-day mortality rate compared to the tigecycline treatment group (n=83) ($p=0.003$). Among those receiving tigecycline, the incidence of gastrointestinal adverse reactions was significantly higher, while allergic reactions were less frequent (both $p<0.05$). In conclusion, prior ICU admission, invasive procedures, and drug abuse are risk factors for developing MDRAB. Severe pneumonia and tigecycline treatment are strongly associated with higher mortality in MDRAB patients, and tigecycline should be used cautiously.

Corresponding authors: Gege Fang Department of Pulmonary Medicine III, The Third People's Hospital of Yichang City, No. 23, Gangyao Road, Xiling District, Yichang City 443000, Hubei Province, China. Email: fgg2343@hotmail.com. Wei Zhang. Department of Critical Care Medicine, The Third People's Hospital of Yichang City, No. 23, Gangyao Road, Xiling District, Yichang City, Hubei Province, China. Email: zw2390Z@hotmail.com

Estrategias de tratamiento y factores de riesgo de mortalidad en pacientes con neumonía por *Acinetobacter baumannii* multirresistente: Un análisis retrospectivo.

Invest Clin 2026; 67 (1): 108 – 124

Palabras clave: *Acinetobacter baumannii*; Neumonía; Resistencia a Múltiples Medicamentos; Factores de riesgo; Tigeciclina.

Resumen. El objetivo del trabajo fue explorar los factores de riesgo de resistencia a múltiples medicamentos en pacientes con neumonía por *Acinetobacter baumannii* (MDRAB), los factores de riesgo de muerte por todas las causas en 30 días y las estrategias de tratamiento. Este estudio retrospectivo (febrero de 2022-febrero de 2025) analizó datos de 168 pacientes con neumonía por MDRAB y de 141 con neumonía por Non-MDRAB. Al segundo día, los pacientes con neumonía por MDRAB presentaron mayor gravedad y mayor uso de carbapenémicos y tigeciclina que los de Non-MDRAB ($p<0,05$). Los factores de riesgo significativamente asociados con neumonía por MDRAB incluyeron estancia en UCI previa a la infección por AB ($p<0,001$), puntuación APACHE II≥18 ($p=0,002$), procedimientos invasivos ($p<0,001$), shock séptico ($p=0,002$) y abuso de drogas ($p<0,001$). La estancia en UCI previa al cultivo, cirugía reciente, puntaje APACHE II ≥ 18, tratamiento con tigeciclina y uso de ≥ 2 antibióticos (todos $p<0,05$) se asociaron significativamente con la mortalidad a 30 días. La cohorte de 168 pacientes con MDRAB mostró una tasa de mortalidad a 30 días significativamente menor en el grupo sin tigeciclina ($n=85$) que en el grupo con tigeciclina ($n=83$) ($p=0,003$). En el tratamiento con tigeciclina, la incidencia de eventos adversos gastrointestinales fue mayor y la de reacciones alérgicas, menor (ambas $p<0,05$). En conclusión, la admisión previa en UCI, los procedimientos invasivos y el abuso de drogas son factores de riesgo para el desarrollo de MDRAB. La enfermedad grave y el tratamiento con tigeciclina se asocian significativamente con una alta mortalidad en pacientes con MDRAB, por lo que debe usarse con precaución.

Received: 24-09-2025 Accepted: 30-12-2025

INTRODUCTION

Acinetobacter baumannii (A. baumannii or AB) is an aerobic, Gram-negative opportunistic pathogen. As a significant pathogen in hospital-acquired infections worldwide, it accounts for approximately 20% of intensive care unit (ICU) infections [1-3]. The bacteria demonstrate strong environmental adaptability, can survive and reproduce across various pH levels and temperatures, and can adhere to surfaces of medical equipment such as surgical instruments, ventilators, catheters, and respiratory measuring devices to form biofilms and continue spreading[4,5]. Because *A. baumannii* closely resembles other strains, phenotypic and biochemical classification methods often misidentify it, resulting in an underestimation of its role in nosocomial infections. *A. baumannii* causes various hospital-associated infections, including ventilator-associated pneumonia and

bloodstream infections [6,7]. As a multidrug-resistant pathogen that has garnered global attention, infections caused by *A. baumannii* are associated with higher mortality rates, ranging from 7.8% to 43%. The risk of death is particularly high among ICU patients. It is the second most common Gram-negative pathogen in hospital-acquired pneumonia, responsible for about 3% to 5% of such cases, with associated mortality rates reaching 30% to 75%.

Recently, the overuse of antibiotics, frequent cross-infections among hospitalized patients, and the horizontal transfer of drug-resistant genes have led to the emergence of multidrug-resistant (MDR), extensively drug-resistant (XDR), and even pan-drug-resistant (PDR) strains of *A. baumannii*. This has severely limited options for clinical anti-infective therapy. Globally, the multidrug resistance rate of *A. baumannii* remains high, at approximately 45%. Currently, mainstream strains show extensive resistance to multiple antibiotics, especially carbapenems. In Asia, bacterial susceptibility to carbapenems is even lower than 27%[8,9]. Many guidelines at home and abroad recommend treating pneumonia caused by MDRAB with polymyxin, tigecycline, and sulbactam, combined with other antibiotics. However, regional differences in bacterial sensitivity to specific drugs necessitate the development of individualized drug combination strategies based on local resistance profiles and current guidelines [10]. Polymyxin and tigecycline remain the effective first-line treatments for infections caused by MDR strains. With MDRAB infections, treatment options are extremely limited, mainly relying on a few classes such as polymyxin and tigecycline. Unfortunately, strains resistant to polymyxin are emerging, and tigecycline resistance is also increasing in *A. baumannii*, further intensifying treatment difficulties.

Tigecycline is a broad-spectrum semi-synthetic glycopeptide antibiotic derived from minocycline. The drug has strong in vitro activity against a variety of MDR bacteria (e.g., *A. baumannii*), but is ineffective against P. *aeruginosa* and *Shigella* [11]. The structural design of tigecycline enables it to avoid the common tetracycline resistance mechanism, thus showing good application potential in dealing with multi-drug resistant bacteria infection [12]. In general, tigecycline alone is not recommended when other effective antibiotics are available. The combination of tigecycline and sulbactam is one of the common strategies for the treatment of hospital-acquired MDRAB infection. For pulmonary and systemic carbapenem-resistant *A. baumannii* infection, high-dose tigecycline regimen is often given priority because of its high drug concentration in plasma and lung tissue, which shows better efficacy than conventional doses in retrospective studies[13]. Despite demonstrating in vitro susceptibility against MDRAB, the clinical efficacy of tigecycline is controversial. Evidence suggests that its antibacterial activity fails to translate into significant clinical benefit, offering little improvement in patient prognosis [14].

This study investigated the risk factors for drug resistance and the determinants of 30-day all-cause mortality in patients with MDRAB pneumonia, and related clinical treatment strategies. At the same time, the safety evaluation of the adverse reactions of Radical Antimicrobial Regimens was carried out to provide evidence-based basis for early identification of high-risk patients, optimization of treatment strategies and improvement of prognosis.

MATERIAL AND METHODS

Study design

This retrospective, single-center, observational study included 343 patients with AB pneumonia treated at the Third People's Hospital of Yichang City, China, between February 2022 and February 2025. After applying exclusion criteria, 168 patients had MDRAB pneumonia, and 141 had non-MDRAB pneumonia. Their basic characteristics, in vitro

antimicrobial susceptibility testing, treatment strategies on the second day of admission, and survival curves of Radical Antimicrobial Regimens were analyzed. Potential risk factors for drug resistance and 30-day all-cause mortality were evaluated using univariate and multivariate logistic regression analyses. The process flow is shown in Fig. 1.

Inclusion criteria

(1) diagnosed as pneumonia; (2) The culture of blood and respiratory tract was AB positive; (3) Age greater than 18 years old; (4) Complete clinical data.

Exclusion criteria

(1) transfer, death, or treatment abandonment within 24 hours of admission; (2) Incomplete clinical data; (3) Lactating women during pregnancy; (4) No clinical manifestations of infection.

Sample size calculation

The mortality rate of *A. baumannii* in hospital-acquired pneumonia ranges from 30% to 75% [15]. This study assumed that the mortality rate could be reduced by 30% with tigecycline treatment. A bilateral test was used to set the significance level α at 0.05, with a test power (1-β) of 0.8. After estimating and adjusting the sample size, the minimum total sample size was 142. Overall, 309 patients were included in this study, of whom 83 with MDRAB infection received a comprehensive treatment regimen containing tigecycline, meeting the preset sample size requirements and providing sufficient statistical power for the research conclusions.

Ethical statement

The study protocol was approved by our hospital's research ethics committee and strictly adhered to the ethical guidelines and norms established by the 'Helsinki Declaration' (latest revision) [16]. It prioritizes the rights, safety, and well-being of the subjects and ensures all research activities follow international ethical standards. We have ef-

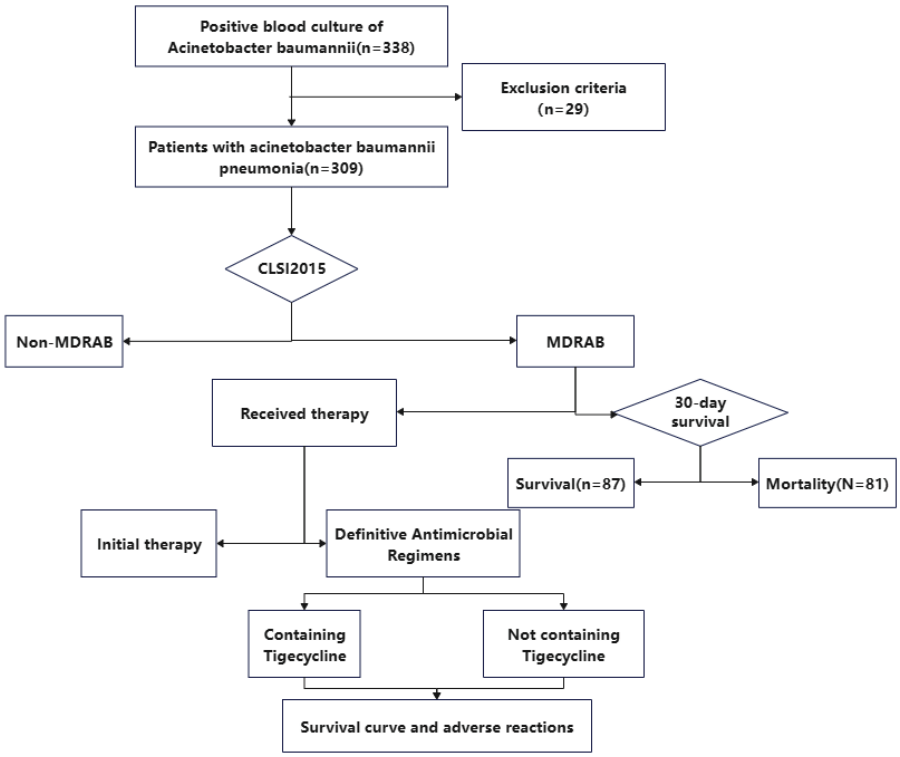

Fig. 1. Case identification flow chart.

fectively protected the legitimate rights and interests of all participants by implementing a thorough informed consent process, safeguarding the privacy and confidentiality of subjects, and adhering to principles of fair benefit and risk reduction.

Basic information collection

Clinical data of patients with AB pneumonia were retrieved from the Hospital Information System (HIS) database. The collected data include age, gender, hospitalization history, past medical history, surgical history, disease diagnosis, clinical outcomes, antibiotic use history, and microbiological data. Disease severity was assessed at the onset of AB using the SOFA and APACHE II scores. All-cause 30-day mortality following the onset of AB pneumonia was the primary clinical outcome. All antibiotic regimens were administered in accordance with the instructions and clinical medication protocols.

Antimicrobial susceptibilities

In this study, the VITEK 2 Compact system (bioMérieux, France) and its supporting MALDI-TOF MS mass spectrometry were used to identify the strains of *A.baumannii* isolates. The drug sensitivity test was performed by the VITEK-2 Compact system combined with the AST-GN16 drug sensitivity card (bioMérieux). Tigecycline susceptibility was determined per FDA breakpoints. For all other antibiotics, susceptibility was interpreted according to the latest CLSI guidelines [17,18].

Adverse reactions

During the treatment, adverse reactions such as nausea and vomiting, Diarrhea, ototoxicity, allergic reactions, liver injury, and kidney injury were observed and recorded.

Definitions

(1) Blood and respiratory cultures should be collected within the first 48 hours of hospitalization. AB isolates were categorized as S (sensitive), I (intermediate), or R (resistant). For this analysis, I and R were considered non-sensitive. MDRAB was defined as any AB resistant to at least one of three or more classes of antimicrobial agents. (2) Complications included cerebrovascular disease, liver disease, chronic lung disease, renal failure, etc. (3) The simultaneous administration of two or more different antibacterial agents is called combination antibacterial therapy. (4) Invasive procedures included tracheotomy, catheterization, abdominal puncture, ventilator use, etc.

Statistical analysis

Continuous and categorical data were expressed as mean ± standard deviation and number (percentage), respectively. For comparisons of mean values between groups, the independent t-test was used under the normality assumption, and categorical data were evaluated using the chi-square test. Statistical analysis was conducted using SPSS version 26. GraphPad Prism was used for plotting. $p<0.05$ indicated statistical significance of each test. Univariate and multivariate logistic regression models were used to examine associations between independent variables and dichotomous outcomes, including MDRAB infection and 30-day mortality.

RESULTS

Antibiotic resistance characteristics of *Acinetobacter baumannii* pneumonia

The drug-sensitivity test results showed that the AB strain was most sensitive to polymyxin and tigecycline, followed by minocycline, cefoperazone/sulbactam, and levofloxacin. Resistance rates to other antibiotics were more than 45%, particularly carbapenems, and resistance to carbapenems was more than 75%. By comparing the antimicrobial susceptibility spectra, we found significant differences in the susceptibility of carbapenems, cephalosporins, quinolones, aminoglycosides, tigecycline, and combination drugs between the MDRAB and Non-MDRAB groups ($p<0.05$). In the MDRAB group, in addi-

tion to tigecycline, polymyxin, minocycline, cefoperazone/sulbactam, and levofloxacin (6.20%, 3.52%, 45.53%, 49.43%, and 63.40%, respectively), the resistance rates to other antibiotics exceeded 75% (Table 1).

Treatment of *Acinetobacter baumannii* pneumonia

By day 2, MDRAB patients exhibited greater disease severity, with higher ICU admission rates (70.8% vs. 18.4%, p<0.001) and mechanical ventilation rates (54.2% vs. 36.2%, p=0.002). The use of carbapenems, extended-spectrum cephalosporins, aminoglycosides, and tigecycline was more frequent than in the Non-MDRAB group (p<0.05). This indicates that MDRAB pneumonia patients have fewer clinical options, which complicates treatment and increases the risk of side effects (Table 2).

Table 1. Antibiotic Resistance characteristics of *Acinetobacter baumannii* pneumonia.

Antimicrobial	Total (N=309)	MDRAB (N=168)	Non-MDRAB (N=141)	χ^2	*p*
Carbapenem antibiotic					
Meropenem	77.35% (239/309)	91.07% (153/168)	60.99%(86/141)	37.885	<0.001
Imipenem	82.85% (256/309)	95.83% (161/168)	67.38% (95/141)	41.708	<0.001
Cephalosporins					
Cefepime	52.10%(161/309)	91.07%(153/168)	5.67%(8/141)	220.61	<0.001
Ceftriaxone	53.21%(141/265)	97.83%(135/138)	4.27%(6/127)	175.9	<0.001
Ceftazidime	54.50%(109/200)	90.27%(102/113)	8.05%(7/87)	101.93	<0.001
Aminoglycosides					
Gentamicin	53.36% (135/253)	94.20%(130/138)	4%(5/125)	168.992	<0.001
Amikacin	50.19% (133/265)	97.73%(129/132)	3.01% (4/133)	171.457	<0.001
Tobramycin	48.51%(129/268)	84.21%(128/152)	1.72%(2/116)	175.136	<0.001
Quinolones					
Ciprofloxacin	56.30%(152/270)	96.58%(141/156)	8.87%(11/124)	177.794	<0.001
Levofloxacin	35.03%(103/294)	63.40%(97/153)	4.26%(6/141)	99.579	<0.001
Tetracycline					
Tigecycline	3.29%(8/243)	6.20%(8/129)	0%(0/114)	5.133	0.024
Minocycline	25.38%(66/260)	45.53%(56/123)	7.30%(10/137)	31.447	0.011
Others					
Colistin	1.87%(5/268)	3.52%(5/142)	0%(0/126)	5.133	0.092
Combined medication					
Trimethoprim/ sulfamethoxazole	54.58%(149/273)	93.06%(134/144)	11.63%(15/129)	146.218	<0.001
Piperacillin/ tazobactam	54.64%(100/183)	97.96%(96/98)	4.71%(4/85)	103.26	<0.001
Cefoperazone/ sulbactam	26.47%(45/170)	49.43%(43/87)	2.41%(2/83)	35.978	<0.001

Data expressed as % (n). MDRAB: multidrug-resistant *Acinetobacter baumannii*; Non-MDRAB: no multidrug-resistant. Comparisons of mean values between groups, was performed by independent χ^2 test.

Table 2. Treatment of *Acinetobacter baumannii* pneumonia.

Treatment	MDRAB (N=168)	Non-MDRAB (N=141)	χ^2	*p*
Illness severity measured by day 2				
ICU admission	119(70.83%)	26(18.44%)	84.399	< 0.001
Mechanical ventilation	91(54.17%)	51(36.17%)	9.909	0.002
Antibiotics administered by day 2				
Extended-spectrum cephalosporins	58(34.52%)	29(20.57%)	7.386	0.007
Fluoroquinolones	63(37.5%)	46(32.627%)	0.783	0.376
Carbapenems	97(57.74%)	31(22%)	40.247	< 0.001
Aminoglycosides	42(25%)	16(11.35%)	9.376	0.002
Combined medication	46(27.38%)	20(14.18%)	7.942	0.005
Tetracyclines	14(8.33%)	6(4.26%)	13.341	< 0.001
Polymyxins	7(4.17%)	0(0%)	6.024	0.014

Data expressed as n (%). MDRAB: multidrug-resistant *Acinetobacter baumannii;* Non-MDRAB: no multidrug-resistant. Comparisons of mean values between groups, was performed by independent χ^2 test.

Baseline characteristics of *Acinetobacter baumannii* pneumonia

Data on 309 patients with AB pneumonia were collected, and their characteristics were analyzed. Patients with MDRAB pneumonia were older (64.72 ± 10.19 years vs 60.72 ± 10.71 years, p = 0.001), and the proportion of males in both groups exceeded 55%. The incidence of AB infection in hospitals was above 90%, and 82.14% of MDRAB pneumonia patients were diagnosed in the ICU. Complications were common in patients with MDRAB pneumonia, among which hypoproteinemia (76.19%) and septic shock (32.14%) were the most common. The APACHE II and SOFA scores of patients with MDRAB pneumonia were higher than those of patients with Non-MDRAB pneumonia. In addition, alcohol abuse and drug abuse also have a greater impact on patients with MDRAB pneumonia. Detailed data are shown in Table 3.

Risk Factors for patients with *Acinetobacter baumannii* pneumonia

Univariate analysis showed that age, ICU stay prior to AB infection, hospital stay over 30 days before AB infection, hemodialysis, immunosuppressive status, APACHE II score of 18 or higher, SOFA score of 10 or higher, invasive procedures, hypoproteinemia, septic shock, alcohol abuse, and drug abuse were associated with MDRAB. After adjusting for confounders, multivariate logistic regression revealed that ICU stay prior to AB infection [p<0.001; OR(95% CI): 17.855 (9.764-32.650)], APACHE II score ≥ 18 [p = 0.002; OR(95% CI): 4.002 (1.658-9.662)], invasive procedures [p<0.001; OR(95% CI): 5.707 (2.933-11.104)], septic shock [p = 0.002; OR(95% CI): 5.059 (1.834-13.956)], and drug abuse [p<0.001; OR(95% CI): 5.092 (2.351-11.024)] were independent risk factors for MDRAB resistance (Table 4).

Risk factors for death within 30 days in patients with *Acinetobacter baumannii* pneumonia

The 30-day all-cause mortality of 168 MDRAB patients was 48.21% (81). Univariate analysis showed that the length of ICU stay prior to culture, recent surgery, immunocompromised status, endotracheal tube, fiberoptic bronchoscopy, and a SOFA score ≥ 10 were associated with culture positivity.

Table 3. Baseline characteristics of *Acinetobacter baumannii* pneumonia.

Baseline characteristics	MDRAB (N=168)	Non-MDRAB (N=141)	χ^2/t	*p*
Age(years)	63.64±10.55	60.92±8.17	2.492	0.013
Gender				
Male	94(56.95%)	82(58.16%)	0.145	0.703
Female	74(44.05%)	59(41.84%)		
Infection				
Nosocomial infection	157(93.45%)	129(91.49%)	0.406	0.524
Community infections	11(6.55%)	12(8.51%)		
Hospital exposure				
ICU stay prior to AB infection	138(82.14%)	31(21.99%)	111.956	<0.001
Hospital stay >30 days prior to AB infection	15(8.93%)	4(2.84%)	4.922	0.027
Operation	64(38.10%)	52(36.88%)	0.048	0.826
Hemodialysis	26(15.48%)	8(5.67%)	7.521	0.006
Illness severity at time of AB				
APACHE II	24.36±8.39	20.31±7.36	4.479	<0.001
SOFA	8.03±5.16	4.11±2.89	7.998	<0.001
Invasive procedures	82(48.81%)	25(17.73%)	32.7	<0.001
Comorbid conditions				
Cerebrovascular diseases	36(21.43%)	27(19.15%)	0.245	0.621
Liver disease	40(23.81%)	31(21.99%)	0.144	0.704
Chronic pulmonary disease	16(9.52%)	14(9.93%)	0.015	0.903
Renal failure	27(16.07%)	16(11.35%)	1.428	0.232
Malignant tumor	32(19.05%)	28(19.86%)	0.032	0.858
Diabetes	28(16.67%)	21(14.89%)	0.181	0.67
Hypoproteinemia	128(76.19%)	89(63.12%)	6.214	0.013
Septic shock	54(32.14%)	11(7.80%)	27.34	<0.001
Immunocompromised status	30(17.86%)	6(4.26%)	13.788	<0.001
Coagulopathy	31(18.45%)	15(10.64%)	3.694	0.055
Paralysis	29(17.26%)	22(15.60%)	0.165	0.684
Gastrointestinal bleeding	20(11.90%)	14(9.93%)	0.305	0.581
Other factors				
Obesity	32(19.05%)	26(18.44%)	0.019	0.891
Weight loss	34(20.24%)	39(27.66%)	2.33	0.127
Fluid and electrolyte disorders	92(54.76%)	79(56.03%)	0.044	0.834
Anemia	64(38.1%)	61(43.26%)	0.85	0.357
Alcohol abuse	28(16.67%)	9(6.38%)	7.723	0.005
Drug abuse	66(39.29%)	18(12.77%)	27.257	<0.001
Mental disorders diseases	31(18.45%)	27(19.15%)	0.024	0.877
Hypertension	102(60.71%)	95(67.38%)	1.451	0.228
Outcome				
30-day mortality	81(48.21%)	10(7.09%)	62.393	<0.001

Data expressed as n (%) or mean ± SD. MDRAB: multidrug-resistant Acinetobacter baumannii; Non-MDRAB: no multidrug-resistant. Comparisons of mean values between groups, was performed by independent t-test or χ^2.

APACHE II ≥ 18 and invasive interventions (n > = 3 types) were significantly associated with 30-day mortality. Multivariate logistic regression showed that independent risk factors included length of ICU stay prior to culture [p = 0.012, OR (*95% CI*): 0.327 (0.137-0.778)], recent surgery [p = 0.001, OR (*95% CI*): 0.063 (0.012-0.338)], APACHE II ≥ 18 [p<0.001, OR (*95% CI*): 0.104 (0.034-0.321)], which were significantly associated with 30-day mortality (Table 5).

The effect of radical antimicrobial regimens on the 30-day mortality of patients with *Acinetobacter baumannii* pneumonia

In this study, 83 MDRAB pneumonia patients received radical treatment containing tigecycline, of which 57 patients (68.67%) died within 30 days. Univariate analysis showed that radical treatment, including tigecycline, polymyxin, and ≥2 antibiotic agents, was significantly associated with 30-day mortality. Multivariate logistic regression analysis showed that Tigecycline + Other drugs, ≥ 2 types of antibiotics, were independent risk factors for 30-day mortality. 168 patients with MDRAB were divided into Non-tigecycline treatment group (n = 85), and tigecycline treatment group (n = 83). The 30-day mortality of the Non-tigecycline group was lower than that of the tigecycline group (p= 0.003) (Table 6 and Fig. 2). This suggests that physicians should select a regimen containing tigecycline to treat MDRAB infection with discretion and prioritize other treatment strategies that may be more effective or safer.

Adverse reaction of radical antimicrobial regimens

The incidence of gastrointestinal adverse reactions, including nausea and vomiting (p = 0.044) and diarrhea (p = 0.035),

Table 4. Risk factors for death within 30 days in patients with MDRAB.

Baseline characteristics	Univariable Analysis OR (95% CI)	p	Multivariable Analysis OR (95% CI)	p
Age(years)	0.970(0.947-0.994)	0.015		
Hospital exposure				
ICU stay prior to AB infection	16.323(9.314-28.604)	<0.001	17.855(9.764-32.650)	<0.001
Hospital stay >30 days prior to AB infection	3.358(1.088-10.361)	0.035	1.364(0.278-6.683)	0.702
Hemodialysis	3.044(1.331-6.960)	0.008	0.565(0.165-1.931)	0.362
Illness severity at time of AB				
APACHE II≥18	2.327(1.460-3.708)	<0.001	4.002(1.658-9.662)	0.002
SOFA≥10	1.619(1.031-2.541)	0.036	0.527(0.2221.254)	0.148
Invasive procedures	4.424(2.611-7.498)	<0.001	5.707(2.933-11.104)	<0.001
Comorbid conditions				
Hypoproteinemia	1.870(1.142-3.061)	0.013	1.233(0.733-2.076)	0.43
Septic shock	5.598(2.793-11.222)	<0.001	5.059(1.834-13.956)	0.002
Immunocompromised status	4.891(1.973-12.128)	0.001	1.042(0.238-3.832)	0.951
Other factors				
Alcohol abuse	2.933(1.334-6.449)	0.007	0.737(0.259-2.059)	0.567
Drug abuse	4.422(2.467-7.925)	<0.001	5.092(2.351-11.024)	<0.001

MDRAB: multidrug-resistant *Acinetobacter baumannii.* Data expressed as n (%). OR(95% CI): Odds Ratio (OR) with a 95% Confidence Interval.

Table 5. Risk factors for mortality of patients with *Acinetobacter baumannii* pneumonia.

Risk factors	Survival (N=87)	Mortality (N=81)	Univariable Analysis OR (95% CI)	*p*	Multivariable Analysis OR (95% CI)	*p*
Age >60 years	51(58.62%)	49(60.49%)	0.833 (0.448-1.550)	0.565		
Male	43(49.43%)	51(62.96%)	0.575 (0.310-1.065)	0.078		
ICU length of stay before AB culture (d)	21(24.14%)	38(46.91%)	0.360 (0.187-0.694)	0.002	0.327 (0.137-0.778)	0.012
Recent surgery (within 1 month)	12(13.79%)	36(44.44%)	0.200 (0.094-0.424)	<0.001	0.063 (0.012-0.338)	0.001
Immunocompromised status	8(9.20%)	22(27.16%)	0.272 (0.113-0.653)	0.004	1.273 (0.322-5.032)	0.731
Endotracheal tube	34(39.08%)	47(58.02%)	0.464 (0.250-0.860)	0.015	0.740 (0.269-2.037)	0.56
Fiberoptic bronchoscopy	25(28.74%)	38(46.91%)	0.448 (0.239-0.839)	0.012	3.872 (0.857-17.507)	0.079
SOFA≥10	39(44.83%)	55(67.90%)	0.367 (0.195-0.688)	0.002	1.579 (0.593-4.206)	0.361
APACHE II≥18	41(51.72%)	39(87.65%)	0.151 (0.069-0.331)	<0.001	0.104 (0.034-0.321)	<0.001
Invasive interventions (n > = 3 types)	11(12.64%)	21(25.93%)	0.414(0.185-0.924)	0.031	0.786(0.280-2.206)	0.647

Data expressed as n (%). OR(95% CI): Odds Ratio (OR) with a 95% Confidence Interval.

Table 6. The Effect of Radical Antimicrobial Regimens on the 30-Day mortality of patients with *Acinetobacter baumannii* pneumonia.

Antimicrobial Regimen	Survival (N=87)	Mortality (N=81)	Univariable Analysis OR (95% CI)	*p*	Multivariable Analysis OR (95% CI)	*p*
Containing Tigecycline	**26(29.89%)**	**57(70.37%)**				
Tigecycline	2(2.30%)	5(6.17%)	0.294 (0.058-1.501)	0.012	0.697 (0.130-3.736)	0.673
Tigecycline+Other drugs	24(27.59%)	52(64.20%)	0.212 (0.110-0.408)	<0.001	0.220 (0.112-0.431)	<0.001
Not containing Tigecycline	**61(70.11%)**	**24(29.63%)**				
Polymyxins	2(2.30%)	8(9.88%)	0.215 (0.044-0.215)	0.056	0.225 (0.044-1.153)	0.074
Cefoperazone/sulbactam	32(36.78%)	35(43.21%)	0.765 (0.412-1.420)	0.396	1.579 (0.721-3.459)	0.254
≥2 types of antibiotic	51(58.62%)	62(76.54%)	0.434 (0.223-0.847)	0.014	0.371 (0.166-0.833)	0.016

Data expressed as n (%). OR(95% CI): Odds Ratio (OR) with a 95% Confidence Interval.

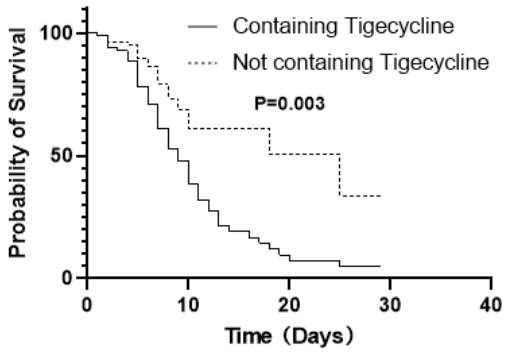

Fig. 2. Kaplan–Meier survival estimates among patients with MDRAB.
MDRAB: multidrug-resistant *Acinetobacter baumannii*.

was significantly higher in regimens containing tigecycline than in regimens without it. In contrast, the occurrence of allergic reactions was lower with the tigecycline treatment ($p = 0.04$). Additionally, there was no significant difference in adverse reactions such as ototoxicity, liver injury, and kidney injury between the two groups. This indicates that clinicians and patients should pay close attention to, and proactively manage, gastrointestinal adverse reactions when using tigecycline in clinical practice. The risk of allergy caused by tigecycline is relatively low, making it a potentially favorable option for patients allergic to other antibiotics (Table 7).

DISCUSSION

Pneumonia poses a major burden on global health, and its high morbidity and mortality make it one of the main causes of in-hospital death in hospitalized patients[19]. *A. baumannii* is a notable opportunistic pathogen responsible for severe nosocomial infections, especially in critically ill patients, which often leads to serious complications such as ventilator-associated pneumonia. Due to its significant drug resistance and susceptibility to clonal transmission, the prevention and control of this bacterium have become a major challenge for global healthcare systems [20]. Recently, the resistance rate of *A. baumannii* to a variety of commonly used antibiotics, including carbapenems, has continued to rise. Therefore, *A. baumannii* has been listed as a 'first-class' key pathogen by the WHO. It is urgent to develop new or more effective antibiotic treatment programs [21]. The emergence of MDRAB has not only increased the morbidity and mortality of patients, but also become one of the core objectives of hospital infection prevention and control, which further highlights the urgent need for effective treatment strategies for MDRAB [22]. Currently, sulbactam-containing combinations, polymyxins, and tigecycline are recommended as standard combination therapies for the treatment of *A. baumannii* infections. However, global reports of drug resistance to these drugs are gradually increasing [23]. Through retrospective analysis, this study summarized the clinical characteristics of patients with AB pneumonia, identified risk factors for MDRAB pneumonia, further evaluated the predictive factors for 30-day mortality in patients with MDRAB

Table 7. Adverse Reaction of Radical Antimicrobial Regimens.

Variables	Containing Tigecycline(n=83)	Not containing Tigecycline(n=85)	χ^2	*p*
Nausea and vomiting	22(26.51%)	11(12.94%)	4.074	0.044
Diarrhea	20(24.10%)	9(10.59%)	4.461	0.035
Allergic reactions	5(6.02%)	14(16.47%)	4.24	0.04
Ototoxicity	2(2.41%)	4(4.71%)	0.149	0.699
Liver injury	7(8.43%)	9(10.59%)	0.045	0.832
renal injury	6(7.23%)	8(9.41%)	0.054	0.816
Other	9(10.84%)	13(15.29%)	0.392	0.531

Data expressed as n (%). Comparison of mean values between groups was performed by the χ^2 test.

pneumonia, and assessed the efficacy and safety of different eradication regimens. It is expected to provide infection control and clinical care for MDRAB.

The emergence of MDRAB has become a major global healthcare challenge, severely compromising treatment options. Numerous studies have demonstrated this pathogen's resistance to a wide range of antimicrobial agents, including carbapenems, cephalosporins, tigecycline, quinolones, aminoglycosides, and sulbactam-containing compounds [24,25]. Several studies have shown that AB strains are highly sensitive to polymyxins and tigecycline and exhibit high resistance to other antimicrobial agents, particularly carbapenems. In the MDRAB group, except for tigecycline, polymyxin, minocycline, cefoperazone/sulbactam, and levofloxacin, the other antibacterial drugs had higher resistance rates, consistent with the trend observed in this study [15,18,26]. However, it has also been reported that there is a high resistance to myxobacterial polyantibodies [27], this difference may be related to factors such as the source and type of the selected sample and the underlying disease of the patient. In addition, the severity of disease in patients with MDRAB pneumonia is significantly higher than that in patients with non-MDRAB pneumonia. This further complicates treatment and increases the risk of adverse drug events. Compared with the Non-MDRAB group, the frequency of carbapenem, extended-spectrum cephalosporin, aminoglycoside, and tigecycline use in patients with MDRAB pneumonia was higher, indicating that, under the pressure of multidrug-resistant infections, the clinic has to rely more on these drugs, which have certain toxicities and side effects.

In terms of clinical impact, drug-resistant strains were associated with previous admission to ICU, APACHE II score ≥ 18, invasive procedures, septic shock, and drug abuse. The most common risk factors for obtaining MDRAB included age, previous admission to ICU, length of hospital stay before AB infection more than 30 days, hemodialysis, immunosuppressive status, APACHE II score ≥ 18, SOFA score ≥ 10, invasive procedures, hypoproteinemia, septic shock, alcohol abuse, and drug abuse[28-30], which were basically consistent with the conclusions of this study. This result may be attributed to AB biofilm formation, which enables bacteria to survive in the hospital environment (especially on the surfaces of medical equipment) for extended periods [31]. The occurrence of MDRAB pneumonia is often due to invasive procedures or certain surgeries that disrupt the patient's skin and mucosal barriers, thereby creating a pathway for bacterial invasion [32]. In addition, prolonged hospitalization, ICU admission, and hemodialysis showed that the patients were in a serious condition and their immune function was impaired. These patients further deteriorated after infection with MDRAB, and they had higher APACHE II and SOFA scores. Septic shock and drug abuse are the most common risk factors for MDRAB infection. ICU patients are mostly in a critic al state and generally have immunosuppression. If they are combined with septic shock and have received multiple drug treatments, their susceptibility to MDRAB will be further increased. It is worth noting that interactions among these factors may attenuate their independent effects. In addition, other studies have reported additional relevant factors, but are limited by specific conditions; this study does not cover all of them.

The mortality rate of infection caused by MDRAB can be as high as 30% -75%, posing a serious threat to human health [33]. Previous studies have explored a variety of factors as potential predictors of mortality risk in patients with MDRAB pneumonia: such as length of ICU stay before AB culture, recent surgical history, immunocompromised status, tracheal intubation, fiberoptic bronchoscopy, SOFA score, APACHE II score ≥ 18 points, and the number of invasive interventions (≥ 3 types)[34-37], which is consistent with the results of this study. Although tigecycline can reach a high concentration in

multiple tissues (such as the concentration in lung tissue can reach twice that in serum)[38], this study divided 168 patients with MDRAB into a non-tigecycline group and a tigecycline group according to the treatment method, and found that the 30-day mortality of the former was lower than that of the latter. This result is consistent with many reports that tigecycline-containing treatment regimens are associated with higher AB infection mortality [39-41].

The limited choice of therapeutic drugs for patients with MDRAB pneumonia not only increases the difficulty of clinical treatment but also increases the risk of drug-related side effects. In the treatment regimen containing tigecycline, the incidence of gastrointestinal adverse events such as nausea, vomiting, and diarrhea was significantly higher than that of the non-tigecycline regimen, which was consistent with the existing research results [42]. In contrast, the incidence of allergic reactions in the tigecycline treatment group was lower. In addition, there was no significant difference in adverse reactions such as ototoxicity, liver injury, and kidney injury between the two groups. The lower allergenicity of tigecycline may make it a better choice for patients allergic to other antibiotics. These findings suggest that tigecycline should be used with caution, and that alternative regimens may yield safer and more effective outcomes.

This study explored risk factors for drug resistance, 30-day all-cause mortality, and associated clinical treatment strategies in patients with MDRAB pneumonia. It provides a new clinical basis for treatment strategies and mortality risk factors in patients with MDRAB pneumonia and has important implications for optimizing clinical prevention and treatment. It is suggested that clinicians should be cautious when prescribing tigecycline for MDRAB pneumonia, as its use may be associated with increased mortality. However, this study also has some limitations. First, because the cases in this study are all from a single center, there are limitations to the representativeness of the sample. Therefore, the extrapolation of the research conclusions may be limited and should not be directly extended to other regions or populations. Furthermore, the study was a retrospective design. Although it can provide clinical reference to a certain extent, there are still unavoidable information biases and confounding factors, which may affect the accuracy of the results. Finally, a limitation of this study is its small sample size, which may limit statistical power and increase uncertainty in some results. Therefore, the current conclusions should be treated as a preliminary reference only. It is recommended that more prospective, multicenter, large-sample studies be conducted in the future, particularly covering patient groups across different institutions and geographical regions, to further verify the risk factors for MDRAB pneumonia and the effectiveness and safety of treatment strategies. Provide a higher level of evidence-based medical evidence for MDRAB pneumonia, so as to optimize clinical practice and improve the prognosis of patients. At the same time, it is necessary to strengthen research on the molecular epidemiology and mechanisms of drug resistance in MDRAB infection, thereby laying a scientific foundation for the development of new antibacterial drugs and precise treatment strategies. Through various efforts, a systematic and efficient comprehensive prevention and control system was ultimately established to address this serious public health challenge.

In summary, the occurrence of MDRAB pneumonia was closely related to the history of ICU hospitalization, APACHE II score ≥ 18, invasive operation, septic shock, and drug abuse. After the diagnosis of MDRAB pneumonia, Severe and tigecycline treatment were significantly associated with patient mortality. Patients with MDRAB pneumonia should be cautious about using tigecycline when receiving treatment. Although there are some limitations, the results of this study still provide an important reference

for the clinical prevention and treatment of MDRAB pneumonia. In the future, more rigorous methodological research is needed to systematically explore treatment strategies and associated mortality risk factors in MDRAB pneumonia, to further improve clinical prevention and treatment.

Acknowledgment

None

Funding

None

Consent to publish

The manuscript has not been published before and is not under review by any other journal. All authors have approved the content of the paper.

Consent to participate

We have effectively protected the legal rights and interests of all participants by carrying out a thorough informed consent process.

Ethic approval

The study protocol was approved by the research ethics committee of The Third People's Hospital of Yichang City and strictly adhered to the ethical guidelines and norms established by the 'Helsinki Declaration' (latest revision).

Data availability statement

The data supporting the findings of this study are available from the corresponding author upon request.

ORCID numbers of authors

- Lili Liu (LL): 0009-0005-0283-3094
- Wen Lu (WL): 0009-0000-1845-3962
- Gege Fang (GF): 0009-0004-5947-6131
- Wei Zhang (WZ): 0009-0003-4892-0973

Author contribution

LL, WL: Conceived and designed the research, and analyzed data. Drafted and critically revised the manuscript for important intellectual content. GF, WZ: Contributed to data acquisition, analysis, and interpretation. Provided substantial intellectual input during manuscript drafting and revision. GF, WZ: Contributed to the study's conception and design. Played a vital role in data interpretation and manuscript writing. All authors have reviewed and approved the final version of the manuscript.

Conflicts of interest

The authors state that they have no financial conflicts of interest.

REFERENCES

1. **Gauba A, Rahman KM.** Evaluation of Antibiotic Resistance Mechanisms in Gram-Negative Bacteria. Antibiotics (Basel). 2023;12(11):1590. *https://doi.org/10.3390/antibiotics12111590.*
2. **Ibrahim S, Al-Saryi N, Al-Kadmy IMS, Aziz SN**. Multidrug-resistant Acinetobacter baumannii as an emerging concern in hospitals. Mol Biol Rep. 2021;48(10):6987-6998. *https://doi.org/10.1007/s11033-021-06690-6.*
3. **Li Y, Xiao S, Huang G.** Acinetobacter baumannii Bacteriophage: Progress in Isolation, Genome Sequencing, Preclinical Research, and Clinical Application. Curr Microbiol. 2023;80(6):199. *https://doi.org/10.1007/s00284-023-03295-z.*
4. **Tiku V.** Acinetobacter baumannii: Virulence Strategies and Host Defense Mechanisms. DNA Cell Biol. 2022;41(1):43-48. *https://doi.org/10.1089/dna.2021.0588.*

5. **Singh S, Singh S, Trivedi M, Dwivedi M.** An insight into MDR Acinetobacter baumannii infection and its pathogenesis: Potential therapeutic targets and challenges. Microb Pathog. 2024;192:106674. *https://doi.org/10.1016/j.micpath.2024.106674.*
6. **Mea HJ, Yong PVC, Wong EH.** An overview of Acinetobacter baumannii pathogenesis: Motility, adherence and biofilm formation. Microbiol Res. 2021;247:126722. h*ttps://doi.org/10.1016/j.micres.2021.126722.*
7. **Shi J, Cheng J, Liu S, Zhu Y, Zhu M.** Acinetobacter baumannii: an evolving and cunning opponent. Front Microbiol. 2024;15:1332108. *https://doi.org/10.3389/fmicb.2024.1332108.*
8. **Luo Q, Chang M, Lu P, Guo Q, Jiang X, Xiao T, et al.** Genomic epidemiology and phylodynamics of *Acinetobacter baumannii* bloodstream isolates in China. Nat Commun. 2025, 16: 3536. *https://doi.org/10.1038/s41467-025-58772-9.*
9. **Gautam D, Dolma KG, Khandelwal B, Mitsuwan W, Mahboob T, Pereira ML, et al.** *Acinetobacter baumannii*: An overview of emerging multidrug-resistant pathogen. Med J Malaysia. 2022;77(3):357-370. PMID: 35638493.
10. **Marino A, Augello E, Stracquadanio S, Bellanca CM, Cosentino F, Spampinato S, et al.** Unveiling the Secrets of *Acinetobacter baumannii*: Resistance, Current Treatments, and Future Innovations. Int J Mol Sci. 2024;25(13):6814. *https://doi.org/10.3390/ijms25136814.*
11. **Jo J, Ko KS.** Tigecycline Heteroresistance and Resistance Mechanism in Clinical Isolates of Acinetobacter baumannii. Microbiol Spectr. 2021;9(2):e0101021. *https://doi.org/10.1128/Spectrum.01010-21.*
12. **Sun C, Yu Y, Hua X.** Resistance mechanisms of tigecycline in Acinetobacter baumannii. Front Cell Infect Microbiol. 2023;13:1141490. *https://doi.org/10.3389/fcimb.2023.1141490.*
13. **Bartal C, Rolston KVI, Nesher L.** Carbapenem-resistant *Acinetobacter baumannii*: Colonization, Infection and Current Treatment Options. Infect Dis Ther. 2022;11(2):683-694. *https://doi.org/10.1007/s40121-022-00597-w.*
14. **Deng Y, Chen L, Yue M, Huang X, Yang Y, Yu H.** Sulbactam combined with tigecycline improves outcomes in patients with severe multidrug-resistant Acinetobacter baumannii pneumonia. BMC Infect Dis. 2022;22(1):795. *https://doi.org/10.1186/s12879-022-07778-5.*
15. **Al-Tamimi M, Albalawi H, Alkhawaldeh M, Alazzam A, Ramadan H, Altalalwah M, et al.** Multidrug-Resistant Acinetobacter baumannii in Jordan. Microorganisms. 2022;10(5):849. *https://doi.org/10.3390/microorganisms10050849.*
16. **Wen B, Zhang G, Zhan C, Chen C, Yi H.** The 2024 revision of the Declaration of Helsinki: a modern ethical framework for medical research. Postgrad Med J. 2025;101(1194):371-382. *https://doi.org/10.1093/postmj/qgae181.*
17. **Humphries R, Bobenchik AM, Hindler JA, Schuetz AN.** Overview of Changes to the Clinical and Laboratory Standards Institute Performance Standards for Antimicrobial Susceptibility Testing, M100, 31st Edition. J Clin Microbiol. 2021;59(12):e0021321. *https://doi.org/10.1128/JCM.00213-21.*
18. **Huang H, Chen B, Liu G, Ran J, Lian X, Huang X, et al.** A multi-center study on the risk factors of infection caused by multidrug resistant Acinetobacter baumannii. BMC Infect Dis. 2018;18(1):11. *https://doi.org/10.1186/s12879-017-2932-5.*
19. **Huang SS, Qiu JY, Li SP, Ma YQ, He J, Han LN, et al.** Microbial signatures predictive of short-term prognosis in severe pneumonia. Front Cell Infect Microbiol. 2024;14:1397717. *https://doi.org/10.3389/fcimb.2024.1397717.*
20. **Müller C, Reuter S, Wille J, Xanthopoulou K, Stefanik D, Grundmann H, et al.** A global view on carbapenem-resistant Acinetobacter baumannii. mBio. 2023;14(6):e0226023. *https://doi.org/10.1128/mbio.02260-23.*
21. **Jo J, Kwon KT, Ko KS.** Multiple heteroresistance to tigecycline and colistin in Acinetobacter baumannii isolates and its implica-

tions for combined antibiotic treatment. J Biomed Sci. 2023;30(1):37. *https://doi.org/10.1186/s12929-023-009 14-6.*

22. **Shein AMS, Hongsing P, Smith OK, Phattharapornjaroen P, Miyanaga K, Cui L, et al.** Current and novel therapies for management of Acinetobacter baumannii-associated pneumonia. Crit Rev Microbiol. 2025;51(3):441-462. https*://doi.org/10.1080/1040841X.2024.2369948.*
23. **Sato Y, Hatayama N, Ubagai T, Tansho-Nagakawa S, Ono Y, Yoshino Y.** Tigecycline Suppresses the Virulence Factors of Multidrug-Resistant Acinetobacter baumannii Allowing Human Neutrophils to Act. Infect Drug Resist. 2022;15:3357-3368. *https://doi.org/10.2147/IDR.S368890.*
24. **Kyriakidis I, Vasileiou E, Pana ZD, Tragiannidis A.** *Acinetobacter baumannii* Antibiotic Resistance Mechanisms. Pathogens. 2021;10(3):373. *https://doi.org/10.3390/pathogens10030373.*
25. **Tu Q, Pu M, Li Y, Wang Y, Li M, Song L, et al.** *Acinetobacter Baumannii* Phages: Past, Present and Future. Viruses. 2023; 15(3):673. *https://doi.org/10.3390/v15030673.*
26. **AlAmri AM, AlQurayan AM, Sebastian T, AlNimr AM.** Molecular Surveillance of Multidrug-Resistant Acinetobacter baumannii. Curr Microbiol. 2020;77(3):335-342. *https://doi.org/10.1007/s00284-019-01836-z.*
27. **Vrancianu CO, Gheorghe I, Czobor IB, Chifiriuc MC.** Antibiotic Resistance Profiles, Molecular Mechanisms and Innovative Treatment Strategies of *Acinetobacter baumannii*. Microorganisms. 2020; 8(6):935. *https://doi.org/10.3390/microorganisms8060935.*
28. **Reina R, León-Moya C, Garnacho-Montero J.** Treatment of *Acinetobacter baumannii* severe infections. Med Intensiva (Engl Ed). 2022;46(12):700-710. *https://doi.org/10.1016/j.medine.2022.08.007.*
29. **Diao H, Lu G, Zhang Y, Wang Z, Liu X, Ma Q, et al.** Risk factors for multidrug-resistant and extensively drug-resistant Acinetobacter baumannii infection of patients admitted in intensive care unit: a systematic review and meta-analysis. J Hosp Infect. 2024;149:77-87. *https://doi.org/10.1016/j.jhin.2024.04.013.*
30. **Gharaibeh MH, Abandeh YM, Elnasser ZA, Lafi SQ, Obeidat HM, Khanfar MA**. Multidrug Resistant Acinetobacter baumannii: Phenotypic and Genotypic Resistance Profiles and the Associated Risk Factors in Teaching Hospital in Jordan. J Infect Public Health. 2024;17(4):543-550. *https://doi.org/10.1016/j.jiph.2024.01.018.*
31. **Roy S, Chowdhury G, Mukhopadhyay AK, Dutta S, Basu S.** Convergence of Biofilm Formation and Antibiotic Resistance in Acinetobacter baumannii Infection. Front Med (Lausanne). 2022;9:793615. *https://doi.org/10.3389/fmed.2022.793615.*
32. **Lan M, Dongmei K, Guodong S, Haifeng Y, Guofeng C, Mengting C, et al.** Risk factors for bacteremic pneumonia and mortality (28-day mortality) in patients with *Acinetobacter baumannii* bacteremia. BMC Infect Dis. 2024;24(1):448. *https://doi.org/10.1186/s12879-024-09335-8.*
33. **Sharma R, Lakhanpal D.** *Acinetobacter baumannii:* A comprehensive review of global epidemiology, clinical implications, host interactions, mechanisms of antimicrobial resistance and mitigation strategies. Microb Pathog. 2025;204:107605. *https://doi.org/10.1016/j.micpath.2025.107605.*
34. **Zhou H, Yao Y, Zhu B, Ren D, Yang Q, Fu Y, et al.** Risk factors for acquisition and mortality of multidrug-resistant *Acinetobacter baumannii* bacteremia: A retrospective study from a Chinese hospital. Medicine (Baltimore). 2019;98(13):e14937. *https://doi.org/10.1097/MD.0000000000014937.*
35. **Černiauskienė K, Vitkauskienė A.** Multidrug-Resistant Acinetobacter baumannii: Risk Factors for Mortality in a Tertiary Care Teaching Hospital. Trop Med Infect Dis. 2025;10(1):15. *https://doi.org/10.3390/tropicalmed10010015.*
36. **Huang C, Gao Y, Lin H, Fan Q, Chen L, Feng Y.** Prognostic Factors That Affect Mortality Patients with Acinetobacter baumannii Bloodstream Infection. Infect Drug Resist. 2024;17:3825-3837. *https://doi.org/10.2147/IDR.S475073.*

37. Yu K, Zeng W, Xu Y, Liao W, Xu W, Zhou T, et al. Bloodstream infections caused by ST2 *Acinetobacter baumannii:* risk factors, antibiotic regimens, and virulence over 6 years period in China. Antimicrob Resist Infect Control. 2021;10(1):16. *https://doi.org/10.1186/s13756-020-00876-6.*

38. Zhang S, Di L, Qi Y, Qian X, Wang S. Treatment of infections caused by carbapenem-resistant *Acinetobacter baumannii*. Front Cell Infect Microbiol. 2024; 14:1395260. *https://doi.org/10.3389/fcimb.2024.1395260.*

39. Niu T, Xiao T, Guo L, Yu W, Chen Y, Zheng B, et al. Retrospective comparative analysis of risk factors and outcomes in patients with carbapenem-resistant *Acinetobacter baumannii* bloodstream infections: cefoperazone-sulbactam associated with resistance and tigecycline increased the mortality. Infect Drug Resist. 2018;11:2021-2030. *https://doi.org/10.2147/IDR.S169432.*

40. Gu S, Xiong J, Peng S, Hu L, Zhu H, Xiao Y, et al. Assessment of Effective Antimicrobial Regimens and Mortality-Related Risk Factors for Bloodstream Infections Caused by Carbapenem-Resistant Acinetobacter baumannii. Infect Drug Resist. 2023;16:2589-2600. *https://doi.org/10.2147/IDR.S408927.*

41. Mei H, Yang T, Wang J, Wang R, Cai Y. Efficacy and safety of tigecycline in treatment of pneumonia caused by MDR Acinetobacter baumannii: a systematic review and meta-analysis. J Antimicrob Chemother. 2019;74(12):3423-3431. *https://doi.org/10.1093/jac/dkz337.*

42. Yaghoubi S, Zekiy AO, Krutova M, Gholami M, Kouhsari E, Sholeh M, et al. Tigecycline antibacterial activity, clinical effectiveness, and mechanisms and epidemiology of resistance: narrative review. Eur J Clin Microbiol Infect Dis. 2022;41(7):1003-1022. *https://doi.org/ 10.1007/s10096-020-04121-1.*

Invest Clin 67(1): 125 - 138, 2026 https://doi.org/10.54817/IC.v67n1a09

Ameliorative potential of astaxanthin in isoproterenol-induced heart failure in rats via the regulation of the renin-angiotensin system.

Liang Chang and Furong Qiao

Department of Cardiology, Xi'an Daxing Hospital, Xi'an, Shaanxi Province, China.

Keywords: Angiotensin-Converting Enzyme;Arterial Pressure; Endomyocardial Fibrosis; Lactate Dehydrogenase; Renin

Abstract. Heart failure (HF) is a condition in which the heart cannot pump blood effectively to the body. Isoproterenol (ISO) induces HF in rodents by affecting the renin-angiotensin system (RAS). Astaxanthin (AST) is known to have protective effects on the cardiovascular system. However, clear evidence showing that AST improves HF through RAS regulation has not yet been reported. This study aimed to investigate the role of AST in ISO-induced HF in rats. HF was induced by intraperitoneal (i.p.) injection of ISO (5 mg/kg/day) for seven consecutive days. AST (25 and 50 mg/kg), aliskiren (30 mg/kg), ramipril (4 mg/kg), and telmisartan (8 mg/kg) were administered orally for 21 days, starting from the last dose of ISO (day 8). Changes in systolic and diastolic blood pressure and heart rate associated with HF were measured on days 0, 7, 14, 21, and 28. Additionally, changes in heart-to-body weight ratio, serum creatine kinase-MB (CK-MB), serum angiotensin-converting enzyme (ACE) activity, plasma renin activity (PRA), tissue hydroxyproline, and lactate dehydrogenase (LDH) activity, along with histopathological alterations, were evaluated. The administration of AST and RAS-modulating agents reduced ISO-induced changes in cardiac function and biochemical markers. It also demonstrated cardioprotective effects. Therefore, AST may be useful for treating cardiotoxic HF due to its RAS-regulatory actions. However, further studies are needed to confirm this therapeutic potential across different HF models and animal species.

Corresponding author. Furong Qiao. Department of Cardiology, Xi'an Daxing Hospital, Xi'an, Shaanxi Province, 710003, China. Telephone: +86 17719654188. Email: furong644759573@sina.com

Potencial mejorador de la astaxantina en la insuficiencia cardíaca inducida por isoproterenol en ratas a través de la regulación del sistema renina-angiotensina.

Invest Clin 2026; 67 (1): 125 – 138

Palabras clave: Enzima Convertidora de Angiotensina; Presión Arterial; Fibrosis Endomiocárdica; Lactato Deshidrogenasa; Renina.

Resumen. La insuficiencia cardíaca (IC) es una alteración de la capacidad funcional del corazón para bombear sangre al organismo. El isoproterenol (ISO) induce IC en roedores mediante la alteración del sistema renina-angiotensina (SRA). Se sabe que la astaxantina (AST) ejerce una acción reguladora sobre el sistema cardiovascular. Sin embargo, aún no se ha descrito evidencia clara de que la AST mejore la IC mediante la regulación del SRA. El presente estudio fue diseñado para investigar el papel de la AST en la IC inducida por ISO en ratas. La IC se indujo mediante administración intraperitoneal (i.p.) de ISO (5 mg/kg/día) durante siete días consecutivos. La AST (25 y 50 mg/kg), aliskiren (30 mg/kg), ramipril (4 mg/kg) y telmisartán (8 mg/kg) se administraron por vía oral durante 21 días consecutivos, desde la última dosis de ISO (día 8). Los cambios asociados a la IC en la presión arterial sistólica y diastólica y en la frecuencia cardíaca se evaluaron en diferentes puntos temporales, es decir, los días 0, 7, 14, 21 y 28. También se evaluaron los cambios en la relación entre el peso corporal y el corazón, la creatinquinasa sérica-MB (CK-MB), la actividad sérica de la enzima convertidora de angiotensina (ECA) y la actividad plasmática de la renina (PRA); y la actividad tisular de la hidroxiprolina y la lactato deshidrogenasa (LDH) junto con los cambios histopatológicos. La administración de agentes moduladores de AST y SRA atenúa los parámetros bioquímicos y funcionales cardíacos inducidos por ISO. También demuestra efectos cardioprotectores. Por lo tanto, la AST puede utilizarse para la IC asociada a cardiotoxinas debido a sus acciones reguladoras del SRA. Sin embargo, se requieren estudios más exhaustivos para demostrar su eficacia terapéutica en diferentes IC y especies animales.

Received: 14-10-2025 Accepted: 21-12-2025

INTRODUCTION

Heart failure (HF) is also known as congestive heart failure (CHF), which indicates impairment of the pumping of blood by the heart. The symptoms of HF are fatigue, shortness of breath, and leg swelling [1]. The global prevalence rate of HF is rising to 24% and affects one person out of four in their lifetime. Furthermore, it is expected to increase by 8.5% among persons aged 65 to 70 years [2]. Isoproterenol (ISO) is widely used to treat bradycardia in patients with arrhythmias. Structurally, it is similar to epinephrine and an agonist of non-selective beta-adrenergic receptors [3]. Experimentally, ISO causes myocardial fibrosis, raises diaphragmatic contractility, and mimics the pathogenesis of cardiomyopathy and human heart failure [4,5] and the mechanism of the effects,

of isoproterenol on diaphragmatic contractility and fatigue in septic peritonitis in vitro. Furthermore, the administration of ISO is known to induce HF by modulating the renin-angiotensin system (RAS) [6–8] changes in circulating and tissue renin-angiotensin system (RAS). Moreover, ISO is known to increase heart rate and systemic arterial blood pressure [9,10]. Even a single dose of ISO also induces type 2 diabetes mellitus-associated myocardial infarctions [11]. Besides, the multiple doses of ISO cause chronic heart failure in mice [12]. A one-week administration of ISO at 5 mg/kg induces changes in hemodynamic parameters in rats by increasing angiotensin II levels and angiotensin-converting enzyme 2 (ACE2) activity [6,13] 5 mg/kg/day, intraperitoneally. The activation of ACE2 may be due to the fact that raising cardiac angiotensin-II peptide concentrations is associated with increased ACE2 expression in normal rats [14]. However, these effects are absent in other conditions and other species [15]. In most cases, ISO does not affect ACE2 expression. An experimental study also demonstrated that ISO increases the cardiac renin-angiotensin system function in a rat model of cardiac hypertrophy [6,16].

Astaxanthin (AST) is a type of keto-carotenoid belonging to the terpene compound group. AST is a metabolite of canthaxanthin and zeaxanthin. It contains hydroxyl and ketone groups, which have key antioxidant properties and act as free radical scavengers and chelators of metal ions [17]. It improves cardiac function and exercise tolerance in HF patients[18]. Additionally, AST provides myocardial protection against steroid-induced cardio-renal dysfunction and related hypertensive complications [19]. Moreover, AST also has modulating effects on the RAS system and enhances vascular function against cardiotoxins [20,21]. However, further research is necessary to fully understand the role of AST in ISO-induced HF and RAS regulation under these conditions. This study examined the effects of specific RAS modulators and AST on cardiovascular dysfunction caused by ISO in rats. Therefore, the impact of AST was evaluated in this research regarding its effects on ISO-induced HF and its possible modulation of the RAS.

METHODS

Animals used

Male Sprague Dawley rats weighing 180–200 g (12–14 months old) were used in this study. The animals had unlimited access to water and a standard laboratory diet. They were housed in the central animal facility, which maintained a 12-hour light:12-hour dark cycle. This experimental protocol was approved by the institutional animal ethics committee (IAEC approval number: IAEC/05/2025). The IAEC guidelines were followed during the trials.

Experimental design

The experimental design consisted of seven groups of eight rats each.

Group I: Animals served as naive controls and did not receive any drug administration.

Animals served as a negative control in Group II. For seven consecutive days, this group of animals received intraperitoneal (i.p.) treatment of ISO (5 mg/kg/day) to induce heart failure (HF). Approximately 0.05% ascorbic acid in 0.9% sodium chloride (NaCl) was used to prepare the ISO solution.

Groups III and IV: Animals served as test subjects for the drug treatments. These groups of animals were administered AST (25 and 50 mg/kg) orally for 21 consecutive days after the last dose of ISO.

Group V-VII: Animals were used as reference drug treatments. These groups of animals received oral administration of specific drugs: a direct renin inhibitor, aliskiren (30 mg/kg); an angiotensin-converting enzyme (ACE) inhibitor, ramipril (4 mg/kg); and an angiotensin II receptor antagonist, telmisartan (8 mg/kg), for 21 consecutive days following the last dose of ISO administration.

At 0, 7, 14, 21, and 28 days, HF-related changes in heart rate (HR), diastolic blood

pressure (DAP), and systolic blood pressure (SAP) were recorded. Blood samples were collected on the twenty-eighth day for biochemical analysis of plasma renin activity (PRA), ACE activity, and serum creatine kinase isoenzyme-MB (CK-MB). Afterwards, all animals were weighed and euthanized with diethyl ether. To assess the heart-to-body weight ratio, the heart was removed and weighed. Immediately, the heart was perfused prior to tissue homogenization, and the cardiac chambers were opened to remove residual blood. Then, cardiac tissue was homogenized in ice-cold phosphate buffer (pH 7.4). Centrifugation at 769 x g was performed to obtain a clear supernatant, which was used to measure lactate dehydrogenase (LDH) activity and hydroxyproline content, both of which are tissue biomarkers. Additionally, ISO-induced histopathological changes were examined using eosin-hematoxylin staining.

Assessment of Isoproterenol-induced functional changes in the heart

The ISO induced the HF with alteration of functional changes of the heart, such as blood pressure and heart rate, using the non-invasive tail-cuff method described by Wang et al. [22]. Briefly, the animal was placed in appropriate holders based on its body size (CODA-HT8, CODA high-throughput noninvasive blood pressure system, Kent Scientific Corporation, Torrington, United States). The tail was positioned into the rear side of the tail port with the screw of the rear hatch without pinching it. The animals were given five minutes to acclimate to the holder. Frequent contact with the animals was avoided to reduce stress and irritation. Without applying any force, the tail occlusion cuff was placed at the base of the tail. The distance between the tail occlusion cuff and the volume pressure recording (VPR) sensor cuff was 2 mm. Body temperature was measured with an infrared thermometer, and it was maintained between 34 and 35°C using a rodent heating pad. Data were recorded as averages of multiple measurements using CODA Data Acquisition Software.

Assessment of Isoproterenol-induced changes in serum and plasma biomarkers

Serum biomarkers, including CK-MB, ACE activity, and PRA, were measured in rat samples. Serum CK-MB was assessed using the rat CK-MB ELISA kit (NBP2-75313, Novus Biologicals, Kuala Lumpur, Malaysia) according to the manufacturer's protocol. Briefly, 100 μL of serum and 100 μL of biotinylated detection antibody working solution were combined in a well plate and incubated at 37 °C for 90 minutes; the plate was then washed with 350 μL of wash buffer. Subsequently, 100 μL of the horseradish peroxidase conjugate working solution was added, and the mixture was incubated at 37 °C for 30 minutes. Importantly, 90 μL of substrate reagent was added after the plate had been washed. After 15 minutes of incubation at 37 °C, 50 μL of stop solution was added to halt the reaction. A microplate reader (Bio-Tek Microplate Instruments, Penang, Malaysia), operating at 450 nanometers, was used to measure the chromogen changes. The reference standard curve was prepared using standards from 31.25 to 2000 pg/mL for CK-MB activity.

Serum ACE levels were measured using the rat ACE ELISA kit (CSB-E04490r; Cusabio Technology LLC, Houston, United States) following the manufacturer's instructions. Briefly, microplate wells were filled with 100 μL of serum and incubated at 37°C for two hours. Afterward, 100 μL of biotinylated detection antibody working solution was added, and the plate was incubated again at 37°C for 60 minutes. The plate was washed with 200 μL of wash buffer solution. Next, 100 μL of horseradish peroxidase conjugate working solution was added, followed by incubation at 37°C for 60 minutes. After washing, 90 μL of 3,3′,5,5′-tetramethylbenzidine (TMB) substrate reagent was added. The reaction was stopped after 15 to 30 minutes of incubation at 37°C in the dark by

adding 50 μL of stop solution. The change in chromogen was measured at 450 nm using a microplate reader (Bio-Tek Microplate Instruments, Penang, Malaysia). A standard curve was prepared with standard concentrations ranging from 31.25 to 2000 ng/mL of ACE activity.

Plasma renin activity (PRA) was measured using the rat PRA ELISA kit (IB59131; Immuno-Biological Laboratories Inc., Minneapolis, United States) following the manufacturer's instructions. Briefly, 500 μL of plasma was added to the microplate wells and incubated for 2 hours at 37°C. Then, 5 μL of phenylmethylsulfonyl fluoride (PMSF) solution was added and vortexed, followed by the addition of 50 μL of the generation buffer. Next, 60 μL of the subtract solution was combined with 250 μL of the sample and transferred to another well plate. After incubating the plate at 37°C for 15 to 30 minutes, 50 μL of stop solution was added to halt the reaction. Changes in chromogen were measured using a microplate reader (Bio-Tek Microplate Instruments, Penang, Malaysia) at 450 nm. The reference standard curve was prepared with standards ranging from 0.2 to 60 ng/mL of PRA activity.

Assessment of Isoproterenol-induced changes in tissue biomarkers

Cardiac tissue biomarkers, such as hydroxyproline content and LDH, were measured. Hydroxyproline, an amino acid, results from the hydrolysis of connective tissue proteins like collagen; therefore, it plays a key role in stabilizing collagen. The tissue hydroxyproline content was determined following the method of Stegemann and Stalder[23], with slight modifications from Cissell et al.[24]. Briefly, about 30 μL of tissue sample was diluted to 100 μL with papain solution to extract maximum collagen, then centrifuged at 1968 G for 10 minutes. Next, 30 μL of this aliquot was mixed with 100 μL of 4 N sodium hydroxide (NaOH), and the mixture was incubated at 120°C for 15 minutes. After cooling to room temperature, 100 μL of 4 N hydrochloric acid (HCl) was added to neutralize the alkaline solution. A mixture containing 0.625 mL of chloramine-T (0.05 M in 74% v/v distilled water), 2-propanolol (26% v/v), NaOH (0.629 M), citric acid (0.140 M), sodium acetate (0.453 M), and glacial acetic acid (0.112 M) was used to oxidize hydroxyproline into pyrrole-2-carboxylate. This mixture was incubated at room temperature for 20 minutes. Each sample was then vortexed immediately after adding 0.625 mL of p-dimethylaminobenzaldehyde (DMAB; 1 M, 15% w/v in 2-propanol plus concentrated acid; Ehrlich's solution). After another 20-minute incubation at 65°C, the samples were cooled to room temperature. The resulting red chromophore was measured with a spectrophotometer (DU 640B, Beckman Coulter Inc., Brea, CA, USA) at 558 nm. A standard curve was prepared using 0.5, 0.75, 1, and 1.5 μg of pure hydroxyproline per milliliter. The hydroxyproline concentration was multiplied by a factor of 8.2 to estimate collagen content. Results were expressed as micrograms of hydroxyproline per milligram of tissue protein.

Lactate dehydrogenase (LDH, EC 1.1.1.27) is a major oxidoreductase enzyme involved in the anaerobic metabolism pathway. When β-nicotinamide adenine dinucleotide (NAD+) is reduced to nicotinamide-adenine dinucleotide hydrogen (NADH), lactate reversibly converts to pyruvate. The tissue LDH content was assessed as described in the method of Singh et al. [25], with a slight modification from Dewi et al. [26]. Briefly, about 50 μL of tris-(hydroxymethyl)-aminomethane hydrochloride (200 mM, pH 8), 50 μL of lithium lactate (50 mM; 49 mg lithium lactate in 2.5 mL water), and 50 μL of phenazine methosulfate (PMS), iodonitrotetrazolium chloride (INT), and NAD solutions (PIN) mixture were combined with 50 μL of sample (adding all reagents first, then the aliquot). The PIN mixture was prepared by mixing 100 μL of PMS (0.9 mg in 100 μL of water), 100 μL of INT (3.3

mg in 100 μL of DMSO), and 2.3 mL of NAD (8.6 mg NAD in 2.3 mL of water). The microplate was incubated at room temperature for 5 minutes. Changes in chromogen were measured using a microplate reader (Bio-Tek Microplate Instruments, Penang, Malaysia) at 490 nm via the endpoint assay method. The standard curve was prepared using 50 μL of standards at 0, 2.5, 5, 7.5, 10, and 12.5 nmoles of NADH. LDH activity was calculated using the following equation:

$$LDH\ Activity\ (mU/mL) = \frac{\Delta A_{Final} - \Delta A_{Initial}\ (B)}{Reaction\ Time\ x\ V}\ x\ DF$$

In this case, B represents the amount of NADH produced (nmole). The sample volume (mL) injected into the well is represented by V, the sample dilution factor by DF, and absorbance changes by ΔA. The amount of LDH enzyme that catalyzes the conversion of lactate to pyruvate, producing 1.0 μmole of NADH per minute at 37°C, is defined as 1 unit of LDH activity. The LDH activity results are expressed as units per gram of protein (U/g protein).

Estimation of tissue total proteins

The total tissue proteins were estimated using the method described by Lowry et al.[27]. The results were expressed as milligrams of total protein per gram of tissue.

Evaluation of histopathological changes

The ISO-induced cardiac histopathological changes were evaluated using eosin-hematoxylin techniques, as described by Grimm [7], with minor modifications by Nikam et al. [28]. Briefly, tissue was fixed in 10% formalin and sectioned into 4 μm transverse slices. Cardiac tissue alterations were observed, and images were captured using an Olympus EP50 microscope camera (Olympus Corporation, Tokyo, Japan). Microscopic analyses were performed with a 400x light microscope, including a 35 μm scale bar.

Statistical analysis

All of the data were represented as mean ± standard deviations (SD). Data on systolic and diastolic blood pressure and heart rate were examined using a two-way analysis of variance (ANOVA) with a Bonferroni post hoc test. Data for CK-MB, ACE & PRA activities, hydroxyproline content, and LDH activity levels were examined using one-way ANOVA and Tukey's Multiple Range tests in GraphPad Prism version 5.0 software. A probability (p) value < 0.05 was judged statistically significant.

RESULTS

Effect of astaxanthin on isoproterenol -induced cardiac functional changes

Administration of ISO (5 mg/kg/day) for seven consecutive days in rats caused a significant ($p<0.05$) decrease in SAP and DAP and a significant increase in HR compared to the normal group. This suggests that ISO may induce potential HF through strong, nonselective β-adrenergic (β1) receptor agonist activity, which enhances inotropic and lusitropic effects in cardiac muscle. Oral administration of AST (25 and 50 mg/kg for 21 consecutive days) alleviates ISO-induced cardiac functional changes in a dose-dependent manner compared to the ISO group. This effect is similar to that seen with aliskiren (30 mg/kg), ramipril (4 mg/kg), and telmisartan (8 mg/kg) in the 21-day treatment groups. The impact of AST on ISO-induced changes in cardiac function, such as SAP, DAP, and HR, is shown in Fig. 1.

Effect of astaxanthin on isoproterenol -induced changes in serum and plasma biomarkers

Administering ISO (5 mg/kg/day) to rats for seven days caused significant ($p<0.05$) increases in CK-MB, ACE, and PRA levels compared to the control group. ISO may induce heart failure by promoting cardiac muscle injury and degeneration,

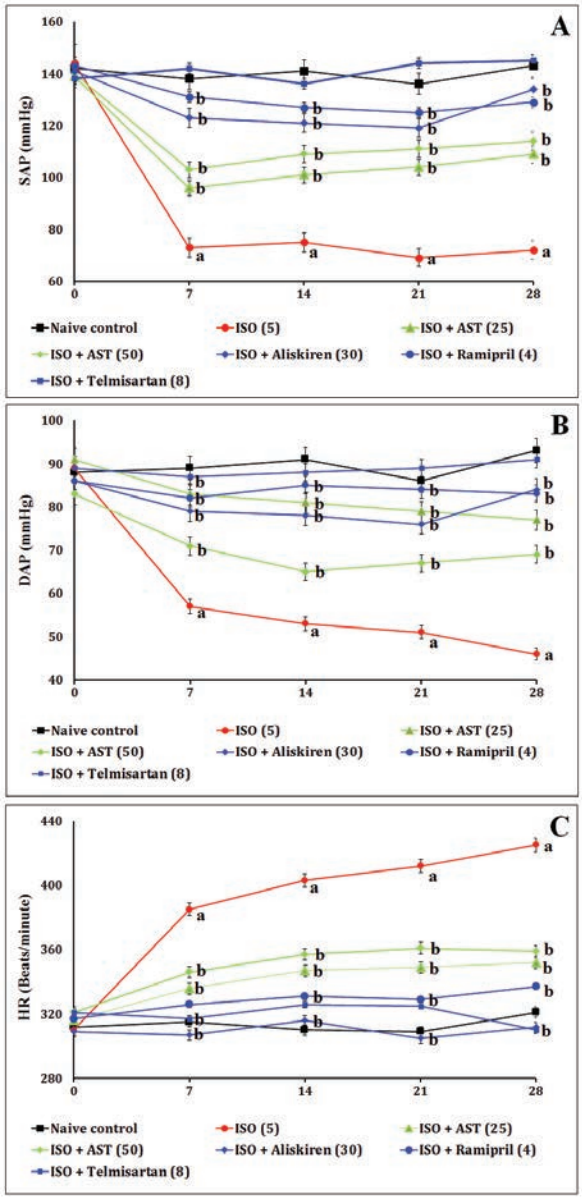

Fig. 1. Effect of AST on ISO-induced cardiac functional changes. Fig. 1A shows changes in SAP; Fig. 1B shows changes in DAP; and Fig. 1C shows changes in heart rate. Values in parentheses indicate the dose in mg/kg. Results are presented as mean ± standard deviation (SD), with n = 8 rats per group, analyzed using a two-way ANOVA with Bonferroni post hoc test. *p<0.05 vs. control group; #p<0.05 vs. ISO group. Abbreviations: AST, astaxanthin; DAP, diastolic blood pressure; HR, heart rate; ISO, isoproterenol; mmHg, millimeter of mercury (blood pressure units); and SAP, systolic blood pressure.

along with elevated circulating RAS mediators. Oral administration of AST (25 and 50 mg/kg) for 21 days decreased ISO-induced changes in serum and plasma biomarkers in a dose-dependent fashion, compared to the ISO group. This effect was comparable to results seen in groups treated for 21 days with aliskiren (30 mg/kg), ramipril (4 mg/kg), and telmisartan (8 mg/kg). Table 1 illustrates how AST influences ISO-induced changes in serum and plasma biomarkers, including CK-MB, ACE, and PRA levels.

Effect of astaxanthin on isoproterenol -induced changes in heart and body weight ratio

Administration of ISO (5 mg/kg/day) for 7 days in rats resulted in a significant ($p<0.05$) increase in the heart-to-body weight ratio compared to the control group. This indicates that ISO may induce potential heart failure (HF) through degeneration of cardiac muscle. Oral administration of AST (25 and 50 mg/kg) for 21 days reduced the ISO-induced changes in the heart-to-body weight ratio in a dose-dependent manner compared to the ISO group. The effect was similar to that observed in the 21-day treatment groups with aliskiren (30 mg/kg), ramipril (4 mg/kg), and telmisartan (8 mg/kg). The impact of AST on the ISO-induced heart and body weight ratio is summarized in Fig. 2.

Effect of astaxanthin on isoproterenol -induced changes in tissue biomarkers

Administering ISO (5 mg/kg/day) for 7 days to rats caused significant ($p<0.05$) increases in hydroxyproline and LDH activity levels compared to the control group. This suggests that ISO may induce potential HF by affecting diastolic function, myocardial structure, muscle mass, and energy metabolism. Oral treatment with AST (25 and 50 mg/kg for 21 days) reduces ISO-induced changes in tissue biomarkers in a dose-dependent way, similar to the effects seen in the groups treated for 21 days with aliskiren

Table 1. Effect of astaxanthin on isoproterenol - induced changes in serum and plasma biomarkers.

Groups	CK-MB (pg/mL)	ACE (ng/mL)	PRA (ng/mL)
Naive control	212 ± 13.5	3.22 ± 1.52	10.3 ± 0.9
ISO (5)	456 ± 14.9*	14.72 ± 1.14*	43.4 ± 1.3*
ISO + AST (25)	293 ± 12.7#	7.48 ± 0.93#	17.5 ± 0.8#
ISO + AST (50)	264 ± 8.6#	5.61 ± 1.04#	11.9 ± 1.2#
ISO + Aliskiren (30)	241 ± 13.1#	4.35 ± 1.47#	9.7 ± 0.4#
ISO + Ramipril (4)	227 ± 11.2#	4.39 ± 0.95#	15.4 ± 0.7#
ISO + Telmisartan (8)	217 ± 9.7#	3.45 ± 1.13#	13.7 ± 0.8#

The values in parentheses represent a dose in mg/kg. The results are presented as mean ± SD, with eight rats in each group. *$p<0.05$ vs. control group; #$p<0.05$ vs. ISO group. ACE, angiotensin-converting enzyme; AST, astaxanthin; CK-MB, creatine kinase isoenzyme-MB; ISO, isoproterenol; PRA, plasma renin activity. Groups were analyzed using a one-way ANOVA and Tukey's Multiple Comparisons test.

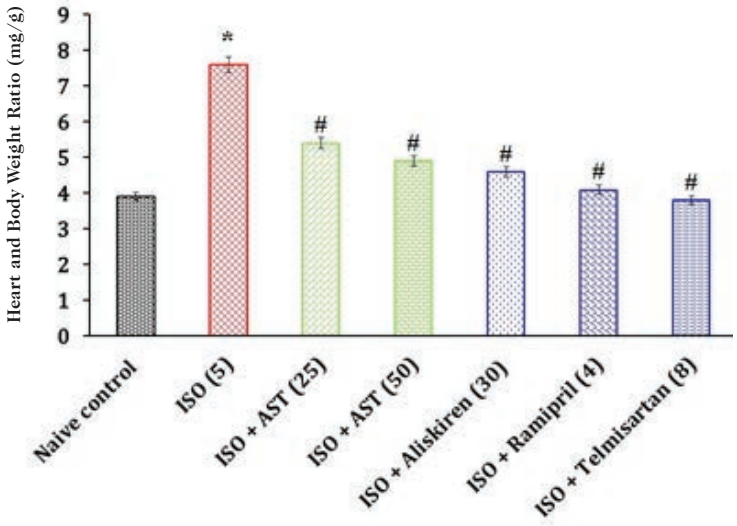

Fig. 2. Effect of AST on ISO-induced changes in the heart and body weight ratio. The values in parentheses indicate a dose in mg/kg. Results are shown as mean ± standard deviation (SD), with n = 8 rats per group, analyzed using a one-way ANOVA and Tukey's Multiple Comparisons test. *p<0.05 compared to the control group; #p<0.05 compared to the ISO group. Abbreviations: AST, astaxanthin; ISO, isoproterenol.

(30 mg/kg), ramipril (4 mg/kg), and telmisartan (8 mg/kg). The impact of AST on ISO-induced alterations in tissue biomarkers, such as hydroxyproline and LDH levels, is illustrated in Table 2.

Effect of astaxanthin on isoproterenol -induced histopathological changes

The histological changes in rat cardiac tissue in naive control animals showed no alterations in rat cardiomyocytes, i.e., branched cardiomyocytes with a central oval vesicular nucleus and mild separation of the connective tissue. In contrast, ISO (5 mg/kg/day; for 7 days) caused potential microscopic changes in cardiac tissue, such as cell destruction, pyknotic and karyolytic nuclei, hemorrhage, edema, and myocyte degeneration. Oral administration of AST (25 and 50 mg/kg) for 21 days alleviated ISO-induced histological alterations in cardiac tissue. These findings were comparable to those seen with reference RAS modulators, i.e., aliskiren (30 mg/kg), ramipril (4 mg/kg), and telmisartan (8 mg/kg) treatment groups. This indicates that AST exhibits cardioprotective effects against ISO-induced myocardial damage and dysfunction (Fig. 3). The changes were observed at 400× magnification (scale bar: 35 μm).

Table 2. Effect of astaxanthin on isoproterenol - induced changes in tissue biomarkers.

Groups	Hydroxyproline (μg/mg of tissue protein)	LDH activity (U/g protein)
Naive control	1.67 ± 0.92	1176.81 ± 12.73
ISO (5)	6.91 ± 1.02*	1492.18 ± 17.62*
ISO + AST (25)	2.29 ± 0.43#	1232.25 ± 9.04#
ISO + AST (50)	2.13 ± 0.67#	1213.94 ± 11.14#
ISO + Aliskiren (30)	2.03 ± 1.05#	1199.07 ± 10.46#
ISO + Ramipril (4)	1.82 ± 0.87#	1204.63 ± 11.06#
ISO + Telmisartan (8)	1.94 ± 1.03#	1191.04 ± 9.83#

The values in parentheses indicate a dose in mg/kg. The results are shown as mean ± SD, with eight rats in each group. *$p<0.05$ versus control group; #$p<0.05$ versus ISO group. AST, astaxanthin; ISO, isoproterenol; and LDH, lactate dehydrogenase.

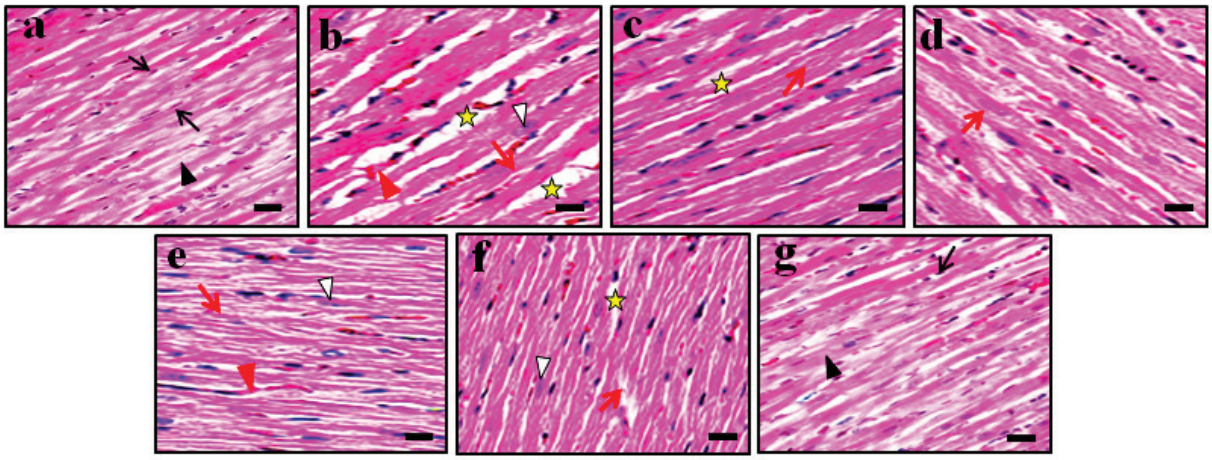

Fig. 3. Effect of AST on ISO-induced histopathological changes in rat cardiac tissue. In each group, two rats were used to evaluate cardiac tissue histopathology. Tissue sections were stained with eosin and hematoxylin. Figures 3a to 3g display histological changes in cardiac tissue from naïve control, ISO (5 mg/kg/day for 7 days), AST (25 mg/kg for 21 days), AST (50 mg/kg for 21 days), aliskiren (30 mg/kg for 21 days), ramipril (4 mg/kg for 21 days), and telmisartan (8 mg/kg for 21 days) groups, respectively. Fig. 3a shows normal cardiac tissue structure. Fig. 3b depicts ISO-associated myocardial damage. Fig. 3c and 3g demonstrate that AST and RAS modulators have cardioprotective effects against ISO toxicity. In this figure, the black arrow points to a normal pyknotic and karyolytic nucleus; the black arrowhead indicates normal cardiac cell structure; the white arrowhead shows cell destruction; the red arrow highlights abnormalities in myocardial fiber arrangement; the red arrowhead signifies hemorrhage and edema; and the yellow star indicates myocyte degeneration. Microscopic examinations were performed at 400× magnification; scale bar, 35 μm.

DISCUSSION

The i.p. administration of ISO (5 mg/kg/day for seven days) in rats demonstrated a significant ($p<0.05$) development of cardiac dysfunction through alterations in hemodynamic parameters, such as reductions in SAP and DAP, along with increases in HR levels and elevated serum CK-MB, ACE, and PRA levels. Furthermore, there was an increase in the heart-to-body weight ratio and in tissue hydroxyproline and LDH activity lev-

els. ISO was also shown to destroy myocytes, resulting in pyknotic cells, karyolytic nuclei, hemorrhage, edema, and myocyte degeneration. These findings indicate that ISO causes potential HF through multiple pathway abnormalities, including free radical-associated cardiac damage, altered energy demands, and RAS pathway disruptions [29,30]. Similar results were observed in ISO-induced HF in rats, which showed changes in the same hemodynamic parameters and myocardial function. These outcomes are consistent with those reported in other studies [31]. Oral AST therapy at 25 and 50 mg/kg for 21 days significantly reduced ISO-related cardiac dysfunctions, biomarker alterations, and histological abnormalities. This effect was comparable to that seen in the RAS modulator treatment groups (aliskiren, ramipril, and telmisartan).

Circulatory and local ACE activity, plasma renin content, and the renin-angiotensin system in the heart and aorta contribute to the development of cardiovascular issues, including myocardial infarction and heart failure [32,33]. Proteomic analysis showed that ISO increases myocardial tissue weight by 55% in hypertrophied rat hearts [34]. Additionally, ISO raises left ventricular tissue weight by 33% and decreases systolic and diastolic blood pressure by 13%. Administering ISO (1, 10, 100, and 500 μg/kg) increases plasma renin activity in a dose-dependent manner [33]. Inhibitors of the renin-angiotensin system are known to improve heart failure in experimental animals [35,36]. RAS modulators, such as spironolactone and captopril, reduce ISO-induced cardiac remodeling in rats[37]. Aliskiren has been shown to lower serum cardiac enzymes like LDH and CK-MB 38, decrease cardiac biomass [39], and also reduce oxidative stress and apoptosis [38,40]. In this study, the AST treatment group exhibited results similar to those of the control group. However, the ACE inhibitor ramipril worsens ISO-induced myocardial dysfunctions by regulating hydroxyproline content in rats[41,42]. The current research demonstrates that AST alleviates ISO-induced cardiac damage by enhancing mitochondrial function and scavenging free radicals in rats [43]. AST is also known to decrease ACE protein expression, mitigate hypertensive conditions [21], prevent ISO-induced loss of cardiac muscle mass [43], and reduce hydroxyproline content [44].

Normally, ISO does not influence ACE2 expression. However, some studies have reported elevated ACE2 levels in Sprague-Dawley rats [6]. Another study indicated that increased cardiac angiotensin-II peptide levels are linked to higher ACE2 expression in normal rats [14]. Nonetheless, these effects are not observed in other conditions or species[15]. Therefore, the impact of ISO on the renin-angiotensin system is complex and varies depending on the specific tissue and animal model. Experimentally, ISO is known to raise plasma angiotensin-II peptide levels, which can lead to left ventricular hypertrophy and worsen heart failure progression[16]. Additionally, angiotensin II directly influences cardiac tissue via the angiotensin II type 2 receptor, resulting in myocardial damage [45]. Furthermore, administering an angiotensin II receptor antagonist, such as telmisartan, can reduce ISO-induced cardiac dysfunction[46]. Similar findings are observed in this study: telmisartan (8 mg/kg) and AST administration normalize elevated blood pressure and modify biomarker levels, including serum CK-MB, ACE, PRA, hydroxyproline, and LDH activity. Moreover, AST has been shown to lower blood pressure in spontaneously hypertensive rats [47] by inhibiting ACE activity and regulating the RAS [48]. Additionally, AST supplementation has demonstrated the ability to decrease blood pressure in humans by suppressing the RAS [49]. Our study also indicates that AST improves ISO-induced cardiac dysfunction and blood pressure control through RAS regulatory mechanisms.

The current study revealed that oral treatment with AST reduces ISO-induced cardiac dysfunction by regulating SAP and DAP, decreasing elevated HR, CK-MB, ACE,

and PRA levels, and lowering the heart-to-body weight ratio, tissue hydroxyproline, and LDH activity levels. Therefore, AST provides cardioprotection against ISO-induced toxicity by regulating the RAS system. It can potentially be used for various heart failure conditions. However, further research using diverse preclinical animal models and human subjects is necessary.

Acknowledgments

The authors acknowledge the Department of Cardiology at Xi'an Daxing Hospital, Xi'an, Shaanxi Province, 710003, China, for its unconditional support.

Funding

The authors received no financial support for this research.

Conflict of interest

The authors declare no conflicts of interest regarding the present study.

ORCID number of authors

- Furong Qiao (FQ): 0009-0008-7478-1109
- Liang Chang (LC): 0009-0003-2808-3522

Contribution of the authors

LC: performed the experiments, collected data, conceived the study, and drafted the manuscript. FQ: supervised the project, secured funding, and critically revised the intellectual content.

REFERENCES

1. **He X, Huang S, Yu C, Chen Y, Zhu H, Li J, et al.** Mst1/Hippo signaling pathway drives isoproterenol-induced inflammatory heart remodeling. Int J Med Sci. 2024;21(9):1718-1729. *https://doi.org/10.7150/ijms.95850.*
2. **Bozkurt B, Ahmad T, Alexander K, Baker WL, Bosak K, Breathett K, et al.** HF STATS 2024: Heart Failure Epidemiology and Outcomes Statistics an Updated 2024 Report from the Heart Failure Society of America. J Card Fail. 2025;31(1):66-116. *https://doi.org/10.1016/j.cardfail.2024.07.001.*
3. **Perez-Bonilla P, LaViolette B, Bhandary B, Ullas S, Chen X, Hirenallur-Shanthappa D.** Isoproterenol induced cardiac hypertrophy: A comparison of three doses and two delivery methods in C57BL/6J mice. PLoS One. 2024;19(7):e0307467. *https://doi.org/10.1371/journal.pone.0307467.*
4. **Fujimura N, Sumita S, Narimatsu E, Nakayama Y, Shitinohe Y, Namiki A.** Effects of isoproterenol on diaphragmatic contractility in septic peritonitis. Am J Respir Crit Care Med. 2000;161(2 Pt 1):440-446. *https://doi.org/10.1164/ajrccm.161.2.9904044.*
5. **Rebrova TY, Korepanov VA, Stepanov I V, Afanasiev SA.** Modeling of isoproterenol-induced chronic heart failure in 24-month-old rats. Bull Exp Biol Med. 2024;178(1):30-33. *https://doi.org/10.1007/s10517-024-06277-8.*
6. **Nadu AP, Ferreira AJ, Reudelhuber TL, Bader M, Santos RA.** Reduced isoproterenol-induced renin-angiotensin changes and extracellular matrix deposition in hearts of TGR(A1–7)3292 rats. J Am Soc Hypertens. 2008;2(5):341-348. *https://doi.org/10.1016/j.jash.2008.04.012.*
7. **Grimm D, Elsner D, Schunkert H, Pfeifer M, Griese D, Bruckschlegel G.** Development of heart failure following isoproterenol administration in the rat: Role of the renin–angiotensin system. Cardiovasc Res. 1998;37(1):91-100. *https://doi.org/10.1016/S0008-6363(97)00212-5.*
8. **Keihanian F, Moohebati M, Saeidinia A, Mohajeri SA, Madaeni S.** Therapeutic effects of medicinal plants on isoproterenol-induced heart failure in rats. Biomed Pharmacother. 2021;134:111101. *https://doi.org/10.1016/j.biopha.2020.111101.*
9. **Driscoll DJ, Gillette PC, Lewis RM, Hartley CJ, Schwartz A.** Comparative hemody-

namic effects of isoproterenol, dopamine, and dobutamine in the newborn dog. Pediatr Res. 1979;13(9):1006-1009. *https://doi.org/10.1203/00006450-197909000-00011.*

10. **Zinzuvadia D, Suthar J, Patel A, Shah U, Solanki N, Koria H.** *Gynostemma pentaphyllum* Makino exerts cardioprotective effects by improving hemodynamic, biochemical and histopathological changes through activation of PI3K signalling in isoproterenol-induced myocardial infarction in rats. Am J Transl Res. 2024;16(6):2290-2300. *https://doi.org/10.62347/GHIX8452.*
11. **Forte E, Panahi M, Baxan N, Ng FS, Boyle JJ, Branca J, et al.** Type 2 MI induced by a single high dose of isoproterenol in C57BL/6J mice triggers a persistent adaptive immune response against the heart. J Cell Mol Med. 2021;25(1):229-243. *https://doi.org/10.1111/jcmm.15937.*
12. **Pan Y, Gao J, Gu R, Song W, Li H, Wang J, et al.** Effect of injection of different doses of isoproterenol on the hearts of mice. BMC Cardiovasc Disord. 2022;22(1):409. *https://doi.org/10.1186/s12872-022-02852-x.*
13. **Krenek P, Kmecova J, Kucerova D, Bajuszova Z, Musil P, Gazova A, et al.** Isoproterenol-induced heart failure in the rat is associated with nitric oxide-dependent functional alterations of cardiac function. Eur J Heart Fail. 2009;11(2):140-146. *https://doi.org/10.1093/eurjhf/hfn026.*
14. **Cano IP, Dionisio TJ, Cestari TM, Calvo AM, Colombini-Ishikiriama BL, Faria FAC, et al.** Losartan and isoproterenol promote alterations in the local renin-angiotensin system of rat salivary glands. PLoS One. 2019;14(5): e0217030 *https://doi.org/10.1371/journal.pone.0217030.*
15. **Kim JE, Kang YJ, Lee KY, Choi HC.** Isoproterenol inhibits angiotensin II-stimulated proliferation and reactive oxygen species production in vascular smooth muscle cells through heme oxygenase-1. Biol Pharm Bull. 2009;32(6):1047-1052. *https://doi.org/10.1248/bpb.32.1047.*
16. **Leenen FH, White R, Yuan B.** Isoproterenol-induced cardiac hypertrophy: Role of circulatory versus cardiac renin-angiotensin system. Am J Physiol Heart Circ Physiol. 2001;281(6):H2410-6. *https://doi.org/10.1152/ajpheart.2001.281.6.H2410.*
17. **Mohammadi SG, Feizi A, Bagherniya M, Shafie D, Ahmadi A-R, Kafeshani M.** The effect of astaxanthin supplementation on inflammatory markers, oxidative stress indices, lipid profile, uric acid level, blood pressure, endothelial function, quality of life, and disease symptoms in heart failure subjects. Trials. 2024;25(1):518. *https://doi.org/10.1186/s13063-024-08339-8.*
18. **Kato T, Kasai T, Sato A, Ishiwata S, Yatsu S, Matsumoto H, et al.** Effects of 3-month astaxanthin supplementation on cardiac function in heart failure patients with left ventricular systolic dysfunction - A pilot study. Nutrients. 2020;12(6): 1896. *https://doi.org/10.3390/nu12061896.*
19. **Sarker M, Chowdhury N, Bristy AT, Emran T, Karim R, Ahmed R, et al.** Astaxanthin protects fludrocortisone acetate-induced cardiac injury by attenuating oxidative stress, fibrosis, and inflammation through TGF-β/Smad signaling pathway. Biomed Pharmacother. 2024;181:117703. *https://doi.org/10.1016/j.biopha.2024.117703.*
20. **Pereira CPM, Souza ACR, Vasconcelos AR, Prado PS, Name JJ.** Antioxidant and anti−inflammatory mechanisms of action of astaxanthin in cardiovascular diseases (Review). Int J Mol Med. 2021;47(1):37-48. *https://doi.org/10.3892/ijmm.2020.4783.*
21. **Gao C, Gong N, Chen F, Hu S, Zhou Q, Gao X.** The effects of astaxanthin on metabolic syndrome: A comprehensive review. Mar Drugs. 2025;23(1):9. *https://doi.org/10.3390/md23010009.*
22. **Wang Y, Thatcher SE, Cassis LA.** Measuring blood pressure using a noninvasive tail cuff method in mice. Methods Mol Biol. 2017;1614:69-73. *https://doi.org/10.1007/978-1-4939-7030-8_6.*
23. **Stegemann H, Stalder K.** Determination of hydroxyproline. Clin Chim Acta. 1967;18(2):267-273. *https://doi.org/10.1016/0009-8981(67)90167-2.*

24. **Cissell DD, Link JM, Hu JC, Athanasiou KA.** A modified hydroxyproline assay based on hydrochloric acid in Ehrlich's solution accurately measures tissue collagen content. Tissue Eng Part C Methods. 2017;23(4):243-250. *https://doi.org/10.1089/ten.tec.2017.0018.*
25. **Singh H, Kaur P, Kaur P, Muthuraman A, Singh G, Kaur M.** Investigation of therapeutic potential and molecular mechanism of vitamin P and digoxin in I/R-induced myocardial infarction in rat. Naunyn Schmiedebergs Arch Pharmacol. 2015;388(5):565-574. *https://doi.org/10.1007/s00210-015-1103-8.*
26. **Dewi S, Ramadhani ANA, Az-zahra KA, Wardaya W.** Specific activity of lactate dehydrogenase in muscle and liver tissues of rats exposed to intermittent hypobaric hypoxia. BIO Integration. 2025; 6: 1–6. *https://doi.org/10.15212/bioi-2024-0074.*
27. **Lowry OH, Rosebrough NJ, Farr AL, Randall RJ.** Protein measurement with the Folin phenol reagent. J Biol Chem. 1951;193(1):265-275. *https://doi.org/10.1016/S0021-9258(19)52451-6.*
28. **Nikam AP, Ghule AE, Piplani P, Bansal J, Bodhankar SL.** Cardioprotective and antiarrythmic activity of oxalate salt of 1-(isopropylamino)-3-(5-((isopropylamino) methyl)-2-methoxyphenoxy) propan-2-ol (PP-24): A newly synthesized aryloxypropanolamine derivative. Biomed Aging Pathol. 2011;1(2):84-89. *https://doi.org/10.1016/j.biomag.2011.06.003.*
29. **Bader Eddin L, Nagoor Meeran MF, Kumar Jha N, Goyal SN, Ojha S.** Isoproterenol mechanisms in inducing myocardial fibrosis and its application as an experimental model for the evaluation of therapeutic potential of phytochemicals and pharmaceuticals. Animal Model Exp Med. 2025;8(1):67-91. *https://doi.org/10.1002/ame2.12496.*
30. **Shakery A, Pourvali K, Shimi G, Zand H.** Isoproterenol Alters Metabolism, Promotes Survival and Migration in 5-Fluorouracil-Treated SW480 Cells with and without Beta-hydroxybutyrate. Int J Mol Cell Med. 2023;12(2):144-158. *https://doi.org/10.22088/IJMCM.BUMS.12.2.144.*
31. **Liu J, Li W, Jiao R, Liu Z, Zhang T, Chai D, et al.** Miglustat ameliorates isoproterenol-induced cardiac fibrosis via targeting UGCG. Mol Med. 2025;31(1): 288. *https://doi.org/10.1186/s10020-025-01360-w.*
32. **Busatto VC, Cunha V, Cicilini MA, Mill JG.** Differential effects of isoproterenol on the activity of angiotensin-converting enzyme in the rat heart and aorta. Braz J Med Biol Res. 1999;32(3):355-360. *https://doi.org/10.1590/s0100-879x1999000300017.*
33. **Leenen FH, McDonald RH Jr.** Effect of isoproterenol on blood pressure, plasma renin activity, and water intake in rats. Eur J Pharmacol.1974;26(2):129-135. *https://doi.org/10.1016/0014-2999(74)90218-0.*
34. **Chowdhury D, Tangutur AD, Khatua TN, Saxena P, Banerjee SK, Bhadra MP.** A proteomic view of isoproterenol induced cardiac hypertrophy: Prohibitin identified as a potential biomarker in rats. J Transl Med. 2013;11:130. *https://doi.org/10.1186/1479-5876-11-130.*
35. **Erokhina IL, Okovityĭ S V, Kulikov AN, Kazachenko AA, Emel'ianova OI.** Effects of renin-angiotensin system inhibitors on density of rat myocardial, pericardial, and pulmonary mast cells in experimental heart failure. Cell Tiss Biol. 2009;3:544-550. *https://doi.org/10.1134/S1990519X09060078.*
36. **Szymanski MW, Singh DP.** Isoproterenol. In: StatPearls [Internet]. Treasure Island (FL); StatPearls Publishing. 2025. Disponible en: https://www.ncbi.nlm.nih.gov/books/NBK526042/
37. **Gallego M, Espiña L, Vegas L, Echevarria E, Iriarte MM, Casis O.** Spironolactone and captopril attenuates isoproterenol-induced cardiac remodelling in rats. Pharmacol Res. 2001;44(4):311-315. *https://doi.org/10.1006/phrs.2001.0865.*
38. **Bin-Jaliah I, Hussein AM, Sakr HF, Eid EA.** Effects of low dose of aliskiren on isoproterenol-induced acute myocardial infarction in rats. Physiol Int. 2018;105(2):127-144. *https://doi.org/10.1556/2060.105.2018.2.11.*

39. **Weng LQ, Zhang WB, Ye Y, Yin PP, Yuan J, Wang XX, et al.** Aliskiren ameliorates pressure overload-induced heart hypertrophy and fibrosis in mice. Acta Pharmacol Sin. 2014;35(8):1005-1014. *https://doi.org/10.1038/aps.2014.45.*
40. **Zhao Z, Liu H, Guo D.** Aliskiren attenuates cardiac dysfunction by modulation of the mTOR and apoptosis pathways. Braz J Med Biol Res. 2020;53(2):e8793. *https://doi.org/10.1590/1414-431X20198793.*
41. **Keles MS, Bayir Y, Suleyman H, Halici Z.** Investigation of effects of Lacidipine, Ramipril and Valsartan on DNA damage and oxidative stress occurred in acute and chronic periods following isoproterenol-induced myocardial infarct in rats. Mol Cell Biochem. 2009;328(1-2):109-117. *https://doi.org/10.1007/s11010-009-0080-y.*
42. **Khloussy HM, Badawy AD, Mohamed YSIE, Maher M.** Role of 17-β estradiol and ramipril in OPG/RANKL pathway in a rat model of post-menopausal osteoporosis. Egypt J Hosp Med. 2023;90(1):522-527. *https://doi.org/10.21608/ejhm.2023.279677.*
43. **Mahmoud DSE, Kamel MA, El-Sayed IE, Binsuwaidan R, Elmongy EI, Razzaq MK, et al.** Astaxanthin ameliorated isoproterenol induced myocardial infarction via improving the mitochondrial function and antioxidant activity in rats. J Biochem Mol Toxicol. 2024;38(8):e23804. *https://doi.org/10.1002/jbt.23804.*
44. **Ni Y, Nagashimada M, Zhuge F, Zhan L, Nagata N, Tsutsui A, et al.** Astaxanthin prevents and reverses diet-induced insulin resistance and steatohepatitis in mice: A comparison with vitamin E. Sci Rep. 2015;5:17192. *https://doi.org/10.1038/srep17192.*
45. **Althammer F, Roy RK, Kirchner MK,** Podpecan Y, Helen J, **McGrath S,** Campos Lira **E, Stern JE.** Angiotensin-II drives changes in microglia-vascular interactions in rats with heart failure. Commun Biol. 2024;7(1):1537. *https://doi.org/10.1038/s42003-024-07229-8.*
46. **Guo BY, Li YJ, Han R, Yang SL, Shi YH, Han DR, et al.** Telmisartan attenuates isoproterenol-induced cardiac remodeling in rats via regulation of cardiac adiponectin expression. Acta Pharmacol Sin. 2011;32(4):449-455. *https://doi.org/10.1038/aps.2010.231.*
47. **Hussein G, Nakamura M, Zhao Q, Iguchi T, Goto H, Sankawa U, et al.** Antihypertensive and neuroprotective effects of astaxanthin in experimental animals. Biol Pharm Bull. 2005;28(1):47-52. *https://doi.org/10.1248/bpb.28.47.*
48. **Preuss HG, Echard B, Bagchi D, Perricone NV, Yamashita E.** Astaxanthin lowers blood pressure and lessens the activity of the renin-angiotensin system in Zucker fatty rats. J Funct Foods. 2009;1(1):13-22. *https://doi.org/10.1016/j.jff.2008.09.001.*
49. **Mokhtari E, Rafiei S, Shokri-Mashhadi N, Saneei P.** Impact of astaxanthin supplementation on blood pressure: A systematic review and meta-analysis of randomized controlled trials. J Funct Foods. 2021;87:104860. *https://doi.org/10.1016/j.jff.2021.104860.*

Invest Clin 67(1): 139 - 151, 2026 https://doi.org/10.54817/IC.v67n1a10

Meta-analysis of the efficacy and safety of bispecific antibodies in immune therapy for lung cancer.

Xing Zhao[1] and Yang Liu[1,2]

[1]School of Clinical Medicine, Southwest Medical University, Luzhou, Sichuan, China.
[2]Chengdu BOE Hospital, Chengdu, Sichuan, China.

Keywords: Antibodies; Bispecific; Lung cancer; Immunotherapy; Meta-Analysis; Efficacy; Safety.

Abstract. This work evaluates the efficacy and safety of bispecific antibodies (BsAbs) in lung cancer immunotherapy through a meta-analysis, providing more comprehensive evidence for their clinical application. A systematic search was conducted in PubMed, Embase, Cochrane Library, and various Chinese databases to identify eligible randomized controlled trials and quasi-randomized controlled trials. Clinical data on bispecific antibody therapy for lung cancer were collected. The primary endpoints included objective response rate (ORR), progression-free survival (PFS), overall survival (OS), and the incidence of immune-related adverse events (irAEs). Data analysis was performed using RevMan 5.3 software, with fixed-effect or random-effects models. Nine studies were included, with a total sample size of 588 patients. The meta-analysis revealed no statistically significant differences between the bispecific antibody group and the traditional treatment group in ORR, OS and PFS, with combined effect sizes of odds ratio (OR)=1.31 and 95% confidence interval (CI)=0.98-1.76, OR=1.36 and 95%CI=0.99-1.87 and OR=1.07 and 95%CI=0.80-1.43, respectively (p 0.07, 0.06, and 0.64, respectively). However, the incidence of irAEs was significantly lower in the bispecific antibody group (OR = 1.56; p = 0.0007), indicating a reduction in such events. Bispecific antibodies demonstrate good safety in lung cancer immunotherapy, particularly in reducing irAEs. Despite some improvements in efficacy (e.g., ORR and OS), BsAbs do not demonstrate a significant superiority over conventional treatments.

Corresponding Author: Yang Liu. School of Clinical Medicine, Southwest Medical University; Chengdu BOE Hospital.No. 1, Section 1, Xianglin Road, Longmatan District, Luzhou, Sichuan 646000, China. Tel: +86 15982013839. Email: liuyang_ly248@163.com

Metaanálisis de la eficacia y la seguridad de los anticuerpos específicos en la inmunoterapia del cáncer de pulmón.

Invest Clin 2026; 67 (1): 139 – 151

Palabras clave: Anticuerpos Biespecíficos; Neoplasias Pulmonares; Cáncer de pulmón; Inmunoterapia; Metaanálisis; Eficacia; Seguridad.

Resumen. Este estudio tiene como objetivo evaluar sistemáticamente la eficacia y la seguridad de los anticuerpos biespecíficos en la inmunoterapia del cáncer de pulmón mediante un metaanálisis, proporcionando evidencia más completa para su aplicación clínica. Se llevó a cabo una búsqueda sistemática en PubMed, Embase, Cochrane Library y bases de datos chinas para identificar ensayos controlados aleatorizados y ensayos controlados cuasialeatorizados elegibles. Se recogieron datos clínicos sobre la terapia con anticuerpos biespecíficos para el cáncer de pulmón. Los puntos finales primarios incluyeron la tasa de respuesta objetiva (ORR), la supervivencia libre de progresión (PFS), la supervivencia general (OS) y la incidencia de eventos adversos relacionados con la inmunidad (AEIs). El análisis de datos se realizó con el software RevMan 5.3, utilizando modelos de efecto fijo o de efecto aleatorio. Se incluyeron nueve estudios, con un total de 588 pacientes. El metaanálisis no reveló diferencias estadísticamente significativas entre el grupo de anticuerpos biespecíficos y el grupo de tratamiento tradicional en ORR, OS y PFS, con tamaños de efecto combinados de OR=1.31, OR=1.36 y OR=1.07, respectivamente (valores de p de 0.07, 0.06 y 0.64, respectivamente). Sin embargo, la incidencia de AEIs fue significativamente menor en el grupo de anticuerpos biespecíficos (OR=1,56, p=0,0007), lo que indica una ventaja de estos anticuerpos en la reducción de AEIs. Los anticuerpos biespecíficos demuestran una alta seguridad en la inmunoterapia del cáncer de pulmón, en particular en la reducción de AEIs. Sin embargo, a pesar de algunas mejoras en la eficacia (tales como ORR y OS), los anticuerpos biespecíficos no muestran una superioridad significativa frente a los tratamientos convencionales.

Received: 30-06-2025 Accepted: 25-11-2025

INTRODUCTION

In 2020, there were 2.48 million new cases of lung cancer (12.4%), making it the most prevalent cancer globally, once again surpassing breast cancer after 2020 [1-2]. The death toll reached 1.8 million (18.7%), maintaining its position as the leading cause of cancer-related deaths. Approximately 50% of global new cases and deaths from lung cancer occur in Asia [3]. In China, lung cancer remains the leading cause of cancer incidence and mortality, with an increasing trend. The main treatment options for lung cancer include surgery, chemotherapy, radiation therapy, and targeted therapy [4]. However, since most patients with lung cancer are diagnosed at an advanced stage, traditional treatments are limited in their efficacy and often come with significant side effects, which significantly impact the quality of life of patients [5].

In recent years, with the rapid development of tumour immunology, immunotherapy has become a research focus and a breakthrough direction in lung cancer treatment[6]. Immune checkpoint inhibitors (ICIs), including those targeting programmed cell death protein 1 (PD-1) and programmed cell death ligand 1 (PD-L1), have achieved significant success in clinical settings, greatly extending survival in patients with lung cancer [7-8]. However, monotherapy with ICIs has notable limitations, including low efficacy, the potential for resistance, and the risk of severe immune-related adverse events (irAEs) [9]. To overcome the limitations of traditional ICI treatments, bispecific antibodies (BsAbs) have gradually attracted research attention as a novel immune therapeutic approach [10-11]. Bispecific antibodies recognise two distinct antigens or receptors simultaneously, enabling precise targeting of tumour cells while activating immune effector cells to enhance the anti-tumour immune response. Studies have shown that BsAbs can not only effectively improve the selectivity and efficacy of cancer treatments but also reduce the toxic side effects of using ICIs alone, thereby maximising the benefits of immunotherapy[10-11]. Several BsAbs have been developed and are currently being evaluated in clinical trials for the treatment of lung cancer. Among them, BsAbs targeting both PD-1/PD-L1 and other immune checkpoints, such as cytotoxic T-lymphocyte antigen 4 (CTLA-4) and lymphocyte-activation gene 3 (LAG-3), are of particular interest [6]. Preliminary results from early clinical trials suggest that these BsAbs demonstrate good anti-tumour efficacy and relatively controllable safety in patients with non-small cell lung cancer (NSCLC) [12]. However, due to significant differences in clinical trial designs, patient populations, and evaluation standards, no consistent conclusion has been reached regarding the overall efficacy and safety of bispecific antibody therapy for lung cancer. Therefore, there is an urgent need to systematically review and integrate the available clinical research data using rigorous evidence-based methods to more comprehensively and objectively evaluate the clinical value of BsAbs in lung cancer immunotherapy.

This study employs a meta-analytic approach to synthesise data from randomized controlled trials (RCTs) and clinical studies on bispecific antibody (BsAb) therapy for lung cancer, systematically evaluating its efficacy and safety to provide stronger evidence for the clinical application of BsAbs in lung cancer immunotherapy.

MATERIALS AND METHODS

Search Strategy

Relevant literature was systematically searched in multiple databases, including PubMed, Embase, the Cochrane Library, China National Knowledge Infrastructure, the Wanfang Database, and the Chinese Medical Journals Database. The literature search combined subject headings (MeSH terms) and free-text terms to comprehensively identify studies that met the research criteria. The Chinese database search terms included: 'Bispecific antibody', 'Bispecific monoclonal antibody', 'Lung cancer', 'Non-small cell lung cancer', 'Small cell lung cancer', 'Immunotherapy', 'Immune checkpoint inhibitors', 'Efficacy', 'Effect', 'Safety', 'Adverse reactions' and 'Randomized controlled trials'. The specific search strategy for English databases was as follows: ('Bispecific antibody' OR 'Bispecific antibodies' OR 'Bispecific monoclonal antibody' OR 'Bispecific mAb' OR 'Dual-target antibody' OR 'BsAb') AND ('Lung cancer' OR 'Lung neoplasms' OR 'Non-small cell lung cancer' OR 'NSCLC' OR 'Small cell lung cancer' OR 'SCLC' OR 'Pulmonary carcinoma') AND ('Immunotherapy' OR 'Immune therapy' OR 'Checkpoint inhibitors' OR 'Immune checkpoint inhibitors' OR 'ICI' OR 'PD-1' OR 'PD-L1' OR 'CTLA-4' OR 'LAG-3' OR 'T cell engager') AND ('Efficacy' OR 'Effectiveness' OR 'Clinical effect' OR 'Response rate' OR 'Objective

response rate' OR 'Survival' OR 'Progression-free survival' OR 'Overall survival') AND ('Safety' OR 'Adverse events' OR 'Adverse reactions' OR 'Adverse effects' OR 'Side effects' OR 'Immune-related adverse events' OR 'irAEs') AND ('RCT' OR 'Randomized controlled trial' OR 'Clinical trial' OR 'Randomized trial').

The inclusion criteria included (1) diagnosis of NSCLC, clinical staging according to the American Joint Committee on Cancer 9th edition lung cancer staging standard (stages IIIB–IV), with negative driver gene mutation; and (2) studies with complete baseline data, with at least one measurable lesion for assessment according to the Response Evaluation Criteria in Solid Tumors (version 1.1.3); (3) study type is an RCT or quasi-randomized controlled trial (CCT), using BsAbs for lung cancer immunotherapy; and (4) the treatment group used BsAbs alone or combined with other treatments (e.g. chemotherapy, targeted therapy or other immunotherapies), and the control group received standard treatment (including placebo, chemotherapy, single immune checkpoint inhibitor therapy or other standard therapies). The **exclusion criteria** were as follows: (1) non-RCTs or studies without a clear control group; (2) multiple primary tumour sites; (3) case reports, expert opinions, literature reviews and meta-analyses; (4) studies with incomplete data or involving the inability to extract valid data; (5) repeatedly published studies or those with obvious data errors or contradictions; (6) treatment lasting fewer than two cycles; and (7) studies where informed consent from all participants was not obtained.

Outcome measures included objective response rate (ORR), categorised as complete response, partial response, stable disease, and disease progression; progression-free survival (PFS); and overall survival (OS). The primary endpoint was OS, defined as the time from receiving immunotherapy to death. The secondary endpoint was PFS, defined as the time from receiving immunotherapy to disease recurrence, progression, or death. Secondary outcomes included the incidence of adverse events (AEs) and irAEs.

Quality Assessment

Two reviewers independently searched the literature, extracted data, and assessed the methodological quality. Any disagreements were cross-checked and resolved through consensus. The quality assessment was based on the Cochrane RCT quality evaluation standards, with the quality classified as low risk, high risk, or unclear. The criteria included random allocation method, allocation concealment, blinding, completeness of outcome data, selective reporting, and other biases.

Statistical Analysis

All statistical analyses were performed using RevMan 5.3 software (The Nordic Cochrane Centre, Copenhagen). Continuous variables were analysed using weighted mean difference or standardised mean difference, and binary variables using odds ratios (ORs). Results were expressed using a 95% confidence interval (CI). If studies were homogeneous ($p>0.05$; $I2 < 50\%$), a fixed-effect model was used; otherwise, a random-effects model was applied. In cases of high heterogeneity, a random-effects model was used, and publication bias was assessed using a funnel plot.

RESULTS

Literature Search and Screening Results

Through systematic searches in the PubMed, Embase, Web of Science, and Cochrane Library databases, a total of 132 potential studies were identified. Following initial screening, where duplicates were removed based on titles and abstracts, 44 studies remained. In a further screening, 26 studies were excluded due to poor quality, irrelevance to the research objectives, duplication, or low-quality or incomplete data. Finally, 9 studies were included, and data were extracted for meta-analysis. The literature screening process is shown in Fig. 1.

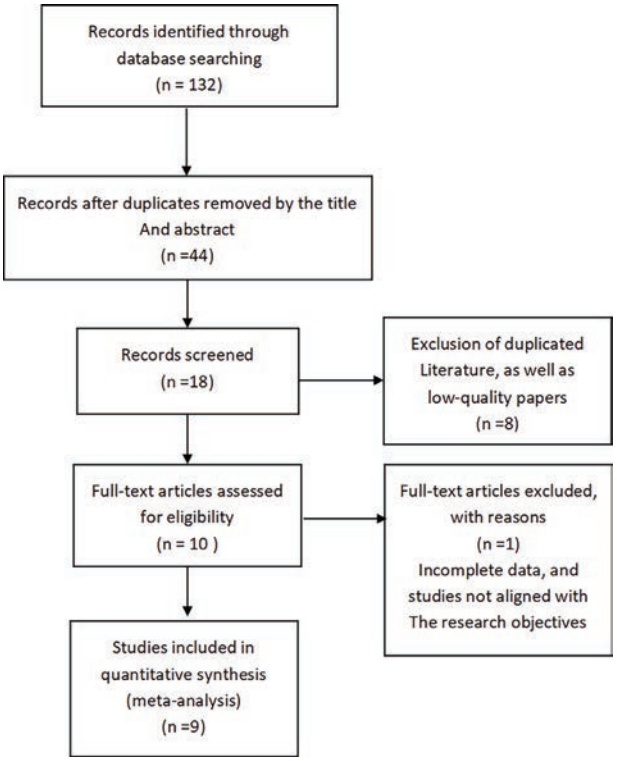

Fig. 1. Literature Screening Flowchart.

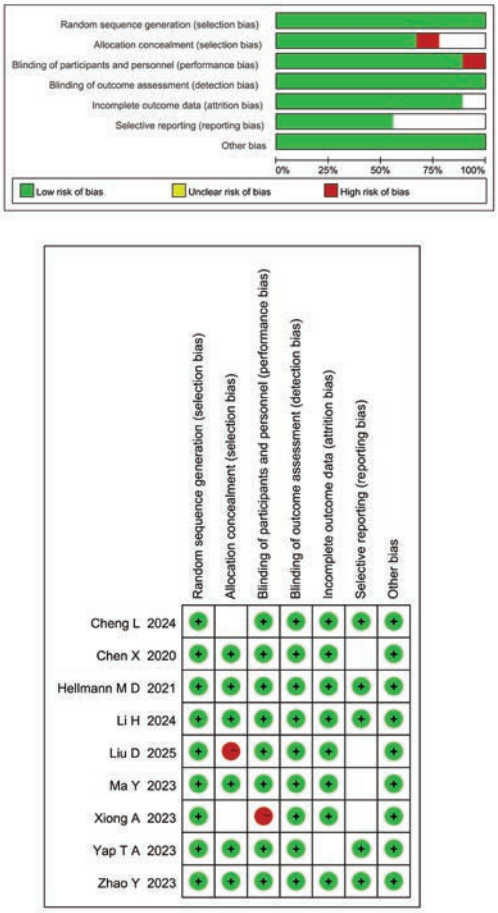

Fig. 2. Literature Quality Assessment.

Quality Assessment of Included Studies

Among the nine studies included in this research [13-21], five studies were of high methodological quality, rated as Grade A; two studies had moderate quality, rated as Grade B; and two studies were of low quality, rated as Grade C. Five studies provided detailed methods, two studies reported concealed allocation methods, and one study had comparable outcome indicators. The quality assessment is shown in Fig. 2.

Basic Characteristics of Included Studies

This analysis included nine clinical studies [13-21], with a total sample size of 588 patients. All studies were RCTs, with high quality (five rated as A). The age range of the study populations was 30–75 years, with treatment and control groups having relatively long disease durations: the treatment group had disease durations of 1-5 years, whereas the control group had durations of 1-3 years. The treatments mainly included combinations of ivosidenib with gefitinib, amivantamab, bevacizumab and other drugs, or the use of immune therapy drugs such as amivantamab, patritumab, pembrolizumab, and nivolumab alone. Treatment duration varied from 1 to 5 years. The main outcome indicators included ORR, PFS, OS, and the incidence of irAEs. All studies compared the effects of different immune therapy regimens across various disease courses and age groups, as shown in Table 1.

Objective Response Rate

This meta-analysis included nine studies comparing the ORR between two groups. All nine studies were clinical trials comparing bispecific antibody drugs with conventional drugs, with $p=0.89$ and $I^2=0\%$. The study data had homogeneity, and the com-

Table 1. Characteristics of included studies.

References	year	Sample (male/ female)	Age	Outcome	Treatment method (treatment group/ control group)	Treatment duration (years)	Disease duration (treatment group/control group)	Value of reference
Cheng L[13]	2024	53/47	60~75	①②③④	**Ivosidenib// Gefitinib, Iressa**	2	2 year/ 1 year	A
Xiong A[14]	2023	67/64	≥54	①③④	**Amivantamab/ Atezolizumab, Tecentriq**	3	2 year/ 3 year	A
Zhao Y[15]	2023	61/63	30~55	①②③	**Patritumab/ Erlotinib, Tarceva**	2	2 year/ 2 year	B
Hellmann MD[16]	2021	38/38	≥45	①②	**Amivantamab/ Nivolumab, Opdivo**	1	4 year/ 2 year	A
Liu D[17]	2025	64/64	<50	②③	**Ivosidenib// Amivantamab, Rybrevant**	2	2 year/ 2 year	C
Li H[18]	2024	43/38	≥50	①④	**Ivosidenib// Nivolumab, Opdivo**	3	1 year/ 2 year	C
Chen X[19]	2020	79/69	40~70	①②	**Patritumab Amivantamab, Rybrevant**	4	2 year/ 2 year	A
Yap TA[20]	2023	54/57	≥50	①②③④	**Ivosidenib/ Bevacizumab, Avastin**	3	5 year/ 3 year	B
Ma Y[21]	2023	34/44	≥50	①②③④	**Ivosidenib/ Pembrolizumab, Keytruda**	5	2 year/ 1 year	A

Note: ①Objective response rate (ORR); ②Progression-free survival (PFS); ③Overall survival (OS); ④Incidence of immune-related adverse events (irAEs).

bined effect size OR was calculated using a fixed-effect model, with OR=1.31 and 95% CI=0.98-1.76. There was no statistically significant difference between the two groups (p= 0.07>0.05), as shown in Fig. 3.

Overall Survival

This meta-analysis included nine studies comparing the OS between two groups. Among them, five studies compared bispecific antibody drugs with conventional drugs. With OR=1.36 and I^2=55%, the study data showed heterogeneity; therefore, the combined effect size was estimated using a random-effects model, yielding OR=1.36 (95% CI=0.99-1.87). There was no statistically significant difference between the two groups (p=0.06>0.05), as shown in Fig. 4.

Progression-Free Survival

This meta-analysis included seven studies comparing PFS between two groups. All seven studies were clinical trials evaluating bispecific antibody drugs against conventional drugs. With p=0.02 and I^2=61%, the data showed heterogeneity, and the combined effect size OR was calculated using a random-effects model, resulting in OR=1.07 and 95% CI=0.80-1.43. There was no statistically significant difference between the two groups (p=0.64 > 0.05), as shown in Fig. 5.

Adverse Event Incidence

This meta-analysis included six studies comparing the incidence of AEs between two groups. All six studies were clinical trials comparing bispecific antibody drugs with conventional drugs. With p=0.31 and I^2=16%, there was no heterogeneity in the study data, and the combined effect size OR was calculated using a fixed-effect model, with OR=1.68 and 95%CI=1.12-2.54. There was a statistically significant difference between the two groups in the incidence of AEs (p=0.01; <0.05), as shown in Fig. 6.

Immune-Related Adverse Event Incidence

This meta-analysis included six studies comparing irAEs between two groups. All six were clinical trials comparing bispecific antibody drugs with conventional drugs. With p=0.17 and I^2=35%, there was no heterogeneity in the data, and the combined effect size OR was calculated using a fixed-effect model, with OR=1.56 and 95% CI=1.13-2.16. A statistically significant difference was observed between the two groups in the incidence of immune-related adverse events (p=0.0007; <0.05), as shown in Fig. 7.

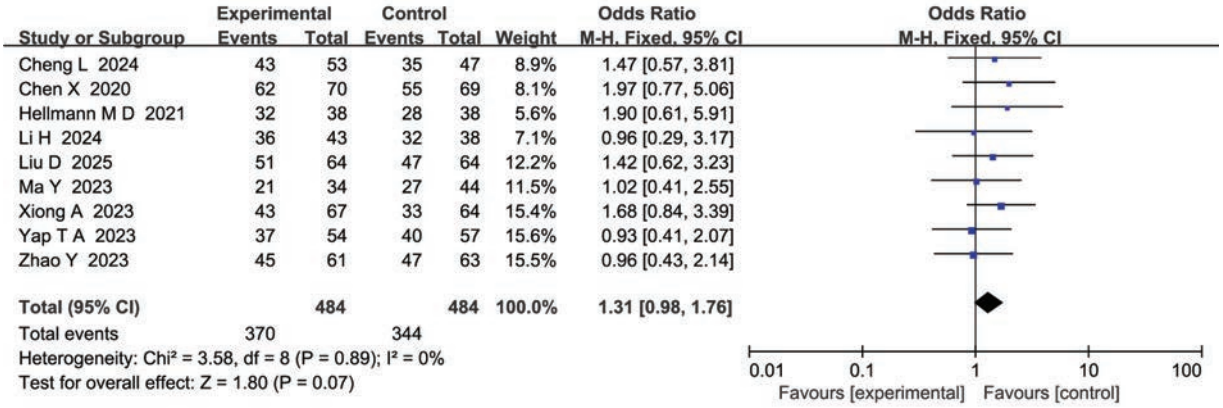

Fig. 3. Forest plot Analysis of Objective Response Rate (ORR) for Bispecific Antibodies in Lung Cancer Immunotherapy.

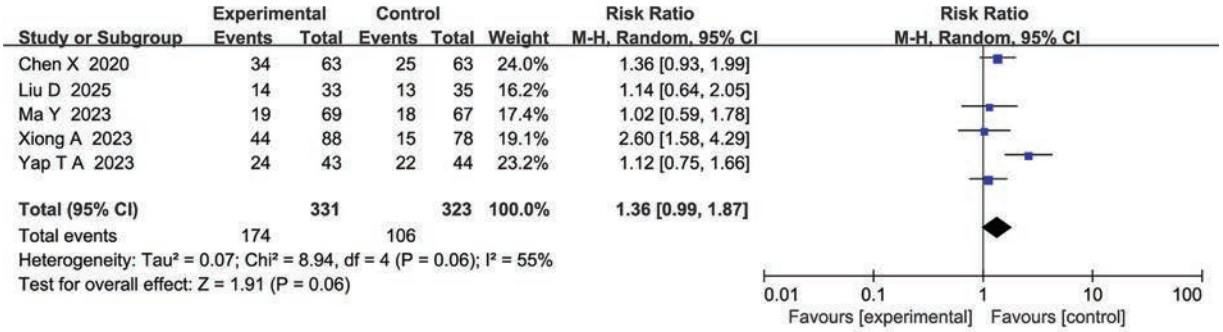

Fig. 4. Forest plot Analysis of Overall Survival (OS) for Bispecific Antibodies in Lung Cancer Immunotherapy.

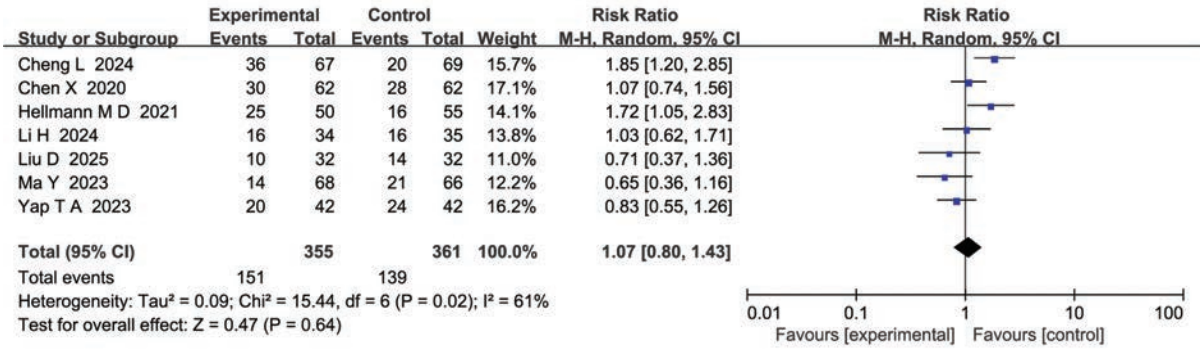

Fig. 5. Forest plot Analysis of Progression-Free Survival (PFS) for Bispecific Antibodies in Lung Cancer Immunotherapy.

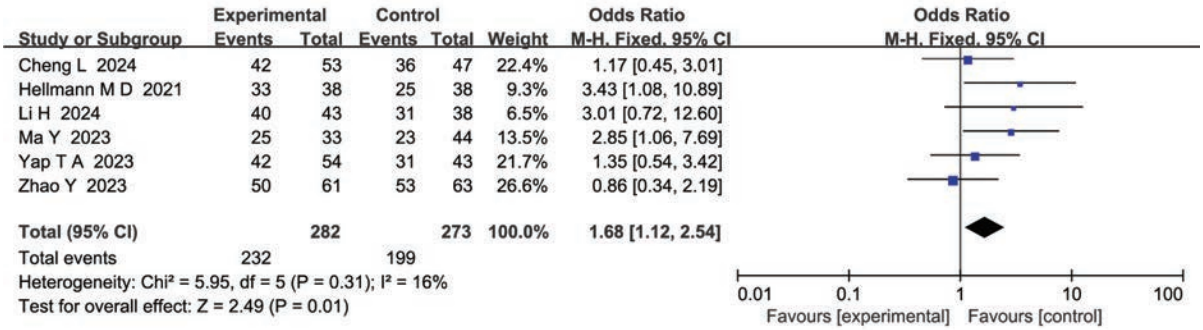

Fig. 6. Forest plot Analysis of Adverse Events (AEs) Incidence for Bispecific Antibodies in Lung Cancer Immunotherapy.

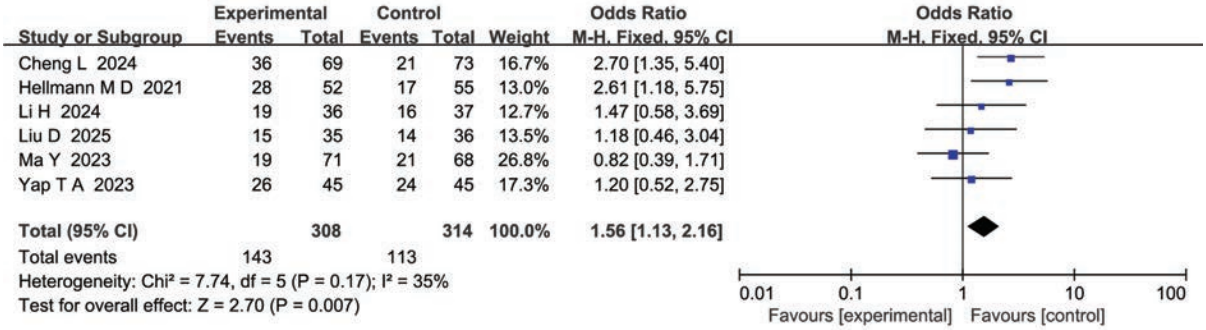

Fig. 7. Forest plot Analysis of Immune-Related Adverse Events (irAEs) Incidence for Bispecific Antibodies in Lung Cancer Immunotherapy.

Publication Bias Assessment

The results of the publication bias assessment for the efficacy and safety of bispecific antibody drugs in lung cancer immunotherapy are displayed in Fig. 8. The studies included were symmetrically spread out in the funnel plot, indicating little publication bias. Most of the scatter points were clustered in the upper part of the funnel plot, implying that the samples in the studies were representative and highly accurate.

DISCUSSION

As the leading cause of cancer-related death worldwide, lung cancer has experienced a steady increase in cases in recent years, particularly in Asia, where it has be-

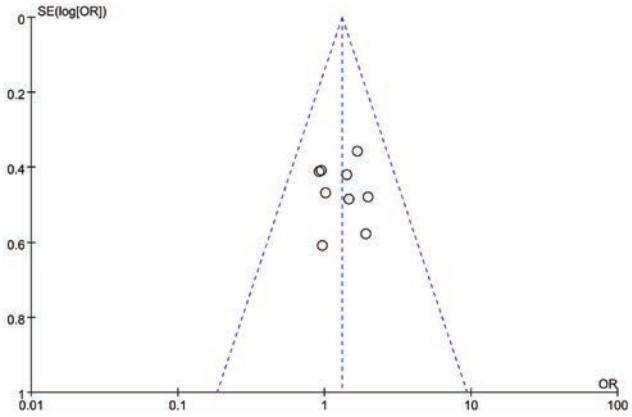

Fig. 8. Funnel plot of Meta-Analysis on the Efficacy and Safety of Bispecific Antibodies in Lung Cancer Immunotherapy.

come the most common type of cancer [22-23]. The treatment approach for lung cancer has gradually shifted from early-stage surgery, chemotherapy, and radiotherapy to targeted therapy and immunotherapy [24]. This meta-analysis indicates that BsAbs may have potential in the efficacy and safety of lung cancer immunotherapy. Although there was no significant difference between the bispecific antibody group and the conventional treatment group in ORR or OS, BsAbs showed an advantage in lowering irAEs.

In this meta-analysis, the bispecific antibody group did not show a significant difference in ORR compared to the conventional treatment group (OR = 1.31; p = 0.07). This result offers initial insight into the potential of BsAbs in lung cancer treatment. Previous studies have demonstrated that BsAbs enhance anti-tumor immune responses through two mechanisms [25]. Although no significant difference in ORR was observed between the bispecific antibody and conventional treatment groups in the overall population, some patients may benefit more from BsAbs. Certain studies have found that, in specific lung cancer patients, combinations of BsAbs exhibit significant synergistic effects [26]. This research indicates that, although the overall ORR in some clinical trials has not shown substantial improvement, BsAbs might be more effective in particular tumor immune phenotypes [27]. The study highlights that small sample sizes can reduce the statistical significance of clinical outcomes, especially in early clinical stages. Therefore, larger-scale clinical trials are needed to provide more definitive evidence.

Regarding OS, the results of this study indicated no statistically significant difference between the bispecific antibody and conventional treatment groups (OR=1.36, p=0.06), although a trend toward effect was observed. This conclusion suggests that BsAbs may not significantly extend patient survival or, at least, no definitive conclusion can be drawn from the current data. Furthermore, with respect to PFS, the study's results showed no significant difference (OR=1.07, p=0.64). This phenomenon may be related to the mechanism of action of BsAbs. Many early clinical trials have indicated that although BsAbs can improve immune responses, their effects often take longer to manifest because of their mechanism of enhancing T-cell-mediated immunity [28]. Therefore, the heterogeneity in this study (I2=55%) may also have contributed to inconsistent PFS results. When BsAbs are combined with other immunotherapies, heterogeneity in efficacy may arise due to differences in combination regimens, dosages, and individual patient characteristics [29]. In the analysis of irAEs, the incidence in the bispecific antibody group was significantly lower than that in the conventional treatment group (OR=1.56, p=0.0007). This result indicates that BsAbs have certain advantages in reducing irAEs. Immune-related adverse events are one of the most significant side effects of traditional immunotherapies, with common adverse effects including rashes, colitis, and immune damage to other organs [30]. However, due to their targeted properties, BsAbs can activate the immune system more precisely, thereby reducing damage to non-target tissues and lowering the occurrence of adverse effects[31]. According to other studies, as a bispecific antibody, amivantamab has shown a lower

incidence of immune-related side effects in clinical studies, which is closely related to its dual-targeting mechanism [22]. By targeting both EGFR and PD-L1, amivantamab can enhance immune responses while reducing attacks on normal tissues, thereby decreasing the occurrence of irAEs [32].

Recently, numerous dual-antibody drugs have been tested in clinical trials and approved for use. First, phase III data published in 2025 (NCT05184795) showed that in patients with EGFR-TKI-resistant NSCLC, ivonescimab (AK112, a PD-1/VEGF dual antibody) combined with chemotherapy significantly prolonged median (m)PFS compared to chemotherapy alone (mPFS: 7.4 months vs. 4.8 months, hazard ratio: 0.55, $p<0.001$), and the incidence of ≥grade 3 irAEs was only 6.8%, which was significantly lower than the historical data of traditional immune combination regimens (approximately 15%). This result suggests that a dual pathway blockade strategy (immunization + anti-angiogenesis) can further reduce the burden of irAEs while improving efficacy, consistent with the present study's conclusion that BsAbs may reduce irAEs, albeit with a greater magnitude of effect [33, 34].

Second, in the DeLLphi-301 study published in 2024, tarlatamab (AMG 757, DLL3×CD3 double antibody) achieved an ORR of 41% with manageable safety, including a cytokine release syndrome ≥ grade 3 incidence of 3% in patients with relapsed small cell lung cancer (SCLC). Although SCLC is not the focus of this study, the success of tarlatamab shows that double antibodies have a comparable breakthrough potential in immune 'cold' tumors, providing new evidence for future meta-analyses that include a broader range of lung cancer subtypes [35].

However, this study has some limitations. In this meta-analysis, heterogeneity among studies may influence how applicable the results are. The sources of heterogeneity can vary, including differences in study design, treatment protocols, and patient groups. For instance, the studies included in this review used different treatment protocols, such as single BsAbs, combined with chemotherapy, or used alongside other immunotherapies. These protocols may have different effects depending on the patient populations. Many studies have pointed out that variations in treatment protocols are a key factor affecting the outcomes of meta-analyses. Treatment length, drug doses, and patient immune status can all impact the overall effectiveness and safety. Therefore, future research should focus on standardizing treatment protocols, increasing sample sizes, and performing more detailed stratified analyses of patient groups to reduce the influence of heterogeneity on the results.

CONCLUSION

Overall, BsAbs show promise in lung cancer immunotherapy, especially in reducing irAEs. However, regarding effectiveness in ORR, OS, and PFS, their impact does not significantly differ from traditional immunotherapy. This may be due to the mechanism of action of BsAbs, the variety of treatment regimens, and the heterogeneity among patient populations.

Funding

No funding or sponsorship was received for this study or the publication of this article.

Competing interest

The authors declare that they have no competing interests.

ORCID numbers of authors

- Xing Zhao (XZ): 0009-0009-2461-7252
- Yang Liu (YL): 0009-0006-7180-7815

Author contributions

Study conception and design: XZ, YL; data collection: XZ, YL; data analysis and interpretation: XZ, YL; drafting of the article: XZ, YL. Critical revision of the article: XZ, YL.

REFERENCES

1. **Khosla AA, Jatwani K, Singh R, Reddy A, Jaiyesimi I, Desai A.** Bispecific Antibodies in Lung Cancer: A State-of-the-Art Review. Pharmaceuticals (Basel). 2023;16(10):1461. *https://doi.org/10.3390/ph16101461*
2. **Kalinka E, Wojas-Krawczyk K, Krawczyk P.** Double Guard Efficiency and Safety-Overcoming Resistance to Immunotherapy by Blocking or Stimulating Several Immune Checkpoints in Non-Small Cell Lung Cancer Patients. Cancers (Basel). 2023;15(13):3499. *https://doi.org/10.3390/cancers15133499.*
3. **Dahlén E, Veitonmäki N, Norlén P.** Bispecific antibodies in cancer immunotherapy. Ther Adv Vaccines Immunother. 2018;6(1):3-17. *https://doi.org/10.1177/2515135518763280.*
4. **Zhang B, Li W, Fan D, Tian W, Zhou J, Ji Z, Song Y.** Advances in the study of CD47-based bispecific antibody in cancer immunotherapy. Immunology. 2022;167(1):15-27. *https://doi.org/10.1111/imm.13498.*
5. **Krishnamurthy A, Jimeno A.** Bispecific antibodies for cancer therapy: A review. Pharmacol Ther. 2018;185:122-134. *https://doi.org/10.1016/j.pharmthera.2017.12.002.*
6. **Li T, Niu M, Zhou J, Wu K, Yi M.** The enhanced antitumor activity of bispecific antibody targeting PD-1/PD-L1 signaling. Cell Commun Signal. 2024;22(1):179. *https://doi.org/10.1186/s12964-024-01562-5.*
7. **Wang W, Qiu T, Li F, Ren S.** Current status and future perspectives of bispecific antibodies in the treatment of lung cancer. Chin Med J (Engl). 2023;136(4):379-393. *https://doi.org/10.1097/CM9.0000000000002460.*
8. **Chames P, Baty D.** Bispecific antibodies for cancer therapy: the light at the end of the tunnel? MAbs. 2009; 1(6): 539-547. *https://doi.org/10.4161/mabs.1.6.10015.*
9. **Ordóñez-Reyes C, Garcia-Robledo JE, Chamorro DF, Mosquera A, Sussmann L, Ruiz-Patiño A, et al.** Bispecific Antibodies in Cancer Immunotherapy: A Novel Response to an Old Question. Pharmaceutics. 2022;14(6):1243. *https://doi.org/10.3390/pharmaceutics14061243.*
10. **Klein C, Brinkmann U, Reichert JM, Kontermann RE.** The present and future of bispecific antibodies for cancer therapy. Nat Rev Drug Discov. 2024;23(4):301-319. *https://doi.org/10.1038/s41573-024-00896-6.*
11. **Wu Y, Yi M, Zhu S, Wang H, Wu K.** Recent advances and challenges of bispecific antibodies in solid tumors. Exp Hematol Oncol. 2021;10(1):56. *https://doi.org/10.1186/s40164-021-00250-1.*
12. **Nejadghaderi SA, Balibegloo M, Noori M, Fayyaz F, Saghazadeh A, Rezaei N.** Clinical efficacy and safety of bispecific antibodies for the treatment of solid tumors: a systematic review and meta-analysis. Expert Rev Anticancer Ther. 2023;23(3):307-318. *https://doi.org/10.1080/14737140.2023.2183847.*
13. **Cheng L, Chen L, Shi Y, Gu W, Ding W, Zheng X, et al.** Efficacy and safety of bispecific antibodies vs. immune checkpoint blockade combination therapy in cancer: a real-world comparison. Mol Cancer. 2024;23(1):77. *https://doi.org/10.1186/s12943-024-01956-6.*
14. **Xiong A, Li W, Li X, Fan Y, Ma Z, Fang J, et al.** Efficacy and safety of KN046, a novel bispecific antibody against PD-L1 and CTLA-4, in patients with non-small cell lung cancer who failed platinum-based chemotherapy: a phase II study. Eur J Cancer. 2023;190:112936. *https://doi.org/10.1016/j.ejca.2023.05.024.*
15. **Zhao Y, Chen G, Chen J, Zhuang L, Du Y, Yu Q, et al.** AK112, a novel PD-1/VEGF bispecific antibody, in combination with chemotherapy in patients with advanced non-small cell lung cancer (NSCLC): an

open-label, multicenter, phase II trial. EClinicalMedicine. 2023;62:102106. *https://doi.org/10.1016/j.eclinm.2023.102106.*

16. **Hellmann MD, Bivi N, Calderon B, Shimizu T, Delafontaine B, Liu ZT, et al.** Safety and Immunogenicity of LY3415244, a Bispecific Antibody Against TIM-3 and PD-L1, in Patients with Advanced Solid Tumors. Clin Cancer Res. 2021;27(10):2773-2781. *https://doi.org/10.1158/1078-0432.CCR-20-3716.*
17. **Liu D, Gong J, Li J, Qi C, Niu Z, Liu B, et al.** Efficacy and safety of KN026, a bispecific anti-HER2 antibody, in combination with KN046, an anti-CTLA4/PD-L1 antibody, in patients with advanced HER2-positive nonbreast cancer: a combined analysis of a phase Ib and a phase II study. Signal Transduct Target Ther. 2025;10(1):104. *https://doi.org/10.1038/s41392-025-02195-x.*
18. **Li H, Zhao W, Li C, Shen H, Li M, Wang C, et al.** The efficacy and safety of a novel PD-1/CTLA-4 bispecific antibody cadonilimab (AK104) in advanced non-small cell lung cancer: A multicenter retrospective observational study. Thorac Cancer. 2024;15(32):2327-2338. *https://doi.org/10.1111/1759-7714.15455.*
19. **Chen X, Amar N, Zhu Y, Wang C, Xia C, Yang X, et al.** Combined DLL3-targeted bispecific antibody with PD-1 inhibition is efficient to suppress small cell lung cancer growth. J Immunother Cancer. 2020;8(1):e000785. *https://doi.org/10.1136/jitc-2020-000785.*
20. **Yap TA, LoRusso PM, Wong DJ, Hu-Lieskovan S, Papadopoulos KP, Holz JB, et al.** A Phase 1 First-in-Human Study of FS118, a Tetravalent Bispecific Antibody Targeting LAG-3 and PD-L1 in Patients with Advanced Cancer and PD-L1 Resistance. Clin Cancer Res. 2023;29(5):888-898. *https://doi.org/10.1158/1078-0432.CCR-22-1449.*
21. **Ma Y, Xue J, Zhao Y, Zhang Y, Huang Y, Yang Y, et al** Phase I trial of KN046, a novel bispecific antibody targeting PD-L1 and CTLA-4 in patients with advanced solid tumors. J Immunother Cancer. 2023;11(6):e006654. *https://doi.org/10.1136/jitc-2022-006654.*
22. **Song X, Xiong A, Wu F, Li X, Wang J, Jiang T, et al.** Spatial multi-omics revealed the impact of tumor ecosystem heterogeneity on immunotherapy efficacy in patients with advanced non-small cell lung cancer treated with bispecific antibody. J Immunother Cancer. 2023;11(2):e006234. *https://doi.org/10.1136/jitc-2022-006234.*
23. **Wei J, Yang Y, Wang G, Liu M.** Current landscape and future directions of bispecific antibodies in cancer immunotherapy. Front Immunol. 2022;13:1035276. *https://doi.org/10.3389/fimmu.2022.1035276.*
24. **Zhang T, Lin Y, Gao Q.** Bispecific antibodies targeting immunomodulatory checkpoints for cancer therapy. Cancer Biol Med. 2023;20(3):181–195. *https://doi.org/10.20892/j.issn.2095-3941.2023.0002.*
25. **Sun Y, Yu X, Wang X, Yuan K, Wang G, Hu L, et al.** Bispecific antibodies in cancer therapy: Target selection and regulatory requirements. Acta Pharm Sin B. 2023;13(9):3583-3597. *https://doi.org/10.1016/j.apsb.2023.05.023.*
26. **Chen B, Yao W, Li X, Lin G, Chu Q, Liu H, et al** A phase Ib/II study of cadonilimab (PD-1/CTLA-4 bispecific antibody) plus anlotinib as first-line treatment in patients with advanced non-small cell lung cancer. Br J Cancer. 2024;130(3):450-456. *https://doi.org/10.1038/s41416-023-02519-0.*
27. **Ruan DY, Wei XL, Liu FR, Hu XC, Zhang J, Ji DM, et al.** The first-in-class bispecific antibody IBI318 (LY3434172) targeting PD-1 and PD-L1 in patients with advanced tumors: a phase Ia/Ib study. J Hematol Oncol. 2024;17(1):118. *https://doi.org/10.1186/s13045-024-01644-4.*
28. **Rader C.** Bispecific antibodies in cancer immunotherapy. Curr Opin Biotechnol. 2020;65:9-16. *https://doi.org/10.1016/j.copbio.2019.11.020.*
29. **Yu S, Li A, Liu Q, Yuan X, Xu H, Jiao D, et al.** Recent advances of bispecific antibodies in solid tumors. J Hematol Oncol. 2017;10(1):155. *https://doi.org/10.1186/s13045-017-0522-z.*

30. **Wang S, Chen K, Lei Q, Ma P, Yuan AQ, Zhao Y, et al.** The state of the art of bispecific antibodies for treating human malignancies. EMBO Mol Med. 2021;13(9):e14291. *https://doi.org/10.15252/emmm.202114291.*
31. **Koopmans I, Hendriks MAJM, van Ginkel RJ, Samplonius DF, Bremer E, Helfrich W.** Bispecific Antibody Approach for Improved Melanoma-Selective PD-L1 Immune Checkpoint Blockade. J Invest Dermatol. 2019;139(11):2343-2351.e3. *https://doi.org/10.1016/j.jid.2019.01.038.*
32. **Rohrberg K S, Brandão M, Castanon Alvarez E, Felip E, Gort E H, Hiltermann T JJN, et al.** Safety, pharmacokinetics (PK), pharmacodynamics (PD) and preliminary efficacy of AZD2936, a bispecific antibody targeting PD-1 and TIGIT, in checkpoint inhibitor (CPI)-experienced advanced/metastatic non-small-cell lung cancer (NSCLC): First report of ARTEMIDE-01. J Clin Oncol. 2023; 41(16). *https://doi.org/10.1200/jco.2023.41.16_suppl.9050.*
33. **Xiong A, Wang L, Chen J, Wu L, Liu B, Yao J, et al.** Ivonescimab versus pembrolizumab for PD-L1-positive non-small cell lung cancer (HARMONi-2): a randomised, double-blind, phase 3 study in China. Lancet. 2025;405(10481):839-849. *https://doi.org/10.1016/S0140-6736(24)02722-3.*
34. **HARMONi-A Study Investigators; Fang W, Zhao Y, Luo Y, Yang R, Huang Y, et al.** Ivonescimab Plus Chemotherapy in Non-Small Cell Lung Cancer with EGFR Variant: A Randomized Clinical Trial. JAMA. 2024;332(7):561-570. *https://doi.org/10.1001/jama.2024.10613.*
35. **Mountzios G, Sun L, Cho BC, Demirci U, Baka S, Gümüş M, et al.** Tarlatamab in Small-Cell Lung Cancer after Platinum-Based Chemotherapy. N Engl J Med. 2025;393(4):349-361. *https://doi.org/10.1056/NEJMoa2502099.*

Instrucciones a los Autores*

Investigación Clínica publica Trabajos Originales, Revisiones y Reportes de Casos Clínicos en español e inglés, que contribuyan al avance del conocimiento en biología humana o animal. También incluye un Editorial y una sección de "Cartas al Editor".

Envío del manuscrito

El manuscrito (Word para Windows®), con su correspondiente lista de verificación y acompañado de una carta de presentación al editor, debe ser enviado por correo electrónico a la dirección:

riclinicas@ gmail.com

Las tablas y las figuras, sí las hubiese, deben estar al final del trabajo, con su correspondiente leyenda. Además del manuscrito, se pueden incluir los nombres de tres posibles árbitros y sus respectivas direcciones institucionales y electrónicas. El Comité Editorial se reserva el derecho de decidir si utilizará alguno de los revisores sugeridos. Todo lo referente a la correspondencia, incluidos la opinión de los árbitros, los requerimientos derivados de la revisión del trabajo y la notificación de la decisión del Comité Editorial, será comunicado por correo electrónico. **La correspondencia de seguimiento del trabajo**, **debe incluir el código asignado por la revista en la carta de recepción.**

Carta de presentación

El manuscrito debe estar acompañado de una carta firmada por todos los autores, en la que manifiestan que han participado activamente en la ejecución del trabajo, que no han utilizado "Inteligencia Artificial" para su elaboración, que este no ha sido publicado con anterioridad, que conocen que se está enviando a Investigación Clínica para su publicación y que no ha sido enviado simultáneamente a otra revista para su consideración.

La autoría debe estar basada en los siguientes criterios:

1) Contribución sustancial a la concepción y al diseño del estudio, a la obtención de datos o a su análisis e interpretación; 2) Revisión crítica del artículo; y 3) Aprobación de la versión final a ser publicada. La obtención de fondos, la recolección de datos o la supervisión del grupo de investigación, por sí solos, no justifican la autoría. Aquellos miembros del grupo que no cumplan con los criterios para ser autores, deben ser mencionados en la sección de Agradecimientos. **Ni el número, ni el orden de aparición de los autores se podrán modificar una vez que el trabajo haya sido aceptado.** Antes de las referencias, es imprescindible incluir: financiamiento, contribución de cada autor, su número ORCID y declarar si hubiere algún conflicto de interés.

Sistema de arbitraje

Para el proceso de arbitraje se utilizará la vía electrónica. Todos los trabajos serán sometidos a la consideración del Comité Editorial de la revista, el cual decidirá si deben ser enviados a arbitraje o si se rechazan por no cumplir las normas editoriales, exceder el alcance editorial definido o no ajustarse a los criterios de calidad científica y metodológica establecidos. El autor de correspondencia recibirá una carta de recepción con un código numérico.

El arbitraje de Trabajos Originales y Reporte de Casos, será realizado por dos expertos en el área y en el caso de las Revisiones, solo por uno. Los árbitros ten-

*Entrarán en vigencia el 01-04-2026

drán un plazo máximo de dos meses para enviar su respuesta. Si las evaluaciones de los árbitros coinciden, el Comité Editorial podrá tomar una decisión; en caso de discrepancia, esperará la evaluación de un tercer árbitro y si la situación lo amerita, se podrán solicitar otras. **La revista sigue la evaluación a doble ciego; el nombre de los árbitros y el de los autores, son estrictamente confidenciales.** Los autores recibirán, tanto en caso de modificaciones como de rechazo, el informe de revisión del manuscrito. El plazo para responder a las recomendaciones de los árbitros será de un máximo de dos meses, transcurridos los cuales, el trabajo será rechazado o readmitido como nuevo.

Costo de la publicación. Todo trabajo aceptado tendrá un costo por concepto de gestión editorial, que se exigirá al momento de su aceptación para publicación.

Normas Editoriales

Los trabajos deben estar escritos a doble espacio, con amplios márgenes y numeración de las páginas en "Word for Windows®" y, preferiblemente, en "Times New Roman 12".

Los **Trabajos Originales**, las **Revisiones** y los **Reportes de Casos,** deben ser contribuciones inéditas de importancia para el avance del conocimiento en el tema objeto de estudio. En la primera página se debe incluir:

El **Título del trabajo** debe ir en letra mayúscula al inicio o cuando se trate de nombres propios, no debe llevar abreviaturas. Luego se coloca el primer nombre, la inicial del segundo y el apellido completo de cada uno de los autores; si usa dos apellidos, deberá separarlos con un guión. El nombre de cada autor llevará superíndices numéricos consecutivos que correspondan a cada una de las instituciones a las que está afiliado. No repetir si pertenecen a la misma institución; solo colocar el superíndice correspondiente. No colocar títulos profesionales.

Un **Título corto** en el idioma original del trabajo, tendrá una extensión máxima de 75 caracteres.

Palabras clave. En renglón aparte, se escribirán de tres a seis palabras clave en español e inglés. Se recomienda colocar palabras que aparezcan en el resumen y evitar aquellas que se encuentren en el título. Para los artículos en español (estas deben formar parte de la lista de Descriptores en Ciencias de la Salud (DeCS), y en inglés usar MeSH (Medical Subject Headings), disponibles en línea: *https://decs.bvsalud.org/es/ y meshb.nlm.nih.gov.*

Autor de correspondencia. Colocar el nombre completo sin títulos académicos, la dirección institucional, la ciudad, el país, el teléfono y el correo electrónico.

A continuación, se presentarán un **Resumen** en español; el título y el resumen en inglés (**Abstract**). Los autores que no posean suficiente dominio del inglés estadounidense deberán solicitar apoyo de un asesor. La revista se reserva el derecho de rechazar trabajos cuyo nivel lingüístico requiera correcciones sustanciales.

Los **Trabajos Originales**, estarán constituidos por: Resumen en español e inglés, Introducción, Material y Métodos o Pacientes y Métodos (si el trabajo se refiere a seres humanos), Resultados, Discusión, Tablas, Figuras, Agradecimientos y Referencias. El texto de los trabajos debe finalizar con una conclusión y no redactarla en una sección aparte.

El **Resumen**, debe constar de un máximo de 250 palabras y establecer los objetivos, la metodología, los hallazgos originales y las conclusiones basadas en los resultados presentados. No debe contener referencias, **ni ser estructurado**. Las abreviaturas deberán evitarse y, si resultan necesarias, definirse en la primera mención.

El **Abstract** debe redactarse en inglés estadounidense y cumplir las mismas indicaciones que el resumen. El resumen y el abstract deberán coincidir en la infor-

mación presentada, sin diferencias en el contenido.

Introducción. Debe incluir antecedentes y generalidades sobre el tema objeto del estudio, hallazgos controversiales, e interrogantes relevantes, aportes propios y, finalmente, **el objetivo principal de la investigación**.

Material y Métodos o Pacientes y Métodos. En esta sección se debe informar sobre el tipo y diseño de la investigación, las características y tamaño de la muestra, su representatividad, así como los criterios de inclusión y exclusión. En los estudios con humanos se debe incluir el consentimiento informado y la aprobación del Comité de Ética de la institución donde se realizó la investigación, o de la institución pertinente para otorgarla, y seguir los lineamientos de la Declaración de Helsinki de 1975, revisada en 2024. Se debe evitar el uso de iniciales o números de historias clínicas; no se aceptarán fotografías del rostro del paciente sin su consentimiento por escrito y se deberá garantizar la protección de la identidad y la dignidad del paciente, evitando rasgos identificatorios. Aquellos estudios que involucren animales, también deben seguir el Código de Ética correspondiente, que cumpla con los estándares internacionales establecidos para el uso, cuidado y tratamiento de los animales de laboratorio. Los procedimientos deben describirse en tiempo pasado y con suficiente detalle para permitir que el trabajo pueda ser duplicado. Los métodos no originales deberán citarse adecuadamente; los equipos y reactivos utilizados deberán ir acompañados del nombre y del país de la compañía proveedora.

Análisis estadístico. Los autores deberán informar el software estadístico utilizado, incluida la versión, y detallar las pruebas estadísticas aplicadas. Asimismo, se recomienda indicar el nivel de significancia y, cuando corresponda, los intervalos de confianza.

Los **Resultados**, deben ser presentados en tiempo pasado, en una secuencia lógica en el texto, Tablas y Figuras. Solo deben resaltarse las observaciones importantes. Los valores de laboratorio y las unidades deben expresarse en el Sistema Internacional de Unidades (SI). No repetir en el texto lo mostrado en las figuras o tablas, solo expresarlo. Las Tablas y figuras se presentarán en páginas separadas. **Las Tablas deben presentarse en formato editable**.

Discusión. Mencionar los hallazgos principales del estudio, comparar los resultados con otros de la literatura, aportes y fortalezas, y mencionar las limitaciones del trabajo, así como sugerir lineamientos para futuras investigaciones. El texto de los trabajos debe finalizar con una conclusión acorde con los resultados y no redactarla en una sección aparte.

Limitar a un máximo de 50 referencias para los artículos originales y de 100 para las revisiones narrativas y sistemáticas o metaanálisis. Se recomienda revisar cuidadosamente el último número de la revista (*http://sites.google.com/site/revista-investigacionesclinicas*) como guía para la preparación del manuscrito.

Las **Revisiones Narrativas** deben estar escritas por especialistas en el campo objeto de las mismas, y contener las contribuciones del autor, ya sea en las referencias o con una discusión del tema revisado. **El número máximo de autores es de cuatro.** No se aceptarán revisiones que consistan meramente en una descripción bibliográfica, sin incluir un análisis. El cuerpo de las revisiones es libre, aunque conviene subdividirlo en secciones. Las **Revisiones Sistemáticas y Metaanálisis** deben seguir las indicaciones internacionales establecidas por PRISMA (Preferred Reporting Items for Systematic reviews and Meta-Analyses) o por cualquier otro método similar.

Los **Reportes de Casos** se refieren a la presentación de casos clínicos poco frecuentes en la práctica médica. Deben incluir una breve introducción sobre la patología a presentar, la descripción del caso y una discusión con el apoyo bibliográfico

correspondiente. Limitar la discusión a lo más notable del caso.

El **Editorial** será presentado por un miembro del Comité Editorial de la revista o por un invitado, propuesto por este cuerpo, seleccionado entre los asiduos colaboradores.

Las **Cartas al Editor**, deben ser comentarios sobre publicaciones recientes en la revista y, en lo posible, no deben exceder de dos páginas, incluidas las referencias.

Tablas. Deben ocupar una página cada una y estar numeradas en números arábigos. Deben contener un título claro y autoexplicativo ubicado en el centro, a seguidas del número de la tabla. No colocar siglas, abreviaturas ni acrónimos en los títulos. Las columnas no deben separarse con líneas. Las notas que aclaren información del cuerpo de la tabla deben escribirse al pie, precedidas por símbolos convencionales. Cada símbolo debe aparecer en la celda correspondiente de la tabla y vincularse con la nota explicativa. D**eben ser comprensibles o poder interpretarse, sin necesidad de recurrir al texto. Por ello, deberán describirse todas las abreviaturas utilizadas, especificar el tipo de análisis estadístico aplicado y señalar a qué grupos corresponde la significancia estadística (p).**

La revista no acepta la expresión "Fuente de información", cuando se refiere a resultados presentados en el mismo artículo, solo si provienen de otro material. Si el artículo está escrito en español, los números decimales se deben separar con una coma y si está escrito en inglés, con un punto. Se aceptará un máximo de 6 tablas y 6 figuras.

Figuras. Cada figura debe ser enviada en un archivo separado, indicando el software donde fue generada (Ej. GraphPad Prism®), identificada con números arábigos consecutivos, de acuerdo con el orden en que aparecen citadas en el texto. El tipo y el tamaño de letra deben ser uniformes y, como mínimo, con resolución de 300 dpi, en formato JPG o TIFF, presentados con un contraste adecuado que garantice su correcta visualización. Las leyendas deben enviarse por separado, con información suficiente para que puedan interpretarse sin recurrir al texto. En el caso de las imágenes radiográficas, no deberán contener leyendas ni marcas que permitan identificar al paciente.

Las fotografías pueden ser en blanco y negro o en color con un contraste adecuado para su reproducción, en formato JPG o TIFF, con las siguientes condiciones: a color o en gradaciones de gris y, tener un mínimo de 600 dpi. En el caso de las microfotografías electrónicas, debe extremarse el cuidado con la nitidez de los hallazgos reportados y señalarlos mediante símbolos claramente distinguibles. También se debe indicar el aumento utilizado; de preferencia, colocar una barra que indique el valor correspondiente (micras, milimicras, nanómetros, entre otros). Las leyendas no deben estar incorporadas a la fotografía ni presentarse en página aparte; deben ser lo suficientemente explicativas. No se aceptarán fotografías ni figuras provenientes de otras publicaciones sin la respectiva autorización.

Referencias. Todas las referencias deben estar en el texto con un número en superíndice sin paréntesis y citadas por orden de aparición, según las normas internacionales *"Recommendations For the Conduct, Reporting, Editing, and Publication of Scholarly Work in Medical Journals"*, actualizadas en enero de 2025 (http:/www. icmje. org); es decir, primero el apellido con la letra inicial en mayúscula, seguido de las iniciales del nombre, también en mayúscula (sin puntos). Cuando una referencia tenga hasta seis autores, deberán incluirse todos. Si son más, se citarán únicamente los primeros seis, seguidos de la abreviatura "et al." o "y col.", según el idioma. **Los nombres de los autores deben ir en negrita y separados entre sí por comas**. A continuación el **título completo del trabajo** y el nombre de la re-

vista abreviado de acuerdo al Index Medicus (http:/ www.nlm.nih.gov), seguido del año de publicación; volumen, y primera y última página, separadas por un guion. Seguidamente, cada referencia deberá incorporar el identificador DOI (Digital Object Identifier). Si el artículo carece de DOI, se indicará el enlace URL (Uniform Resource Locator) del documento. El DOI o la URL debe presentarse de forma completa y verificable. No se aceptarán como referencias, observaciones no publicadas, comunicaciones personales o trabajos enviados a publicación; sin embargo, estos podrán citarse entre paréntesis en el texto. Si el autor es una organización, se coloca el nombre de la organización como responsable de la referencia.

Ejemplos:

Publicaciones periódicas: Jaspe RC, Sulbaran Y, Hidalgo M, Loureiro CL, Moros ZC, Garzaro D, et al. A simple method for detecting of mutations in amino acid 452 of the Spike protein of SARS-CoV-2 using restriction enzyme analysis. Invest Clin. 2021; 62(4): 371-377. https://doi.org/10.22209/IC.v62n4a07.

Libros: Hall JE, Guyton AC. Guyton and Hall textbook of medical physiology. 13th ed. Philadelphia: Elsevier; 2016. https://doi.org/10.1016/C2015-0-00477-0.

Capítulo de Libro: Kumar V, Abbas AK, Aster JC. Robbins and Cotran pathologic basis of disease. 9th ed. Philadelphia: Elsevier; 2015. Chapter 7, Neoplasia. *https://doi.org/10.1016/B978-1-4557-7016-2.00007-0.*

De León DD, Pinney SE. Permanent Neonatal Diabetes Mellitus. 2025. In: Adam MP, Bick S, Mirzaa GM, Pagon RA, Wallace SE, Amemiya A, editors. GeneReviews® [Internet]. Seattle (WA): University of Washington, Seattle; 1993–2026. Disponible en: https://www.ncbi.nlm.nih.gov/books/NBK1116/

Memorias de Congresos:

Stepenka V, Rivas Y, Casal J, Gutiérrez R, Ryder E, Florez H. Metabolic benefits of lifestyle intervention in the clinical setting: a pilot study in Latinos with prediabetes from Venezuela, South America. En: 70th Scientific Sessions of the American Diabetes Association; 2010 Jun 25–29; Orlando, USA. Si las memorias fueron publicadas en un libro o suplemento de revista, se añade después del nombre del congreso, junto a las páginas o identificador si el abstract aparece publicado en un suplemento con paginación o DOI.

Tesis: León NI. Caracterización de aislamientos del complejo *Sporothrix* spp. provenientes de diferentes regiones de Venezuela [Tesis de Maestría]. Caracas: IVIC; 2013. Disponible en: https://ivic.gob.ve/biblioteca/.

Revista en formato electrónico: Calvo B, Melo A, Perozo A, Hernández M, Francisco E, Hagen F, et al. First report of *Candida auris* in America: clinical and microbiological aspects of 18 episodes of candidaemia. J Infect. 2016; 73(4):369-374 [citado, 2017 febrero 10]. http://doi.org/10.1016/j.inf.2016.07.008. o Disponible en: URL

Erratum: Si la publicación tiene un erratum y afecta información crítica, se recomienda incluir ambas referencias en la lista (original y errata). Si solo se consulta la corrección, se cita únicamente el erratum.

Ejemplo:

García M, López R, Pérez J. Impacto de la COVID-19 en la salud mental de estudiantes universitarios. Rev Salud Acad. 2023;15(2):123-30. http://doi.org/doi:10.1234/rsa.2023.5678. Erratum in: García M, López R, Pérez J. Impacto de la COVID-19 en la salud mental de estudiantes universitarios. Rev Salud Acad. 2023;15(3):210. *https://doi.org/10.1234/rsa.2023.5678e.*

Política sobre preprints como referencias

La revista permite citar manuscritos en versión preprint, siempre que se indique claramente su condición de documento

no revisado por pares. Los autores deberán proporcionar el enlace permanente (DOI o URL del servidor correspondiente) y la fecha de consulta. Se recomienda utilizar los preprints como referencias complementarias y no sustituir la evidencia publicada en revistas científicas revisadas por pares.

Política antiplagio

Con el fin de garantizar la ética y la transparencia de las publicaciones científicas, esta revista aplica una política estricta de prevención del plagio y del autoplagio. Todos los manuscritos recibidos serán sometidos a revisión mediante software especializado en detección de similitud o antiplagio.

La revista Investigación Clínica establece que la responsabilidad por la integridad ética de los trabajos publicados recae exclusivamente en sus autores.

Alineada con las prácticas editoriales internacionales del Comité de Ética de publicación (COPE) (*https://publicationethics.org/*) y el Comité Internacional de Editores de Revistas Médicas (ICMJE) (*www.icmje.org*), la revista establece que las retractaciones deberán publicarse de manera visible y permanente, en una página numerada dentro del sistema editorial o índice de contenidos, para garantizar su correcta indexación. La nota de retractación incluirá el título del artículo original, estará vinculada digitalmente al manuscrito y el artículo será claramente identificado como retractado en todas sus versiones (resumen, texto completo y PDF). El texto de la retractación explicará la causa e incluirá la referencia completa al artículo afectado. Los artículos retractados permanecerán de acceso público y estarán inequívocamente señalados como retractados. La retractación podrá ser solicitada por los autores, los editores o la institución correspondiente.

Lista de Verificación

- ☐ Carta firmada por todos los autores, donde se indique el autor de correspondencia, la participación de cada autor en la elaboración del trabajo, y se manifieste que este no ha sido publicado con anterioridad, ni está siendo enviado a otra revista para publicación.
- ☐ Páginas numeradas en forma secuencial.
- ☐ Título en español.
- ☐ Título en inglés.
- ☐ Título corto en el idioma principal del manuscrito.
- ☐ Lista de Autores con nombres completos, sin títulos profesionales.
- ☐ Resumen **no estructurado** en inglés y en español de no más de 250 palabras, que incluya una introducción, procedimientos básicos, resultados y una conclusión.
- ☐ Introducción breve, referida al objeto de estudio.
- ☐ Material y Métodos o Pacientes y Métodos, descritos con precisión y con referencias adecuadas.
- ☐ Especificación del análisis estadístico (cuando se requiere).
- ☐ Resultados presentados en forma clara y en orden lógico sin discusión de los mismos.
- ☐ Discusión basada en los hallazgos obtenidos.
- ☐ Referencias presentadas en orden de aparición, en superíndices sin paréntesis, citadas en el texto y de acuerdo con las especificaciones de la revista.
- ☐ No se aceptan comunicaciones personales, ni presentaciones en congresos cuyos resúmenes no hayan sido publicados.
- ☐ Tablas numeradas en arábigos, con las notas en la parte inferior.
- ☐ Las ilustraciones y fotografías de acuerdo con las especificaciones de la revista.
- ☐ Leyendas de las ilustraciones, figuras y fotografías en páginas separadas.
- ☐ Número ORCID de todos los autores.
- ☐ Fuente de financiamiento.
- ☐ Participación de los autores en el trabajo.
- ☐ Conflictos de interés.

Instructions to Authors*

Investigación Clínica publishes Original Articles, Reviews, and Reports of Clinical Cases in both Spanish and English that significantly contribute to advancing knowledge in human or animal biology. It also features an Editorial section and a 'Letters to the Editor' segment.

Manuscript submission

The manuscript (Word for Windows®), along with its corresponding checklist and accompanied by a letter of submission to the editor, must be sent by email to the following address: riclinicas@gmail.com.

Tables and figures, if any, should be placed at the end of the work with their corresponding captions. In addition to the manuscript, the following may be included: the names of three potential referees and their respective institutional and email addresses. The Editorial Committee reserves the right to decide whether to use some of the reviewers suggested. All correspondence, including the Referees' opinions, requirements arising from the review of the work, and notification of the Editorial Committee's decision, will be communicated via email. Follow-up correspondence regarding the work should include the journal-assigned code in the reception letter.

Cover letter

The manuscript must be accompanied by a letter, addressed to the Editor, signed by all authors, stating that they have actively participated in the execution of the work, that they have not used "Artificial Intelligence" for its preparation, that it has not been previously published, that they are aware it is being sent to Investigación Clínica for publication, and that it has not been simultaneously submitted to another journal for consideration.

Authorship must be based on the following criteria:

1) Substantial contribution involves the conception and design of the study, data collection, or analysis and interpretation; 2) Drafting or critically reviewing the manuscript; and 3) Approving the final version for publication. Obtaining funding, collecting data, or supervising the research group, by themselves, do not justify authorship. Group members who do not meet the authorship criteria should be acknowledged in the Acknowledgments section. Once the work has been accepted, neither the number nor the order of authors may be changed. Before the references, it is essential to include: funding, each author's contribution, their ORCID number, and a declaration of any conflicts of interest.

System of arbitration

The arbitration process will be carried out electronically. All submissions will be reviewed by the journal's Editorial Committee, which will decide whether to send them for peer review or reject them for failing to meet editorial guidelines, exceeding the editorial scope, or failing to comply with established scientific and methodological quality standards. The corresponding author will receive a confirmation letter with a numerical code.

The arbitration of Original Works and Reports of Cases will be conducted by two experts in the field, while reviews will be handled by only one. Referees will have up to two months to submit their responses. If the referees' evaluations are consis-

*These will take effect from April 1st, 2026

tent, the Editorial Committee may make a decision; if they differ, a third referee's evaluation will be sought and, if needed, additional reviews may be requested. The journal uses a double-blind peer-review process, keeping referees' and authors' identities strictly confidential. Authors will receive the manuscript review report whether revisions are needed or the work is rejected. Authors have two months to respond to the referees' recommendations; after that, the work will be either rejected or considered for readmission as new.

Publication costs. All accepted works will require an editorial management fee, payable upon publication.

Editorial Guidelines

Papers must be double-spaced with wide margins, page numbers, written in "Word for Windows®," and preferably in "Times New Roman 12."

Original Articles, Reviews, and Case Reports must be original contributions of substantial importance to the advancement of knowledge on the subject. The first page should include:

The **title of the work** must start with a capital letter and should not contain abbreviations. Then, place the first name, the initial of the second name, and the full surname of each author. If an author has two surnames, separate them with a hyphen. Each author's name should be followed by numerical superscripts indicating their institutional affiliations. Do not repeat names from the same institution; only use the corresponding superscript. Do not include professional titles.

A short title in the original language of the work should not exceed 75 characters.

Keywords. On a separate line, list three to six keywords in both Spanish and English. It is recommended to include words that appear in the summary and avoid those found in the title. For Spanish articles, use terms from the Descriptors in Health Sciences (DeCS) list, and for English, use MeSH (Medical Subject Headings). Both are accessible online: https://decs.bvsalud.org/es/ and meshb.nlm.nih.gov.

Author of correspondence. Include the full name without academic titles, the institutional address, city, country, phone number, and email address.

Next, a summary will be provided in Spanish, and the title and abstract in English. Authors without sufficient command of American English should seek assistance from an advisor. The journal reserves the right to reject submissions that require extensive language corrections.

The original articles will include a summary in both Spanish and English, an introduction, materials and methods (or patients and methods if the work involves human subjects), results, discussion, tables, figures, acknowledgments, and references. The paper must end with a conclusion, which should not be written as a separate section.

The summary should be no longer than 250 words and clearly outline the objectives, methodology, original findings, and conclusions based on the presented results. It should not include references or have a specific structure. Abbreviations should be avoided; if necessary, they must be defined when first used.

The abstract should be written in American English and adhere to the same guidelines as the Spanish summary. Both the summary and the abstract must contain the same information; there should be no discrepancies in content.

Introduction. It should provide background and general information on the study topic, address controversial findings, pose relevant questions, highlight your own contributions, and conclude with the main objective of the research.

Materials and Methods or Patients and Methods. This section should describe the type and design of the study, the characteristics and size of the sample, its representa-

tiveness, and the inclusion and exclusion criteria. For studies involving human subjects, informed consent and approval from the Ethics Committee of the institution where the research was conducted, or from the relevant institution authorized to grant such approval, must be included, and the guidelines of the 1975 Declaration of Helsinki, revised in 2024, must be followed. The use of initials or medical record numbers should be avoided. Photographs of the patient's face will not be accepted without their written consent, and the patient's identity and dignity must be protected by avoiding any identifying features. Studies involving animals must also comply with the applicable Code of Ethics and established international standards for the use, care, and treatment of laboratory animals. Procedures should be described in the past tense and in sufficient detail to enable replication of the work. Non-original methods must be properly cited. The equipment and reagents used must include the company name and the supplier's country.

Statistical analysis. Authors should specify the statistical software used, including the version, and describe the statistical tests performed. It is also advisable to mention the significance level and, if relevant, the confidence intervals.

Results should be presented in the past tense and follow a logical order throughout the text, tables, and figures. Only key observations should be emphasized. Laboratory values and units must be expressed in the International System of Units (SI). Do not repeat information shown in the figures or tables within the text; simply state it. Tables and figures should be presented on separate pages. Tables must be submitted in an editable format.

Discussion. Summarize the main findings of the study, compare the results with others in the literature, highlight the contributions and strengths, and acknowledge the limitations of the work. Also, suggest guidelines for future research. The paper's final section should be a conclusion that aligns with the results and should not be written as a separate section.

References. Limit to a maximum of 50 references for original articles and 100 for narrative and systematic reviews or meta-analyses. It is recommended that you carefully review the latest issue of the journal (http://sites.google.com/site/revistainvestigacionesclinicas) as a guide for preparing the manuscript.

Narrative reviews must be written by experts in the field and include the author's contributions, either in the references or within a discussion of the topic. The maximum number of authors is four. Reviews that are simply bibliographic descriptions without analysis will not be accepted. The structure of the reviews is flexible, though it is recommended to divide them into sections. Systematic reviews and meta-analyses must follow the international PRISMA (Preferred Reporting Items for Systematic Reviews and Meta-Analyses) guidelines or similar standards.

Case reports emphasize rare clinical cases in medical practice. They should include a brief introduction to the pathology being discussed, a case description, and a discussion supported by relevant references. Limit the discussion to the most important aspects of the case.

The Editorial will be presented by a member of the journal's Editorial Committee or by a guest, proposed by this group and selected from among the regular contributors.

Letters to the editor should comment on recent journal publications and, if possible, should not exceed two pages, including references.

Tables. Each must fit on one page and be numbered with Arabic numerals. They should include a centered clear, self-explanatory title following the Table number. Do not use acronyms, abbreviations, or initialisms in the titles. Columns should not be separated by lines. Notes clarifying information in the table body should be placed at the

bottom, preceded by conventional symbols. Each symbol should appear in the corresponding cell of the table and be linked to the explanatory note. These notes should be understandable without referring to the text. Therefore, all abbreviations used should be explained, the type of statistical analysis applied should be specified, and the groups related to the statistical significance (p) should be indicated.

The journal does not accept the phrase "Source of information" when referring to results presented in the same article, unless they come from other material. If the article is written in Spanish, decimal numbers should be separated by a comma, and if it is written in English, by a period. A maximum of six tables and six figures will be accepted.

Figures. Each figure must be submitted as a separate file, indicating the software used to create it (e.g., GraphPad Prism®) and numbered consecutively with Arabic numerals in the order they appear in the text. The font type and size should be consistent, and the image should have a minimum resolution of 300 dpi in JPG or TIFF format, with adequate contrast for proper viewing. Legends must be submitted separately and include enough information to interpret them without referencing the text. For radiographic images, no legends or markings that could identify the patient are allowed.

Photographs should be in black-and-white or color, with sufficient contrast for reproduction, in JPG or TIFF format, and must be at least 600 dpi. For electron micrographs, extreme care is required to ensure the clarity of the reported findings, which must be marked with clearly distinguishable symbols. The magnification used must also be indicated; preferably, include a scale bar to show the corresponding measurement (microns, nanometers, etc.). Captions should not be embedded in the photograph and must appear on a separate page; they should be detailed enough that the viewer does not need to refer to the main text. Photographs and figures from other publications will not be accepted without proper authorization.

References. All references must be included in the text with a superscript number, without parentheses, and cited in the order they appear, in accordance with the standards of the international "Recommendations for the Conduct, Reporting, Editing, and Publication of Scholarly Work in Medical Journals," updated in January 2025 (http://www.icmje.org). This means the surname should be in capital letters, followed by the first name initials in capital letters, without periods. When a reference has up to six authors, list all authors. If there are more, only the first six should be cited, followed by the abbreviation "et al." or "y col.", depending on the language. The authors' names should be in bold and separated by commas. Next, include the full title of the work and the abbreviated journal name per Index Medicus (http://www.nlm.nih.gov), followed by the year of publication, volume, and first and last page numbers, separated by a hyphen. Each reference must then include the DOI (Digital Object Identifier). If the article does not have a DOI, provide the document URL (Uniform Resource Locator). The DOI or URL must be complete and verifiable. Unpublished observations, personal communications, or works submitted for publication are not acceptable as references; however, they can be cited in parentheses within the text. If the author is an organization, list the organization's name as the responsible party.

Examples:

Periodical publications: Jaspe RC, Sulbaran Y, Hidalgo M, Loureiro CL, Moros ZC, Garzaro D, et al. A simple method for detecting mutations in amino acid 452 of the Spike protein of SARS-CoV-2 using restriction enzyme analysis. Invest Clin. 2021; 62(4): 371-377. https://doi.o rg/10.22209/IC.v62n4a07.

Books: Hall JE, Guyton AC. Guyton and Hall textbook of medical physiol-

ogy. 13th ed. Philadelphia: Elsevier; 2016. *https://doi.o rg/10.1016/C2015-0-00477-0.*

Book Chapter: Kumar V, Abbas AK, Aster JC. Robbins and Cotran pathologic basis of disease. 9th ed. Philadelphia: Elsevier; 2015. Chapter 7, Neoplasia. *https://doi.o rg/ 10.1016/B978-1-4557-7016-2.00007-0* .

De León DD, Pinney SE. Permanent Neonatal Diabetes Mellitus. 2025. In: Adam MP, Bick S, Mirzaa GM, Pagon RA, Wallace SE, Amemiya A, editors. GeneReviews ® [Internet]. Seattle (WA): University of Washington, Seattle; 1993–2026. Available at: https:// www.ncbi.nlm.nih.gov/books/NBK1116/

Conference Proceedings:

Stepenka V, Rivas Y, Casal J, Gutiérrez R, Ryder E, Florez H. Metabolic benefits of lifestyle intervention in the clinical setting: a pilot study in Latinos with prediabetes from Venezuela, South America. In: 70th Scientific Sessions of the American Diabetes Association; 2010 Jun 25–29; Orlando, USA. If the proceedings were published in a book or journal supplement, it is added after the name of the congress, next to the pages or identifier if the abstract appears published in a supplement with pagination or DOI.

Thesis: León NI. Characterization of isolates of the *Sporothrix* spp. complex from different regions of Venezuela [Master 's Thesis]. Caracas: IVIC; 2013. Available from: https://ivic.gob.ve/biblioteca/.

Electronic journal: Calvo B, Melo A, Perozo A, Hernández M, Francisco E, Hagen F, et al. First report of *Candida auris* in America: clinical and microbiological aspects of 18 episodes of candidaemia. J Infect. 2016; 73(4):369-374 [cited 2017 February 10]. http://doi.org/10.1016/j.inf.2016.07.008. Available from: URL

Erratum: If the publication contains an erratum affecting critical information, it is recommended to include both references in the list (original and erratum). If only the correction is consulted, only the erratum is cited. Example:

García M, López R, Pérez J. Impact of COVID-19 on the mental health of university students. Rev Salud Acad. 2023;15(2):123-30. http://doi.org/ doi :10.1234/rsa.2023.5678. Erratum in: García M, López R, Pérez J. Impact of COVID-19 on the mental health of university students. Rev Salud Acad. 2023;15(3):210. *https://doi.org/10.1234/rsa.2023.5678e.*

Policy on preprints as references

The journal permits citing preprints as long as their non-peer-reviewed status is clearly indicated. Authors need to include the permanent link (DOI or URL) and the date accessed. It is advised that preprints serve as supplementary references rather than replacing evidence published in peer-reviewed scientific journals.

Anti-plagiarism policy

To ensure the ethical and transparent publication of scientific work, this journal adheres to a strict policy on plagiarism and self-plagiarism. All submitted manuscripts will be checked with specialized plagiarism detection software.

The journal Investigación Clínica states that the ethical integrity of published works rests exclusively with their authors.

In accordance with the international editorial standards of the Committee on Publication Ethics (COPE) (https://publicationethics.org/) and the International Committee of Medical Journal Editors (ICMJE) (www.icmje.org), the journal requires that retractions be published prominently and permanently on a numbered page within the editorial system or table of contents to ensure proper indexing. The retraction notice will include the title of the original article, be digitally linked to the manuscript, and clearly identify the article as retracted in all its versions (abstract, full text, and PDF). The retraction text will state the reason for the retraction and include the full reference to the affected article. Retracted articles will remain publicly accessible and be unmistakably marked as retracted. Requests for retractions can come from the authors, editors, or the corresponding institution.

Checklist

- ☐ A letter signed by all authors, confirming the corresponding author, each author's contribution to the work, and stating that it has not been published before and is not being submitted to another journal.
- ☐ Pages numbered sequentially.
- ☐ Title in Spanish.
- ☐ Title in English.
- ☐ Short title in the main language of the manuscript.
- ☐ List of authors with full names, excluding professional titles.
- ☐ Provide a summary in both English and Spanish, not exceeding 250 words, including an introduction, basic procedures, results, and a conclusion.
- ☐ Brief introduction, referring to the subject of study.
- ☐ Material and Methods or Patients and Methods, described clearly and with proper references.
- ☐ Specification of the statistical analysis when needed.
- ☐ Results are presented clearly and in a logical order without discussing the same.
- ☐ Discussion based on the findings obtained.
- ☐ References listed in order of appearance, using superscripts without parentheses, cited in the text and in accordance with the journal's specifications.
- ☐ Personal communications and conference presentations are not accepted if abstracts have not been published.
- ☐ Tables numbered with Arabic numerals, with notes at the bottom.
- ☐ The illustrations and photographs meet the journal's specifications.
- ☐ Legends for the illustrations, figures, and photographs are on separate pages.
- ☐ All authors'ORCID numbers.
- ☐ Source of funding.
- ☐ Authors' involvement in the job.
- ☐ Conflicts of interest.

Investigación Clínica
Vol. 67 Nº 1 / March 2026
Bilingual - Abstracts in Spanish and English

Contents

EDITORIAL

Recognitions and achievements in our 65th Anniversary.
Ryder E (*E-mail: elenaryder@gmail.com*) 1
https://doi.org/10.54817/IC.v67n1a00

In Memoriam. *Slavia Cristina Ryder Jaksic*
Esparza J (*E-mail: Jose.esparza5@live.com*). 3

ORIGINAL PAPERS

Effects of Vitamin D deficiency and supplementation on 25(OH)D3 levels and neuropsychobehavioral development in premature infants. (English)
Guo X (*E-mail: guoxiaohui3212919@163.com*), Sun Y, Chen Y, Xu F, Li Y 5
https://doi.org/10.54817/IC.v67n1a01

The impact of complement C1q/tumor necrosis factor-related protein 6-mediated cardiomyocyte pyroptosis on myocardial fibrosis in rats with myocardial infarction. (English)
Zhang Q, Chen X, Pan H, Chen Z (*E-mail:zengguangchen@126.com*) 19
https://doi.org/10.54817/IC.v67n1a02

Assessment of the efficacy of tamsulosin and potassium citrate in promoting spontaneous ureteral stone expulsion. (English)
Liu L, Zhang K, Li D (*E-mail: Li1908chang@hotmail.com*) 30
https://doi.org/10.54817/IC.v67n1a03

Virulence factors and their effect on antifungal sensitivity of *Candida albicans* causing recurrent vulvovaginal candidiasis. (Spanish)
Moreno-Calderón X (*E-mail: xmorenoc1356@gmail.com*), Cantero-Alvarado A, Vivas-Parababire MG, Panizo-Domínguez MM 45
https://doi.org/10.54817/IC.v67n1a04

Study on the predictive model of response of patients with inflammatory bowel disease to infliximab treatment. (English)
Ding R, Fan M, Gu J, Zhou Z (*E-mail: zjsrxy2024@hotmail.com*) 57
https://doi.org/10.54817/IC.v67n1a05

Withaferin-A induces apoptosis and autophagy in colorectal cancer cell lines via down-regulated expression of histone deacetylase 1. (English)
Wang Q (*E-mail: Wangqiong7979@163.com*), Li C.. 73
https://doi.org/10.54817/IC.v67n1a06

Phyllanthin identified from *Phyllanthus amarus* attenuates arsenite-induced liver and kidney damage: Role of NF-kB pathway inhibition. (English)
Xu J, Sadar S, Kamble H, Zhang Y (*E-mail: snkzyt@sina.com*) 92
https://doi.org/10.54817/IC.v67n1a07

Treatment strategies and mortality risk factors in patients with multidrug-resistant *Acinetobacter baumannii* pneumonia: A retrospective analysis. (English)
Liu L, Lu W, Fang G, Zhang W (*E-mail: fgg2343@hotmail.com*) 108
https://doi.org/10.54817/IC.v67n1a08

Ameliorative potential of astaxanthin in isoproterenol-induced heart failure in rats via the regulation of the renin-angiotensin system. (English)
Chang L, Qiao F (*E-mail: furong644759573@sina.com*) 125
https://doi.org/10.54817/IC.v67n1a09

REVIEW

Meta-analysis of the efficacy and safety of bispecific antibodies in immune therapy for lung cancer. (English)
Zhao X, Liu Y (*E-mail: liuyang_ly248@163.com*) 139
https://doi.org/10.54817/IC.v67n1a10

INSTRUCTIONS TO AUTHORS 2026 159

Investigación Clínica
Vol. 67 Nº 1 /Marzo 2026
Bilingüe - Resúmenes en Español e Inglés

Contenido

EDITORIAL

Reconocimientos y logros alcanzados en nuestro 65° Aniversario.
Ryder E (*Correo electrónico: elenaryder@gmail.com*) 1
https://doi.org/10.54817/IC.v67n1a00

In Memoriam. *Slavia Cristina Ryder Jaksic*
Esparza J (*Correo electrónico: Jose.esparza5@live.com*) 3

TRABAJOS ORIGINALES

Efectos de la deficiencia de vitamina D y la suplementación sobre los niveles de 25(OH)D3 y el desarrollo neuropsicológico-conductual en bebés prematuros. (Inglés)
Guo X (*Correo electrónico: guoxiaohui3212919@163.com*), Sun Y, Chen Y, Xu F, Li Y. 5
https://doi.org/10.54817/IC.v67n1a01

Impacto de la piroptosis de cardiomiocitos mediada por CTRP6 en la fibrosis miocárdica en ratas con infarto de miocardio. (Inglés)
Zhang Q, Chen X, Pan H, Chen Z (*Correo electrónico:zengguangchen@126.com*). 19
https://doi.org/10.54817/IC.v67n1a02

Evaluación de la eficacia de tamsulosina y citrato de potasio en la promoción de la expulsión espontánea de cálculos ureterales. (Inglés)
Liu L, Zhang K, Li D (*Correo electrónico: Li1908chang@hotmail.com*). 30
https://doi.org/10.54817/IC.v67n1a03

Factores de virulencia y su efecto sobre la sensibilidad a los fármacos antifúngicos de *Candida albicans* causante de vulvovaginitis candidiásica recurrente. (Español)
Moreno-Calderón X (*Correo electrónico: xmorenoc1356@gmail.com*),Cantero-Alvarado A, Vivas-Parababire MG, Panizo-Domínguez MM 45
https://doi.org/10.54817/IC.v67n1a04

Estudio sobre el modelo predictivo de la respuesta de los pacientes con enfermedad inflamatoria intestinal al tratamiento con infliximab. (Inglés)
Ding R, Fan M, Gu J, Zhou Z (*Correo electrónico: zjsrxy2024@hotmail.com*). 57
https://doi.org/10.54817/IC.v67n1a05

La withaferina-A induce la apoptosis y la autofagia en líneas celulares de cáncer colorrectal mediante la regulación negativa de la expresión de la histona deacetilasa 1. (Inglés)
Wang Q (*Correo electrónico: Wangqiong7979@163.com*), Li C. 73
https://doi.org/10.54817/IC.v67n1a06

La filantina identificada en *Phyllanthus amarus* atenúa el daño hepático y renal inducido por arsenito: papel de la inhibición de la vía NF-Kb. (Inglés)
Xu J, Sadar S, Kamble H , Zhang Y (*Correo electrónico :snkzyt@sina.com*) 92
https://doi.org/10.54817/IC.v67n1a07

Estrategias de tratamiento y factores de riesgo de mortalidad en pacientes con neumonía por *Acinetobacter baumannii* multirresistente: Un análisis retrospectivo. (Inglés)
Liu L, Lu W, Fang G, Zhang W (*Correo electrónico: fgg2343@hotmail.com*) 108
https://doi.org/10.54817/IC.v67n1a08

Potencial mejorador de la astaxantina en la insuficiencia cardíaca inducida por isoproterenol en ratas a través de la regulación del sistema renina-angiotensina. (Inglés)
Chang L, Qiao F (*Correo electrónico: furong644759573@sina.com*). 125
https://doi.org/10.54817/IC.v67n1a09

REVISIÓN

Metaanálisis de la eficacia y la seguridad de los anticuerpos específicos en la inmunoterapia del cáncer de pulmón. (Inglés)
Zhao X, Liu Y (*Correo electrónico: liuyang_ly248@163.com*) 139
https://doi.org/10.54817/IC.v67n1a10

INSTRUCCIONES A LOS AUTORES 2026. 152